Identification and Characterisation of Novel T3SS Effector Proteins of *Salmonella enterica* serovar Typhi

Alexander Mathew Patrick Byrne

2017

Ph.D. Thesis

Submitted to the Department of Life Sciences, Imperial College London, in partial fulfilment of the requirements for the degree of Doctor of Philosophy

Abstract

Salmonella enterica serovar Typhi (*S.* Typhi) is a Gram-negative, intracellular, human pathogen that is the causative agent of typhoid fever, responsible for 200,000 deaths worldwide, per year. Central to *S. enterica* pathogenesis are two type III secretion systems (T3SS), that are used to translocate up to 40 effector proteins to enable invasion, replication and manipulation of host immune responses. These proteins have been largely characterised in other *S. enterica* serovars and many are pseudogenes or absent from the genome of *S.* Typhi. The identification of a putative effector protein in *S.* Typhi, StoD, a member of the NleG family of bacterial E3 ubiquitin-ligase effectors, suggested that there may be more effectors in *S.* Typhi, than previously thought. In this study, a containment level three laboratory was established to enable the study of *S.* Typhi pathogenesis, and the role of novel T3SS effector proteins in this. A genome-wide machine-learning approach was then used to identify five putative effectors in *S.* Typhi, four of which, as well as StoD, were experimentally validated as being T3SS effectors. Whilst none of these novel effectors were found to be required for *S.* Typhi invasion or replication, StoD, and another novel effector, StoE, were found to localise in a punctate fashion in HeLa cells. For StoE, this localisation was shown to be dependent on a N-terminal transmembrane domain, whilst StoD was found to colocalise with the eukaryotic protein, ubiquitin, involved in protein regulation and cellular signalling. This colocalisation was demonstrated to be dependent on the E3 ubiquitin-ligase activity of StoD and whilst it was not possible to identify any substrates of StoD, further biochemical characterisation found that StoD preferentially bound K63-linked, di-ubiquitin. These findings increase the known repertoire of *S.* Typhi T3SS effectors from 23 to 28 proteins and suggest that further effectors could be identified.

Candidate's Declaration

I, Alexander Byrne, declare that the work contained within this thesis is my own. Any work performed by others that has been used in this thesis is appropriately acknowledged and referenced in the text or appropriate figure legends.

Copyright Declaration

The copyright of this thesis rests with the author and is made available under the Creative Commons Attribution Non-Commercial No Derivatives licence. Researchers are free to copy, distribute or transmit the thesis on the condition that they attribute it, that they do no use it for commercial purposes and that they do not alter, transform or build upon it. For any reuse or distribution, researchers must make clear to others the licence terms of this work.

Acknowledgements

Firstly, I would like to thank Gadi for the opportunity to undertake a PhD in his research group, and for the continued support and guidance that he has provided throughout. I would also like to thank Valerie for her direction, teaching and, for knowing when I needed to be pushed. Both Gadi and Valerie have taught me so much, without them I would never have become the scientist I now am, and for this I will never be able to thank you enough.

I would also like to the BBSRC for funding this work and everyone who contributed to this work. Thank you to Vassillis Koronakis, for the SipA and SipD antibodies, Sophie Helaine, for the SseB antibody and *S.* Typhimurium strains and Gordon Dougan, for the *S.* Typhi strains. Thank you to my collaborators, Tal Pupko and Dafna Shkedy, for running the genome-wide machine-learning algorithm on *S.* Typhi, as well as, Susan Lea and Melanie McDowell, for the structural work on StoD and for several constructs.

I would like to thank everyone in the CMBI and Frankel group for helping me to enjoy my PhD, even when times were tough, and would like to thank a few individuals in particular. Elli, you were an amazing master's student and are quickly becoming an excellent researcher. I am truly honoured to have been able to supervise you and to have benefitted from your help with my own project. Becky, without you I would never have been able to set up the CL3 laboratory and work on Typhi. You always had answers to my questions and were always happy to help when I needed it. I would also like to thank you for your comments and suggestions on several chapters of my thesis, I owe you so much for this. Ernie, you always knew when to tell me to stop stressing and were always so helpful with anything. Agnes, you provided me with so much kindness and support when I most needed it. You were always positive and you made the lab a much happier place. Chris, you not only helped with ideas and planning with respect to science, but you also made me feel so welcome at Imperial, from the moment I met you at our interviews. Finally, Dom, you were not only an awesome housemate, who put up with my complaining about work and other things, but you also helped me so much throughout my

PhD. You've always been an amazing friend ever since we met in Durham, for this I thank you.

I would also like to thank David and Anna Yallop for their ever-present support, especially when times were tough, and for your stories which made me laugh and cry. You taught me never to take things at face value and to always question everything.

Mum, Dad and Nan, you raised me and have always supported me in all my endeavours. Without you I wouldn't be where I am today. I will never be able to thank you enough for all your loving support and hard work that you put into raising me and Dom. I must also thank you Dom, for always making me laugh and keeping me sane.

Finally, Katherine, I can honestly say that without you I would not have been able to get through my PhD. You were always so strong and supportive when times were both good and bad. You never fail to make me laugh, and you always cared for me whenever I got stressed or upset. I will never truly be able to thank you for everything that you've done, I can only hope that I can repay you in kind.

Contents

Abstract **2**
Candidate's Declaration **3**
Copyright Declaration **3**
Acknowledgements **4**
Contents **6**
List of Figures **9**
List of Tables **10**
Abbreviations **11**
Chapter 1: Introduction **16**
1.14. The *Salmonella* Genus **17**
1.14.1. Discovery and Taxonomy 17
1.14.2. *Salmonella* Pathogenesis in Humans 19
1.14.2.1. Gastroenteritis 19
1.14.2.2. Bacteraemia 20
1.14.2.3. Enteric fever 21
1.14.2.4. Vi-antigen 22
1.14.2.5. The typhoid toxin 23
1.14.3. Epidemiology of Typhoidal Serovars 24
1.14.4. Diagnosis, Treatment and Vaccination 26
1.15. Bacterial Secretion Systems **29**
1.15.1. General Secretion Mechanisms 29
1.15.2. Type I Secretion System 31
1.15.3. Type II Secretion System 32
1.15.4. Type IV Secretion System 32
1.15.5. Type V Secretion System 33
1.15.6. Type VI Secretion System 35
1.15.7. Type III Secretion System 35
1.15.7.1. Assembly of the T3SS 36
1.15.7.2. T3SS chaperones 38
1.15.7.3. Regulation of the T3SSs in *Salmonella* 39
1.16. T3SS Effector Proteins and Manipulation of the Host Cell by *Salmonella* **43**
1.16.1. Invasion of Non-Phagocytic Host Cells 44
1.16.2. Formation of a Replicative Niche 44
1.16.3. Subversion of the Innate Immune System 46
1.16.4. Comparison of the Effector Repertoires of *S.* Typhimurium and *S.* Typhi 47
1.16.5. Identification of Novel Effector Proteins 49
1.17. The Ubiquitination System **51**
1.17.1. T3SS Effectors that Mimic Components of the Ubiquitination System 54
1.17.2. The NleG Family of T3SS Effectors 59
1.18. Hypothesis and Aims **60**
Chapter 2: Materials and Methods **61**
2.1. Bacterial strains **62**
2.2. Tissue Culture **63**
2.2 Cloning **64**
2.3 Generating Mutants in *S.* Typhi **70**
2.4 Transfection **71**

2.5 *Salmonella* Infection Assays 72
2.5.1 *Salmonella* Infection of HeLa cells 72
2.5.2 *Salmonella* Infection of RAW264.7 Murine Macrophages 72
2.5.3 *Salmonella* Infection of THP-1 Human Monocytes 73
2.5.4 Colony Forming Unit Enumeration 74
2.5.5 Protein Expression during *S.* Typhi Infection 74
2.6 β-lactamase Translocation Assays 74
2.7 Paraformaldehyde Fixation of Cells 75
2.8 Staining of Fixed Cells for Immunofluorescence 75
2.9 *Salmonella SPI-1* Secretion Assays 77
2.10 *Salmonella SPI-2* Secretion Assays 77
2.11 Protein Expression and Purification 78
2.11.1 StoD Variants 78
2.11.2 UBE2E1 79
2.11.3 UBE2L3 80
2.12 Autoubiquitination Assays 81
2.13 SDS-PAGE, Western Blotting and Coomasie Staining 81
2.15. Transformation of S. cerevisiae 82
2.16. Yeast Two-Hybrid 83
2.16.1. Control experiment – Autoactivation test 83
2.16.2. Control experiment – Toxicity test 84
2.16.3. Y2H Screen 84
2.16.4. Direct Y2H assays 85
2.16 Yeast Toxicity Assays 85
2.14 Genome-Wide Machine-Learning 85
2.15 Bioinformatics 86
2.17. Statistical Analyses 86

Chapter 3: Establishing a Containment Level 3 Laboratory for the Study of *S.* Typhi. 87

3.1. Introduction 88
3.2. Hazard Group Definitions and Containment Levels 88
3.3. Code of Practice: The Use of the CL3 Laboratory to Work with *S.* Typhi 90
3.3.1. Health Surveillance and Vaccinations 91
3.3.2. CL3 Laboratory Training 91
3.3.3. Producing SOPs for Work Involving *S.* Typhi 92
3.3.4. Practical Considerations for Work with *S.* Typhi in a CL3 Laboratory 92
3.4. Preliminary Work involving *S.* Typhi 97
3.4.1. Determination of the Antibiotic Susceptibilities of Several *S.* Typhi Strains 97
3.4.2. Optimisation of Protocols for Use with *S.* Typhi 99
3.4.2.1. Optimising infection of human epithelial cells with *S.* Typhi 99
3.4.2.2. Optimising infection of human macrophages with *S.* Typhi 101
3.4.2.3. Optimising secretion assays using *S.* Typhi 102
3.5. Discussion 105

Chapter 4: Identification and Characterisation of Novel T3SS Effectors in *S.* Typhi . 110

4.1. Introduction 111
4.2. Identification of Putative T3SS effectors in *S.* Typhi using a Genome-Wide Machine-Learning Approach 111
4.3. Assessing Secretion and Translocation of Putative T3SS Effectors 116
4.3.1. Assessing Secretion of Putative T3SS Effectors from *S.* Typhi 116
4.3.1.1. *SPI-1* secretion assays 116
4.3.1.2. *SPI-2* secretion assays 119
4.3.2. Evaluating the Translocation of the Novel Effector Proteins 121
4.4. Characterisation of the Novel Effector Proteins 124
4.4.1. Bioinformatic Analysis of the Novel Effector Proteins 124

4.4.2. Bioinformatic Analysis of the Promoter Region of *stoD* 128
4.4.3. Investigating the Localisation of the Novel Effectors in HeLa Cells 129
4.4.4. Assessing the Role of the Novel Effectors in *S*. Typhi Invasion and Replication 131
4.4.5. Investigating the Localisation of StoD and StoE during *S*. Typhi Infection 133
4.4.6. Evaluating StoD Expression during *S*. Typhi Infection of THP-1 Human Macrophages 136
4.4.7. Assessing the Effect of StoD on *S*. Typhimurium Invasion and Replication .. 137
4.5. Discussion 138

Chapter 5: Investigating the Biological Activity of StoD 146

5.1. Introduction 147
5.2. StoD is a Putative Member of the NleG Family of T3SS Effectors 147
5.3. Assessing the Enzymatic Activity of StoD 150
5.3.1. Optimising the Expression and Purification of Recombinant StoD 150
5.3.2. Assessing the Autoubiquitination Activity of StoD 152
5.3.3. Evaluating the Effect of the P204K Mutation on StoD Autoubiquitination 154
5.3.4. Investigating the Effect of StoD Expression on BY4741 S. cerevisiae 156
5.4. Identifying Interacting Partners of StoD 157
5.4.1. Assessing the Suitability of $StoD_{P204K}$ for use in a Y2H Screen 157
5.4.2. Y2H Screen with $StoD_{P204K}$ 159
5.4.3. Evaluating the Interaction between StoD and UBE2L3 160
5.4.4. Assessing the Ability of StoD to Ubiquitinate UBE2L3 in vitro 163
5.5. Investigating the Localisation of Vesicular Proteins upon StoD Expression in HeLa Cells 164
5.6. Determining the Effect of StoD on Host Ubiquitin Localisation 166
5.6.1. Assessing the Localisation of Ubiquitin-Like Proteins upon StoD Expression in HeLa Cells 166
5.7. Investigating a Direct Interaction between StoD and Ubiquitin 169
5.7.1. Evaluating the Binding of StoD and Di-Ubiquitin Moieties 171
5.7.2. Assessing if StoD can Directly Interact with ISG15 173
5.8. Discussion 174

Chapter 6: Conclusions 182

6.1. Overview 183
6.2. Conclusions and Future Directions 183

Bibliography 186

Appendices 210

Appendix 1 211
Appendix 2 214
Appendix 3 234
Appendix 4 235
Appendix 5 238

List of Figures

Figure 1.1. Phylogeny of the *Salmonella* genus. 18
Figure 1.2. *Salmonella* pathogenesis. 20
Figure 1.3. The secretion systems of Gram-negative bacteria. 30
Figure 1.4 The T3SSs of *Salmonella*. 36
Figure 1.5. Regulation of *SPI-1* and *SPI-2*. 39
Figure 1.6. *Salmonella* T3SS effectors involved in invasion, replication and subversion of the host innate immune system. 43
Figure 1.7. The ubiquitination system. 52
Figure 1.8. The varying forms of ubiquitination. 54
Figure 3.1. SOPs for use in the CL3 laboratory. 93
Figure 3.2. A CL3 laboratory for handling *S*. Typhi. 94
Figure 3.3. Optimising *S*. Typhi infection protocols. 100
Figure 3.4. Optimising T3SS secretion assays for *S*. Typhi. 103
Figure 4.1. Assessing secretion of the putative effector proteins from the *SPI-1* T3SS. 117
Figure 4.2. Assessing secretion of the putative effector proteins from the *SPI-2* T3SS. 120
Figure 4.3. Novel effector proteins are secreted by a *SPI-2* mutant in *S*. Typhimurium. 122
Figure 4.4. Assessing translocation of novel effector proteins. 123
Figure 4.5. Assessing translocation of the *S*. Typhimurium homologue of StoB. 126
Figure 4.6. Genomic localisation of the novel effector proteins in *S*. Typhi 127
Figure 4.7. The upstream region of *stoD* contains two putative promoters. 129
Figure 4.8. Localisation of the novel effectors during ectopic expression in HeLa cells. 130
Figure 4.9. Assessing the role of the novel effectors in *S*. Typhi invasion and replication. 132
Figure 4.10. Investigating the localisation of StoD and StoE during *S*. Typhi infection. 135
Figure 4.11. Investigating the expression of StoD during *S*. Typhi infection. 136
Figure 4.12. Assessing the effect of StoD on *S*. Typhimurium invasion and replication. 137
Figure 5.1. StoD is a member of the NleG family of effector proteins. 149
Figure 5.2. Structural model of StoD. 150
Figure 5.3. Optimising expression and purification of recombinant StoD. 152
Figure 5.4. Screening E2 ubiquitin-conjugating enzymes with StoD. 153
Figure 5.5. Purification of 6His-UBE2E1 and autoubiquitination assays with StoD. 155
Figure 5.6. StoD is toxic to BY4741. 156
Figure 5.7. $StoD_{P204K}$ does not autoactivate or cause a growth defect in AH109 *S. cerevisiae*. 158
Figure 5.8. $StoD_{P204K}$ interacts with the UBE2L3 Hit. 161
Figure 5.9. StoD does not interact with UBE2L3. 162
Figure 5.10. StoD does not ubiquitinate UBE2L3. 163
Figure 5.11. StoD does not colocalise with vesicular proteins. 165
Figure 5.12 Ubiquitin is relocalised during ectopic expression of StoD. 167
Figure 5.13. StoD does not cause relocalisation of ubiquitin-like proteins. 168
Figure 5.14. StoD directly interacts with ubiquitin. 170
Figure 5.15. StoD binds to di-ubiquitin. 172
Figure 5.16. StoD does not interact with ISG15. 173

List of Tables

Table 2.1. Strains used in this study. 62
Table 2.2. Vectors used in this study. 64
Table 2.3. Primers used in this study. 67
Table 2.4. Antibodies used in this study. 76
Table 3.1. Hazard group classifications. 89
Table 3.2. Antibiotic sensitivity profiles of *S.* Typhi strains. 98
Table 4.1. Table of known Salmonella T3SS effector and non-effector genes used in the machine-learning algorithm. 113
Table 4.2. Top 100 ranked genes from the machine-learning algorithm. 114
Table 4.3. Genes selected for further investigation based on the machine-learning algorithm results. 116
Table 4.4. Putative homologues of the novel effectors in other species of Gram-negative pathogenic bacteria. 125
Table 4.5. Putative homologues of the novel effectors in *S. enterica* serovars. 125
Table 5.1. Shortlisted hits from Y2H screen with $StoD_{P204K}$ selected for further investigation. 160

Abbreviations

%GC	Guanosine-cytosine content
6His	Polyhistidine
ABC	ATP-binding cassette
ACDP	Advisory committee on dangerous pathogens
ADP	Adenosine diphosphate
Amp	Ampicillin
Amp^R	Ampicillin resistant
ATP	Adenosine triphosphate
B	Binding
BLAST	Basic local alignment search tool
BSA	Bovine serum albumin
cAMP	Cyclic adenosine monophosphate
CL2	Containment level two
CL3	Containment level three
Cm	Chloramphenicol
Cm^R	Chloramphenicol resistant
COP	Code of practice
CSA	Common structural antigen
Csr	Carbon storage regulator
DDO	SD agar plates lacking L-leucine and L-tryptophan
DMEM	Dulbecco's modified Eagle's medium
DPBS	Dulbecco's phosphate-buffered saline
DTT	DL-dithiothreitol
DUB	Deubiquitinase
E1	Ubiquitin-activating enzyme
E2	Ubiquitin-conjugating protein
E3	Ubiquitin-ligase
EHEC	Enterohaemorrhagic *E. coli*
EPEC	Enteropathogenic *E. coli*
EV	Empty vector
F	Elution fraction

FBS	Foetal bovine serum
FRT	Flp recombination target
FT	Flow-through
GAP	GTPase activating protein
GEF	Guanine nucleotide exchange factor
Gent	Gentamicin
GFP	Green fluorescent protein
GST	Glutathione S-transferase
GTP	Guanosine triphosphate
h	Hour
H58	Haplotype 58
HA	Haemagglutinin
HBSS	Hank's buffered saline solution
HECT	Homologous to the E6-AP carboxyl terminus
Hil	Hyper invasion locus
HIV	Human Immunodeficiency Virus
HMW	High molecular weight
HSE	Health and safety executive
I	Insoluble
IL	Interleukin
IMC	Inner-membrane complex
In	Induced
inv/Inv	Invasion
IPTG	Isopropyl β-D-1-thiogalactopyranoside
ISG15	Interferon-stimulated gene 15
K6	Lysine-6
K11	Lysine-11
K27	Lysine-27
K29	Lysine-29
K33	Lysine-33
K48	Lysine-48
K63	Lysine-63
K_D	Dissociation constant

kDa	Kilodalton
KEGG	Kyoto encyclopaedia of genes and genomes
Kn	Kanamycin
Kn^R	Kanamycin resistant
LB	Lysogeny broth
LC-MS/MS	Liquid chromatography coupled to tandem mass spectroscopy
LEE	Locus of enterocyte effacement
LPS	Lipopolysaccharide
LRR	Leucine-rich repeat
LUBAC	Linear ubiquitin assembly complex
M cells	Microfold cells
M1	Methionine-1
MAC	Membrane-associated complex
MDR	Multi-drug resistant
MES	2-(N-morpholino)ethanesulfonic acid
MFP	Membrane fusion protein
min	Minute
MOI	Moiety of infection
MSC	Microbiological safety cabinet
NAIP	NOD-like receptor family apoptosis inhibitor protein
Nal	Nalidixic acid
NCBI	National Centre for Biotechnology Information
NEL	New E3-like
Nle	Non-LEE encoded protein
NMR	Nuclear magnetic resonance
NOD	Nucleotide-binding oligomerisation domain-containing
nt	Nucleotide
NTS	Non-typhoidal *Salmonella*
OD_{600}	Optical density at 600 nm
OMC	Outer-membrane complex
OMP	Outer membrane pore
ORF	Open reading frame
Pag	PhoP-activated gene

PBS	Phosphate-buffered saline
PBST	PBS with 0.05% Tween 20
PCR	Polymerase chain reaction
PFA	Paraformaldehyde
PMA	Phorbol 12-myristate 13-acetate
PMN	Polymorphonuclear neutrophil
Pre	Pre-induced
PVDF	Polyvinylidene difluoride
QDO	SD agar plates lacking L-leucine, L-tryptophan, L-adenine containing X-α-Gal
RBR	RING-between-RING
RING	Really interesting new gene
RPMI-1640	Roswell Park Memorial Institute medium
Rts	Regulator of *SPI-1*
S	Soluble
s	Second
S. Choleraesuis	*Salmonella enterica* serovar Choleraesuis
S. Dublin	*Salmonella enterica* serovar Dublin
S. Enteritidis	*Salmonella enterica* serovar Enteritidis
S. Paratyphi A, B and C	*Salmonella enterica* serovar Paratyphi A, B and C
S. Typhi	*Salmonella enterica* serovar Typhi
S. Typhimurium	*Salmonella enterica* serovar Typhimurium
Sbo	*S. bongori* outer protein
SCV	*Salmonella*-containing vacuole
SD	Synthetic dextrose
SD/-Ade/-His/-Trp	SD medium lacking adenine, L-histidine and L-tryptophan
SD/-Trp	SD medium lacking L-tryptophan
SDS-PAGE	Sodium dodecyl sulfate polyacrylamide gel electrophoresis
Sec	General secretion
Sif	*Salmonella*-induced filament
Sip	*Salmonella* invasion protein
SNP	Single nucleotide polymorphism
SOC	Super optimal broth with catabolite repression

SOP	Standard operating procedures
Sop	*Salmonella* outer protein
Spec	Spectinomycin
$Spec^R$	Spectinomycin resistant
SPI	*Salmonella* pathogenicity island
SSOP	*Salmonella* standard operating procedures
ST	Sequence type
STM	Signature-tagged mutagenesis
Sto	*S.* Typhi outer protein
T1SS	Type I Secretion System
T2SS	Type II Secretion System
T3SS	Type III Secretion System
T4SS	Type IV Secretion System
T5SS	Type V Secretion System
T6SS	Type VI Secretion System
Tat	Twin arginine translocation
TCF	T-cell factor
TEM1	β-lactamase
Tet	Tetracycline
Tet^R	Tetracycline resistant
TLR	Toll-like receptor
Tn	Transposon
TNFα	Tumour necrosis factor alpha
Tts	Typhoid toxin secretion protein
UPEC	Uropathogenic *E. coli*
v/v	Volume-to-volume
Vi-antigen	Virulence antigen
W	Wash
w/v	Weight-to-volume
WT	Wild-type
Y2H	Yeast two-hybrid
YPDA	Yeast peptone dextrose adenine

Chapter 1: Introduction

1.14. The Salmonella Genus

1.14.1. Discovery and Taxonomy

The *Salmonella* genus is comprised of Gram-negative, rod-shaped bacteria of the family *Enterobacteriaceae*. The genus was first recognised by Theobald Smith and Daniel Elmer Salmon; after whom the genus is named, who isolated the causative agent of hog cholera in 1886 – now understood to be *Salmonella enterica* serovar Choleraesuis (*S.* Choleraesuis) (Kass 1987). However, *Salmonella enterica* serovar Typhi (*S.* Typhi) had been isolated from the lymph nodes and spleen of typhoid fever patients by Karl Joseph Eberth, in 1880, but not identified (Marineli et al. 2013).

The taxonomy of *Salmonellae* is complicated due to the common misconception that different serovars represent separate species. However, it is now recognised that the *Salmonella* genus consists of only two species: *Salmonella enterica* and *Salmonella bongori* (Figure 1.1). Both species possess *Salmonella* pathogenicity islands *(SPI)-1*, *SPI-3*, *SPI-4* and *SPI-9* as well as fimbriae, all of which are thought to have been obtained by a common ancestral organism of the two species (Fookes et al. 2011). After divergence of the two species, *S. bongori* obtained a single additional *SPI*, *SPI-22*, whilst *S. enterica* gained an additional nine pathogenicity islands including *SPI-2* and *SPI-6* (Fookes et al. 2011). The two species also differ in their ability to metabolise substrates. For example, *S. bongori* lacks the ability to utilise ethanolamine as an energy source (Porwollik et al. 2002), whereas, *S. enterica* is unable to metabolise complex acid sugars (Fookes et al. 2011).

S. enterica is divided into seven subspecies: *enterica* (I), *salamae* (II), *arizonae* (IIIa), *diarizonae* (IIIb), *houtenae* (IV), *indica* (VI) and a seventh, as yet unnamed subspecies (VII) (Figure 1.1), based on differences in multilocus enzyme electrophoresis (Boyd et al. 1996). *S. bongori* was originally identified as subspecies V, but was later reclassified as a separate

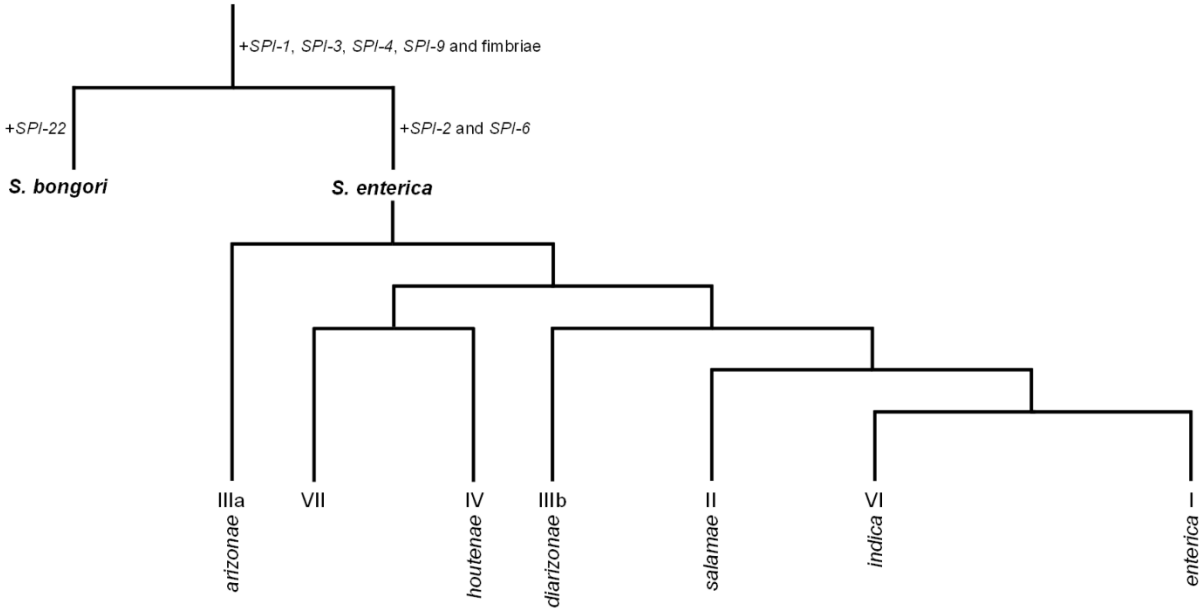


Figure 1.1. Phylogeny of the *Salmonella* genus. A common ancestor of the *S. bongori* and *S. enterica* species obtained *SPI-1*, *SPI-3*, *SPI-4*, *SPI-9* and fimbriae, before divergence, after which *S. bongori* obtained *SPI-22* and *S. enterica* gained *SPI-2* and *SPI-6*. The *S. enterica* species then diverged more, leading to the evolution of seven subspecies. Please note, distances between species and subspecies are not to scale. Adapted from (McQuiston et al. 2008; Fookes et al. 2011).

species (Reeves et al. 1989). The subspecies differ in their *SPI* and metabolic repertoires (Fookes et al. 2011), as well as their host. *S. enterica* subspecies I and II usually inhabit warm-blooded animals, whereas, *S. bongori* and *S. enterica* subspecies III-VII are usually isolated from cold-blooded animals (Brenner et al. 2000), but can become pathogenic in humans (Woodward et al. 1997). However, most of the human pathogens belong to subspecies I. Subspecies are then further classified into more than 2,600 serovars based on the White-Kauffmann-Le Minor scheme using the somatic “O” and “H” antigens present in lipopolysaccharide (LPS) and flagellar, respectively (Gal-Mor et al. 2014; Grimont & Weill 2007). To denote which species and subspecies a particular serovar belongs to, there is a defined nomenclature. For example, *S. enterica* subspecies *enterica* (I) serovar Typhi, where the species and subspecies are italicised, unless the numeral is used, whilst the serovar is not italicised and has a capitalised first letter (Grimont & Weill 2007). This can be shortened to *S.* Typhi, where it is assumed that the serovar belongs to *S. enterica* subspecies I, unless stated otherwise.

The majority of *Salmonella* serovars belongs to *S. enterica* subspecies I (Lan et al. 2009) and can be broadly distinguished into two groups: typhoidal and non-typhoidal. Serovars *S.* Typhi, *S.* Paratyphi A, B and C are human-restricted (McClelland et al. 2004), typhoidal serovars that cause systemic infections, resulting in the enteric fevers known as typhoid fever and paratyphoid fever, respectively (Darton et al. 2014). Non-typhoidal serovars, such as *S.* Typhimurium and *S.* Enteritidis are generalist pathogens infecting humans, livestock (Feasey et al. 2012) and mice (de Jong et al. 2012) and cause a self-limiting diarrhoeal disease in humans (Feasey et al. 2012). Although the disease outcome and host ranges of *Salmonella* serovars can differ, all have the ability to cause disease to humans and are transmitted by the faecal-oral route via contaminated food or water (Feasey et al. 2012).

1.14.2. *Salmonella* Pathogenesis in Humans

Once ingested, *Salmonellae* pass through the stomach and attach to the mucosa of the small intestine, where entry into the body occurs, primarily via antigen sampling microfold (M) cells, located within Peyer's patches (Clark et al. 1994). However, non-typhoidal *Salmonella* (NTS) serovars, such as *S.* Typhimurium are capable of directly invading the epithelial cells of the small intestine (de Jong et al. 2012). It is after this initial invasion that three different forms of *Salmonellosis* can occur: gastroenteritis, bacteraemia or enteric fever (Figure 1.2) (de Jong et al. 2012). These *Salmonelloses* have distinct clinical symptoms, and are caused by different *Salmonellae*.

1.14.2.1. Gastroenteritis

Gastroenteritis is caused by an infection of immunocompetent individuals with NTS serovars and occurs within 72 h of ingestion (Raffatellu et al. 2008). NTS remain in the intestinal mucosa (Raffatellu et al. 2008) where they replicate within phagocytic cells (Figure 1.2A) (Alpuche-Aranda et al. 1994) and induce a pro-inflammatory response enabling them to outcompete the resident microbiota and establish an infection (Stecher et al. 2007). This mucosal response results in the recruitment of neutrophils to the site of infection (McCormick et al. 1993), and

causes watery diarrhoea, vomiting and abdominal pain (Gal-Mor et al. 2014). The disease is self-limiting and usually resolves within 10 days with the provision of fluids (Raffatellu et al. 2008) and is not usually associated with further complications.

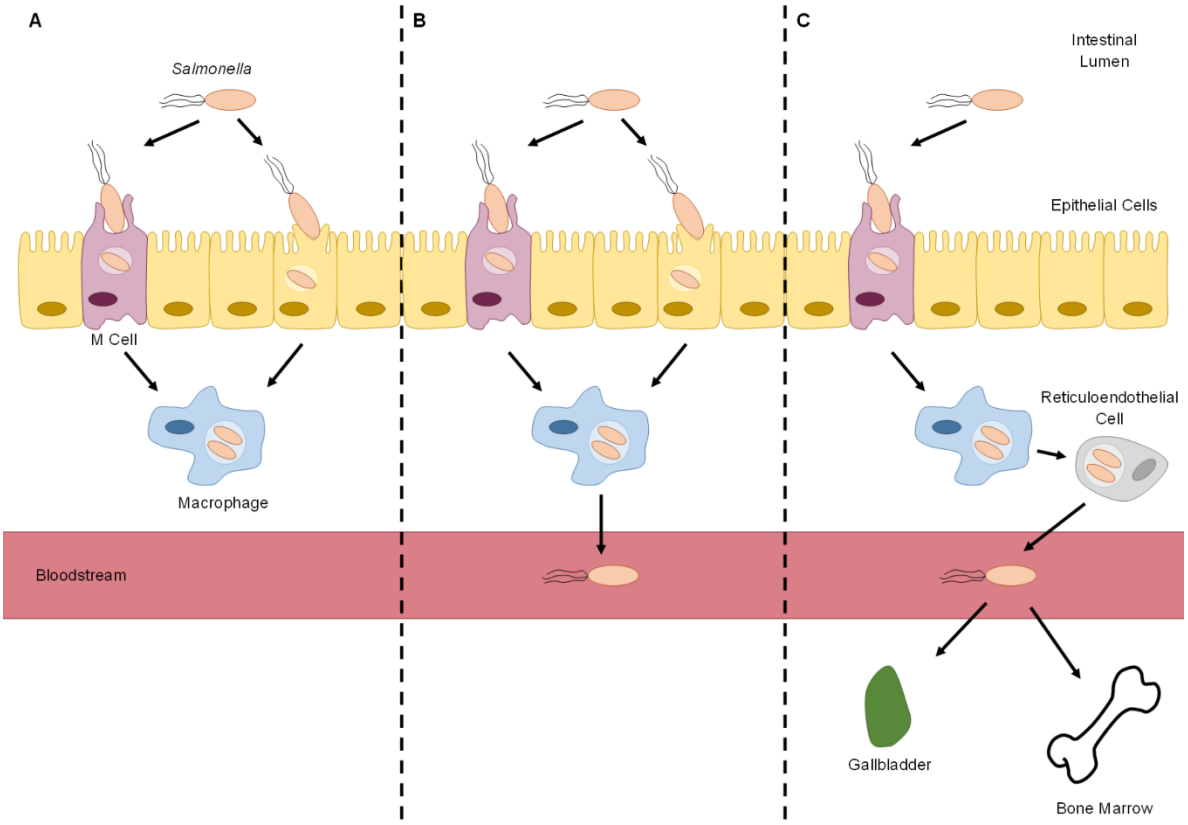


Figure 1.2. *Salmonella* pathogenesis. *Salmonellae* are ingested via contaminated food or water and pass through the stomach to the small intestine. **(A)** NTS serovars are either taken up by microfold (M) cells or through invasion of intestinal epithelial cells, before replicating within phagocytic cells. **(B)** Invasive strains of NTS, such as *S.* Typhimurium ST313, invade the intestinal mucosa in a similar manner to other NTS strains, but then enter the bloodstream to disseminate systemically. **(C)** Typhoidal *Salmonellae* enter the intestinal mucosa through M cells before replicating within phagocytic cells. These serovars then translocate to reticuloendothelial cells in the liver and spleen, before entering the bloodstream and colonising secondary infection sites such as the gallbladder and bone marrow, resulting in systemic infection. Adapted from (Lhocine et al. 2015; Sansonetti 2004; Parry et al. 2002).

1.14.2.2. Bacteraemia

Within Sub-Saharan Africa and South-East Asia, individuals that suffer from immunodeficiencies, such as those arising from Human Immunodeficiency Virus (HIV) infection, sickle cell anaemia, malaria and malnutrition, can develop an invasive *Salmonellosis* caused by NTS serovars (Feasey et al. 2012; Phu Huong Lan et al. 2016). This disease is a

stark contrast to gastroenteritis, and is marked by the migration of NTS from the intestinal mucosa and entering the bloodstream, resulting in systemic dissemination (Figure 1.2B) (Gilchrist et al. 2015). Clinically, invasive NTS infection lacks diarrhoea and is associated with a high fever, enlarged liver and spleen, respiratory conditions, sepsis and meningitis, resulting in up to 47% patient fatality, even after antibiotic treatment (Gal-Mor et al. 2014; Feasey et al. 2012). Whilst *S.* Enteritidis and *S.* Typhimurium, are the NTS serovars primarily associated with bacteraemia, the sequence type (ST) 313 lineage of *S.* Typhimurium is the predominant cause in sub-Saharan Africa (Feasey et al. 2012). This lineage exhibits resistance to several antibiotics and has undergone a significant accumulation of pseudogenes compared to other *S*. Typhimurium isolates (Kingsley et al. 2009).

1.14.2.3. Enteric fever

Typhoidal serovars replicate within phagocytic cells before translocating to lymphoid tissue within the intestine, and reticuloendothelial cells in the spleen and liver (de Jong et al. 2012). These serovars then enter the blood stream, allowing dissemination and colonisation of secondary infection sites such as the gallbladder and bone marrow, resulting in systemic infection (Figure 1.2C) (Parry et al. 2002). Unlike the NTS serovars responsible for bacteraemia, typhoidal serovars are capable of inducing a systemic infection in immunocompetent hosts that results in an enteric fever (Feasey et al. 2012) called typhoid or paratyphoid fever, depending on which serovar is the cause (Bhan et al. 2005).

Symptoms of typhoid fever can take up to two weeks to develop but include: a progressively increasing fever which is then sustained around 40°C, malaise, constipation and a rash on the abdomen and chest which can be seen from four days post-infection (Parry et al. 2002; Waddington et al. 2014). Complications are unlikely, but can result in intestinal perforation or haemorrhage (Wain et al. 2014).

Paratyphoid fever is a similar infection that is caused predominantly by *S.* Paratyphi A (Meltzer et al. 2005). Paratyphoid fever presents with similar symptoms to typhoid fever, but has

generally been considered to be less severe (Buckle et al. 2012). However, recent reports suggest that the symptoms of paratyphoid fever can be indistinguishable from those of typhoid fever, and that complications, such as splenic abscesses and endocarditis, are more likely (Meltzer et al. 2005).

1.14.2.3.1. Gallbladder carriage

S. Typhi and *S.* Paratyphi A are able to persist within the gallbladder in up to 2% of patients, even after convalescence (Parry et al. 2002; Khatri et al. 2009). This persistence within the gallbladder can result in shedding, leading to infection of other individuals, as well as re-infection, and is known as the "Carrier State" (Dougan & Baker 2014; Parry et al. 2002). The first documented, and most infamous incidence of this was Mary Mallon, also known as "Typhoid Mary", an Irish émigré who worked as a cook in America in the early 1880s (Marineli et al. 2013). Mary had previously contracted typhoid fever, but acted as an asymptomatic carrier resulting in the infection of over 100 people in the New York area (Marineli et al. 2013). The mechanisms that allow *S.* Typhi to persist inside the gallbladder are still not fully understood. One recent study suggested that *Salmonella* can invade and persist in the epithelium of the gallbladder (Gonzalez-Escobedo & Gunn 2013), whereas other work has suggested that *Salmonella* can form biofilms on the surface of gallstones and that this allows persistence (Crawford et al. 2010). However, the consensus opinion is that both mechanisms allow gallbladder carriage (Gonzalez-Escobedo & Gunn 2013).

1.14.2.4. Vi-antigen

The virulence (Vi)-antigen is a capsular polysaccharide, composed of linear α-1,4-linked 2-deoxy-2-N-acetylgalactosamine uronic acid monomers, that covers the surface of the bacterium (Virlogeux et al. 1995). The Vi-antigen is found in most *S.* Typhi strains, as well as *S.* Paratyphi C, *Citrobacter freundii* and some strains of *S. enterica* serovar Dublin (*S.* Dublin) (Virlogeux et al. 1995), but is absent in *S.* Typhimurium and *S.* Paratyphi A (Seth-Smith 2008). In *S.* Typhi and *S.* Paratyphi C, the genes required for the synthesis and export of the

Vi-antigen are encoded within *SPI-7* and are split between two loci, *viaA* and *viaB* (Seth-Smith 2008). Whilst the *viaB* locus is specific to Vi-antigen producing bacteria, the *viaA* locus is found in both Vi-positive and Vi-negative bacteria including *Escherichia coli* (Virlogeux et al. 1995). The *viaA* locus encodes the *rcsB* and *rcsC* genes, of which *rcsB* is involved in regulating the expression of the Vi-antigen (Kaur & Jain 2012), whilst the *viaB* locus encodes 10 genes that are required for the synthesis, export and anchoring of the Vi-antigen to the bacterial surface (Wetter et al. 2012). The *tviA* gene encodes a regulatory protein that binds to RcsB and induces expression of the remainder of the *viaB* locus (Virlogeux et al. 1996). The enzymes involved in polymerisation of N-acetylglucosamine within the bacterial cytoplasm are encoded by *tviB-E*, whilst *vexA-D* encode components of an ATP-binding cassette (ABC) transporter, that exports the polymerised Vi-antigen through the bacterial cell membrane, where VexE anchors the capsule to the cell surface (Wetter et al. 2012).

During infection, the Vi-antigen acts as a physical barrier to prevent LPS being detected by Toll-like receptor (TLR) 4 and complement components, preventing a pro-inflammatory response being generated by the intestinal mucosa and preventing bacterial complement-dependent clearance (Wilson et al. 2008; Raffatellu et al. 2005; Wilson et al. 2011). The expression of the Vi-antigen regulatory protein, TviA, also results in repression of flagellin expression and therefore detection by TLR5, which also contributes to the lack of a pro-inflammatory response (Winter et al. 2008)

1.14.2.5. The typhoid toxin

The typhoid toxin is an AB-type, cytolethal distending toxin, similar to that found in *Campylobacter* species, encoded by *S.* Typhi (Haghjoo & Galán 2004), and consists of three proteins: CdtB, PltA and PltB (Song et al. 2013). The typhoid toxin has two A-subunit proteins, CdtB and PltA, unlike other AB toxins, and one B-subunit protein, PltB, which are arranged in a pyramidal, A_2B_5 structure formed from one molecule each of CdtB and PltA in complex with five PltB monomers (Song et al. 2013). The A-subunits possess the activity domains of the toxin, which are a DNase, CdtB, (Haghjoo & Galán 2004) and an ADP-ribosyl transferase,

PltA (Song et al. 2013). Each PltB protein contains a polysaccharide-binding domain, which binds to N-acetylneuramidic acid in the host cell glycocalyx, whilst the PltB pentamer forms a channel through which CdtB and PltA are translocated through the host cell membrane (Song et al. 2013).

The typhoid toxin causes disintegration of eukaryotic cell chromatin, resulting is cell elongation and cell cycle arrest, through the activity of CdtB (Haghjoo & Galán 2004), and treatment of mice with purified typhoid toxin results in the development of symptoms associated with typhoid fever including malaise, but not a fever (Song et al. 2013). Further work has found that PltB specifically binds to N-acetylneuramidic acid moieties (Song et al. 2013), which are only present in humans, whereas other mammals, including mice, convert N-acetylneuramidic acid to N-glycolylneuramidic acid (Deng et al. 2014). Due to these findings, it has been suggested that the typhoid toxin is the determinant of the differing host specificities and disease outcomes between typhoidal and NTS serovars (Song et al. 2013; Deng et al. 2014). However, whilst the typhoid toxin is also encoded by *S.* Paratyphi A, another human-specific, typhoidal serovar (Galán 2016), it is also present in some NTS serovars (Miller & Wiedmann 2016), suggesting that the disease outcome and host-specificity may be due to factors aside from the typhoid toxin.

1.14.3. Epidemiology of Typhoidal Serovars

Globally, there are approximately 21 million cases of typhoid fever each year, resulting in 200,000 deaths (WHO 2013). The highest incidences occur within Sub-Saharan Africa (724.6 cases per 100,000 people) and South Asia (394.2 cases per 100,000 people), with the majority of cases involving children under five years of age (Buckle et al. 2012). Europe and North America have the lowest incidence (less than 0.1 case per 100,000 people) (Buckle et al. 2012) and in the UK specifically, there are approximately 500 cases of typhoid fever per year, mostly in people who have travelled to the Indian subcontinent (NHS 2016).

The development of multi-drug resistant (MDR) strains of *S.* Typhi, defined as strains with

resistance to chloramphenicol, ampicillin and co-trimoxazole (Zaki & Karande 2011), have become an increasing problem. The first MDR strains of *S.* Typhi were identified in South-east Asia in the early 1980s, carrying plasmids that conferred resistance to the antibiotics listed above (Ling & Chau 1984). In 1995, *S.* Typhi strains resistant to quinolone antibiotics, such as ofloxacin and nalidixic acid, were isolated in Vietnam, with resistance conferred by mutations in the DNA gyrase subunit A (*gyrA*) gene (Wain et al. 1997). The spread of MDR *S.* Typhi strains has since been so extensive, that during an outbreak in Tanzania between 2009 and 2010, up to 100% of isolates from infected patients demonstrated MDR (Wain et al. 2014).

Over the last 30 years, one particularly dominant MDR lineage of *S.* Typhi, haplotype 58 (H58) also known as subclade 4.3.1 (Wong et al. 2016), has emerged from South Asia, and then spread throughout Asia and Africa (Wong et al. 2015). These *S.* Typhi strains are separated from the nearest non-H58 isolates by 151 single-nucleotide polymorphisms (SNPs) and have been shown to be resistant to ampicillin, trimethoprim and streptomycin, as well as having reduced susceptibility to fluoroquinolones (Wong et al. 2015). Resistance is conferred by the presence of the IncH1 MDR plasmid and genomic mutations (Wong et al. 2015). Just under 50% of globally collected isolates since 1992 have belonged to H58 and there is also evidence that H58 strains are outcompeting antibiotic-sensitive strains (Wong et al. 2015), suggesting that in the coming years the H58 lineage may become the sole global haplotype of *S.* Typhi.

The incidence of paratyphoid fever has been greatly underestimated due to the difficulty in distinguishing whether patients exhibiting symptoms of enteric fever are infected with *S.* Typhi or *S.* Paratyphi (Gupta et al. 2008). However, in 2004, it was estimated that there were approximately 5.4 million cases globally, per year (Crump et al. 2004). More recent work has shown that the highest incidences of paratyphoid fever occur in South Asia and Sub-Saharan Africa (both 77.4 cases per 100,000 people), with a much lower incidence in Europe (<0.1 cases per 100,000 people) similar to typhoid fever (Buckle et al. 2012). The similarities in geographic incidence is to be expected as both diseases are transmitted by the same

faecal-oral route which can be exacerbated by poor sanitation and food preparation. It has been suggested that *S.* Paratyphi A is beginning to outcompete *S.* Typhi in endemic regions resulting in serovar replacement, which is thought to be somewhat due to the use of the Vi-antigen-based vaccine in certain areas of Asia, which would selectively benefit the survival of *S.* Paratyphi A, which does not encode the Vi-antigen, over *S.* Typhi (Darton et al. 2014).

1.14.4. Diagnosis, Treatment and Vaccination

Diagnosis of typhoid fever is currently performed using two methods: culture of *S.* Typhi from blood or bone marrow, or serological assays, such as the Felix-Widal test (Steele et al. 2016).

Culture methods involve inoculating tryptic soy broth with samples from the patient, followed by incubation at 37°C and sub-culturing onto non-selective agar plates, such as blood or desoxycholate agar (WHO 2003). Growth of *S.* Typhi and *S.* Paratyphi A on blood agar results in smooth, white, non-haemolytic colonies, whereas growth on desoxycholate agar results in lactose non-fermenting colonies with black centres for *S.* Typhi, whilst *S.* Paratyphi A colonies do not have black centres (WHO 2003). Therefore, growth of blood culture on desoxycholate agar can be one means of differentially diagnosing typhoid and paratyphoid fever infections. Culturing methods of diagnosis are very sensitive, but do require specialist experience and equipment as well as taking a minimum of two days to provide a diagnosis (Steele et al. 2016).

The Felix-Widal test involves mixing blood from a suspected typhoid fever patient with antibodies raised against the O and H antigens, which can be detected between six and 12 days after onset of infection, and then assessing agglutination (WHO 2003). This method of diagnosis is relatively cheap, quick and does not require expertise, but is less sensitive than culture methods of diagnosis and due to the cross-reaction of antibodies with other *Salmonella* serovars can result in false positives (Steele et al. 2016; WHO 2003).

Polymerase chain reaction (PCR) methodologies for the detection of *S.* Typhi and *S.* Paratyphi A (Levy et al. 2008; Nga et al. 2010) have been developed and are attractive diagnostic tools due to their ability to differentiate between patients infected with different

Salmonella serovars, based on the presence or absence of particular genes. However, the sensitivity of these assays is limited (Andrews & Ryan 2015) and often require a culture step to amplify bacterial numbers prior to the PCR (Zhou & Pollard 2010; Darton et al. 2017).

The increasing prevalence of MDR *S.* Typhi strains, has meant that antibiotic treatment is now limited to the use of fluoroquinolones, azithromycin, and third-generation cephalosporins (Wain et al. 2014). But, reports of fluoroquinolone-resistance in *S.* Typhi (Tatavarthy et al. 2014) highlight the need for new, effective treatments and vaccines.

There are currently two licensed vaccines that protect against typhoid fever. Firstly, a live-attenuated oral vaccine based on the Ty21a strain, which was produced by chemical mutagenesis and contains a mutation in a gene involved in galactose metabolism, Δ*galE* (Germanier & Fiirer 1975), which was first licensed in 1993 and has an efficacy of 53-78% (WHO 2008). Secondly, the Vi-antigen polysaccharide vaccine, which was licensed in 1994 and has an efficacy of 70% (WHO 2008). Currently, neither vaccine provides protection for children under two years of age, which are most at risk of contracting a fatal infection, or against *S.* Paratyphi A (McGregor et al. 2013; Darton et al. 2014). However, there are currently vaccines in development that are based on both the Ty21a live-attenuated vaccine and Vi-antigen vaccines that hope to address the shortfalls of the two current vaccines.

M01ZH09 and CVD909 are two possible single-dose, live attenuated oral vaccines (Tran et al. 2010; Tacket & Levine 2007). Both are Ty2-derivatives with mutations in aromatic amino acid synthesis, Δ*aroC* for M01ZH09 (Tran et al. 2010) and Δ*aroC*Δ*aroD* for CVD909 (Tacket & Levine 2007). These mutations in amino acid synthesis have then been combined with further mutations that prevent *S.* Typhi from causing infection. In M01ZH09 the additional mutation is in a structural component of the *SPI-2* T3SS, Δ*ssaV* (Tran et al. 2010), and in CVD909 the additional mutation is to a heat shock protein, Δ*htrA* (Tacket & Levine 2007) which not only prevents *S*. Typhi replicating intracellularly, but also causes constitutive Vi-antigen expression (Wang et al. 2000). Both vaccines have been shown to be well tolerated

and to induce the production of anti-LPS antibodies in clinical trials (Tran et al. 2010; Tacket & Levine 2007).

Vi-rEPA and Vi-CRM_{197} are both variations on the Vi-antigen polysaccharide vaccine, where the Vi-antigen has been conjugated to other proteins. In the Vi-rEPA vaccine, the Vi-antigen has been fused to recombinant exoprotein A from *Pseudomonas aeruginosa* (Thiem et al. 2011), whereas the Vi-CRM_{197} vaccine has the Vi-antigen coupled to the carrier protein of the diphtheria toxin from *Corynebacterium diphtheriae* (van Damme et al. 2011). Both vaccines have been demonstrated to stimulate the production of anti-Vi-antigen antibodies (Thiem et al. 2011; van Damme et al. 2011), but only the Vi-rEPA vaccine has been shown to be efficacious in infants under two years of age (Thiem et al. 2011).

Although the Vi-conjugate vaccines have been shown to induce the same, if not higher levels of anti-Vi-antigen antibodies compared the current Vi-antigen vaccine, they do not protect against Vi-negative *Salmonella* serovars. To achieve this, an improved live-attenuated vaccine would be required that can protect children under the age of two as well as demonstrating protection against other serovars, such as *S.* Paratyphi A, neither of which have been shown to date. In answer to this lack of coverage by current typhoid fever vaccines, several vaccines against paratyphoid fever are currently in development. The O:2-CRM_{197} vaccine contains the *S.* Paratyphi A O-antigen conjugated to the diphtheria toxin carrier protein (Micoli et al. 2011) similar to the Vi-CRM_{197} vaccine, whereas, the CVD1902 vaccine contains a live attenuated strain of *S.* Paratyphi A (Gat et al. 2011), analogous to the M01ZH09, CVD909 or Ty21a live-attenuated typhoid fever vaccines. Both of these paratyphoid fever vaccine candidates have been shown to be immunogenic (Micoli et al. 2011; Gat et al. 2011), but, since uptake of vaccination can be low in endemic areas due to limited resources and infrastructure required for mass vaccination programs (Martin et al. 2016), work is being undertaken to assess the suitability of dual typhoid and paratyphoid vaccines. Examples of these include combining recombinant Vi- and O:2-antigens or the CVD909 and CVD1902 live attenuated strains in an attempt to provide protection against both typhoid and paratyphoid fevers without confounding

the difficulties required to coordinate the administration of two separate vaccines (Martin et al. 2016).

1.15. Bacterial Secretion Systems

Bacteria have evolved many mechanisms to secrete proteins into their extracellular environment, which are not only used by pathogenic bacteria but also commensal species (Green & Mecsas 2016). As such, these secretion systems not only secrete proteins that interfere with, or manipulate cellular processes in eukaryotic and other prokaryotic cells, but also proteins involved in nutrient acquisition (Green & Mecsas 2016; Costa et al. 2015).

In this section, the following secretion systems of Gram-negative bacteria will be discussed: the general secretion (Sec) and twin arginine translocation (Tat) pathways, the type I secretion system (T1SS), type II secretion system (T2SS), type III secretion system (T3SS), type IV secretion system (T4SS), type V secretion system (T5SS) and type VI secretion system (T6SS) (Figure 1.3). The canonical features of each secretion system will be discussed and where appropriate, the features of the secretion system in *Salmonella* species will be highlighted, however, due to the nature of my project, the focus of this section will reside on the T3SS.

1.15.1. General Secretion Mechanisms

The Sec and Tat pathways are used to transport proteins across the cytoplasmic membrane and have been identified in bacteria, archaea and eukaryotes (Natale et al. 2008).

The Sec pathway translocates unfolded proteins into the bacterial periplasm, which are kept in a unfolded, translocation-competent state by the Sec chaperone, SecB (Driessen 2001). SecB delivers substrates to the ATPase, SecA, which hydrolyses ATP to power the translocation of substrates through the Sec translocase, composed of SecY, SecE and SecG, located in the bacterial plasma membrane (Figure 1.3) (Natale et al. 2008).

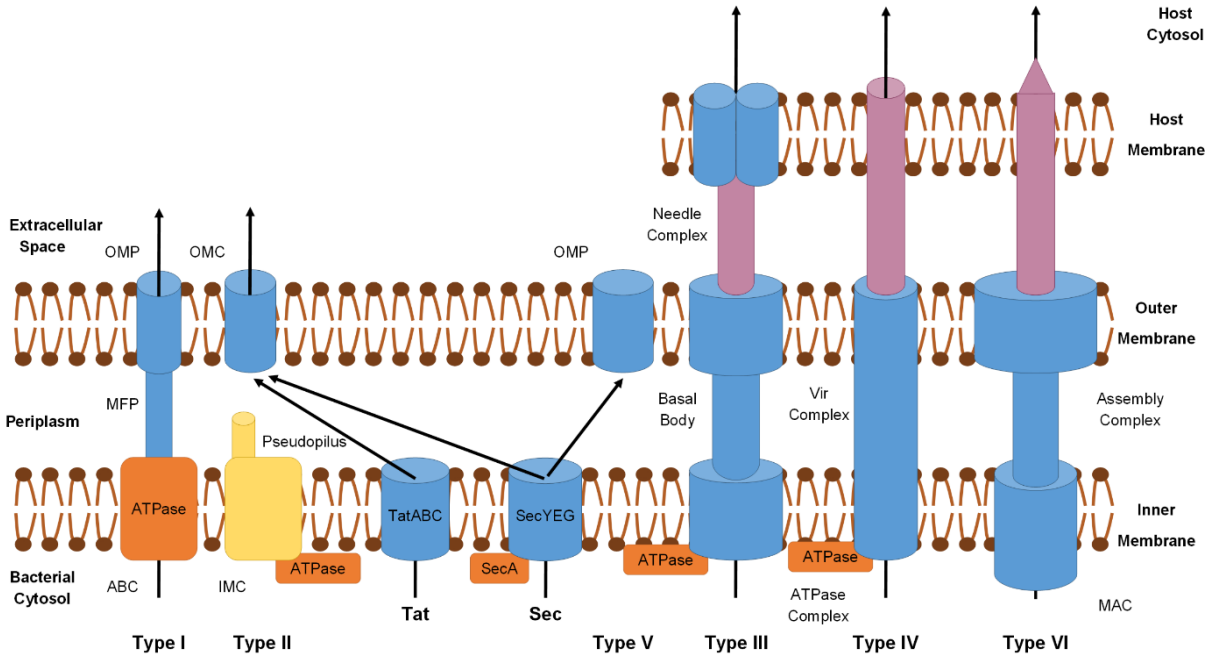


Figure 1.3. The secretion systems of Gram-negative bacteria. A schematic showing the known Gram-negative secretion systems. Arrows show the direction of protein transport. Abbreviations are as follows: ATP-binding cassette, ABC; membrane-fusion protein, MFP; outer-membrane pore, OMP; inner-membrane complex, IMC; outer-membrane complex, OMC; membrane-associated complex, MAC. ATPase components are shown in orange, secretion apparatus in blue and translocons in purple. See text for details. Adapted from (Green & Mecsas 2016; Tseng et al. 2009).

The Tat pathway secretes folded proteins into the periplasm through the Tat translocase in the bacterial plasma membrane, consisting of TatA, TatB and TatC and is powered by a difference in proton motive force between the cytoplasm and periplasm (Figure 1.3) (Natale et al. 2008).

Proteins secreted by the Sec and Tat pathways require secretion sequences. For the Sec pathway, the secretion sequence is a 20 amino acid, N-terminal signal sequence consisting of three regions: an amino-terminal region, a hydrophobic middle region and a polar region (Natale et al. 2008). This is bound by SecB and cleaved from the substrate by a periplasmic, membrane-anchored signal peptidase following translocation (Natale et al. 2008). Tat signal sequences are also N-terminal and share the same three regions as Sec secretion signals, but tend to be longer and must contain the consensus amino acid sequence of

S/T-**R**-**R**-x-F-L-K before the hydrophobic region (Berks 1996). The Tat signal sequence is also cleaved following translocation (Natale et al. 2008).

The Sec secretion system is required for secretion of the typhoid toxin into the periplasm in *S.* Typhi (Haghjoo & Galán 2004). Once in the periplasm, the typhoid toxin secretion protein (Tts) A facilitates secretion of the toxin across the outer bacterial membrane (Hodak & Galán 2013). The Tat secretion system has been demonstrated to be required for the virulence of several pathogenic bacterial species including *S.* Typhimurium, where it is essential for maintaining the integrity of the bacterial envelope (Craig et al. 2013), as well as, *P. aeruginosa* (Ochsner et al. 2002) and enterohaemorrhagic *E. coli* (EHEC) (Pradel et al. 2003).

1.15.2. Type I Secretion System

The T1SS consists of three proteins: an ABC transporter, a membrane fusion protein (MFP) and an outer membrane protein (OMP) (Figure 1.3) (Thomas et al. 2014). This multiprotein complex is used to transport a range of proteins, up to 900 kDa in size, directly from the bacterial cytoplasm, through the periplasm, into the extracellular space (Thomas et al. 2014). The T1SS was identified, and has been best studied in uropathogenic *E. coli* (UPEC) where it is required for the secretion of the HlyA toxin, but T1SSs have been identified in other pathogenic bacteria (Thomas et al. 2014). In *Salmonella,* there are two T1SSs, one encoded by *SPI-4*, which is required for the secretion of SiiE, an adhesion molecule essential for *SPI-1* T3SS-independent invasion in *S.* Typhimurium (Gerlach et al. 2008), however, SiiE is a pseudogene in *S.* Typhi (Sabbagh et al. 2010). The second T1SS is encoded by *SPI-9* which is also thought to be required for the secretion of a putative adhesion protein (Velasquez et al. 2016).

The SiiE T1SS is the most well understood T1SS in *Salmonella* and will be used here as an example for how T1SSs function. The ABC transporter, SiiF, forms a complex with the MFP, SiiD, which connects the bacterial inner membrane with the OMP, SiiC, that forms a pore in the outer-membrane (Thomas et al. 2014; Green & Mecsas 2016; Wille et al. 2014). The ABC

transporter recognises substrates via a C-terminal secretion signal and then hydrolyses ATP to allow the secretion of unfolded substrates through the periplasm and into the extracellular space (Thomas et al. 2014).

1.15.3. Type II Secretion System

The T2SS is evolutionarily related to the Type IV pilus, the archaeal flagellum and the transformation system found in Gram-positive bacteria (Korotkov et al. 2012). Composed of 12-15 proteins, the T2SS can be divided into four sub-complexes: the pseudopilus, the outer-membrane complex (OMC), the inner-membrane complex (IMC) and the ATPase (Figure 1.3) (Korotkov et al. 2012). The IMC resides in the bacterial inner-membrane and interacts with the other three sub-complexes to control secretion of substrates from the periplasm (Korotkov et al. 2012). Proteins secreted into the periplasmic lumen by either the Sec or Tat secretion pathways are allowed to fold, and are then recognised by the secretin, which comprises the majority of the OMC, and the end of the retracted pseudopilus; found on the periplasmic side of the inner membrane (Korotkov et al. 2012). This interaction causes a conformational change in the ATPase, which is associated with the IMC but resides in the bacterial cytosol, resulting in its activation and hydrolysis of ATP (Korotkov et al. 2012). This allows the pseudopilus to polymerise and push the substrate protein through a pore in the OMC into the extracellular space (Korotkov et al. 2012).

The T2SS is used to secrete a range of varying substrates from the periplasm and has been found in both pathogenic and non-pathogenic bacteria (Korotkov et al. 2012). The T2SS has not been demonstrated to be required for virulence of *Salmonella* but has been shown to be required for *Legionella pneumophila* and *Yersinia enterocolitica* virulence (Rossier et al. 2004; Iwobi et al. 2003).

1.15.4. Type IV Secretion System

There are three main types of T4SS: conjugative T4SSs, found in Gram-positive and Gram-negative bacteria and used for the exchange of DNA between bacteria; transformation

T4SSs, found in *Helicobacter pylori* and *Neisseria gonorrhoeae* and used to take up or secrete DNA into the extracellular environment; and protein secretion T4SSs, found in pathogenic bacteria such as *H. pylori*, *Bordetella pertussis* and *L. pneumophila* and used to translocate virulence proteins into host cells (Wallden et al. 2010).

The best characterised T4SS is the VirB conjugative T4SS found in *Agrobacterium tumefaciens* and is made up of 12 proteins VirB1-11 and VirD4 (Wallden et al. 2010), most of which are involved in the formation of a cylindrical tube that spans the periplasm providing a channel for protein or DNA transport (Figure 1.3) (Wallden et al. 2010). VirD4 recognises substrates and then transfers them onto the ATPase complex (Green & Mecsas 2016), which is located on the cytoplasmic side of the inner membrane, and hydrolyses ATP to power the translocation of substrates across the periplasm (Wallden et al. 2010). Another example of a T4SS is the Dot/Icm T4SS of *L. pneumophila* used to translocate virulence proteins into eukaryotic cells (Wallden et al. 2010). T4SSs involved in DNA secretion and translocation, such as the VirB T4SS, use a pilus to transport DNA in and out of the cell, but the exact mechanism of how the pilus is involved, still remains to be elucidated (Wallden et al. 2010; Green & Mecsas 2016).

The Dot/Icm T4SS in *L. pneumophila* is required for the translocation of around 200 effector proteins, required for invasion and intracellular replication and contain a C-terminal secretion signal (Green & Mecsas 2016). *S.* Typhi encodes a putative T4SS on *SPI-7* which is absent in *S.* Typhimurium, and is thought to be involved in the transfer of genomic islands (Juhas et al. 2007) and would therefore be more similar to a conjugative T4SSs, than a protein secretion T4SS.

1.15.5. Type V Secretion System

The T5SS is used to transport proteins across the outer membrane that have previously been secreted into the bacterial periplasm by the Sec pathway (Figure 1.3). The T5SS is used to

describe a family of proteins that are divided into three types: type Va (T5aSS), type Vb (T5bSS) and type Vc (T5cSS).

The majority of proteins secreted by the T5SS are secreted in the autotransporter fashion, also known as the T5aSS (Green & Mecsas 2016). These proteins are able to transport themselves across the bacterial outer membrane and have three or four modular domains: a C-terminal translocator domain, forms a β-barrel-based pore in the outer-membrane through which the protein will be secreted; a passenger domain, containing the functional portion of the protein; a linker domain, connecting the translocator and passenger domains; and in some cases a protease domain to cleave the passenger domain after secretion (Green & Mecsas 2016). These proteins also contain a signal sequence required for Sec secretion into the periplasm, which is cleaved following translocation. The *Salmonella* proteins MisL and SdhA are secreted by this autotransporter mechanism and are involved in intestinal colonisation during *S.* Typhimurium infection of mice (Dorsey et al. 2005; Kingsley et al. 2003). Both of these proteins are pseudogenes in *S.* Typhi, suggesting that they are not required for *S.* Typhi infection of humans (Sabbagh et al. 2010).

The T5bSS is also known as two-partner secretion and involves two proteins: one to form the β-barrel-based pore in the outer-membrane and the other is the protein to be secreted (Green & Mecsas 2016). The secretion of the High Molecular Weight (HMW) adhesins of *Haemophilus influenzae* are secreted through the outer membrane by HMW1B, which forms a pore in the outer membrane and recognises the HMW adhesins via a pro-peptide revealed after the cleavage of the Sec secretion signal (McCann & St. Geme 2014).

The T5cSS involves a trimer of proteins that oligomerise and a part of each protein contributes to the formation of a functional β-barrel pore in the bacterial outer membrane (Tseng et al. 2009). Once the pore is formed, the remaining portion of the proteins are secreted through the pore lumen (Tseng et al. 2009). The SadA protein of *S.* Typhimurium is secreted in a T5cSS fashion, and has been demonstrated to be involved in biofilm formation, as well as cellular adhesion during infection (Raghunathan et al. 2011).

1.15.6. Type VI Secretion System

The T6SS is used to translocate effector proteins across the bacterial inner and outer membranes into both eukaryotic and prokaryotic hosts and was first identified in *Vibrio cholerae* (Williams et al. 1996). The overall architecture can be broadly divided into a membrane-associated complex (MAC), thought to anchor the T6SS to the bacterial cell wall (Silverman & Brunet 2012), and an assembly complex, which is similar to an inverted T4 bacteriophage tail, that is surrounded by a sheath and through which effector proteins may travel into the host cell (Figure 1.3) (Russell et al. 2014). It is thought that the contraction of the sheath provides the energy required to translocate effector proteins into host cells (Russell et al. 2014).

Many of the proteins secreted by the T6SS are toxins demonstrated to be involved in competition between different bacterial species, but some of these proteins are designed to target eukaryotic cells (Russell et al. 2014). *S.* Typhi and *S.* Typhimurium encode a T6SS in the *sci* operon of *SPI-6,* and has been demonstrated to play a role in *S.* Typhimurium replication and survival in both mice and macrophage cell lines (Liu et al. 2013), suggesting that the T6SS in *Salmonella* may be involved in bacterial-host interaction.

1.15.7. Type III Secretion System

The T3SS has similarity to the flagellum apparatus (Diepold & Wagner 2014), and was first discovered in *Y. enterocolitica* as being required for the translocation of Yop proteins into host cells (Michiels et al. 1991). Since this finding, T3SSs have been identified in other species including *Salmonella*, *Shigella flexneri* and pathogenic *E. coli*, amongst others (Notti & Stebbins 2016). *S. enterica* serovars encode two T3SSs, located on pathogenicity islands, both of which are required for virulence. The invasion (*inv*) operon, which is located within *SPI-1* was originally identified as being required for *S.* Typhimurium invasion of cultured epithelial cells in 1989 (Galán & Curtiss 1989) and was not identified as forming a multiprotein complex until 1994 (Ginocchio et al. 1994). The *SPI-2* T3SS was identified in 1996 by

signature-tagged mutagenesis (STM) and was demonstrated to be required for virulence of *S.* Typhimurium in mice (Shea et al. 1996). The *SPI-1* and *SPI-2* T3SSs of *Salmonella* are each composed of more than 20 individual proteins, but the structures can be generally described as being composed of two sections: the basal body, which spans the inner and outer bacterial membranes and includes the export apparatus and secretin, and the needle complex, which extends from the bacterial cell surface and contacts the host cell membrane via a translocation pore (Figure 1.3 and Figure 1.4) (Costa et al. 2015).

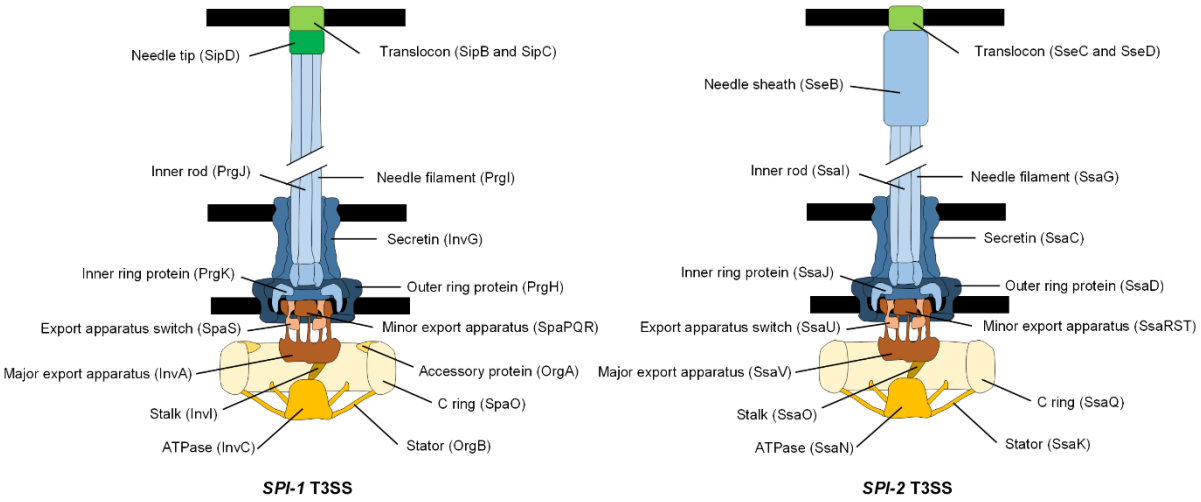


Figure 1.4 The T3SSs of *Salmonella*. A schematic showing the *SPI-1* and *SPI-2* T3SSs of *Salmonella*. See text for details. Adapted from (Diepold & Wagner 2014).

1.15.7.1. Assembly of the T3SS

The assembly of the Salmonella T3SS will be described using the *SPI-1* T3SS as an example, but the process is believed to be similar for the assembly of the *SPI-2* T3SS.

Formation of the T3SS begins with SpaP and SpaR recruiting SpaQ and SpaS to the bacterial inner membrane, where PrgH and PrgK are then recruited, to form the export apparatus (Wagner et al. 2010). The major export apparatus, InvA, is thought to be recruited at the same time as PrgH and PrgK, although it is not essential for formation of the export apparatus (Diepold & Wagner 2014). InvG, is secreted from the bacterial cytoplasm by the Sec pathway (Burkinshaw & Strynadka 2014), and oligomerises to form the secretin, in a process requiring

the pilotin, InvH (Daefler & Russel 1998). SpaO, OrgB, OrgA self-assemble into the sorting complex, along with the ATPase, InvC, in the cytosol and then attach to the export apparatus (Lara-Tejero et al. 2011). The function of the sorting-complex is to ensure that the translocon proteins, *Salmonella* invasion protein (Sip) B, SipC and SipD, are secreted before the effector proteins, but after the needle has been fully assembled (Lara-Tejero et al. 2011).

Once the basal body has been completed, the needle complex can then be assembled. The inner rod is a polymer consisting of PrgJ subunits which spans the periplasm and connects the inner membrane ring of the basal body to the secretin (Marlovits et al. 2004). The needle filament attaches to the inner rod and is 80 nm in length and 13 nm in width and is formed by the polymerisation of PrgI (Kubori et al. 1998). The method by which the length of the T3SS needle is controlled is still under debate, but currently there are two theories (Diepold & Wagner 2014). The “ruler model” suggests that the inner rod protein directly samples the length of the T3SS needle during elongation, until the correct needle length is achieved (Journet et al. 2003). The second model states that whilst PrgJ is polymerising to form the inner rod, PrgI is free to polymerise into the needle filament, but once the inner rod is complete, the needle filament stops polymerising and the T3SS is complete (Marlovits et al. 2006). In both models, the inner rod protein does control the final length of the needle filament, but differ in how this is exactly achieved. Although there is evidence to support both theories, there is currently no consensus answer for how the needle filament length is controlled.

Once the needle filament is formed, the cytoplasmic gatekeeper protein, InvE, is displaced allowing secretion of the translocon proteins which form a pore in the host cell membrane and subsequent translocation of effector proteins (Lara-Tejero et al. 2011).

One major difference between the *SPI-1* and *SPI-2* T3SS is the presence of a sheath, composed of SseB, SseC and SseD, at the end of the needle within the *SPI-2* T3SS that eventually forms the translocon pore in the *Salmonella*-containing vacuole (SCV) membrane, which surrounds replicating *Salmonellae* inside host cells, to allow effector protein translocation (Chakravortty et al. 2005).

1.15.7.2. T3SS chaperones

For the T3SS to assemble correctly and to perform secretion, there are many small proteins, called chaperones, that reside in the bacterial cytosol and maintain T3SS effector proteins and structural components in a secretion-competent state (Thomas et al. 2012). These chaperones have no conserved sequence but can be categorised according to what proteins they bind to.

Class I chaperones bind to T3SS effector proteins and are subdivided into Class IA or Class IB (Lohou et al. 2013). Class IA chaperones bind to only one specific effector (Lohou et al. 2013), and includes SicP, which binds to SptP (Stebbins & Galán 2001), and SigE, which binds to *Salmonella* outer protein (Sop) B (Luo et al. 2001). Class IB chaperones bind multiple effectors, and include InvB, which interacts with SipA (Bronstein et al. 2000), SopE (Lee & Galán 2003; Ehrbar et al. 2003), SopE2 (Ehrbar et al. 2003) and SopA (Ehrbar et al. 2004), as well as SrcA, which interacts with the SseL and PipB2 effector proteins (Cooper et al. 2010).

Class II chaperones bind to components of the T3SS translocon, such as SscA, which interacts with SseC (Cooper et al. 2013), and SicA, which binds to SipB and SipC (Tucker & Galán 2000). Class III chaperones bind to components of the flagellar T3SS (Lohou et al. 2013), as well as the T3SS needle proteins (Burkinshaw & Strynadka 2014), however no chaperone for the needle proteins of the *SPI-1* or *SPI-2* T3SSs have been identified in *Salmonella*.

These chaperones bind to a region in the N-terminus of these proteins that is located within the first 50-100 amino acids (Stebbins & Galán 2001; Lilic et al. 2006) after the secretion signal which is located within the first 15 amino acids (Lloyd et al. 2001; Ehrbar et al. 2003). Unlike the secretion signals of the general secretion pathways, the T3SS effector secretion signal has no known consensus sequence (Tobe et al. 2006).

1.15.7.3. Regulation of the T3SSs in *Salmonella*

As the T3SS is essential for virulence but is energetically costly and immunogenic, both the *SPI-1* and *SPI-2* T3SSs are under strict environmental regulation (Figure 1.5).

The regulation of the *SPI-1* T3SS is complex but converges on the transcription regulators of the hyper invasion locus (Hil), HilA, HilC and HilD (Fàbrega & Vila 2013). The *hilA*, *hilC* and *hilD* genes are encoded within *SPI-1* and activate the expression of *SPI-1* genes (Bajaj et al. 1995; Schechter et al. 1999). HilD is the main regulator, but works cooperatively with HilC or the regulator of *SPI-1* (Rts) A, a non-*SPI-1*-encoded transcriptional regulator (Cott Chubiz et al. 2010), to induce the expression of *hilA* (Ellermeier et al. 2005; Ellermeier & Slauch 2003).

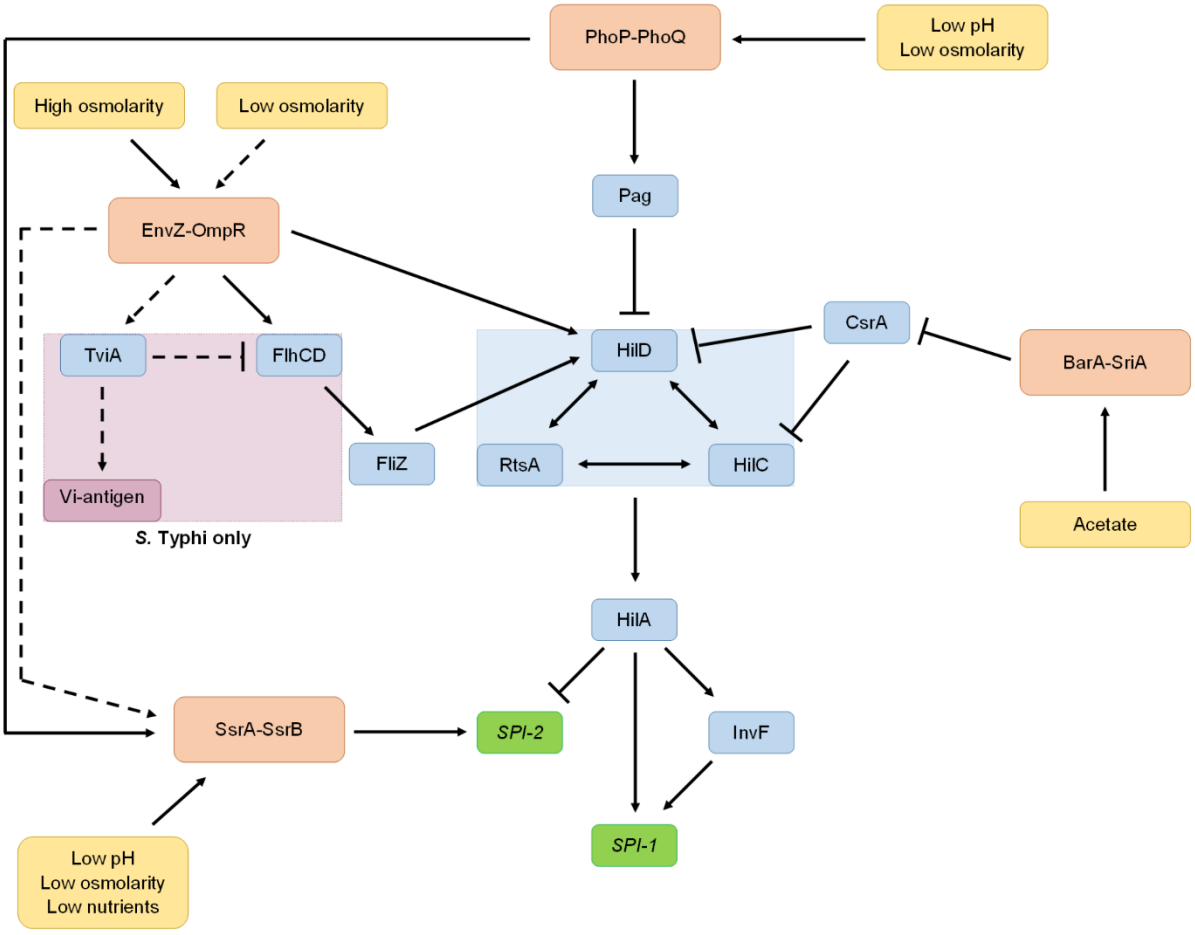


Figure 1.5. Regulation of *SPI-1* and *SPI-2*. A schematic representation of the pathways involved in regulating the expression of *SPI-1* and *SPI-2* in *Salmonella*. Environmental stimuli are shown in yellow, two-component regulatory systems are shown in orange, regulatory proteins are shown in blue, *SPIs* are shown in green and other virulence factors in purple. When a two-component system is capable of responding to opposing environmental stimuli, these are differentiated using solid and dashed arrows. See text for details. Adapted from (Winter et al. 2009; Fàbrega & Vila 2013).

Once expressed, HilA directly induces expression of several genes within *SPI-1* including those required for a functional *SPI-1* T3SS (Bajaj et al. 1996) and effector proteins (Thijs et al. 2007), as well as inducing the expression of another transcription regulator, *invF*, by binding to their promoters within the *SPI-1* operon (Bajaj et al. 1996). InvF then induces expression of T3SS effector chaperones and further effector proteins (Darwin et al. 1999) by binding to their promoters within the *SPI-1* operon and activating their expression (Bajaj et al. 1996). HilA also inhibits the assembly of the *SPI-2* T3SS, by binding to the promoters of *SPI-2* T3SS genes and preventing their expression during invasion (Thijs et al. 2007).

HilD is regulated by several two-component systems that respond to environmental stimuli. The PhoQ-PhoP two-component system is activated by low nutrient levels (Garcia Vescovi et al. 1996) and low pH (Foster & Hall 1990), as has been shown to occur inside the SCV (Garcia-del Portillo et al. 1992; Rathman & Sjaastad 1996). Once activated, PhoP activates the expression of PhoP-activated gene (Pag) proteins (Belden & Miller 1994) which act on the HilD protein to prevent *hilA* expression (Boddicker et al. 2003) therefore repressing the expression of *SPI-1* genes (Pegues et al. 1995). The BarA-SirA two-component system is activated by acetate (Chavez et al. 2010), a metabolite that is found in high abundance in the mammalian intestine, and once activated reduces the expression of carbon storage regulator (*csr*) A (Lawhon et al. 2002). CsrA itself inhibits *hilA* expression through degradation of the *hilC* and *hilD* mRNA, therefore preventing expression of *SPI-1* T3SS structural components and effector proteins (Altier et al. 2000; Ahmer et al. 1999). The EnvZ-OmpR two-component system detects extracellular osmolarity (Hall & Silhavy 1981) and once activated results in the post-transcriptional activation of HilD, which in turn induces expression of *hilA* (Ellermeier et al. 2005) under high osmolarity (Bajaj et al. 1996). Overall, these two-component systems ensure that the *SPI-1* T3SS and its associated effector proteins are only expressed when the extracellular environment is optimal: high osmolarity, neutral pH and in the presence of specific metabolites, as found in the intestinal lumen (Bajaj et al. 1996; Lawhon et al. 2002).

S. Typhi also has another level of regulation over the *SPI-1* T3SS in the form of the *viaA* and *viaB* loci of *SPI-7* (Winter et al. 2014). The Vi-antigen biosynthesis regulatory protein, TviA, induces Vi-antigen expression (Virlogeux et al. 1995), but also represses expression of *SPI-1* T3SS structural genes and effector proteins, until *S.* Typhi is ready to invade the intestinal epithelium (Winter et al. 2014). Under low osmolarity, EnvZ-OmpR activation results in an interaction between TviA and RcsB, which then bind to the promoter of the flagellar regulators, *flhDC*, inhibiting their expression and subsequently the expression of another flagellar regulator, *fliZ* (Winter et al. 2009). Under high osmolarity, FliZ activates the HilD protein, resulting in expression of *hilA* and therefore *SPI-1* genes (Cott Chubiz et al. 2010). This extra level of regulation ensures that the *S.* Typhi *SPI-1* T3SS, is not detected by the nucleotide-binding oligomerisation domain-containing protein (NOD)-like receptor family apoptosis inhibitory protein (NAIP) (Rayamajhi et al. 2013) within intestinal epithelial cells, and therefore preventing a pro-inflammatory response in the intestinal lumen that is characteristic of NTS serovars (Winter et al. 2014).

The *SPI-2* T3SS is only expressed once *Salmonellae* are intracellular (Cirillo et al. 1998) and within the SCV. This environmental sensing is controlled by two-component regulatory systems such as: EnvZ-OmpR, SsrA-SsrB and PhoQ-PhoP (Fàbrega & Vila 2013) which respond to low osmolarity, nutrient levels (Garcia-del Portillo et al. 1992) and low pH (Rathman & Sjaastad 1996) shown to occur inside the SCV (Cirillo et al. 1998). As previously mentioned, the EnvZ-OmpR system detects extracellular osmolarity (Hall & Silhavy 1981) and under low osmolarity induces the expression of *ssrA* and *ssrB* (Feng et al. 2003). SsrA-SsrB is another two-component response system which is located within *SPI-2* itself (Cirillo et al. 1998) and is activated by low nutrient levels, low osmolarity and acidic pH (Garmendia et al. 2003). Once activated SsrA-SsrB induces the expression of the *SPI-2* T3SS and associated effector proteins through interactions with promoters of genes within *SPI-2* (Garmendia et al. 2003). PhoQ-PhoP is activated by low nutrient levels (Garcia Vescovi et al. 1996) and low pH (Foster

& Hall 1990) and results in the expression of *ssrB* (Bijlsma & Groisman 2005), thus feeding back into the SsrA-B two-component system activation.

Once the *SPI-2* T3SS is expressed and assembled, it will not translocate any effector proteins until the neutral pH of the host cell cytosol causes a complex of three *SPI-2* T3SS proteins, SsaM, SpiC and SsaL, to dissociate from the export apparatus (Yu et al. 2010). However, how the pH of the host cell cytosol outside of the SCV is detected and this signal transmitted to the T3SS proteins is not known (Yu et al. 2010). This demonstrates that the *SPI-2* T3SS is regulated at both the transcriptional and post-translational level to ensure that its activity remains tightly controlled.

The interplay in regulation of both the *SPI-1* and *SPI-2* T3SSs ensure that once *Salmonellae* are intracellular, the *SPI-1* T3SS is down-regulated, due to reduced HilA expression in response to low osmolarity (Ellermeier et al. 2005), reduced nutrient levels, pH (Boddicker et al. 2003) and metabolites (Altier et al. 2000; Ahmer et al. 1999; Lawhon et al. 2002) inside the SCV to prevent cell apoptosis (Hersh et al. 1999). The *SPI-2* T3SS is then up-regulated in response to these same environmental stimuli (Garcia-del Portillo et al. 1992) enabling intracellular survival (Ochman et al. 1996). These environmental stimuli that differentially affect the expression of the *SPI-1* and *SPI-2* T3SSs, and their respective effectors, are largely sensed by the two component systems, EnvZ-OmpR and PhoP-PhoQ, but it is the downstream signalling proteins, as well as the other two component systems, BarA-SirA and SsrA-SsrB, that result in the differing outcome in expression of the two T3SSs (Fàbrega & Vila 2013).

1.16. T3SS Effector Proteins and Manipulation of the Host Cell by *Salmonella*

Salmonella uses the *SPI-1* and *SPI-2* T3SSs to translocate over 40 effector proteins (Appendix 1), with a variety of enzymatic activities and functions, into host cells (LaRock et al. 2015). Broadly, the effector proteins translocated by the *SPI-1* T3SS are involved in the invasion of non-phagocytic host cells and initial formation of the SCV, whereas those translocated across the SCV membrane by the *SPI-2* T3SS are required for intracellular survival and replication (Figure 1.6) (LaRock et al. 2015). However, more recent work has shown that this is an oversimplified view and that *SPI-1* effectors can influence *Salmonella* replication and survival. In this section I will broadly discuss the effectors concerned with invasion of host cells, formation of a replicative niche and subversion of the host innate immune system.

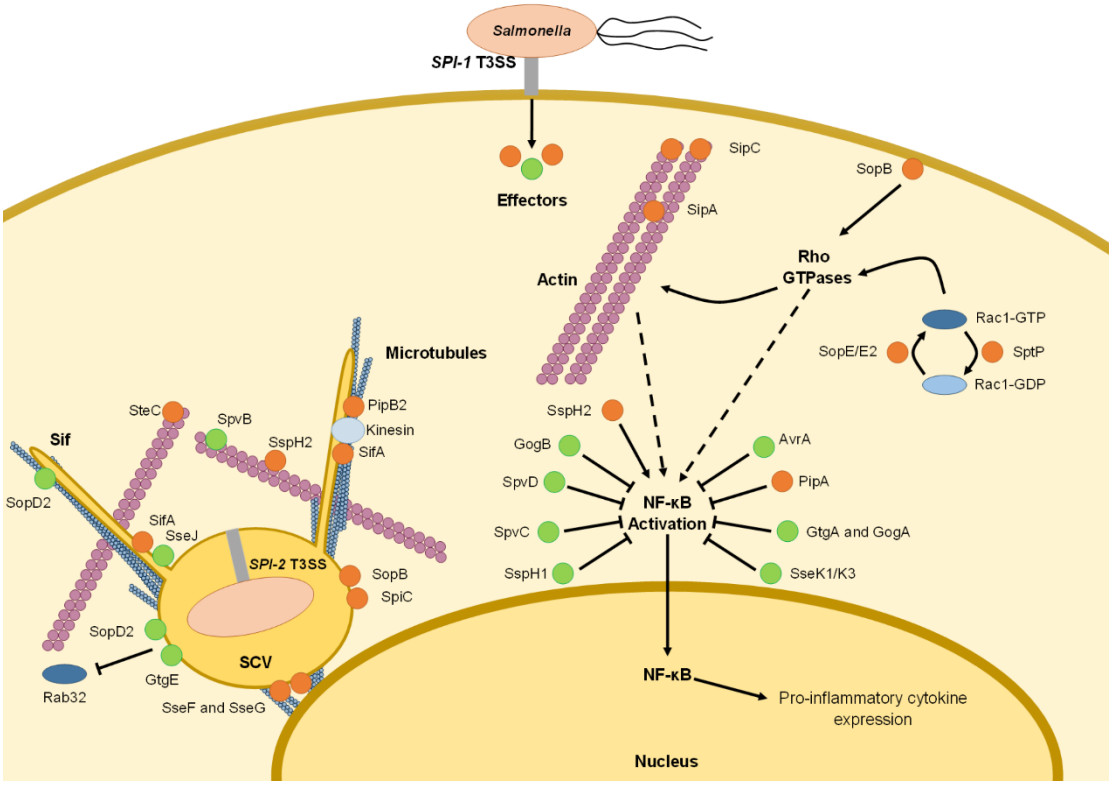


Figure 1.6. *Salmonella* T3SS effectors involved in invasion, replication and subversion of the host innate immune system. A schematic showing the prominent effector proteins involved in manipulating the host cell to allow *Salmonella* to invade, replicate and survive within the host. See text for details. Effectors in green are absent or pseudogenes in *S.* Typhi. Adapted from (LaRock et al. 2015).

1.16.1. Invasion of Non-Phagocytic Host Cells

SopE and SopE2 are guanine nucleotide exchange factors (GEFs) that directly activate the host Rho family GTPases, Cdc42 and Rac1 (Friebel et al. 2001). SopB is an inositol phosphate phosphatase that indirectly activates Cdc42 by production of the inositol tetra-phosphate (Zhou et al. 2001). The concomitant activity of SopE, SopE2 and SopB activates Rho GTPases causing actin rearrangement within non-phagocytic cells and leads to plasma membrane ruffling, which allows bacterial internalisation (Hardt et al. 1998; Zhou et al. 2001). SipA and SipC are actin-binding proteins that inhibit actin depolymerisation (Zhou et al. 1999) and increase actin bundle formation, respectively (Hayward & Koronakis 1999), to extend the plasma membrane ruffles initially formed by the action of SopE, SopE2 and SopB on actin (Zhou et al. 1999).

Once internalised, SptP, a GTPase-activating protein (GAP), activates the GTP hydrolysis activity of Cdc42 and Rac1 resulting in their inactivation (Fu & Galán 1999). SopE is also rapidly degraded by the proteasome after translocation (Kubori et al. 2003). The degradation of SopE and the antagonistic activity of SptP, work to ensure that the host cell cytoskeleton is restored to its normal state, following bacterial internalisation (Fu & Galán 1999; Kubori et al. 2003; Johnson et al. 2017).

1.16.2. Formation of a Replicative Niche

The membrane-ruffling induced during invasion forms the initial SCV encapsulating *Salmonellae* (Friebel et al. 2001), before it buds off from the inner surface of the host plasma membrane due to action of SopB and SopD (Hernandez et al. 2003; Bakowski et al. 2007). SopB then undergoes ubiquitination by a host E3 ubiquitin-ligase, causing it to relocate from the host plasma membrane to the surface of the SCV (Patel et al. 2009) where it prevents fusion with lysosomes (Bakowski et al. 2010). The *SPI-2* T3SS effector SpiC is thought to aid SopB in this activity by disrupting the host endocytic pathway (Shotland et al. 2003).

As the SCV matures it migrates towards the perinuclear region of the host cell, close to the Golgi apparatus (Deiwick et al. 2006), to allow the bacteria to obtain nutrients and replicate (Ramsden et al. 2007). This relocation is thought to involve SopB-mediated activation of the actin-based motor protein, myosin (Wasylnka et al. 2008), as well as SipA, which persists on the SCV surface after internalisation (Brawn et al. 2007). Once perinuclear, the two *SPI-2* effectors, SseF and SseG, interact with each other on the surface of the SCV (Deiwick et al. 2006), and anchor the SCV in the perinuclear region by interacting with microtubules (Kuhle et al. 2004). SseF and SseG have also been demonstrated to redirect host vesicles towards the SCV, which may provide the replicating bacteria with nutrients and membranes (Kuhle et al. 2006).

The *SPI-2* T3SS effector, SseJ localises to the SCV after translocation (Freeman et al. 2003) and catalyses the esterification of cholesterol at the SCV membrane (Christen et al. 2009), which is thought to recruit another *SPI-2* effector, SifA, to the SCV (Figueira & Holden 2012; LaRock et al. 2015). SifA interacts with the host microtubule network (Boucrot et al. 2005) and along with SseJ, induces the formation of *Salmonella*-induced filaments (Sifs) and maintains the integrity of the SCV membrane (Beuzón et al. 2000; Ohlson et al. 2008). PipB2 and SifA recruit the microtubule motor protein, kinesin, to the SCV which then acts to enable Sif extension along the microtubule network (Boucrot et al. 2005; Henry et al. 2006; Knodler & Steele-Mortimer 2005). SopD2 prevents Sif formation and the interplay between SifA, PipB2 and SopD2 may act to ensure that the optimal environment is maintained within the SCV to allow bacterial replication (Schroeder et al. 2010).

Actin is deposited around the SCV during *Salmonella* infection (Méresse et al. 2001) and this has been demonstrated to control bacterial replication (Lesnick et al. 2001; Odendall et al. 2012). This actin deposition is regulated by three *SPI-2* effectors: SteC, a kinase that stimulates actin remodelling and deposition (Odendall et al. 2012), SpvB, an ADP-ribosyltransferase, and SspH2, an E3 ubiquitin-ligase, both of which inhibit actin polymerisation (Lesnick et al. 2001; Miao et al. 2003).

The E3 ubiquitin-ligase SopA (Diao et al. 2008), is a *SPI-1* T3SS effector and its degradation has been demonstrated to promote bacterial escape from the SCV (Zhang et al. 2005) which may be involved in the eventual spread of *Salmonella* between host cells, although this has yet to be characterised.

1.16.3. Subversion of the Innate Immune System

Salmonella is recognised by the host cell through several innate immune receptors. TLR4 detects bacterial LPS (Royle et al. 2003), TLR5 recognises bacterial flagellin (Hayashi et al. 2001), and NAIP proteins detect the T3SS itself (Rayamajhi et al. 2013), all resulting in the release of pro-inflammatory cytokines such as tumour necrosis factor alpha (TNFα), and interleukins (IL)-1β, IL-6, IL-8 and IL-18, which cause intestinal inflammation (Keestra-Gounder et al. 2015). Although NTS serovars require an inflammatory response to outcompete the intestinal microbiota and colonise the gut (Stecher et al. 2007), this must be controlled, through the activities of several T3SS effectors, to ensure that *Salmonellae* can maintain a suitable environment for survival.

The *SPI-1* effector proteins SipA, SopA, SopB, SopD and SopE2 induce fluid secretion, a marker of inflammation, during *S.* Typhimurium infection of bovine ligated ileal loop (Zhang et al. 2002), which is thought to be a consequence of their role in actin rearrangement during invasion (Keestra et al. 2013). SspH2 can also increase pro-inflammatory cytokine secretion by ubiquitinating NOD1, a host immune receptor involved in recognising pathogen signals and stimulating a pro-inflammatory response (Bhavsar et al. 2013). The *SPI-1* T3SS translocon protein, SipB also induces autophagy and cell death in macrophages through interfering with host mitochondria (Hernandez et al. 2003).

By reversing the actin remodelling required for invasion, SptP also down-regulates the expression of TNFα (Lin et al. 2003), as well as the expression and secretion of IL-8 through the NF-κB pathway caused by these alterations (Murli et al. 2001). Multiple other effector proteins translocated by both the *SPI-1*, *SPI-2* or both, act on the NF-κB pathway to inhibit

pro-inflammatory cytokine expression and secretion including the deubiquitinase (DUB) AvrA (Ye et al. 2007), the E3 ubiquitin-ligase SspH1 (Haraga & Miller 2006), the phosphothreonine lyase, SpvC (Haneda et al. 2012), the F-box protein, GogB (Pilar et al. 2012), the proteases PipA, GtgA and GogA (Sun et al. 2016), the N-acetylglucosamine transferases SseK1 and SseK3 (Günster et al. 2017) and SpvD (Rolhion et al. 2016).

It should be noted that the study of the majority of these effectors has been performed in *S.* Typhimurium, and due to the different host specificity and disease outcome associated with *S.* Typhi, they may have different roles during *S.* Typhi infection, although this has yet to be substantially investigated.

1.16.4. Comparison of the Effector Repertoires of *S.* Typhimurium and *S.* Typhi

S. Typhi has undergone genome degradation and accumulated 145 pseudogenes, all of which are intact in *S.* Typhimurium (Parkhill et al. 2001). This gradual degradation is thought to have contributed to the host-specificity and disease outcome exhibited by *S.* Typhi (Parkhill et al. 2001), as several genes known to be involved in causing gastroenteritis in *S.* Typhimurium are pseudogenes in *S.* Typhi (McClelland et al. 2004).

Many T3SS effector proteins are absent or pseudogenes in *S.* Typhi: SopA, SopE2, GogA, GogB, SopD2, SseI, SseJ, SseK1, SseK2, SseK3, SpvB, GtgA, CigR, SrfJ, SlrP, AvrA, SspH1, SpvC, SpvD, SteB, SteE and GtgE (Appendix 1) (Figure 1.6) (Parkhill et al. 2001; Deng et al. 2003; Sabbagh et al. 2010). One *Salmonella* T3SS effector absent in *S.* Typhi, GtgE, has been linked with *S.* Typhi host restriction. This effector has been demonstrated to be involved in the proteolytic degradation of Rab29 and Rab32 (Spanò et al. 2011; Spanò & Galán 2012), two related proteins involved in lysosomal trafficking (Wang et al. 2014). By degrading Rab29 and Rab32, these proteins are not recruited to the *S.* Typhimurium SCV in murine macrophages, allowing *S.* Typhimurium to replicate (Spanò et al. 2011; Spanò & Galán 2012). When *S.* Typhi infects murine macrophages, Rab29 and Rab32 are recruited to the SCV and

restrict its replication, but this can be avoided by ectopically expressing GtgE in *S.* Typhi, which then allows it to replicate within murine macrophages and to survive during infection of mice, a non-permissive host (Spanò et al. 2011; Spanò & Galán 2012). It has also been shown that GtgE may work synergistically with the GAP, SopD2, also absent in *S.* Typhi, which also prevents Rab32 recruitment to the *S.* Typhimurium SCV (Spanò et al. 2016).

To date, much of the work to characterise *Salmonella* T3SS effector proteins has been performed using *S.* Typhimurium and these findings have then been applied to *S.* Typhi with the assumption that they perform the same role. However, we have recently shown that SptP in *S.* Typhi is not involved in reformation of the host cytoskeleton after *S.* Typhi invasion and this is thought to be due to decreased stability of *S.* Typhi SptP caused by mutations in its chaperone-binding domain (Johnson et al. 2017) (entire article can be found in Appendix 2). This finding suggests that *S*. Typhi may have another effector to antagonise the effects of SopE and SopB, allowing reformation of the host cytoskeleton. This work also showed that *S.* Typhi only requires SopE for invasion when grown under microaerobic conditions to stationary phase, whereas, *S.* Typhimurium requires SopE for invasion when grown under microaerobic conditions to stationary phase, as well as when grown under aerobic conditions to late exponential phase (Johnson et al. 2017). Overall, this work has shown that one T3SS effector identified in *S.* Typhimurium may be non-functional in *S.* Typhi, whilst another is only essential depending on the growth conditions of the bacteria. This work is supported by the findings of another study which suggests that the *Salmonella* T3SS effectors, SptP, SifA and SseF, as well as components of the *SPI-1* and *SPI-2* T3SS apparatus, SipD, SseC and SseD, have evolved differentially between human-restricted serovars, such as *S.* Typhi and *S.* Paratyphi A, compared to generalist serovars such as *S.* Typhimurium and *S.* Enteritidis and these differences may account for the different host ranges of the serovars (Eswarappa et al. 2008).

Whilst *S.* Typhi has accumulated many pseudogenes, it also has 601 genes not found in *S.* Typhimurium, accounting for approximately 13% of the genome (Parkhill et al. 2001). This

includes *SPI-7*, encoding the Vi-antigen biosynthetic enzymes (Pickard et al. 2003), and genes encoding components on the typhoid-toxin (Parkhill et al. 2001), both previously discussed. *S.* Typhi may also contain novel T3SS effectors that may enable *S.* Typhi to inhabit specific niches, such as the human gallbladder, which are not present in *S.* Typhimurium.

1.16.5. Identification of Novel Effector Proteins

Due to the lack of a consensus secretion signal or other identifiable features, identification of new T3SS effectors proteins is difficult (Tobe et al. 2006). Nevertheless, several different approaches have been used to date.

One method of identifying effectors is using sequence homology. SspH1 was found to be related to the IpaH family of T3SS effectors, from *S. flexneri* and YopM, from *Y. pestis*, and using the N-terminal DNA sequence of SspH1 as a probe, SspH2 was identified in the *S.* Typhimurium genome by southern blot analysis (Miao et al. 1999). The SspH1 DNA sequence was later used to identify three more T3SS effectors: SifA (Brumell et al. 2000), SseI and SseJ (Miao & Miller 2000).

Transposon-based methods have also been used. David Holden developed the technique of STM, where transposon (Tn) 5 is used to insert unique DNA sequence tags, at random, into the *S.* Typhimurium genome to create a pool of transposon mutants, each of which identifiable by PCR or southern blot using the unique DNA tag (Hensel et al. 1995). These mutants are then pooled, and used to infect mice, before harvesting the remaining bacteria from the spleen and identification (Hensel et al. 1995). By comparing the recovered transposon mutants to those used to infect the mice in the inoculum, several genes, including *invA* and *invG* were demonstrated to be essential for virulence (Hensel et al. 1995). This method was also used to identify the T3SS effector SlrP, another homologue of IpaH and YopM, shown to be essential for *S.* Typhimurium virulence in mice (Tsolis et al. 1999).

Geddes and colleagues also used Tn5 to create a transposon library in *S.* Typhimurium, but instead of inserting DNA tags, the adenylate cyclase toxin, CyaA, from *Bordetella pertussis*

was inserted within *S.* Typhimurium genes, creating translational fusions of the genes with the CyaA protein (Geddes et al. 2005). The CyaA protein acts as a reporter and upon translocation into eukaryotic cells, results in the accumulation of cyclic AMP (cAMP) which can be quantified (Sory & Cornelis 1994). In this way any proteins that have an in-frame CyaA fusion and are translocated during infection can be observed (Geddes et al. 2005; Sory & Cornelis 1994). Using this approach, the T3SS effectors SteA, SteB and SteC were identified (Geddes et al. 2005).

The increase in the use of proteomics in biological sciences has also aided in the identification of novel effector proteins. By using liquid chromatography coupled to tandem mass spectroscopy (LC-MS/MS), Niemann and coworkers identified six T3SS effector proteins SpvD, GtgA, GtgE, CigR, SteD and SteE, from the secreted fraction of *S.* Typhimurium that had been grown under *SPI-2*-inducing conditions (Niemann et al. 2011).

With the amassing number of bacterial genomes now available, bioinformatic approaches have also been developed. These methods use sequence homology, similar to the approaches used to identify SspH1 and SspH2 (Miao et al. 1999), but instead of using a DNA probe to screen a target genome by southern blot analysis, computers are used to screen a target genome using the sequences of known effectors from other bacteria. In EHEC, the genome of the O157:H7 Sakai strain was screened for novel T3SS effector proteins using the sequences of over 300 known effectors from various human and plant bacterial pathogens (Tobe et al. 2006). This was then combined with a proteomics-based approach similar to that used by Niemann and colleagues described above (Niemann et al. 2011), and resulted in the identification of 28 translocated effector proteins that were then confirmed experimentally (Tobe et al. 2006). More complex bioinformatic approaches have also been used such as genome-wide machine-learning which was first used in 2009 to identify 40 novel T4SS effector proteins in *L. pneumophila* (Burstein et al. 2009). Putative effectors were identified based on several features including: guanine-cytosine content (%GC), as effectors often have a %GC that differs from surrounding genes due to horizontal gene transfer; sequence similarity to

known effectors or eukaryotic proteins; genome organisation; and the presence of a C-terminal secretion sequence found in T4SS effectors (Burstein et al. 2009). The screen started with 53 known *L. pneumophila* T4SS effectors, which were then used to scan the *L. pneumophila* genome using an algorithm based on the features detailed above (Burstein et al. 2009). Out of a selected 15 predicted genes, 11 were confirmed using the CyaA system to be translocated by the T4SS during infection (Burstein et al. 2009). These 11 new effectors were then fed back into the computer algorithm to scan the genome again and 21 out of 25 predicted genes were confirmed to be T4SS effectors (Burstein et al. 2009). The process was then repeated a third time with the additional 21 effectors that they had identified, resulting in the identification and confirmation of a further eight T4SS effectors (Burstein et al. 2009). This method of continual genomic-based prediction and experimental validation has since been used to identify novel T4SS effectors in *Coxiella burnetti* (Lifshitz et al. 2014), as well as T3SS effectors in *P. aeruginosa* (Burstein et al. 2015) and *Xanthomonas euvesicatoria* (Teper et al. 2016).

To date, none of these approaches have been used in *S.* Typhi, to identify *S.* Typhi-specific T3SS effector proteins.

1.17. The Ubiquitination System

Ubiquitination is a key post-translational modification involved in a multitude of central processes in eukaryotic cells including: protein regulation and degradation, cell signalling, DNA repair and cell cycle control (Ashida et al. 2014). Ubiquitin itself is a small, 8.5 kDa conserved protein that is attached to a lysine residue of a protein substrate by a sequential enzymatic cascade involving three classes of enzymes: E1 ubiquitin-activating enzymes, E2 ubiquitin-conjugating enzymes and E3 ubiquitin-ligase enzymes (Figure 1.7) (Ashida et al. 2014).

The E1 ubiquitin-activating protein attaches ubiquitin to itself via a thioester bond between the C-terminal glycine of ubiquitin, and a cysteine residue within the E1 in a reaction powered by

ATP hydrolysis (Foot et al. 2017). Ubiquitin is then transferred to a cysteine residue within an E2 ubiquitin-conjugating protein, forming another thioester bond (Foot et al. 2017). The E2-ubiquitin complex is brought together with the substrate by the E3 ubiquitin-ligase protein and ubiquitin is transferred onto the substrate protein, forming an isopeptide bond between the C-terminal glycine of ubiquitin and the R group of a lysine residue within the substrate (Foot et al. 2017). The E3 ubiquitin-ligase protein acts to determine substrate-specificity and mediates the final transfer of ubiquitin onto the substrate differently, depending on the type of E3 ubiquitin-ligase present (Foot et al. 2017). The two main types of E3 ubiquitin-ligase proteins are the really interesting new gene (RING)/U-box-type and, the homologous to the E6-AP carboxyl terminus (HECT)-type. RING/U-box-type E3 ubiquitin-ligases transfer ubiquitin directly from the E2 ubiquitin-conjugating enzyme to the substrate, whereas HECT-

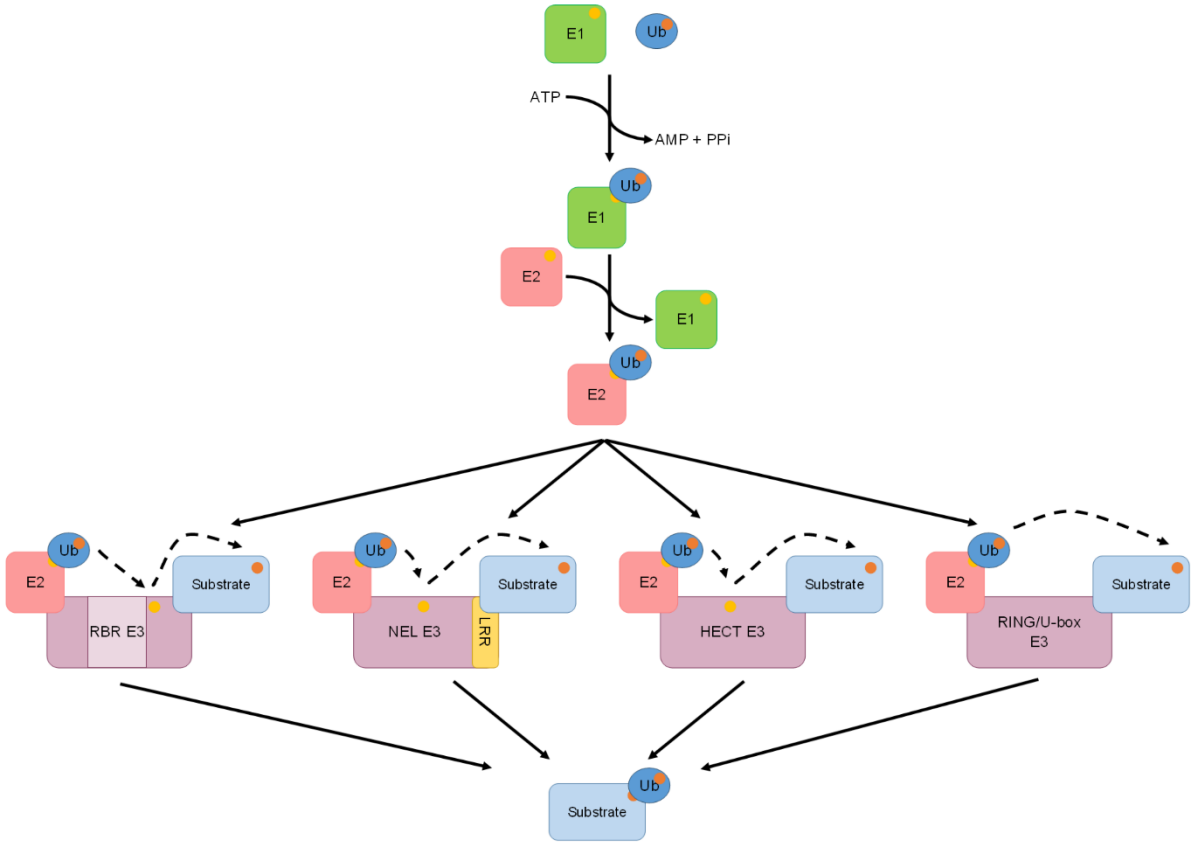


Figure 1.7. The ubiquitination system. E1 ubiquitin-activating enzymes (E1), activate ubiquitin (Ub) in a reaction involving ATP, resulting in ubiquitin bound to a cysteine residue (yellow) in the E1. Ubiquitin is then transferred to a cysteine in the E2 ubiquitin-conjugating enzyme (E2). From here, ubiquitin can be directly transferred onto a lysine residue (orange) in the target protein, in the case of RING/U-box E3 ubiquitin-ligases (E3), or via transfer onto a cysteine residue of the E3 itself, in the case of HECT, NEL and RBR E3s. This results in the formation of an isopeptide bond between the amine group of the lysine R group and the carboxyl group of the C-terminal glycine of ubiquitin. Adapted from (Jung et al. 2009; Ashida et al. 2014; Foot et al. 2017).

type E3 ubiquitin-ligases, first transfer ubiquitin from the E2 ubiquitin-conjugating protein onto a cysteine residue within the E3 ubiquitin-ligase, before then conjugating ubiquitin onto the substrate (Foot et al. 2017). There are two other types of E3 ubiquitin-ligase proteins, new E3-like (NEL)-type and RING-between-RING (RBR)-type E3 ubiquitin-ligases, which transfer ubiquitin in a manner similar to HECT-type E3 ubiquitin-ligases. NEL-type E3 ubiquitin-ligases have only been identified from T3SS effectors of pathogenic bacteria, and have an N-terminal leucine-rich repeat (LRR) domain for substrate recognition, and a conserved C-terminal ligase domain, that contains a cysteine residue required to bind ubiquitin before it is transferred onto the substrate (Ashida et al. 2014). The LRR domain remains bound to the C-terminal domain resulting in inhibition of the E3 which is relieved upon substrate-binding and structural rearrangement of the LRR domain (Ashida et al. 2014). RBR-type E3 ubiquitin-ligases have two RING domains, one to bind the E2-ubiquitin complex and one to catalyse the transfer of ubiquitin onto a cysteine within the E3 ubiquitin-ligase domain and then onto the substrate protein (Foot et al. 2017).

Ubiquitin can be conjugated onto a single lysine residue within the substrate (monoubiquitination) or multiple lysine residues (multi-monoubiquitination). But, ubiquitin itself ubiquitin is conjugated the outcome for the modified substrate will differ (Figure 1.8). (Foot et al. 2017). For example, lysine-48 (K48)-linked polyubiquitination is a signal that the substrate also contains seven lysine residues and a methionine residue which can be used to attach other ubiquitin molecules by isopeptide bonds (polyubiquitination) and depending on how is to undergo proteasomal degradation, whereas lysine-63 (K63)-linked polyubiquitination is involved in cell signalling (Foot et al. 2017). There are also proteases called DUBs that can remove ubiquitin from substrates or polyubiquitin chains to modify the signalling outcome (Ashida et al. 2014).

In addition to ubiquitin, there are several ubiquitin-like proteins, including SUMO-1, 2 and 3, NEDD8, ISG15 and LC3 that modify proteins in a similar way to ubiquitin by using components of the ubiquitination system and are also involved in cell signalling (Ashida et al. 2014). Some

of these ubiquitin-like proteins, such as SUMO and NEDD, can be used to modify ubiquitin chains and change the signalling outcome (Swatek & Komander 2016).

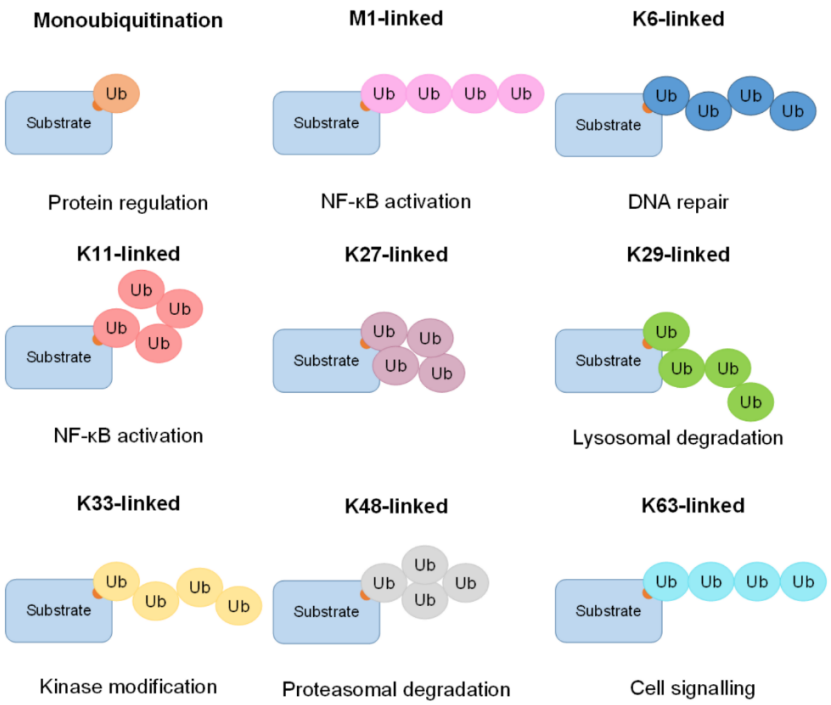


Figure 1.8. The varying forms of ubiquitination. Ubiquitin can be conjugated onto the lysine residue of a substrate protein in a number of different ways with diverse outcomes for the substrate. Monoubiquitination is involved in protein regulation, but ubiquitin molecules can be conjugated onto conjugated ubiquitin molecules via a surface exposed methionine as well as several lysine residues resulting in the formation of polyubiquitin chains. These different ubiquitin linkages are involved in various cellular signalling pathways. Adapted from (Jung et al. 2009; Ashida et al. 2014; Foot et al. 2017; Komander 2009).

1.17.1. T3SS Effectors that Mimic Components of the Ubiquitination System

Although some bacteria, such as *M. tuberculosis*, have a process similar to ubiquitination (Pearce et al. 2008), ubiquitination itself is exclusive to eukaryotes. This, coupled with the many processes that ubiquitination is involved in within host cells, make it an attractive target for T3SS effectors to manipulate host cell processes (Ashida et al. 2014). As such, pathogenic bacteria, such as *Salmonella*, have evolved effector proteins that mimic components of the ubiquitination system.

SopA is a HECT-type E3 ubiquitin-ligase (Zhang et al. 2006; Diao et al. 2008), translocated by the *SPI-1* T3SS and is found in *S.* Dublin, *S.* Typhimurium and *S.* Enteritidis (Wood et al. 2000), but is a pseudogene in *S.* Typhi (Parkhill et al. 2001) and *S.* Paratyphi A (McClelland et al. 2004; Holt et al. 2009). SopA also has a homologue, NleL, in EHEC (Lin et al. 2012), which is also a HECT-type E3 ubiquitin-ligase (Lin et al. 2011). The ubiquitin-ligase activity of SopA is dependent on a conserved cysteine residue and *in vitro* studies have shown that SopA can utilise several host E2 ubiquitin-conjugating enzymes including UBE2D1, UBE2D3 and UBE2L3 for autoubiquitination (Zhang et al. 2006). SopA is required for the stimulation of polymorphonuclear neutrophil (PMN) influx and fluid secretion into the intestinal lumen of ligated ileal calf loops (Wood et al. 2000), with this activity being dependent on the ubiquitin-ligase activity of SopA (Zhang et al. 2006). Other work has also shown that SopA is ubiquitinated by a host E3 ubiquitin-ligase, HsRMA1, resulting in proteasomal degradation of SopA, which is thought to enable bacterial escape from the SCV (Zhang et al. 2005). More recent work has demonstrated that SopA can ubiquitinate the eukaryotic RING-type E3 ubiquitin-ligases, TRIM56 and TRIM65, which are involved in innate immune responses to pathogens, resulting in their degradation by the proteasome (Fiskin et al. 2017). This may provide a molecular basis for the induction of PMN translocation and fluid secretion by SopA.

SlrP is a NEL-type E3 ubiquitin-ligase and is a homologue of YopM from *Y. pestis* and IpaH from *S. flexneri* (Tsolis et al. 1999; Zouhir et al. 2014), and translocated by both the *SPI-1* and *SPI-2* T3SSs in *Salmonella* (Miao & Miller 2000). SlrP is found in *S.* Typhimurium (Tsolis et al. 1999) and *S.* Enteritidis (Rehman et al. 2015), but is a pseudogene in *S.* Typhi (Sabbagh et al. 2010) and *S.* Paratyphi A (McClelland et al. 2004; Holt et al. 2009). SlrP is a member of the LRR *Salmonella* T3SS effector protein family, along with SspH1 and SspH2 (Tsolis et al. 1999), and has been shown to be required for colonisation of Peyer's patches during *S.* Typhimurium infection of mice (Tsolis et al. 1999). SlrP has been demonstrated to interact with the reduction/oxidation-regulatory protein, thioredoxin-1 (Bernal-Bayard & Ramos-Morales 2009) and the protein chaperone, ERdj3 (Bernal-Bayard et al. 2010). SlrP

ubiquitinates thioredoxin-1 *in vitro* (Zouhir et al. 2014), resulting in decreased activity (Bernal-Bayard & Ramos-Morales 2009). Interaction of SlrP with ERdj3 causes SlrP to localise partially with the endoplasmic reticulum, and a decreased ability of ERdj3 to bind unfolded proteins, however, this is not dependent on the E3 ubiquitin-ligase activity of SlrP (Bernal-Bayard et al. 2010). A recent, proteomic-based approach showed that HeLa cells, stably-transfected with SlrP showed a decrease in the proteins CKB and S100A4, which have been demonstrated to be involved in clearance of bacterial pathogens, which may explain its role in *S.* Typhimurium colonisation although the ubiquitination of these proteins by SlrP was not confirmed (Cordero-Alba et al. 2016).

SspH1 is a NEL-type E3 ubiquitin-ligase that, like SlrP and SspH2, requires a catalytic cysteine residue for activity (Rohde et al. 2007; Quezada et al. 2009). SspH1 is translocated by the *SPI-1* and *SPI-2* T3SSs (Miao et al. 1999), and is present in only one *S.* Typhimurium strain (ATCC 14028) and is absent in *S.* Enteritidis, *S.* Typhi and *S.* Paratyphi A (Tsolis et al. 1999; McClelland et al. 2004; Sabbagh et al. 2010; Holt et al. 2009). During infection, SspH1 localises to the nucleus (Haraga & Miller 2003), resulting in decreased IL-8 secretion (Haraga & Miller 2003), due to downregulation of NF-κB-dependent gene expression (Haraga & Miller 2006). A yeast two-hybrid (Y2H) screen identified PKN1 as an interacting partner of SspH1 (Haraga & Miller 2006) resulting in ubiquitination of PKN1 and proteasomal degradation, leading to abrogation of neutrophil and macrophage activation during infection (Keszei et al. 2014). Although PKN1 has also been shown to be involved in NF-κB-dependent gene expression (Haraga & Miller 2006), the effect of SspH1 on NF-κB-dependent gene expression is independent of PKN1 (Keszei et al. 2014).

SspH2 is translocated by the *SPI-2* T3SS only, and is found in many different strains of *S.* Typhimurium, as well as *S.* Enteritidis and *S.* Typhi, but is absent in *S.* Paratyphi A (Tsolis et al. 1999; McClelland et al. 2004; Sabbagh et al. 2010; Holt et al. 2009). A yeast two-hybrid screen identified filamin and profilin, proteins involved in actin polymerisation and cross-linking, as binding partners of SspH2 (Miao et al. 2003). The interaction between SspH2 and

filamin is dependent on the N-terminus of SspH2, but not the LRR domain, whereas the interaction with profilin is dependent on the C-terminus (Miao et al. 2003). During infection, SspH2 undergoes *S*-palmitoylation on an N-terminal cysteine residue by host palmitoyltransferases, allowing it to localise to the host plasma membrane (Hicks et al. 2011). This allows SspH2 to colocalise with filamin at membrane ruffles induced during *Salmonella* invasion, where actin is actively undergoing polymerisation (Miao et al. 2003). SspH2 also localises to actin filaments around the SCV and has been shown to inhibit actin polymerisation, but not sufficiently to abrogate the accumulation around the SCV (Miao et al. 2003). Other work has shown that the LRR domain of SspH2 is required for interaction with Sgt1, a host protein that acts as a co-chaperone for NOD1 (Bhavsar et al. 2013; da Silva Correia et al. 2007; Mayor et al. 2007). The SspH2-Sgt1 interaction enables SspH2 to ubiquitinate NOD1, resulting in its degradation and an increase in IL-8 secretion (Bhavsar et al. 2013).

SseL is a DUB that uses a conserved cysteine residue to preferentially hydrolyse K63-linked polyubiquitin chains *in vitro* (Rytkönen et al. 2007). SseL is translocated by the *SPI-2* T3SS and is present in *S.* Typhimurium, *S.* Typhi and *S.* Paratyphi A (Coombes et al. 2007). During infection of macrophages, SseL has been shown to be involved in the deubiquitination, and subsequent stabilisation of IκBα, the regulator of NF-κB-dependent gene expression, and therefore inhibits the expression of pro-inflammatory NF-κB-dependent genes (Negrate et al. 2008). However, other studies found that SseL had no effect on the stability of IκBα and did not inhibit NF-κB-dependent gene expression during macrophage infection (Rytkönen et al. 2007; Mesquita et al. 2013), but was involved in macrophage killing (Rytkönen et al. 2007). Therefore, the role of SseL in modulation of NF-κB signalling remains to be confirmed, but it does appear that SseL may be involved in modulation of cellular immunity. Other work has demonstrated that SseL is capable of preventing the accumulation K63-linked polyubiquitin chains around the SCV, which are responsible for the recruitment of autophagy markers, p62 and LC3, therefore preventing autophagosomal degradation of *Salmonella* (Mesquita et al. 2012). This suggests that SseL may be crucial in preventing the fusion of the SCV with

lysosomes in host cells. A recent proteomics-based study identified several novel interacting partners of SseL, the biological relevance of which remains to be determined (Sontag et al. 2016). However, one interesting finding from this study was the ability of SseL to bind the ubiquitin-like protein NEDD8, and whilst SseL was shown to lack deNEDDylase activity, this suggests that it may interfere with NEDD8 signalling by another method (Sontag et al. 2016).

AvrA is a homologue of YopJ from *Y. pseudotuberculosis* and AvrRvx from *X. capestris* and is found in *S.* Typhimurium and *S.* Enteritidis, but not *S.* Typhi (Hardt & Galán 1997) or *S.* Paratyphi A (Holt et al. 2009). AvrA is a DUB (Ye et al. 2007), encoded downstream of the *SPI-1* T3SS in *S.* Typhimurium and has been shown to be translocated in a *SPI-1* T3SS-dependent manner during infection (Hardt & Galán 1997). AvrA is capable of inhibiting NF-κB-dependent gene expression (Collier-Hyams et al. 2002), by deubiquitinating and subsequently stabilising IκBα, both in cell lines and during murine infection, which is dependent on a conserved catalytic cysteine residue (Ye et al. 2007). AvrA can also deubiquitinate β-catenin, a transcription factor that translocates to the nucleus and interacts with T-cell factor (TCF), to induce expression of genes involved in proliferation of intestinal epithelial cells during murine infection (Ye et al. 2007). Other work has shown that AvrA can stimulate cell proliferation through STAT3 activation (Lu et al. 2016), but whether this involves deubiquitination has not been determined. AvrA has also been demonstrated to be involved in maintaining cellular tight junctions, and therefore the integrity of the intestinal epithelium, which reduces inflammation during *Salmonella* infection (Liao et al. 2008). However, AvrA has also been demonstrated to possess acetyl transferase activity that is involved in the inhibition of JNK-dependent inflammatory gene expression (Jones et al. 2008) and this may also be responsible for the AvrA-dependent maintenance of cellular tight junctions (Zhang et al. 2015). AvrA has also been shown to be capable of acetylating β-catenin, and this is thought to be able to contribute to the AvrA-dependent increase in β-catenin-dependent gene expression (Lu et al. 2012). Therefore, the DUB activity of AvrA has been shown to be important for the reduction of NF-κB-dependent inflammatory response during *Salmonella* infection (Ye et al.

2007), but the role of AvrA in maintenance of the intestinal epithelium (Liao et al. 2008) and cell proliferation (Ye et al. 2007) may involve acetyl transferase activity (Jones et al. 2008; Zhang et al. 2015).

These effectors demonstrate that *Salmonella* has a range of T3SS effectors that have evolved to mimic components of the eukaryotic ubiquitination system. These effectors target host proteins involved in many cellular pathways and significantly contribute to the successful infection of the host by *Salmonella*.

1.17.2. The NleG Family of T3SS Effectors

The non-locus of enterocyte effacement (LEE)-encoded (Nle) G family, are the largest family of T3SS effectors in EHEC, with homologues also found in enteropathogenic *E. coli* (EPEC), *Citrobacter rodentium* and *Salmonella* (Tobe et al. 2006). This family of proteins share a conserved C-terminal domain, that has structural similarity to eukaryotic RING/U-box-type E3 ubiquitin-ligase domains (Wu et al. 2010). The N-terminus is more variable between NleG proteins, and is thought to be required for substrate recognition (Wu et al. 2010), however, whilst some putative interacting partners have been identified by proteomic methods (Sontag et al. 2016), this has yet to be substantiated.

During investigations into novel T3SS effectors in *S. bongori*, three proteins were identified that were homologous to the NleG family of effectors, these were *S. bongori* outer protein (Sbo) D, SboF and SboG (Fookes et al. 2011). Interestingly, one of these proteins, SboD had a homologue in *S.* Typhi, but not *S.* Typhimurium or *S.* Enteritidis (Fookes et al. 2011). This gene, *t1865* in *S.* Typhi Ty2, was uncharacterised and had not previously been investigated, but was renamed as *S.* Typhi outer protein (Sto) D, to correspond with the *S. bongori* homologue. Preliminary work was performed to investigate StoD, but not using *S.* Typhi, as an appropriate containment level three (CL3) laboratory was not available.

1.18. Hypothesis and Aims

The hypothesis underlying this project is that *S.* Typhi has a suite of T3SS effectors that are different to those found in *S.* Typhimurium, and that these are instrumental to the differences in disease outcome and host between these two *Salmonella* serovars. To investigate this hypothesis the following aims were set:

- To establish a CL3 laboratory, including the optimisation and documentation of protocols required to enable the study and manipulation of *S.* Typhi.
- To identify any novel T3SS effector proteins in *S.* Typhi and to assess the role these T3SS effector proteins have in *S.* Typhi pathogenesis.
- To characterise the biochemical activity of one of the novel T3SS effectors, StoD.

Chapter 2: Materials and Methods

2.1. Bacterial strains

Salmonella strains (Table 2.1) were routinely cultured in Lennox lysogeny broth (LB; Sigma or Invitrogen) at 37°C, 200 rpm overnight, unless otherwise stated. Where appropriate, antibiotics were used at the following concentrations: chloramphenicol (Cm^R); 30 µg/mL, tetracycline (Tet^R); 12.5 µg/mL, kanamycin (Kn^R); 50 µg/mL, ampicillin (Amp^R); 100 µg/mL and spectinomycin ($Spec^R$); 100 µg/mL. All antibiotics were purchased from Sigma. All other bacterial strains (Table 2.1) were cultured in Miller LB (Sigma).

Table 2.1. Strains used in this study.

Name	Description	Source or Reference
***E. coli* strains**		
Top10	F- *mcrA* Δ*(mrr-hsd*RMS-*mcrBC)* Φ80*lacZ*Δ*M15* Δ*lacX74 recA1 adaD139* Δ*(ara-leu)7697 galU galK rpsL endA1 nupG*.	Invitrogen
BL21 Star	F- *ompT hsdS$_B$*($r_B^-m_B^-$) *galdcm rne131* λ(DE3[*lacI lacUV5-T7p07 ind1 sam7 nin5*]) [*malB*$^+$]$_{K-12}$(λ^S).	Invitrogen
BL21 pLysS	F- *ompT gal dcm lon hsdS$_B$*($r_B^-m_B^-$) λ(DE3[*lacI lacUV5-T7p07 ind1 sam7 nin5*]) [*malB*$^+$]$_{K-12}$(λ^S) p*LysS*[*T7p20 ori$_{P15A}$*] (Cm^R).	Promega
***S.* Typhimurium strains**		
Wild-type	ATCC 14028 *S.* Typhimurium wild-type.	ATCC
Δ*prgH*	ATCC 14028 *S.* Typhimurium Δ*prgH*::Tet (Tet^R).	(Beuzon et al. 2001)
Δ*ssaV*	ATCC 14028 *S.* Typhimurium Δ*ssaV*::Kn (Kn^R).	(Beuzón et al. 2000)
Δ*prgH/ΔssaV*	ATCC 14028 *S.* Typhimurium Δ*prgH*::Tet and Δ*ssaV*::Kn (Tet^R, Kn^R).	(Beuzon et al. 2001)
***S.* Typhi strains**		
Wild-type	Ty2 *S.* Typhi wild-type.	Gordon Dougan
Δ*invA*	Ty2 *S.* Typhi Δ*invA*::Kn (Kn^R).	(Johnson et al. 2017)
Δ*ssaV*	Ty2 *S.* Typhi Δ*ssaV*::Kn (Kn^R).	This study
Δ*tviB*	Ty2 *S.* Typhi Δ*tviB*::Kn (Kn^R).	Rebecca Johnson
Δ*tviB*Δ*invA*	Ty2 *S.* Typhi Δ*tviB*::FRTΔ*invA*::Kn (Kn^R).	Rebecca Johnson
Δ*tviB*Δ*invA*Δ*ssaV*	Ty2 *S.* Typhi Δ*tviB*::FRTΔ*invA*::FRTΔ*ssaV*::Kn (Kn^R).	Rebecca Johnson
Δ*tviB*Δ*invA*Δ*fliF*	Ty2 *S.* Typhi Δ*tviB*::FRTΔ*invA*::FRTΔ*fliF*::Kn (Kn^R).	Rebecca Johnson
Δ*stoA*	Ty2 *S.* Typhi Δ*stoA*::Kn (Kn^R).	This study
Δ*stoB*	Ty2 *S.* Typhi Δ*stoB*::Kn (Kn^R).	This study
Δ*stoC*	Ty2 *S.* Typhi Δ*stoC*::Kn (Kn^R).	This study

Name	Description	Source or Reference
Δ*stoD*	Ty2 *S.* Typhi Δ*stoD*::Kn (Kn^R).	This study
Δ*stoE*	Ty2 *S.* Typhi Δ*stoE*::Kn (Kn^R).	This study
CT18	CT18 *S.* Typhi wild-type.	Gordon Dougan
ERL12148	ERL12148 *S.* Typhi wild-type. H58 clinical isolate obtained from the stool of a patient in India.	Gordon Dougan
129-0238	129-0238 *S.* Typhi wild-type. H58 clinical isolate obtained from the blood of a patient in Tanzania.	Gordon Dougan
Lupe Gen0059	Lupe Gen0059 *S.* Typhi wild-type. Clinical isolate obtained from a patient in Samoa.	Gordon Dougan
***S. cerevisiae* strains**		
AH109	*MATa trp1-901 leu2-3 112 ura3-52 his3-200 gal4Δ gal80Δ LYS2:GAL1$_{TATA}$-HIS3 GAL2$_{UAS}$-GAL2$_{TATA}$-ADE2 URA3::MEL1$_{UAS}$-MEL1$_{TATA}$-lacZ*	Clontech
BY4741	*MATa his3Δ1 leu20Δ0 met15Δ) ura3Δ0*	(Brachmann et al. 1998)

2.2. Tissue Culture

Human epithelial cervical adenocarcinoma cells (HeLa; ATCC) were cultured in Dulbecco's Modified Eagle's Medium (DMEM) containing 4500 mg/L glucose (Sigma), supplemented with 10% (v/v) heat-inactivated foetal bovine serum (FBS; Gibco) and 2 mM GlutaMAX (Gibco), referred to as Complete HeLa Medium.

Abelson murine leukaemia virus-induced tumour macrophages (RAW 264.7; ATCC) were cultured in DMEM containing 4500 mg/L glucose and L-glutamine (Sigma) and supplemented with 10% (v/v) heat-inactivated FBS, referred to as Complete RAW264.7 Medium.

Human acute monocytic leukaemia cells (THP-1; ATCC) were cultured in suspension in Roswell Park Memorial Institute medium (RPMI-1640) containing L-glutamine (Sigma) supplemented with 10% (v/v) heat-inactivated FBS and 10 μM HEPES buffer (Sigma), referred to as Complete THP-1 Medium.

All cells were kept at 37°C and 5% CO2 in a humidified environment and were regularly tested for mycoplasma using the MycoAlert mycoplasma detection kit (Lonza).

2.2 Cloning

Vectors and primers used in this study are shown in Table 2.2 and Table 2.3, respectively. The following genes were amplified from Ty2 *S.* Typhi genomic DNA by PCR: *t0733*, *t1875* (*stoA*), *t2863* (*stoC*), *t4218* (*stoB*), *t05880* (*stoE*) and *stoD*. The following genes were amplified from ATCC 14028 *S.* Typhimurium genomic DNA by PCR: *sopB*, *sseJ* and *stoBTm*. The following genes were amplified from the stated vectors by PCR: *UBE2E1* was amplified from pET28-*UBE2E1*, *Ubiquitin* was amplified from pCW7, *ISG15* was amplified from pcDNA3.1-*hISG15* and *UBE2L3* was amplified from pGEX-*UBE2L3*.

All PCRs were performed using either: One*Taq* (New England Biolabs), Q5 High-Fidelity (New England Biolabs), Phusion High-Fidelity (New England Biolabs) or KOD Hot Start (Invitrogen) DNA polymerases. All cloning was carried out using restriction enzyme digest (New England Biolabs) and T4 DNA ligase (New England Biolabs) ligation and transformed into chemically competent Top10. Vector sequences were confirmed by sequencing (GATC Biotech).

To generate the *stoD*$_{P204K}$ mutation, a vector containing the *stoD* gene was amplified using the appropriate primers (Table 2.3) before phosphorylation using T4 polynucleotide kinase (New England Biolabs) and blunt-end ligation with T4 DNA ligase, before transformation into chemically competent Top10. The insertion of the P204K mutation was confirmed by KasI (New England Biolabs) restriction enzyme digest, as this restriction site was introduced upon insertion of the P204K mutation, and sequencing.

Table 2.2. Vectors used in this study.

Name	Description	Source or Reference
Bacterial expression vectors		
pKD46	Temperature unstable bacterial expression vector encoding the λ Red Recombinase under the control of an arabinose-inducible promoter (Amp^R).	(Datsenko & Wanner 2000)
pKD4	PCR template vector with Kn resistance cassette (Kn^R).	(Datsenko & Wanner 2000)

Name	Description	Source or Reference
pWSK29	Low copy-number bacterial expression vector containing a T3 RNA polymerase promoter (Amp^R).	(Wang & Kushner 1991)
pWSK29-*stoD*	pWSK29 containing *stoD* (Amp^R).	This study
pWSK29-*stoD*-4HA	pWSK29 containing *stoD* with a C-terminal 4HA tag (Amp^R).	This study
pWSK29-Spec	pWSK29 with a spectinomycin resistance cassette ($Spec^R$).	(Johnson et al. 2017)
pWSK29-Spec-*stoD*-4HA	pWSK29-Spec containing *stoD* with a C-terminal 4HA tag ($Spec^R$).	This study
pWSK29-Spec-p*stoD*-4HA	pWSK29-Spec containing *stoD* and the 499 nucleotides upstream with a C-terminal 4HA tag ($Spec^R$).	This study
pWSK29-Spec-*t0733*-4HA	pWSK29-Spec containing *t0733* with a C-terminal 4HA tag ($Spec^R$).	This study
pWSK29-Spec-*t1875*-4HA	pWSK29-Spec containing *t1875* (*stoA*) with a C-terminal 4HA tag ($Spec^R$).	This study
pWSK29-Spec-*t2863*-4HA	pWSK29-Spec containing *t2863* (*stoC*) with a C-terminal 4HA tag ($Spec^R$).	This study
pWSK29-Spec-*t4218*-4HA	pWSK29-Spec containing *t4218* (*stoB*) with a C-terminal 4HA tag ($Spec^R$).	This study
pWSK29-Spec-*t05880*-4HA	pWSK29-Spec containing *t05880* (*stoE*) with a C-terminal 4HA tag ($Spec^R$).	This study
pWSK29-*sopB*-TEM1	pWSK29 containing *sopB* from ATCC 14028 *S.* Typhimurium with a C-terminal β-lactamase (TEM1) tag (Amp^R).	This study
pWSK29-*sseJ*-TEM1	pWSK29 containing *sseJ* from ATCC 14028 *S.* Typhimurium with a C-terminal TEM1 tag (Amp^R).	This study
pWSK29-*stoA*-TEM1	pWSK29 containing *stoA* with a C-terminal TEM1 tag (Amp^R).	This study
pWSK29-*stoB*-TEM1	pWSK29 containing *stoB* with a C-terminal TEM1 tag (Amp^R).	This study
pWSK29-*stoBTm*-TEM1	pWSK29 containing *stoB* from ATCC 14028 *S.* Typhimurium with a C-terminal TEM1 tag (Amp^R).	This study
pWSK29-*stoC*-TEM1	pWSK29 containing *stoC* with a C-terminal TEM1 tag (Amp^R).	This study
pWSK29-*stoD*-TEM1	pWSK29 containing *stoD* with a C-terminal TEM1 tag (Amp^R).	This study
pWSK29-*stoE*-TEM1	pWSK29 containing *t05880* (*stoE*) with a C-terminal TEM1 tag (Amp^R).	This study
pET28	Bacterial expression vector with an N-terminal polyhistidine (6His) tag and an IPTG-inducible T7 RNA polymerase promoter (Kn^R).	Novagen
pET28-*stoD*	pET28 containing *stoD* (Kn^R).	Mariella Lomma

Name	Description	Source or Reference
pET28-*stoD*$_{P204K}$	pET28 containing *stoD* with a P204K mutation (Kn^R).	This study
pET28-*stoD* [1-95]	pET28 containing *stoD* amino acids 1-95 (Kn^R).	Susan Lea
pET28-*stoD* [134-233]	pET28 containing *stoD* amino acids 134-233 (Kn^R).	This study
pET28-*stoD*$_{P204K}$ [134-233]	pET28 containing *stoD* amino acids 134-233 with a P204K mutation (Kn^R).	This study
pET28-*UBE2E1*	pET28 containing *UBE2E1* (Kn^R)	Susan Lea
pGEX-*UBE2L3*	Bacterial expression vector containing *UBE2L3* with a N-terminal glutathione S-transferase (GST) tag (Amp^R).	(Eldridge et al. 2017)
Mammalian expression vectors		
pRK5	Mammalian expression vector containing the SP6 promoter.	Clontech
pRK5-*mCherry*	pRK5 containing *mCherry* with an N-terminal HA tag (Amp^R).	(Harding et al. 2013)
pRK5-*stoA*	pRK5 containing *stoA* with an N-terminal HA tag (Amp^R).	This study
pRK5-*stoB*	pRK5 containing *stoB* with an N-terminal HA tag (Amp^R).	This study
pRK5-*stoC*	pRK5 containing *stoC* with an N-terminal HA tag (Amp^R).	This study
pRK5-*stoD*	pRK5 containing *stoD* with a C-terminal HA tag (Amp^R).	This study
pRK5-*stoD*$_{P204K}$	pRK5 containing *stoD* with a P204K mutation and a C-terminal HA tag (Amp^R).	This study
pRK5-*stoE*	pRK5 containing *stoE* with an N-terminal HA tag (Amp^R).	This study
pRK5-*stoE* [41-273]	pRK5 containing *stoE* amino acids 41-273 with an N-terminal HA tag (Amp^R).	This study
pGFP-*Rab11a*	Mammalian expression vector containing Rab11a with a GFP tag (Kn^R).	(Clements et al. 2014)
pGFP-*Vamp3*	Mammalian expression vector containing Vamp3 with a GFP tag (Kn^R).	(Clements et al. 2014)
pEGFP-*LC3*	Mammalian expression vector containing LC3 with an EGFP tag (Kn^R).	(Dupont et al. 2009)
pCW7	Mammalian expression vector containing ubiquitin from *S. cerevisiae* with N-terminal 6His and c-myc tags (Amp^R).	(Ward et al. 1995)
pcDNA3.1-*hISG15*	Mammalian expression vector containing *ISG15* (Amp^R).	(Kim et al. 2004) Addgene plasmid #12447
***S. cerevisiae* expression vectors**		
pGBKT7	Yeast expression vector containing the Gal4 DNA-binding domain, a c-myc tag, the *ADH1* promoter and the *TRP1* gene for selection in *S. cerevisiae* (Amp^R).	Clontech

Name	Description	Source or Reference
pGBKT7-*stoD*	pGBKT7 containing *stoD* fused to the Gal4 DNA-binding domain at the N-terminus (Kn^R).	Mariella Lomma
pGBKT7-*stoD*$_{P204K}$	pGBKT7 containing *stoD* with a P204K mutation fused to the Gal4 DNA-binding domain at the N-terminus (Kn^R).	This study
pGBKT7-*stoD* [1-133]	pGBKT7 containing *stoD* amino acids 1-133 fused to the Gal4 DNA-binding domain at the N-terminus (Kn^R).	This study
pGBKT7-*stoD* [134-233]	pGBKT7 containing *stoD* amino acids 134-233 fused to the Gal4 DNA-binding domain at the N-terminus (Kn^R).	This study
pGBKT7-*stoD*$_{P204K}$ [134-233]	pGBKT7 containing *stoD* amino acids 134-233 containing a P204K mutation fused to the Gal4 DNA-binding domain at the N-terminus (Kn^R).	This study
pGADT7	Yeast expression vector containing the Gal4 activation domain, a HA tag, the *ADH1* promoter and *LEU2* gene for selection in *S. cerevisiae* (Amp^R).	Clontech
pGADT7-*Ubiquitin*	pGADT7 containing a synthetic sequence of *Ubiquitin* fused to the Gal4 activation domain at the N-terminus (Amp^R).	This study
pGADT7-*ISG15*	pGADT7 containing *ISG15* fused to the Gal4 activation domain at the N-terminus (Amp^R).	This study
pGADT7-*UBE2L3*	pGADT7 containing *UBE2L3* fused to the Gal4 activation domain at the N-terminus (Amp^R).	This study
pYes2	Yeast expression vector containing the galactose-inducible *GAL1* promoter and *URA3* gene for selection in *S. cerevisiae* (Amp^R).	Invitrogen
pYes2-*stoD*	pYes2 containing *stoD* (Amp^R).	This study
pYes2-*stoD*$_{P204K}$	pYes2 containing *stoD* with a P204K mutation (Amp^R).	This study

Table 2.3. Primers used in this study.

Name	5' to 3' Nucleotide Sequence
pWSK29	
NotI t0733 FW	CATGGCGGCCGCGTTGGTTAGTTCTACTTATGGTG
PacI t0733 REV	CATGTTAATTAATTTAACCTTGAATGAGCG
BamHI StoD FW	CGCGGATCCAGAAGGAGATATACCTACGTAATGTTCTTAACATTTCC TAATGTAG
EcoRI StoD REV	CCGGAATTCTTATGCATAATCAGGCACATCATACGGATAAGCGTAGT CTGGGACGTCGTATGGGTATGGGATTATAAAATTACCTTTGG
SacI StoD with promoter FW	GGAGCTCCCAGATTTTCCCTGATGCC
PacI StoD with promoter REV	GCTTAATTAATGGGATTATAAAATTACCTTTGG

Name	5’ to 3’ Nucleotide Sequence
NotI t1875 FW	CATGGCGGCCGCGATGAGTTTAGCGCAGCCTAAATC
PacI t1875 REV	CATGTTAATTAAGAAGTCTCCTGCCTGGAAAC
NotI t2863 FW	CATGGCGGCCGCGTTGCCTGATGGACTTGAATCC
PacI t2863 REV	CATGTTAATTAATTCGTAGGGTATCAAAACGGT
NotI t4218 FW	CATGGCGGCCGCGTTGGGTCGCTTAGAAGCTC
PacI t4218 REV	CATGTTAATTAAGTTATCAGGCATAATCATTTCATCTAC
NotI t05880 FW	CATGGCGGCCGCGATGAAAGTTAGTCTTGATTTGGTTATCAATAG
PacI t05880 REV	CATGTTAATTAATACCCCATCCACCTCAATAATTAAG
BamHI Typhimurium SopB FW	GCCGGATCCAAGAAGGAGATATACCTACGTAATGCAAATACAGAGC TTCTATCAC
EcoRI Typhimurium SopB REV	GCCGAATTCCGAGATGTGATTAATGAAGAAATGCC
BamHI Typhimurium SseJ FW	GCCGGATCCAAGAAGGAGATATACCTACGTAATGCCATTGAGTGTT GGACAGG
EcoRI Typhimurium SseJ REV	CCGCCGGGAATTCCGTTCAGTGGAATAATGATGAGCTATAAAACTTT C
NotI t4218 from Typhimurium FW	CATGGCGGCCGCGATGGATACACAACCGTCCG
EcoRI t4218 from Typhimurium REV	GCCGAATTCGCGGCATGATTTTCTTCATCAAC
BamHI StoD-TEM1 FW	GCCGGATCCAAGAAGGAGATATACCTACGTAATGTTCTTAACATTTC CTAATGTAGC
EcoRI StoD-TEM1 REV	CCGCCGGGAATTCCGTGGGATTATAAAATTACCTTTGG
StoD no HA FW	CGCGGATCCAGAAGGAGATATACCTACGTAATGTTCTTAACATTTCC TAATGTAG
StoD no HA REV	CCGGAATTCTTATGGGATTATAAAATTACCTTTGG
pET28	
BamHI StoD FW	CGCGCGGATCCATGTTCTTAACATTTCCTAATGTAGC
NotI StoD REV	GAATGCGGCCGCTTATGGGATTATAAAATTACCTTTGG
BamHI StoD [134-233] FW	CGCGCGGATCCATGAATAAACAACAATTAGTGGATAAGATTG
NotI StoD [134-233] REV	GAATGCGGCCGCTTATGGGATTATAAAATTACCTTTGG
pRK5	
BamHI StoA FW	GCCGGATCCCATATGAGTTTAGCGCAGCCTAAATC
PstI StoA REV	AAAACTGCAGTTAGAAGTCTCCTGCCTGGAAAC
BamHI StoB FW	GCCGGATCCCATATGGGTCGCTTAGAAGCTC
PstI StoB REV	AAAACTGCAGTTAGTTATCAGGCATAATCATTTCATCTAC
BamHI StoC FW	GCCGGATCCCATATGCCTGATGGACTTGAATCC
PstI StoC REV	AAAACTGCAGTTATTCGTAGGGTATCAAAACGGT
BamHI StoD FW	CGCGCGGATCCCGGCCACCATGGCGATGTTCTTAACATTTCCTAAT GTAGC

Name	5’ to 3’ Nucleotide Sequence
HindIII StoD REV	GCCAAGCTTTTAAGCGTAGTCTGGGACGTCGTATGGGTAACCTGCT CCGAATTCTGGGATTATAAAATTACCTTTGGTAG
BamHI StoE FW	GCCGGATCCCATATGAAAGTTAGTCTTGATTTGGTTATCAATAG
PstI StoE REV	AAAACTGCAGTCATACCCCATCCACCTCAATAATTAAG
BamHI StoE [41-273] FW	GCCGGATCCCATATGCGAGGTAAAGTTAAAGAAAACAGAC
PstI StoE REV	AAAACTGCAGTCATACCCCATCCACCTCAATAATTAAG
pGBKT7	
EcoRI StoD FW	CCGCCGGGAATTCATGTTCTTAACATTTCCTAATGTAGC
PstI StoD REV	TGCACTGCAGATTATGGGATTATAAAATTACCTTTGG
EcoRI StoD [1-133] FW	CCGCCGGGAATTCATGTTCTTAACATTTCCTAATGTAGC
PstI StoD [1-133] REV	TGCACTGCAGATCAAGATGTATCAAAAATAGCAGGTGCTCC
EcoRI StoD [134-233] FW	GCCGAATTCAATAAACAACAATTAGTGGATAAG
BamHI StoD [134-233] REV	GCCGGATCCTTATGGGATTATAAAATTACCTTTGG
NdeI UBE2E1 FW	GCCCATATGTCAGATGATGATTCACGCGCC
EcoRI UBE2E1 REV	GCCGAATTCTTAGGTCGCATAGCGTTTGGTC
EcoRI Ubiquitin FW	GCCGAATTCATGCAGATCTTCGTCAAGACG
BamHI Ubiquitin REV	GCCGGATCCTCAACCACCTCTTAGTCTTAAG
EcoRI UBE2L3 FW	GCCGAATTCATGGCGGCCAGCAGGAGG
BamHI UBE2L3 REV	GCCGGATCCTTAGTCCACAGGTCGCTTTTC
NdeI ISG15 FW	GCCCATATGGGCTGGGACCTGACG
BamHI ISG15 REV	GCCGGATCCTTAGCTCCGCCCGCCAGGCTCTGTGCCGCCTCCCCG CAGGCGCAGATTCATGAACAC
pYes2	
BamHI StoD FW	CGCGCGGATCCATGTTCTTAACATTTCCTAATGTAGC
NotI StoD REV	GAATGCGGCCGCTTATGGGATTATAAAATTACCTTTGG
Primers for generating StoD$_{P204K}$	
KasI StoD P204K FW	CACACAT<u>GCA</u>GTTAGTAGGGCTCCATTATCAC
KasI StoD P204K REV	GCGCCGTCAATAATAAGTTGGATAAGTG
Generating mutants in *S.* Typhi Ty2	
SsaV KanR FW	GGCGCAACAGTGGCTCAGTGTATGCGCGGGTCGTCAGGATATGGTT CTGGTGTGTAGGCTGGAGCTGCTTCG
SsaV KanR REV	GCTAAGGTCAATACTTTCTACCACTTGTATAAGGCTCTCCTCTCCTAA TTCATATGAATATCCTCCTTAG
SsaV Confirmation FW	GCGCGATGGGCTTGCAATG
SsaV Confirmation REV	CACGCATTTAACTTCGTTGCGC
StoA KanR FW	ATCCGGAGAGCTTTTAGAGATCCTTGGTCCCTCACTCACTCAGGGA GAAATGTGTAGGCTGGAGCTGCTTCG

Name	5’ to 3’ Nucleotide Sequence
StoA KanR REV	CAGCAGCGATGAGTTCATTGGCAAGGTCGTTATTCACTTTTGACAAA AGTCATATGAATATCCTCCTTAG
StoA Confirmation FW	CATCGTGCTGTCGTTTTCC
StoA Confirmation REV	GGGCTGAATGATACATGCC
StoB KanR FW	CTGTTCCGCAATCCGCTATTCTGTCGGGGGAGAATCAGTATACCATA ACGTGTGTAGGCTGGAGCTGCTTCG
StoB KanR REV	TTTCATCTACGCCGGAACTCTTGTTGACCGGATTTTCCGTGGGCGAT GTACCATATGAATATCCTCCTTAG
StoB Confirmation FW	CTGACGATAGACTCTACACC
StoB Confirmation REV	CGGCAGCGTAGTCTGCCG
StoC KanR FW	CCACTCTTGAGTTTGATCCATCAACTTCTTTCATCAATACAACCGCTG TCGTGTGTAGGCTGGAGCTGCTTCG
StoC KanR REV	CGGTAATTGCACAAGTTGTATCGATGTTGACTCTCTCCCAGGTACCC TTTACATATGAATATCCTCCTTAG
StoC Confirmation FW	GATCCTACATTCGATACCATCC
StoC Confirmation REV	CATATCATTCAATTCGGCATTGATC
StoD KanR FW	CCTAATGTAGCAATAACTCGAGATAACAGGATAGACAAATTATCTGA AAATGTGTGTAGGCTGGAGCTGCTTCG
StoD KanR REV	ATTACCTTTGGTAGTGTCAAAATAACATTCATTTTTATTTATTATCATA TCCATATGAATATCCTCCTTAG
StoD Confirmation FW	GTCTTAATCTGTACAAAGGC
StoD Confirmation REV	CAACATCGAAACATAGACTGC
StoE KanR FW	ACTACCTCACCATTACTGATGGTTAAATCTCTAACTTTTAATAACAAA TATGTGTAGGCTGGAGCTGCTTCG
StoE KanR REV	GTTATCAATAGCGGCGACGATGAAATAGATATGGATTATGCTCTCCA GACCATATGAATATCCTCCTTAG
StoE Confirmation FW	CTTTGTTTTCAGAAAGAGTGG
StoE Confirmation REV	GTTGATCACTATCATAAATTTAG
Primers for screening yeast two-hybrid colonies	
pGADT7 FW	CTATTCGATGATGAAGATACCCCACCAAACCC
pGADT7 REV	GTGAACTTGCGGGGTTTTTCAGTATCTACGATT

2.3 Generating Mutants in *S.* Typhi

The Ty2 *S.* Typhi Δ*ssaV*, Δ*stoA*, Δ*stoB*, Δ*stoC*, Δ*stoD* and Δ*stoE* mutants were generated using the λ Red Recombinase system with the pKD46 vector (Table 2.2) (Datsenko & Wanner 2000). The kanamycin cassette from pKD4 (Table 2.2) was amplified using primers (Table 2.3) that introduced 50 nucleotide overhangs to the 5’ and 3’ ends of the kanamycin cassette

that were homologous to the gene of interest. This linear PCR product was then introduced into *S.* Typhi by electroporation to generate the mutation as follows. *S.* Typhi containing the pKD46 vector were grown overnight at 30°C, 200 rpm with 50 µg/mL ampicillin to maintain the vector. *S.* Typhi was then subcultured 1:100 into fresh Lennox LB containing 50 µg/mL ampicillin and grown at 30°C, 200 rpm for 2.5 h, before the addition of 10 mM arabinose. *S.* Typhi was then grown for a further 30 min at 30°C, 200 rpm to induce the expression of the λ Red Recombinase. Bacteria were then made electrocompetent and transformed with the linear PCR product described above. Transformants were recovered at 30°C, 200 rpm in super optimal broth with catabolite repression (SOC) media for at least 1 h. Transformants were then plated on LB agar (Merck) plates containing 50 µg/mL kanamycin to select for transformants where the kanamycin resistance cassette had been successfully integrated into the genome. Mutagenesis of the respective gene was confirmed using a primer pair that were 100 nucleotides up- and downstream of the gene (Table 2.3) and this PCR product was confirmed by sequencing following the curing of the transformants by growth at 37°C, 200 rpm overnight to remove the pKD46 vector.

2.4 Transfection

HeLa cells were seeded at $4.5x10^4$ cells/well on coverslips in 24-well plates (BD Falcon) 24 h before transfection. Cell medium was replaced with fresh Complete HeLa Medium before transfection with eukaryotic expression vectors (Table 2.2). GeneJuice transfection reagent (Novagen) was used as per the manufacturer's instructions. Briefly, 0.75 µL GeneJuice transfection reagent was mixed with Opti-MEM containing GlutaMAX (Gibco) for 5 min at room temperature before the addition of 0.25 µg DNA, giving a 3:1 ratio of GeneJuice reagent to DNA, and incubation for 15-30 min at room temperature. For co-transfections, 0.25 µg of each vector was incubated with 1.5 µL of GeneJuice transfection reagent. This mixture was then added to the cells and incubated for 24 h at 37°C and 5% CO_2 in a humidified environment.

For transfections using the pRK5-*stoA* construct, a GeneJuice:DNA ratio of 6:1 was used instead of the standard 3:1, and the media was replaced 16 h after transfection.

2.5 *Salmonella* Infection Assays

2.5.1 *Salmonella* Infection of HeLa cells

Salmonella infection of HeLa cells was adapted from a previously described protocol (Beuzón et al. 2000). HeLa cells were seeded in 1 mL of media in a 24-well plate (BD Falcon), at a density of $7x10^4$ cells/well, 24 h prior to infection. *Salmonella* strains were either grown as subcultures or static overnights from glycerol stocks. For subcultures, *Salmonella* were grown overnight at 37°C, 200 rpm in 5 mL Lennox LB with appropriate antibiotics, before being diluted 1:33 into 5 mL of fresh Lennox LB, with appropriate antibiotics, and grown at 37°C, 200 rpm, until an OD_{600} of 1.8-2.0. For static overnights, *Salmonella* were grown in 5 mL Lennox LB with appropriate antibiotics at 37°C without shaking overnight.

Salmonella cultures were then normalised according to an optical density at 600 nm (OD_{600}) and used to infect HeLa cells at a moiety of infection (MOI) of 100. Bacterial invasion was allowed to occur for 15-60 min at 37°C and 5% CO_2, before cells were washed three times with Dulbecco's phosphate-buffered saline (DPBS; Sigma) and incubated in 1 mL Complete HeLa Medium containing 100 µg/mL gentamicin (Sigma) for 1 h at 37°C and 5% CO_2 to kill extracellular bacteria. Cells were then washed once with DPBS and incubated in 1 mL Complete HeLa Medium containing 20 µg/mL gentamicin at 37°C and 5% CO_2 for the remainder of the experiment.

2.5.2 *Salmonella* Infection of RAW264.7 Murine Macrophages

Salmonella infection of RAW 264.7 murine macrophages was adapted from a previously described protocol (Beuzón et al. 2000). RAW264.7 murine macrophages were seeded in 1 mL of media in a 24-well plate, at a density of $1x10^5$ cells/well, 24 h prior to infection. *Salmonella* strains were grown overnight at 37°C, 200 rpm in 5 mL Lennox LB with appropriate

antibiotics from glycerol stocks, before 30 µL of overnight culture was mixed with 20 µL mouse serum (Sigma) and 170 µL Complete RAW264.7 Medium for 20 min at room temperature to opsonise bacteria. Opsonised bacteria were diluted with 600 µL Complete RAW264.7 Medium before being used to infect the cells at a MOI of 10. Infected cells were then centrifuged at 100 g for 5 min to synchronise infection, before phagocytosis was allowed to occur for 25 min at 37°C and 5% CO_2. Cells were then washed three times with DPBS and incubated in 1 mL Complete RAW264.7 Medium containing 100 µg/mL gentamicin for 1 h at 37°C and 5% CO_2. The cells were then washed once with DPBS and incubated in 1 mL Complete RAW264.7 Medium containing 20 µg/mL gentamicin at 37°C and 5% CO_2 for the remainder of the experiment.

2.5.3 *Salmonella* Infection of THP-1 Human Monocytes

THP-1 human monocytes were differentiated into macrophages by seeding in a 6-well (BD Falcon) or 24-well plate at a density of $3.36x10^6$ cells/well or $7.5x10^5$ cells/well, respectively, with 250 nM or 162 nM phorbol 12-myristate 13-acetate (PMA; Sigma) 72 h prior to infection. The day before infection, the medium was removed and replaced with Complete THP-1 Medium without PMA. Prior to infection, THP-1 cells were washed three times with DPBS and incubated in 1 mL Complete THP-1 Medium without FBS (Serum-free THP-1 Medium).

Salmonella strains were grown overnight in 5 mL Lennox LB with appropriate antibiotics, at 37°C as static cultures from glycerol stocks, before being washed twice with phosphate-buffered saline (PBS). Cultures were normalised according to OD_{600} and used to infect THP-1 cells at a MOI of 10. Infected cells were centrifuged at 100 g for 5 min to synchronise infection, before phagocytosis was allowed to occur for 25 min at 37°C and 5% CO_2. Infected cells were then washed three times with DPBS and incubated in 1 mL Serum-free THP-1 Medium containing 100 µg/mL gentamicin for 1 h at 37°C and 5% CO_2. The cells were then washed once with DPBS and incubated in 1 mL serum-free THP-1 Medium containing 20 µg/mL gentamicin at 37°C and 5% CO_2 for the remainder of the experiment.

2.5.4 Colony Forming Unit Enumeration

Infected cells were washed three times with DPBS, before lysis using 1 mL of 0.1% (v/v) Triton X-100 (Sigma) in DPBS for 5 min at room temperature. Bacteria were then diluted in PBS and plated onto LB agar plates containing appropriate antibiotics.

2.5.5 Protein Expression during *S.* Typhi Infection

THP-1 cells were infected as above in 6-well plates. Infected cells were washed three times with DPBS before lysis with 150 µL 20% (v/v) glycerol (VWR Chemicals), 60 mM tris pH 6.8 (Sigma), 2% (v/v) SDS (Sigma), 5% (v/v) β-mercaptoethanol (Sigma) and 0.05% (w/v) bromophenol blue (Sigma) (2xSDS loading buffer). Samples were boiled for 10 min at 100°C, before analysis by western blot.

2.6 β-lactamase Translocation Assays

The β-lactamase translocation assays were adapted from a previously described protocol (Charpentier & Oswald 2004). HeLa cells were seeded in 200 µL of Complete HeLa Medium at a density of $3.5x10^4$ cells/well in black-walled 96-well plates (BD Biosciences). *Salmonella* strains containing pWSK29 vectors with TEM1-tagged proteins (Table 2.2) were grown overnight at 37°C, 200 rpm in 5 mL Lennox LB containing 100 µg/mL ampicillin, from glycerol stocks. Overnight cultures were diluted 1:33 in fresh Lennox LB containing 100 µg/mL ampicillin and grown at 37°C, 200 rpm until an OD_{600} of 1.8-2.0.

Salmonella cultures were then normalised according to OD_{600} and used to infect HeLa cells at a MOI of 100. Infected cells were then centrifuged at 500 g for 5 min to synchronise infection, before bacterial invasion was allowed to occur for 60 min at 37°C and 5% CO_2 to maximise translocation of T3SS effectors.

Complete HeLa Medium was replaced with 100 µL of 3 mM probenecid (Sigma), 20 mM HEPES in Hank's Balanced Salt Solution (HBSS; Gibco) (Probenecid Solution) and 20 µL CCF2-AM LiveBLAzer FRET – B/G loading kit (Invitrogen), before incubation at room

temperature, in the dark until 3 h post-infection. Probenecid was used to ensure that the CCF2-AM substrate was not secreted from the host cells.

After incubation with CCF2-AM LiveBLAzer FRET – B/G loading kit, cells were washed four times with Probenecid Solution before the fluorescence was measured using a FLUOstar Optima plate reader (BMG Labtech) with an excitation wavelength of 410 nm and emission wavelengths of 450 nm and 520 nm. Response ratios were calculated by first subtracting the average background fluorescence for both 450 nm and 520 nm wavelengths from the fluorescence reading for each sample. The ratio of fluorescence at 450 nm to fluorescence at 520 nm for each sample was then divided by the uninfected ratio of fluorescence at these wavelengths to give the final response ratio.

2.7 Paraformaldehyde Fixation of Cells

Infected or transfected cells were washed three times with DPBS before fixation with 3.2% paraformaldehyde (PFA; Agar Scientific) for 15-30 min at room temperature. Fixed cells were then washed twice and stored in DPBS at 4°C until required.

2.8 Staining of Fixed Cells for Immunofluorescence

Fixed cells were quenched in 50 mM ammonium chloride for 10 min at room temperature before permeabilisation with either 0.2% (v/v) Triton X-100 in DPBS or 0.1% (w/v) Saponin (Sigma) in DPBS for 4-30 min at room temperature. Saponin is a selective detergent, unlike Triton X-100, meaning that it will not permeabilise all host or bacterial cell membranes (Jamur & Oliver 2009). Cells were then washed twice with PBS before saturation with 0.2% (w/v) bovine serum albumin (BSA; Sigma) in DPBS for 5 min at room temperature. Once saturated, cells were incubated with primary antibodies (Table 2.4) diluted in 0.2% BSA in DPBS for 45-90 min at room temperature, in a humidified environment. Cells were washed twice with PBS for 5 min at room temperature, before saturation with 0.2% BSA in DPBS for 5 min at room temperature. Coverslips were then incubated with secondary antibodies (Table 2.4), as

Table 2.4. Antibodies used in this study.

Antibody	Origin	Dilution		Source
		Immunofluorescence	Western blot	
Primary antibodies				
SipD	Rabbit	-	1:5,000	Vassillis Koronakis
SipA	Rabbit	-	1:5,000	Vassillis Koronakis
SseB	Rabbit	-	1:2,000	Sophie Helaine
DnaK clone 8E2/2	Mouse	-	1:10,000	Enzo Life Sciences
Haemagglutinin (HA)	Rabbit	1:500	1:1,000	Sigma
HA.11 clone 16B12	Mouse	1:1,000	-	Cambridge Bioscience
β-lactamase (TEM1)	Mouse	-	1:1,000	QED Biosciences
Salmonella Common Structural Antigen (CSA) 1	Goat	1:200	-	Insight Biotechnology
Polyhistidine clone HIS-1 HRP	Mouse	-	1:2,000	Sigma
Ubiquitin clone FK2	Mouse	1:200	1:1,000	Enzo Life Sciences
NEDD8	Rabbit	1:200	-	Cell Signalling Technology
SUMO-1	Rabbit	1:100	-	Cell Signalling Technology
SUMO-2/3	Rabbit	1:100	-	Cell Signalling Technology
GFP	Rabbit	1:1,000	-	Abcam
Salmonella Vi-antigen	Mouse	-	-	Stratens Serum Institute
Secondary antibodies				
Anti-rabbit HRP	Goat	-	1:50,000	Jackson Immunoresearch
Anti-mouse HRP	Goat	-	1:1,000	Jackson Immunoresearch
Anti-mouse Alexa Fluor-488	Donkey	1:200	-	Jackson Immunoresearch
Anti-mouse RRX	Donkey	1:200	-	Jackson Immunoresearch
Anti-goat RRX	Donkey	1:200	-	Jackson Immunoresearch
Anti-goat Cy2	Donkey	1:200	-	Jackson Immunoresearch
Anti-rabbit Alexa Fluor-488	Donkey	1:200	-	Jackson Immunoresearch
Anti-rabbit RRX	Donkey	1:200	-	Jackson Immunoresearch

well as: Alexa Fluor-647 Phalloidin (1:100 dilution; Invitrogen) or Phalloidin-iFluor 647 conjugate (1:1,000 dilution; Stratech) and Hoechst 33258 (1:1,000 dilution; Sigma) diluted in 0.2% BSA in DPBS, for 30 min at room temperature in a dark, humidified environment. Cells were washed three times with PBS for 5 min at room temperature before mounting on microscope slides with Prolong Gold Antifade Reagent (Invitrogen). Stained cells were then viewed and analysed using Zeiss Axio Imager M1 or Zeiss Axio Observer Z1 (Carl Zeiss Microscopy) microscopes. If Saponin was used for permeabilisation, it was maintained throughout the staining protocol at a concentration of 0.1% (w/v) in DPBS.

2.9 *Salmonella SPI-1* Secretion Assays

The *SPI-1* secretion assay was adapted from a previously described protocol (Kaniga, Tucker, et al. 1995). *Salmonella* strains were grown overnight at 37°C, 200 rpm in 5 mL Lennox LB with appropriate antibiotics at 37°C, 200 rpm, from glycerol stocks. Overnight cultures were then diluted 1:33 into 50 mL fresh Lennox LB with appropriate antibiotics and grown to an OD_{600} of 1.8-2.0 to induce *SPI-1* expression and secretion. A 1 mL sample of the bacterial culture was then pelleted and resuspended in 10 µL 2xSDS loading buffer per OD_{600} of 0.1, for the expression sample. The remaining culture was cleared by centrifugation for 20 min at 4°C, 3,300 g, before the supernatant was filtered through a 0.2 µm filter to remove any bacteria. Proteins were precipitated from filtered supernatant by adding 10% (v/v) trichloroacetic acid (Sigma) and incubating at 4°C overnight. Precipitated proteins were collected by centrifugation for 15 min, 20,000 g at 4°C, before being washed twice with ice-cold acetone. Protein pellets were air-dried before being resuspended in 10 µL 2xSDS loading buffer per OD_{600} of 0.1, providing the secreted sample. Both the expression and secreted samples were then boiled for 10 min at 100°C, before analysis by western blot.

2.10 *Salmonella SPI-2* Secretion Assays

The *SPI-2* secretion assay was adapted from a previously described protocol (Beuzón et al. 2000; Yu et al. 2010). *Salmonella* strains were grown overnight at 37°C, 200 rpm in 5 mL

Lennox LB with appropriate antibiotics, from glycerol stocks. The next day, 120 µL of overnight culture was washed twice with 0.5 mL of 170 mM 2-(N-morpholino)ethanesulfonic acid (MES) (Sigma) pH 5.0, 7.5 mM ammonium sulfate (BDH Chemicals), 0.5 mM potassium sulfate (BDH Chemicals), 1 mM potassium dihydrogen orthophosphate (BDH Chemicals), 5 mM potassium chloride (Sigma), 8 µM magnesium chloride (Sigma), 38 mM glycerol (VWR) and 0.1% (w/v) casamino acids (BD Biosciences) (Mg-MES Medium pH 5.0). Washed bacteria were then grown in 5 mL Mg-MES Medium pH 5.0 overnight (*S.* Typhi) or for 4 h (*S.* Typhimurium) at 37°C, 200 rpm in a 50 mL centrifuge tube to induce *SPI-2* expression and secretion (Beuzón et al. 1999).

For *S.* Typhimurium, bacteria were then washed twice with 0.5 mL Mg-MES Medium pH 7.4 (same recipe as Mg-MES Medium pH 5.0, but the MES is buffered to a pH of 7.4 rather than 5.0) and then grown in 5 mL Mg-MES Medium pH 7.4 for 2 h at 37°C, 200 rpm. This causes dissociation of the *SPI-2* T3SS gatekeeper complex and secretion of effector proteins (Yu et al. 2010). This step was found to be unnecessary for *S.* Typhi secretion.

A 1 mL sample of the bacterial culture was then pelleted and resuspended in 10 µL 2xSDS loading buffer per OD_{600} of 0.1, for the expression sample and the remaining culture was discarded. Following secretion, effector proteins are bound to the inside of the centrifuge tube in which they are cultured (Beuzón et al. 1999), these were then washed twice with PBS to remove any residual bacteria and 10 µL of 2xSDS loading buffer per OD_{600} of 0.1 was added to the centrifuge tube and incubated at 37°C, 200 rpm for 1 h to dislodge the secreted proteins, to produce the secreted sample. Both the expression and secreted samples were then boiled for 10 min at 100°C, before analysis by western blot.

2.11 Protein Expression and Purification

2.11.1 StoD Variants

BL21 pLysS strains (Table 2.1) containing pET28a-*stoD* constructs (Table 2.2) were grown overnight at 37°C, 200 rpm in 5 mL LB with appropriate antibiotics, before being diluted 1:100

into 500 mL fresh LB with appropriate antibiotics and grown at 37°C, 200 rpm to an OD_{600} of 0.4-0.6. Protein expression was then induced with 1 mM isopropyl β-D-1-thiogalactopyranoside (IPTG; Sigma) and incubated at 30°C, 200 rpm for 6 h. Bacteria were collected by centrifugation and resuspended in 20 mM tris pH 7.9, 500 mM sodium chloride (Sigma) (His Lysis buffer) containing: 1 mg/mL chicken egg white lysozyme (Sigma), 25 Units benzonase nuclease (Novagen) per gram of bacterial pellet and cOmplete Mini EDTA-free protease inhibitor cocktail (Roche). Bacteria were then lysed using an EmulsiFlex B15 cell disruptor (Avestin). Soluble and insoluble fractions were separated by centrifugation at 40,000 g for 45 min at 4°C. Proteins were purified by affinity chromatography from the soluble fraction using His-bind Resin (Novagen) as follows: 2 mL of resin (4 mL of 50% slush) was allowed to settle in a plastic 5 mL column (Qiagen) before being equilibrated with three volumes of water and charged with five volumes of 50 mM nickel sulfate hexahydrate. The resin was then washed with three volumes of 20 mM tris pH 7.9, 500 mM sodium chloride and 5 mM imidazole (Sigma) (Binding buffer), before the soluble fraction was loaded onto the charged resin. The resin was washed with ten volumes binding buffer and six volumes 20 mM tris pH 7.9, 500 mM sodium chloride and 60 mM imidazole (Wash buffer). Proteins were eluted from the resin with six volumes of 20 mM tris pH 7.9, 500 mM sodium chloride and 1.5 M imidazole (Elution buffer). Protein fractions were collected and analysed by SDS-PAGE and Coomasie stain. Selected protein fractions were then dialysed using SnakeSkin dialysis tubing (10 K molecular weight cut off; Thermo Fisher Scientific) for 1-4 h and then again overnight in fresh His lysis buffer. Protein concentration was then determined using a NanoDrop 1000 (Thermo Fisher Scientific).

2.11.2 UBE2E1

UBE2E1 protein was either purchased from Ubiquigent, or produced in-house as follows. BL21 Star (Table 2.1) containing pET28b-*UBE2E1* (Table 2.2) were grown overnight at 37°C, 200 rpm in 5 mL LB with 50 µg/mL kanamycin before being diluted 1:100 in 500 mL fresh LB containing 50 µg/mL kanamycin, and grown at 37°C, 200 rpm to an OD_{600} of 0.4-0.6. Protein

expression was then induced with 1 mM IPTG and incubation at 37°C, 200 rpm for 3 h. Bacterial cells were collected by centrifugation and resuspended in His lysis buffer containing: 1 mg/mL chicken egg white lysozyme, 25 Units benzonase nuclease per gram of bacterial pellet and cOmplete Mini EDTA-free protease inhibitor cocktail. Bacteria were then lysed using an EmulsiFlex B15 cell disruptor. Soluble and insoluble fractions were separated by centrifugation at 40,000 g for 45 min at 4°C. Proteins were purified by affinity chromatography using an Äktaprime (GE Healthcare Life Sciences) with a 1 mL HiTrap TALON Crude column (GE Healthcare Life Sciences) from the soluble fraction. The column was equilibrated with 10 mL Binding buffer, before the soluble fraction was loaded onto the column, and then washed with 25 mL 20 mM tris pH 7.9, 500 mM sodium chloride and 30 mM imidazole before elution with a gradient of 20 mM tris pH 7.9, 500 mM sodium chloride and 1 M imidazole over 20 mL. The flow rate was maintained at 0.5 mL/min throughout equilibration and purification. Protein fractions were collected and analysed by Coomasie stain. Selected protein fractions were then dialysed using SnakeSkin dialysis tubing for 1-4 h and then again overnight in fresh 50 mM tris pH 7.9 and 150 mM sodium chloride. Protein concentration was then determined using a NanoDrop 1000.

2.11.3 UBE2L3

UBE2L3 protein was either purchased as part of the Ubc (E2) enzyme set (Boston Biochem) or produced in-house for substrate ubiquitination assays with StoD as follows. BL21 Star (Table 2.1) containing pGEX-*UBE2L3* (Table 2.2) were grown overnight at 37°C, 200 rpm in 5 mL LB with 100 µg/mL ampicillin before being diluted 1:100 in 500 mL fresh LB containing 100 µg/mL ampicillin, and grown at 37°C, 200 rpm to an OD_{600} of 0.4-0.6. Protein expression was then induced with 1 mM IPTG and incubation at 37°C, 200 rpm for 3 h. Bacterial cells were collected by centrifugation and resuspended in 50 mM Tris pH 8, 2 mM EDTA (Sigma), 10% (v/v) glycerol, 150 mM sodium chloride and 5 mM DL-dithiothreitol (DTT; Sigma) (GST lysis buffer) containing: 1 mg/mL chicken egg white lysozyme, 25 Units benzonase nuclease per gram of bacterial pellet and cOmplete Mini protease inhibitor cocktail (Roche). Bacteria

were then lysed using an EmulsiFlex B15 cell disruptor. Soluble and insoluble fractions were separated by centrifugation at 40,000 g for 45 min at 4°C. Proteins were purified by affinity chromatography using an Äktaprime with a 1 mL GSTrap 4B column (GE Healthcare Life Sciences) from the soluble fraction. The column was equilibrated with 10 mL GST lysis buffer at 0.3 mL/min, before the soluble fraction was loaded onto the column at 0.2 mL/min. The column was then washed with 20 mL 50 mM Tris pH 8, 2 mM EDTA, 10% (v/v) glycerol, 300 mM sodium chloride and 5 mM DTT at 0.3 mL/min, before elution with 20 mL 100 mM Tris pH 8, 150 mM sodium chloride, 5 mM DTT and 10 mM reduced glutathione (Sigma) at 0.3 mL/min. Protein fractions were collected and analysed by Coomasie stain. Selected protein fractions were then dialysed using SnakeSkin dialysis tubing for 1-4 h and then again overnight in fresh 50 mM tris pH 8, 150 mM sodium chloride and 1 mM DTT. Protein concentration was then determined using a NanoDrop 1000.

2.12 Autoubiquitination Assays

The ability of StoD to autoubiquitinate was assessed using a protocol adapted from the E2 Scan Kit (Ubiquigent) (Ubiquigent 2013). Variants of StoD were incubated at a concentration of 1 µM with 0.1 µM His_6-UBE1 (Ubiquigent), 100 µM ubiquitin (Ubiquigent) or biotinylated ubiquitin (Boston Biochem), 0.05 nmoles His_6-UBE2E1 in 50 mM HEPES pH 7.5, 5 mM $MgCl_2$ (Sigma) and 5 mM DTT (Sigma) with or without 2 mM ATP (Thermo Fisher Scientific) for 1 h at 30°C. The reaction was then stopped by adding 50% (v/v) glycerol, 0.3 M tris pH 6.8 (Sigma), 10% (w/v) SDS (Merck), 5% (v/v) β-mercaptoethanol (Sigma) and 0.05% (w/v) bromophenol blue (5xSDS loading buffer) and boiled for 5 min at 100°C before analysis by western blot.

2.13 SDS-PAGE, Western Blotting and Coomasie Staining

Samples for western blot or Coomasie staining were run on discontinuous sodium dodecyl sulfate polyacrylamide gel electrophoresis (SDS-PAGE) gels using Tris-Glycine-SDS running buffer (Geneflow) before: incubation in InstantBlue Protein Stain (Expedeon) for Coomasie

staining, or transfer onto polyvinylidene difluoride (PVDF) membrane (GE Healthcare) for western blotting. PVDF membrane was activated for 5 min with methanol before transfer using Tris-Glycine-Ethanol transfer buffer (Geneflow). Once transferred, membranes were saturated with PBS containing 0.05% (v/v) Tween 20 (PBST; Sigma) and 5% (w/v) semi-skimmed milk powder (Sigma) before incubation with primary antibodies (Table 2.4) diluted in either PBST containing 5% semi-skimmed milk powder or PBST containing 3% (w/v) BSA for between 2 h and overnight. Membranes were then washed twice with PBST before incubation with secondary antibodies (Table 2.4) diluted in either PBST containing 5% semi-skimmed milk powder or PBST containing 3% BSA for 1-3 h. Western blots were visualised by the addition of EZ-ECL detection solution (Geneflow) for 3 min and developed using a LAS-3000 imager (Fuji).

2.15. Transformation of *S. cerevisiae*

The protocol for transformation of *S. cerevisiae* was adapted from a previously published method (Agatep et al. 1998). AH109 or BY4741 *S. cerevisiae* strains (Table 2.1) were streaked onto 10 g/L yeast extract (Merck), 20 g/L bacto peptone (BD Biosciences), 2% (v/v) dextrose (Sigma), 0.003% (v/v) adenine (Sigma) and 50 µg/mL kanamycin, to prevent bacterial contamination (YPDA), agar plates and grown at 30°C for 2-3 days. One colony from this plate was used to inoculate 10 mL YPDA broth and then grown overnight at 30°C, 200 rpm. The overnight culture was then diluted 1:10 into 50 mL fresh YPDA broth per 10 transformations and grown at 30°C, 200 rpm for 4 h. *S. cerevisiae* cells were collected by centrifugation at 3,300 g for 5 min, before being washed with sterile water. *S. cerevisiae* cells were again collected by centrifugation at 3,300 g for 5 min before being resuspended in 1 mL 100 mM lithium acetate (Sigma). *S. cerevisiae* cells were then collected by centrifugation at 20,000 g for 15 s, before resuspension in 50 µL 100 mM lithium acetate per transformation, and aliquoted into separate microcentrifuge tubes for each transformation. *S. cerevisiae* cells were again collected by centrifugation at 20,000 g for 15 s and the lithium acetate removed.

Each aliquot of *S. cerevisiae* cells was then resuspended in 240 µL 50% (w/v) polyethylene glycol, 36 µL 1 mM lithium acetate, 25 µL 2 mg/mL herring sperm DNA (Sigma); boiled and cooled prior to use, 50 µL sterile water and 0.1-10 µg of purified vector (Table 2.2). *S. cerevisiae* cells were then incubated at 30°C for 30 min, before heat shock at 42°C for 20-25 min. *S. cerevisiae* cells were collected by centrifugation at 20,000 g for 15 s, before resuspension in sterile water and plated onto synthetic dextrose (SD) agar plates containing 6.7 g/L yeast nitrogen base without amino acids (BD Biosciences), 2% (v/v) glucose and appropriate nutrients to select for the transformants.

2.16. Yeast Two-Hybrid

AH109 *S. cerevisiae* (Table 2.1) was transformed with the pGBKT7-*stoD*$_{P204K}$ vector (Table 2.2), as described above, and used to perform a yeast two-hybrid (Y2H) screen with the Mate & Plate HeLa S3 Normalised Library (Clontech). Prior to the use of this AH109 strain in the Y2H screen, control experiments were used to assess its suitability.

2.16.1. Control experiment – Autoactivation test

To assess if StoD$_{P204K}$ was capable of activating the reporter genes within AH109 in the absence of an interacting partner an autoactivation test was used. AH109 *S. cerevisiae* containing either empty pGBKT7 vector (Table 2.2) or pGBKT7-*stoD*$_{P204K}$ were streaked onto SD agar lacking L-tryptophan (SD/-Trp), to maintain the pGBKT7 vectors, and grown at 30°C for up to 3 days. One colony was then used to inoculate 10 mL SD/-Trp broth containing 50 µg/mL kanamycin and grown overnight at 30°C, 200 rpm. These cultures were then streaked onto SD agar lacking adenine, L-histidine and L-tryptophan (SD/-Ade/-His/-Trp), to assess autoactivation of reporter genes, and SD/-Trp agar plates and incubated at 30°C for up to 5 days prior to imaging.

2.16.2. Control experiment – Toxicity test

To assess if the expression of $StoD_{P204K}$ caused a growth defect in AH109, a toxicity test was used. AH109 *S. cerevisiae* containing either empty pGBKT7 vector or pGBKT7-*stoD*$_{P204K}$ (Table 2.2) were streaked onto SD/-Trp agar, to maintain the vectors, and grown at 30°C for up to 3 days. One colony was then used to inoculate 10 mL SD/-Trp broth containing 50 µg/mL kanamycin and grown overnight at 30°C, 200 rpm. This culture was then diluted to an OD_{600} of 0.1 in a 96-well plate and incubated at 30°C with shaking and OD_{600} readings taken every 30 min in a FLUOstar Optima plate reader.

2.16.3. Y2H Screen

AH109 *S. cerevisiae* containing pGBKT7-*stoD*$_{P204K}$ (Table 2.2) was streaked onto a SD/-Trp agar and grown at 30°C for 3 days, before one colony was used to inoculate 50 mL SD/-Trp broth and grown at 30°C, 200 rpm until an OD_{600} of 0.8. *S. cerevisiae* cells were collected by centrifugation at 3,000 g for 5 min and resuspended in 5 mL SD/-Trp broth. This was combined with 1 mL of the library strain and made up to 50 mL with 20 g/L yeast extract, 40 g/L bacto peptone, 4% (v/v) dextrose and 0.006% (v/v) adenine containing 50 µg/mL kanamycin (2xYPDA broth) and grown at 30°C, 30 rpm for 24 h or until zygotes were observed. *S. cerevisiae* cells were collected by centrifugation at 3,000 g for 10 min before resuspension in 10 mL 5 g/L yeast extract, 10 g/L bacto peptone, 1% (v/v) dextrose and 0.0015% (v/v) adenine containing 50 µg/mL kanamycin (0.5xYPDA broth) and plated onto SD agar plates lacking L-leucine, L-tryptophan, L-adenine and containing X-α-Gal (Clontech) (QDO). Plates were incubated at 30°C for 14 days and the development of colonies was observed.

The cDNA insert from these colonies was amplified using One*Taq* 2X Master Mix (New England Biolabs) using the pGADT7-FW and pGADT7-REV primer pair (Table 2.3), before sequencing. The vectors of shortlisted hits were isolated using the Plasmid Miniprep Kit I (Peqlab) according to the manufacturer's instructions with one addition: during the incubation

in the RNA lysis buffer, glass beads (Sigma) were added and vortexed for 5 min to aid in the lysis of *S. cerevisiae* cells.

2.16.4. Direct Y2H assays

For direct Y2H assays, AH109 *S. cerevisiae* was co-transformed, as described above, with 500 ng of both pGBKT7-*bait* and pGADT7-*prey* vectors (Table 2.2) and plated onto SD agar plates lacking L-leucine and L-tryptophan (DDO) to select for co-transformants. Transformants were allowed to grow for 3 days at 30°C before being resuspended in sterile water and spotted onto DDO and QDO plates to assess the interaction of bait and prey proteins.

2.16 Yeast Toxicity Assays

BY4741 *S. cerevisiae* (Table 2.1) containing pYes2 constructs (Table 2.2) were grown at 30°C, 200 rpm in SD media lacking L-uracil overnight to maintain the pYes2 vector. BY4741 cultures were then diluted in PBS before plating onto SD agar plates lacking L-uracil with either glucose or galactose as a carbon source to either repress or induce expression of the pYes2 construct, respectively.

2.14 Genome-Wide Machine-Learning

The genome-wide machine-learning algorithm was run by Professor Tal Pupko and Dafna Shkedy of Tel Aviv University, Israel and was adapted from previously published work (Burstein et al. 2009; Lifshitz et al. 2014; Burstein et al. 2015; Teper et al. 2016). Briefly, a training set of open reading frames (ORFs), containing both known T3SS effectors and non-effector proteins were used to train the algorithm to characterise effectors and differentiate them from non-effector ORFs according to a number of features. The list of known effectors contained those validated in other *Salmonella* serovars, but excluded those that are absent or pseudogenes in *S.* Typhi. StoD was also included as a T3SS effector ORF as this represented the first putative effector present in *S.* Typhi and not *S.* Typhimurium (Fookes et al. 2011) and may enable the identification of other effectors that are not present in *S.* Typhimurium. The

non-effector list was curated using UniProt (http://www.uniprot.org/), to identify ORFs with a subcellular localisation defined as either 'cytoplasm' or 'cell inner membrane'. In total, the training set contained 23 known effectors and 29 non-effectors (Table 4.1). The classification algorithms then used the data from the training set to classify all ORFs within the Ty2 *S.* Typhi genome (NCBI Accession number: NC_004631.1) as to the likeliness of the ORF containing a T3SS effector. The classification algorithms used were: Naïve Bayes classifier, Bayesian Network, Sequential Minimal Optimisation and Random Forest. The scores from the different classification algorithms were then averaged (Vote classifier) and weighted according the performance of each algorithm based on the area under the precision-recall curve (wVote). The ORFs of the Ty2 genome were then ranked according to descending wVote value (and therefore decreasing likeliness of encoding a T3SS effector).

2.15 Bioinformatics

Bacterial transcriptional promoters were identified using BPROM (Solovyev & Salamov 2011). Nucleotide Basic Local Alignment Search Tool (BLAST) searches were performed using default settings (Boratyn et al. 2013) from the National Centre for Biotechnology Information (NCBI) website (https://blast.ncbi.nlm.nih.gov/Blast.cgi). The Kyoto Encyclopaedia of Genes and Genomes (KEGG) (Kanehisa et al. 2016) and NCBI website were used to retrieve sequences for sequence alignments performed using Clustal Omega (Sievers et al. 2011) and formatted using Strap (Gille et al. 2014). Genomic localisation of novel effector proteins was determined in Ty2 *S.* Typhi strain using SyntTax with default settings (Oberto 2013). The presence of any domains or motifs within novel effector proteins was determined using InterPro with default settings (Finn et al. 2017).

2.17. Statistical Analyses

All data was analysed using GraphPad Prism 7 (GraphPad Software).

Chapter 3: Establishing a Containment Level 3 Laboratory for the Study of *S.* Typhi

3.1. Introduction

In the United Kingdom, *S.* Typhi is classified as a hazard group 3 biological agent by the Health and Safety Executive (HSE), meaning that it must be handled in a laboratory that complies with the Advisory Committee on Dangerous Pathogens (ACDP) CL3 (HSE 2013). In addition to this, *S.* Typhi is listed under Schedule 5 of the Anti-terrorism, Crime and Security Act 2001, meaning that it may *"pose the greatest risk to human life if misused by terrorists"* (Crown 2001). For these reasons, much of the work studying *Salmonella* is performed using *S.* Typhimurium, a hazard group 2 biological agent, which requires less specialised facilities and security provisions. However, it was deemed necessary that if novel *S.* Typhi T3SS effector proteins, such as StoD, were going to be identified and studied, then this should be performed using *S.* Typhi, wherever possible, and consequently a CL3 laboratory was required. At the beginning of this project, Imperial College London did not possess a CL3 laboratory that would allow the use of *S.* Typhi and therefore, such a laboratory was established by my colleague, Rebecca Johnson and myself, an accomplishment for which we were awarded the Student Prize for Excellence in Health and Safety from the Faculty of Natural Sciences at Imperial College London.

In this chapter, I will provide an overview of the different hazard groups as classified by the HSE, the requirements for a CL3 laboratory suitable for the handling and study of *S.* Typhi, and preliminary work to adapt experimental protocols for use.

3.2. Hazard Group Definitions and Containment Levels

The approved list of biological agents is a resource, provided by the HSE, detailing all the biological agents that may be used within the UK, and provides guidance on how these should be handled to minimise the possibility of infection or injury (HSE 2013). As part of this, each biological agent is provided with a hazard group classification (Table 3.1) that describes how

Table 3.1. Hazard group classifications. Adapted from (HSE 2013).

Hazard Group	Likeliness to cause human disease	Severity of disease	Possibility of spread through community	Effective prophylaxis or treatment available?	Containment level required
1	Low	Low	Unlikely	Yes	≥1
2	Medium	Medium	Unlikely	Yes	≥2
3	High	High	Likely	Yes	≥3
4	Very high	Very high	Very likely	No	4

likely it is to cause human disease, the severity of the disease, the risk of spread within the community, and whether there are methods for preventing or treating any resulting disease (HSE 2013). As previously mentioned, *S.* Typhi is classified as a hazard group three biological agent as it results in a serious disease, but there are two different prophylactic vaccines available (WHO 2008), as well as effective antibiotic therapy. *S.* Typhimurium is classified as hazard group two, because although it is potentially hazardous when handled, the disease outcome is considerably less severe and effective treatment is readily available.

The hazard group in which a biological agent is classified then determines which containment level is required (Table 3.1). For example, a hazard group two biological agent must be handled at a minimum of containment level two (CL2), whereas a hazard group three organism must be handled at a minimum of CL3 (HSE 2013). The main differences between a CL2 and a CL3 laboratory are (HSE 2005):

- A CL3 laboratory must be maintained at a negative air pressure compared to the atmosphere.
- All air leaving a CL3 laboratory must be filtered using a high efficiency particulate absorption filter.
- A CL3 laboratory should contain its own equipment, and must be separated from any other activities.

- Any handling of biological agents in a CL3 laboratory must be performed inside a microbiological safety cabinet (MSC).
- A CL3 laboratory must be sealable to allow disinfection.

As previously mentioned, *S.* Typhi is also listed under Schedule 5 of the Anti-terrorism, Crime and Security Act 2001 (Crown 2001) which includes another set of provisions that must be considered on top of the CL3 requirements. These features cannot be discussed here for reasons of security; however, inspections are routinely carried out by the Metropolitan Police Service to ensure that the CL3 laboratory is secure and all security requirements are adhered to.

Anyone wishing to work with a hazard group three organism must apply to the HSE and be granted permission before any work can begin. After this, an application to Imperial College must also be made. Permission to work with *S.* Typhi was obtained by Professor Gad Frankel and Dr Valerie Crepin prior to the beginning of my PhD and will therefore not be discussed here.

3.3. Code of Practice: The Use of the CL3 Laboratory to Work with *S.* Typhi

Before work with *S.* Typhi could begin, a Code of Practice (COP) was written, which in conjunction with a Bio1 risk assessment, details the scope of the work that can be carried out using *S.* Typhi, and how this should be performed. This includes information regarding health surveillance and vaccinations, personnel training, details for disposal of any waste generated within the CL3, emergency procedures and all standard operating procedures (SOPs) for manipulation of *S.* Typhi.

3.3.1. Health Surveillance and Vaccinations

All researchers working with *S.* Typhi must first undergo a health assessment by the Occupational Health department at Imperial College London. The aim of this assessment is to identify any pre-existing health conditions that could potentially increase the risk of developing an infection with *S.* Typhi.

Upon completion of this initial health assessment all researchers are enrolled upon a health surveillance program to monitor them in the event of an accident that results in infection. All researchers must also undergo vaccination against *S.* Typhi. Initially this was using the Vi-antigen vaccine, however, this was rendered ineffective by the later expansion of the scope of work to include the use of Vi-negative strains of *S.* Typhi. This meant that an alternative vaccine, the live-attenuated Ty21a vaccine, had to be administered, which provides protection against both Vi-positive and Vi-negative strains (Dougan & Baker 2014). It is now standard procedure for researchers to only receive the live-attenuated vaccine.

3.3.2. CL3 Laboratory Training

Training to work in the CL3 laboratory involved working with the Biosafety department at Imperial College London and covered how to work safely within the CL3 laboratory, and developing an understanding about the systems that were in place to ensure that the risk of infection is minimised. This includes the use of MSCs for all manipulation of infectious material, and how to fumigate the MSCs, as well as how to deal with the spillage of infectious material both inside and outside of a MSC, and what to do in the event of the contamination of any personal protective equipment.

Following training, initial work was performed using *S.* Typhimurium to allow researchers to gain confidence and to identify any alterations that needed to be made to SOPs for them to be suitable for use in the CL3 laboratory.

A training record was then produced that details any relevant training courses, enrolment onto the health surveillance program, vaccination and competency to carry out SOPs. This record

demonstrates competency to work at CL3 with *S.* Typhi and is continually updated with any further related training that is undertaken. This allows us to confirm that before someone is allowed to work independently in the CL3 laboratory, they are competent to do so.

3.3.3. Producing SOPs for Work Involving *S.* Typhi

All protocols that are used in the CL3 laboratory must first be documented and approved by the Biosafety team before they can be put into practice. This ensures that all protocols have considered any activity that could increase the risk of infection to anyone using the procedure. The Biosafety team also oversee the purchase of any new equipment purchased for the CL3 laboratory to ensure suitability and a protocol for its use must first be written and approved before the equipment can be acquired.

The protocols are called *Salmonella* SOPs (SSOPs) and explain how to perform each procedure in a step-by-step manner, including how to disinfect any material that is to be taken out of the MSC and how to proceed in the event of a spillage (Figure 3.1). SOPs also highlight whether a procedure or part of it, must be performed in a particular MSC, as well as indicating where other SOPs should be consulted in relation to certain steps (Figure 3.1). The SOP also states how any material that is required to be removed from the CL3 laboratory should be tested for sterility to ensure that live *S.* Typhi is not removed from the laboratory.

At present, there are 31 SOPs within the *S.* Typhi COP which were written either by myself or Rebecca Johnson and approved by the Biosafety team. For all new researchers joining the group, all relevant SOPs must be performed in a CL2 laboratory using *S.* Typhimurium and competency assessed, before they can perform them in the CL3 laboratory with *S.* Typhi. Competency with regards to each SOP is then detailed within the researchers training record.

3.3.4. Practical Considerations for Work with *S.* Typhi in a CL3 Laboratory

The CL3 laboratory contains two MSCs (Figure 3.2A), one Class 1 and one Class 2. As mentioned previously, the SOP states whether a particular MSC should be used for a specific procedure (Figure 3.1). The details of the differences between a Class 1 and Class 2 MSC will

15.14 SSOP14: SPI-1 secretion assay

As this assay requires the manipulation of large culture volumes (50ml total), steps 1-8 should be performed within the Class I MSC where possible. From step 8 onwards, all further steps MUST be performed in the Class I MSC.

1. Grow 5ml o/n culture of *S.* Typhi strains according to **SSOP1.**
2. Take the container to the MSC. Open the container and check for any sign of leakage.

In the event of a leakage contained within the secondary container 3% Virkon should be added and the container left for 30 minutes in the MSC. After this time, contaminated material should be disposed of in the disposable autoclave jars/boxes within the MSC and the secondary container disinfected with 70% ethanol.

3. Mix o/n by swirling the culture and dilute 1:33 (1.51 mL) in 50 mL fresh Lennox LB containing appropriate antibiotics (±0.3M NaCl) in a 125 mL non-vented conical flask.
4. Place the conical flask in a sealed secondary container padded with tissue paper to minimise movement within biohazard pot.
5. Disinfect gloves and the outside of the secondary container with 70% ethanol, remove from MSC and secure in the shaking incubator.
6. Incubate for 3 hr at 37°C, 200 rpm (until OD_{600} = 1.8 to 2.0).
7. Take the container to the Class I MSC. Open the container and check for any sign of leakage.

In the event of a leakage contained within the secondary container 3% Virkon should be added and the container left for 30 minutes in the MSC. After this time, contaminated material should be disposed of in the disposable autoclave jars/boxes within the MSC and the secondary container disinfected with 70% ethanol.

8. Record OD_{600} of each subculture according to **SSOP12.**
9. Take 1 mL and centrifuge at 13,200 rpm for 1 minute to pellet bacteria according to **SSOP5.**
10. Discard supernatant into waste centrifuge tube inside the MSC and resuspend pellet in 10 µl of 2x SDS loading buffer per 0.1 OD_{600} of the subculture. This is the pellet fraction. *E.g. a subculture OD_{600} of 1.8 would require resuspension in 180 µl 2x SDS loading buffer.*
11. Centrifuge the remaining culture at 4000 rpm for 5 minutes according to **SSOP5.**
12. Filter sterilise the cleared supernatant using centrifugation filter unit (0.22µM) according to **SSOP5**.
13. Disinfect gloves and the outside of the 50 mL centrifuge tube with 70% ethanol and remove from MSC.
14. Boil the pellet fraction sample in a heat block at 100°C for 10 minutes.

The sterility of the pellet fraction and the filter sterilised supernatant has been confirmed by plating 10µl on LB plates followed by incubation at 37°C overnight. No growth was observed. These sterility tests must be repeated each time the protocol is used and before the samples are taken out of the CL3 lab.

Figure 3.1. SOPs for use in the CL3 laboratory. An example SSOP used in the CL3 laboratory. SSOPs identified in red, indicate a reference to another SSOP that should be consulted. Emergency procedures are highlighted in bold and details of how sterility was, and should be demonstrated are shown in italics at the end of the SOP.

not be discussed in detail here, but the handling of any *S.* Typhi culture greater than 25 mL in volume, or any manipulations that would disturb the airflow of the MSC, such as vortexing, must be performed inside the Class 1 MSC, as this provides the greatest protection to the user. The Class 2 MSC provides limited protection to the user but does protect the samples and therefore tends to be used for any procedure that requires the samples to be kept sterile, such as infections of tissue culture cell lines. Inside each MSC is a set of pipettes, a Bio-bin,



Figure 3.2. A CL3 laboratory for handling *S.* Typhi. **(A)** A photograph of the CL3 laboratory used for work with *S.* Typhi. **(B)** A photograph of the Class I MSC. **(C)** A photograph of the Class II MSC. **(D)** An image of the tube top filter units used for sterilising larger volumes (>0.5 mL) of liquid *S.* Typhi cultures. Image taken from the Sigma Aldrich website (Sigma 2017). **(E)** Photographs of the inside (left) and outside (right) of a secondary container used for growing liquid cultures of *S.* Typhi.

racks, a bottle of 70% ethanol, a bottle of 3% Virkon solution and a container for any liquid waste (Figure 3.2B and C). Pipettes are kept inside the MSCs, and only removed after fumigation due to the risk of contamination of the internal workings of the pipettes, that cannot be addressed by surface decontamination with 70% ethanol or 3% Virkon. The Bio-bin is used for disposal of any solid waste generated within the MSC, including: pipette tips, plates and cuvettes, amongst other items. These Bio-bins are then enclosed within two autoclavable bags and undergo surface decontamination before removal from the MSC. Any liquid waste generated within the MSC is contained within separate suitable containers. Volumes greater than 50 mL must first be treated with Virkon before being removed from the MSC and autoclaved. Racks are kept inside the MSC for general use but can be removed after surface decontamination, provided there have been no spillages of infectious material. In this case, any contaminated racks are submerged in 3% Virkon solution for at least 30 min before wiping with 70% ethanol and removal from the MSC. The spray bottles of 70% ethanol and 3% Virkon solution are kept inside the MSC, and are used for surface decontamination of anything that is being removed from the MSC, including an individual's gloved hands, after handling anything inside the MSC. The 3% Virkon solution is also for dealing with any small spillages inside the MSC.

The Class 2 MSC contains all items mentioned above as well as a vacuum pump system used for the removal of liquid, such as that generated during *S.* Typhi infection of tissue culture cell lines (Figure 3.2C). This liquid waste is constantly treated with Virkon and is removed from the MSC and autoclaved when full. It should also be noted that the vacuum pump itself is located outside of the MSC due to space constraints meaning that the extract tubing from the vacuum pump waste bottle has to leave the MSC. For this reason, a 0.2 µm filter was introduced into the extract line to ensure that no infectious material leaves the MSC by this means.

Certain procedures require the removal of liquid samples from the CL3. Whilst for particular protocols, any infectious material is lysed using SDS loading buffer and then boiled, other procedures are not compatible with this. One example is the *SPI-1* secretion assay (Figure

3.1), where upwards of 10 mL of cleared culture supernatant must be sterilised before removal from the CL3 and further processing elsewhere. The most convenient method of sterilising these samples is through a 0.2 µm filter using a syringe. However, due to the risks associated with using syringe-filtration, namely over-pressurisation of the filter unit resulting in expulsion of infectious material, this is not permitted in the CL3 laboratory. Due to this restriction, tube top vacuum filters (Figure 3.2D) are used to filter larger (>0.5 mL) volumes, whereas smaller volumes (<0.5 mL) are filtered using centrifugal filter units. Both methods draw the solution through a 0.2 µm filter and collect the filtrate in a sterile container, but just differ in what method is used to draw the solution through the filter.

Some protocols require infectious material to be removed from the MSC, such as overnight cultures and incubation of infected cell lines. However, in the CL3 laboratory, infectious material cannot be stored outside of the MSC in just the primary container: the centrifuge tube or tissue culture plate, in case there is a leak that would result in the escape of any infectious material. To address this issue, all infectious material is double contained within sealable, plastic containers (Figure 3.2E) in case the primary container fails, to prevent the release of any infectious material into the laboratory.

Due to the required isolation of CL3 work from any other laboratory (HSE 2005), several pieces of equipment and consumables also had to be obtained (Appendix 3) and were carefully assessed before being taken into the CL3 laboratory. For example, the buckets used in the centrifuge required rubber O-rings to ensure that these are sealed and that any breakage within the bucket would be contained. These O-rings are also present on secondary containers mentioned above. Another example was the use of an electroporator that allowed the power supply to be kept outside of the MSC, whilst only the cuvette chamber was required inside the MSC. This was to ensure that cuvettes containing *S.* Typhi were not removed from the MSC, in the event the electric pulse caused aerosolisation of the bacterial culture. These adaptations required consideration to ensure any new equipment was suitable for use in the CL3 laboratory.

Therefore, whilst certain procedures had to be modified for use in the CL3 laboratory, this has meant that a greater understanding of these protocols has been gained, enabling them to be tailored to better suit the requirements of the experiment.

3.4. Preliminary Work involving *S.* Typhi

Once the CL3 laboratory had been established, and all researchers had undergone the appropriate training, work with *S.* Typhi could begin. Professor Gordon Dougan at the Wellcome Trust Sanger Institute, Cambridge, provided two reference *S.* Typhi strains (Ty2 and CT18), as well as three clinical isolates from the H58 (ERL12148 and 129-0238) and non-H58 lineages (Lupe Gen0059).

3.4.1. Determination of the Antibiotic Susceptibilities of Several *S.* Typhi Strains

Determination of the antibiotic susceptibility profile of the *S.* Typhi strains that had been acquired was assessed to inform which antibiotics would be suitable for use in antibiotic-based selection techniques.

All strains were grown overnight as liquid cultures in Lennox LB supplemented with different antibiotics and growth was confirmed by visual inspection (Table 3.2). The antibiotics chosen are all routinely used within the research setting.

S. Typhi Ty2 was found to been sensitive to almost all the antibiotics tested, except the quinolone antibiotic, nalidixic acid. The second reference strain, CT18 was resistant to chloramphenicol, tetracycline, nalidixic acid and the β-lactam, ampicillin. The H58 clinical isolates showed differential sensitivities to the antibiotics tested: ERL12148 was resistant to chloramphenicol, ampicillin and nalidixic acid, whereas, 129-0238 was only resistant to ampicillin. The final clinical isolate, Lupe Gen0059, was sensitive to all antibiotics tested.

In terms of future work, this was very informative. The plasmid containing the λ Red Recombinase for introducing genomic mutations contains an ampicillin-resistance cassette

Table 3.2. Antibiotic sensitivity profiles of *S.* Typhi strains. Antibiotic sensitivity was assessed visually after overnight growth in chloramphenicol (Cm), kanamycin (Kn), tetracycline (Tet), gentamicin (Gent), spectinomycin (Spec), ampicillin (Amp) or nalidixic acid (Nal). Concentration of antibiotic is shown in brackets. S – sensitive, R – resistant.

Strain	Cm (30 µg/mL)	Kn (50 µg/mL)	Tet (50 µg/mL)	Gent (10 µg/mL)	Spec (50 µg/mL)	Amp (100 µg/mL)	Nal (50 µg/mL)
Ty2	S	S	S	S	S	S	R
CT18	R	S	R	S	S	R	R
ERL12148	R	S	S	S	S	R	R
129-0238	S	S	S	S	S	R	S
Lupe Gen0059	S	S	S	S	S	S	S

(Table 2.2) (Datsenko & Wanner 2000). This would therefore be unsuitable for use with CT18 and the H58 clinical isolates, but would be appropriate for use with Ty2 and Lupe Gen0059. However, a pKD46 variant is available that contains a gentamicin-resistance cassette, an antibiotic that all strains were sensitive to, which could be used for these ampicillin-resistant strains. None of the *S.* Typhi strains showed resistance to kanamycin, meaning that the kanamycin resistance cassette within pKD4 used to make genomic deletions would be suitable for all strains (Table 2.2). The complementation vector used for work with *Salmonella*, pWSK29, contains an ampicillin-resistance cassette (Table 2.2) (Wang & Kushner 1991), meaning it would be unsuitable for use with CT18 and the H58 strains. Therefore, a pWSK29 variant containing a spectinomycin resistance cassette was generated that could be used with all *S.* Typhi strains. Finally, the infection protocols used with *Salmonella* are based upon the gentamicin-protection assay (Weinstein et al. 1998). Since all *S.* Typhi strains were sensitive to gentamicin, this meant these protocols could still be used.

Therefore, understanding the antibiotic susceptibilities of the *S.* Typhi strains aided in the development of future experimental methodologies.

3.4.2. Optimisation of Protocols for Use with *S.* Typhi

There were several protocols that would be routinely used with *S.* Typhi that had to be adapted from use with *S.* Typhimurium and optimised for *S.* Typhi. These included infection of human epithelial and macrophage cells lines, as well as *SPI-1* and *SPI-2* secretion assays.

3.4.2.1. Optimising infection of human epithelial cells with *S.* Typhi

An invasion protocol for epithelial cells that was robust and provided maximal invasion with *S.* Typhi was required to allow the assessment of how particular genes influence *S.* Typhi invasion of host cells.

Firstly, varying the MOI of Ty2 *S.* Typhi used to infect HeLa cells was assessed (Figure 3.3A). All bacteria were subcultured in fresh Lennox LB and grown to late exponential phase before being used to infect HeLa cells for 15 min. Cells were then treated with gentamicin to kill any extracellular bacteria, as described elsewhere (Beuzón et al. 2000). Cells were then lysed at 2 h post-infection, CFU enumerated and compared to the inoculum to calculate the percentage invasion. Wild-type (WT) and Δ*prgH S.* Typhimurium were used as controls. WT *S.* Typhimurium invasion was highest at 0.2% and Δ*prgH S.* Typhimurium the lowest with 0% invasion. This is to be expected as PrgH is a structural component of the *SPI-1* T3SS (Figure 1.4) which has been shown to be required for invasion of epithelial cells (Galán & Curtiss 1989). *S.* Typhi showed an increase in invasion with increasing MOI from 0.03% at an MOI of 50 up to 0.05% at an MOI of 300.

It was then investigated if increasing the length of the assay could increase *S.* Typhi invasion of HeLa cells (Figure 3.3B). A MOI of 100 was used to infect HeLa cells for either 15, 30 or 60 min before treatment with gentamicin. The length of invasion was not increased passed 60 min to ensure that the gentamicin treatment had sufficient time to kill any extracellular bacteria, prior to the 2 h timepoint used to assess bacterial invasion. Based on previous experiments, an MOI of 100 was chosen as this should not lead to the cells being over-encumbered with bacteria and should therefore reduce the amount of invasion-associated cell

death. As anticipated, by increasing the length of time the bacteria were allowed, the amount of invasion also increased, from 0.03% with 15 min infection up to 0.08% invasion with 60 min infection.

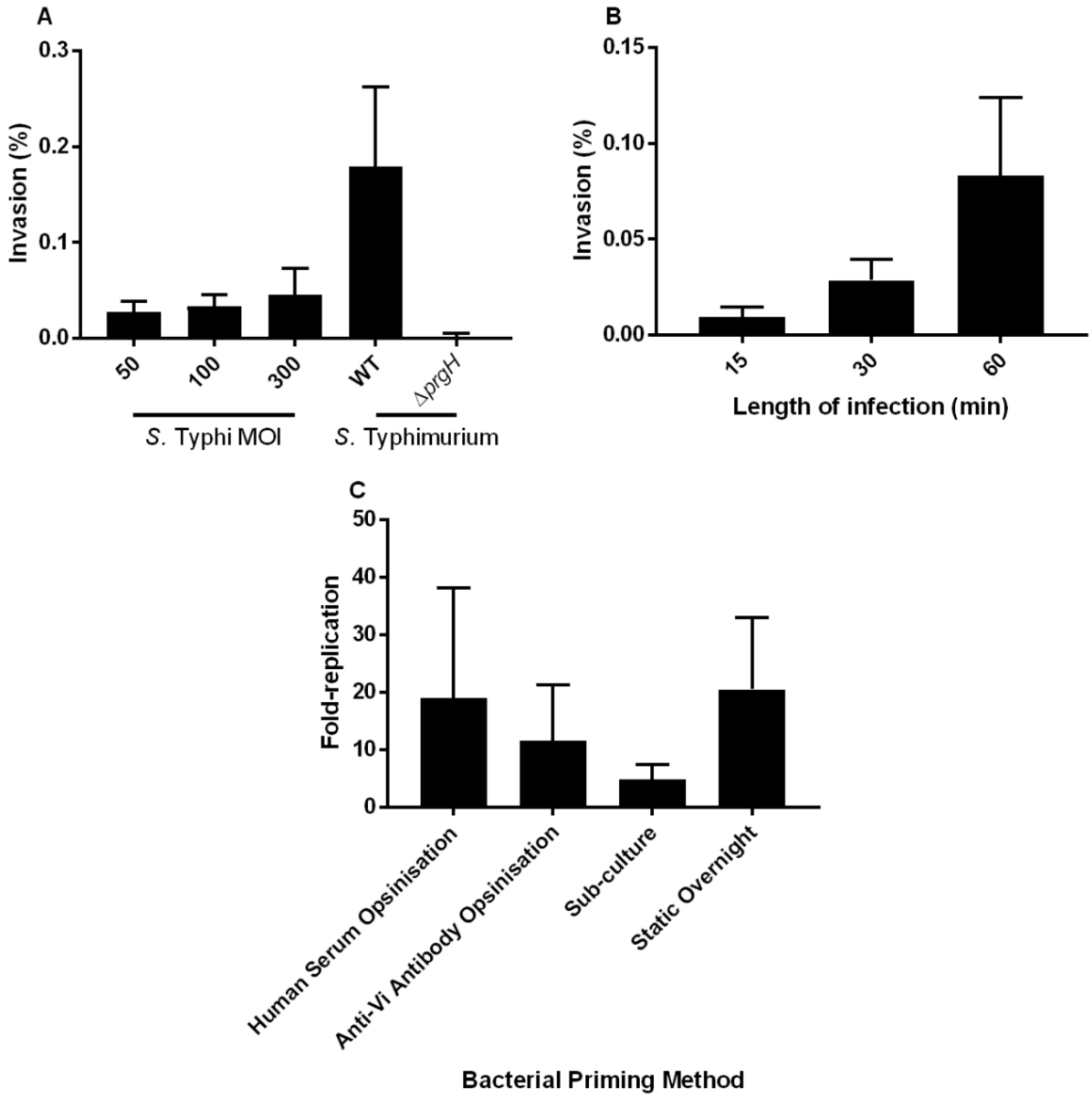


Figure 3.3. Optimising *S.* Typhi infection protocols. (A) The ability of Ty2 *S.* Typhi to invade HeLa cells was assessed at 2 h post-infection using a MOI of 50, 100 or 300. **(B)** The capability of *S.* Typhi to invade HeLa cells was assessed at 2 h post-infection after either 15, 30 or 60 min infection. **(C)** The ability of *S.* Typhi to replicate within THP-1 cells was assessed at 24 h post-infection, after the bacteria had been primed either by human serum opsonisation, anti-Vi-antigen antibody opsonisation, subcultured in Lennox LB or static overnight culture in Lennox LB. Graph shows mean + SD. These experiments were performed in combination with Rebecca Johnson.

Using the data from these experiments, it was determined that future infections of HeLa cells with *S.* Typhi would use an MOI of 100 with an infection time of 60 min.

3.4.2.2. Optimising infection of human macrophages with *S.* Typhi

Future experiments would also require the ability to assess the role of particular genes in the replication of *S.* Typhi within human macrophages. Therefore, a suitable protocol that would allow the study of *S.* Typhi intracellular replication was required.

To develop such a protocol for *S.* Typhi, bacteria were primed by several methods, before being used to infect THP-1 macrophages at an MOI of 10. Phagocytosis was then allowed to occur for 30 min before treatment with gentamicin. Cells were then lysed at 2 and 24 h post-infection and CFU enumerated to determine the amount of replication the bacteria had undergone (Figure 3.3C). The methods used to prime bacteria were as follows: opsonisation with either human serum or an antibody raised against the *S.* Typhi Vi-antigen, subcultured in Lennox LB and grown to late exponential phase, or grown overnight as static cultures in Lennox LB. The opsonisation and static overnight methods of priming were adaptations of those used with *S.* Typhimurium for infection of murine macrophages (Beuzón et al. 2000; Cardenal-Muñoz & Ramos-Morales 2011), whereas, the subculture to late exponential phase and static overnight methods are usually used to prime *Salmonella* for infection of epithelial cells due to the induction of the *SPI-1* T3SS, but do differ in the intensity of *SPI-1* induction (Ibarra et al. 2010).

Infection of THP-1 macrophages with *S.* Typhi primed by these methods had mixed effects on the amount of intracellular bacterial replication (Figure 3.3C). Subculture priming resulted in the least amount of intracellular replication with only a 4.9-fold increase in intracellular bacteria at 24 h compared to 2 h post-infection, whereas, static overnight priming resulted in the highest amount of replication with a 20.5-fold increase. Opsonisation of *S.* Typhi with either human serum or an antibody raised against the Vi-antigen resulted in a 19.0-fold increase and a 11.6-fold increase at 24 h, respectively.

Based on this experiment, it was concluded that the static overnight culture method of priming *S.* Typhi for infection of THP-1 macrophages should be used in future.

3.4.2.3. Optimising secretion assays using *S.* Typhi

In the process of identifying novel T3SS effectors, one of the techniques that would be required was the ability to identify whether any putative effectors can be secreted from *S.* Typhi in a T3SS-dependent manner, and if they are secreted, whether the *SPI-1* or *SPI-2* T3SS is required. Therefore, methods for inducing T3SS secretion from *S.* Typhi needed to be optimised.

SPI-1 secretion assays have been developed for *Salmonella*, primarily using *S.* Typhimurium, in which bacteria are grown to late exponential phase in LB, in the presence of sodium chloride, to stimulate expression of the *SPI-1* T3SS and induce secretion (Kaniga et al. 1995; Bajaj et al. 1996). However, the Vi-antigen has been demonstrated to reduce the amount of secretion from the *SPI-1* T3SS in Ty2 *S.* Typhi, and removal of the Vi-antigen by mutating genes involved in its synthesis has been shown to relieve this (Arricau et al. 1998). Based on this, TviB, an enzyme required for synthesis of the Vi-antigen (Virlogeux et al. 1995), was mutated in *S.* Typhi and *SPI-1* secretion assays were performed (Figure 3.4A). Under these conditions, SipD secretion, a component of the *SPI-1* T3SS needle tip (Figure 1.4) that is translocated into host cells (Collazo & Galán 1997), could be seen in the secreted fraction. DnaK is a bacterial chaperone that is not secreted and since no DnaK signal was observed in the secreted fraction, this indicates no bacterial lysis had occurred and that the presence of SipD in the secreted fraction is due to secretion and not lysis. Therefore, this indicates that *SPI-1* secretion can be detected from *S.* Typhi using a mutant lacking the Vi-antigen.

The secretion of proteins by the *SPI-2* T3SS of *S.* Typhi would also need to be assessed. However, prior to beginning work to optimise this assay, a Ty2 *S.* Typhi strain lacking a functional *SPI-2* T3SS (Δ*ssaV*) was generated using the λ Red Recombinase system (Datsenko & Wanner 2000) as described in the materials and methods and confirmed by PCR

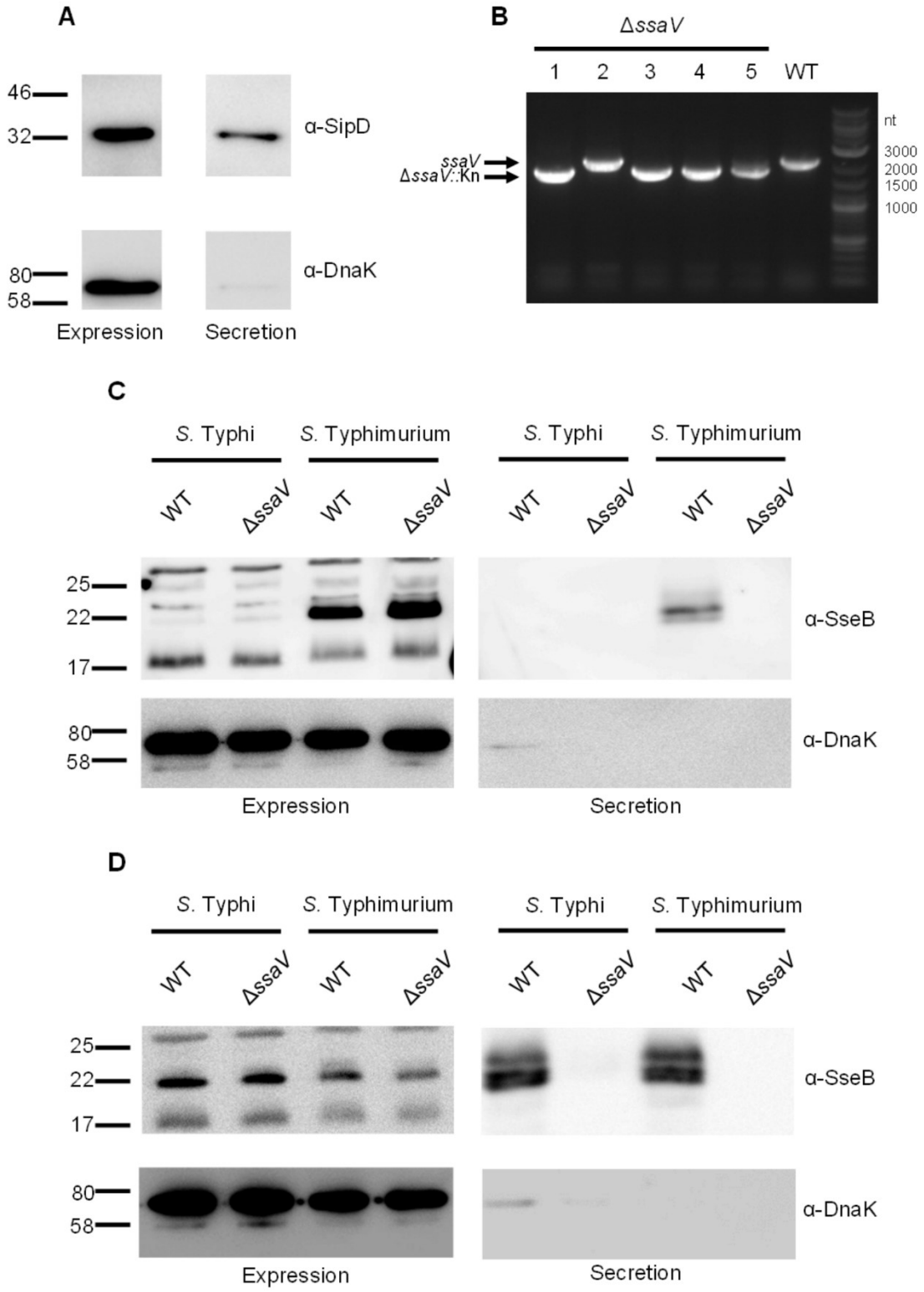


Figure 3.4. Optimising T3SS secretion assays for *S.* Typhi. (A) *SPI-1* secretion assay using a mutant strain of Ty2 *S.* Typhi lacking the ability to produce the Vi-antigen (Δ*tviB*). The presence of the *SPI-1* T3SS component, SipD, in expressed and secreted fractions was assessed by SDS-PAGE and western blot. **(B)** Agarose gel showing PCR screening products from Δ*ssaV* Ty2 *S.* Typhi mutants, along with a WT Ty2 *ssaV* control. **(C) and (D)** *SPI-2* secretion assays were performed using wild-type (WT) and a mutant lacking the *SPI-2* T3SS (Δ*ssaV*) strains of *S.* Typhimurium and *S.* Typhi incubated in MgMES medium, pH 5.0 for either **(C)** 4 h or **(D)** overnight. The presence of the *SPI-2* T3SS component, SseB, in expressed and secreted fractions was assessed by SDS-PAGE and western blot. Both expression and secreted fractions were also analysed for the presence of the protein chaperone, DnaK, to assess bacterial lysis.

(Figure 3.4B) and sequencing. PCR of the WT Ty2 *S.* Typhi strain using primers 100 nucleotides (nt) up- and downstream of *ssaV* (Table 2.3) produced a PCR product ~2200 nt in length, as expected. Of the five mutant colonies screened, four produced a PCR product ~1800 nt in length, indicating successful integration of the kanamycin resistance cassette. Integration and localisation of the kanamycin cassette for colony three was then confirmed by sequencing, and found to be correct.

This meant that work to optimise the *SPI-2* secretion assays could then begin. However, unlike *SPI-1* secretions assays, no work on *SPI-2* secretion has been conducted in *S.* Typhi, to the best of our knowledge. Therefore, a protocol previously described for use with *S.* Typhimurium was used as a starting point (Beuzón et al. 2000; Yu et al. 2010). *SPI-2* secretion assays involve replicating the conditions inside the SCV by growing the bacteria at low pH with limited nutrients, in MgMES medium, pH 5.0 for 4 h at 37°C, 200 rpm, to induce expression of the *SPI-2* T3SS (Beuzón et al. 1999). Bacteria are then transferred to MgMES medium with a neutral pH (pH 7.4) for 2 h at 37°C; to remove the *SPI-2* T3SS gatekeeper complex and allow secretion (Yu et al. 2010) (Figure 3.4C). Under these conditions, SseB, a protein that is involved in the formation of the *SPI-2* T3SS translocon (Figure 1.4) (Nikolaus et al. 2001), was observed in the secreted fraction of WT *S.* Typhimurium, but not Δ*ssaV S.* Typhimurium, a mutant lacking a structural component of the *SPI-2* T3SS (Figure 1.4). However, SseB was not observed in the *S.* Typhi secreted fraction. However, increasing the period in which the bacteria are grown at pH 5.0 from 4 h to overnight (Figure 3.4D), resulted in SseB secretion by WT *S.* Typhi, but not the Δ*ssaV* mutant. DnaK was again used to assess whether bacterial lysis had occurred in the secreted fraction. A weak DnaK band was seen in the WT *S.* Typhi secreted fraction after both 4 h and overnight incubation in MgMES pH 5.0, but SseB was only seen after overnight incubation, suggesting that the SseB signal is due to *SPI-2* secretion and not lysis. Therefore, this demonstrates optimisation of the *SPI-2* secretion assay for use with *S.* Typhi.

3.5. Discussion

S. Typhi is classified as a hazard group 3 pathogen in the United Kingdom due to the severity of the disease it can cause and the risk of its spreading through a community (HSE 2013), for this reason a CL3 laboratory for use of *S.* Typhi was established, including the procurement of equipment and completion of all relevant documentation. The process, from applying to the HSE to the commencing of work with *S.* Typhi, took approximately three years to complete. Although HSE permission to work with *S.* Typhi was granted prior to my starting on this project, a significant proportion of procuring equipment for the CL3 laboratory and writing the associated COP and SOPs was completed during this study. However, once established, the CL3 laboratory has required constant assessment not only by the Biosafety team at Imperial College, but also the HSE and Metropolitan Police Service, to ensure that the laboratory is adhering to all relevant requirements.

The practicalities of working in a CL3 laboratory mean that certain methods that are appropriate for use in a CL2 laboratory, have had to be adapted. However, whilst the CL3 laboratory is suitable for its current use, the scope of the protocols that can be used are limited due to a lack of certain pieces of equipment. For example, it would be beneficial to be able to demonstrate the translocation of novel effector proteins from *S.* Typhi using the β-lactamase translocation assay (Charpentier & Oswald 2004). For this, a plate reader capable of detecting fluorescent emission would be required. However, since this is not available in the CL3 laboratory, *S.* Typhimurium is currently used to assess effector protein translocation in a CL2 laboratory where a plate reader is present, as will be discussed in subsequent chapters. Another example would be the use of live-cell imaging to study *S.* Typhi pathogenesis. This would be beneficial, as the effect *S.* Typhi has on the cell biology of host cells, as well as assessing T3SS effector localisation during infection could be performed in real-time instead of at discrete timepoints. This type of work has not been performed with *S.* Typhi and would allow further comparisons with *S.* Typhimurium to be drawn. However, there is no facility at Imperial College that allows live-cell imaging of hazard group 3 organisms, meaning that at

present, this work cannot be performed. Future development of the CL3 laboratory may seek to address these constraints to enable such work to be performed.

Initial screening of the antibiotics sensitivities of the *S.* Typhi strains that had been obtained did provide some interesting results. It was found that Ty2 was resistant to nalidixic acid, whereas, previous reports claimed that it was sensitive (Phung et al. 2002). However, spontaneous resistance to nalidixic acid can be easily generated in laboratory strains of bacteria by repeated passage in the presence of increasing antibiotic concentrations (Greenwood & O'Grady 1978) and is sometimes used as a method of ensuring that bacterial stocks do not become contaminated with exogenous bacterial species. CT18 was demonstrated to be resistant to several different antibiotics and this was anticipated as it was originally identified as an MDR strain of *S.* Typhi (Parkhill et al. 2001) with clinical resistance to quinolone antibiotics (Parry et al. 1998). The H58 strains, ERL12148 and 129-0238, were differentially resistant to the antibiotics tested. This is to be expected as greater than 65% of H58 isolates have been demonstrated to contain antibiotic resistance genes, but resistance profiles do differ between isolates, and as these isolates are from different H58 sub-lineages, this could contribute to the differences observed here (Wong et al. 2015). The other clinical isolate, Lupe Gen0059, was sensitive to all antibiotics tested. Lupe Gen0059 was known to be a non-H58 clinical isolate, and as less than 10% of such isolates have been shown to contain antibiotic resistance genes (Wong et al. 2015), this is understandable. The determination of antibiotics sensitivities was to enable the design of appropriate antibiotic-based selection techniques. However, future work may seek to investigate the susceptibility of these strains to clinically-relevant antibiotics, such as third generation cephalosporins, as well as screening further clinical isolates and determining the genetic basis for any antibiotic resistance. Although recent work has answered some of these questions with regard to the overall antibiotic resistance profile of H58 and non-H58 clinical isolates (Wong et al. 2015). It would be beneficial to identify any particularly prominent H58 and non-H58 isolates and

identify which antibiotic resistances these carry, and whether current antibiotics would be sufficient for the treatment of infected individuals.

It was found that *S.* Typhi was much less invasive than *S.* Typhimurium during infection of HeLa cells, even at an MOI three times greater than that used for *S.* Typhimurium. This could be increased by allowing *S.* Typhi longer to invade, but still never reached a level comparable to *S.* Typhimurium. *S.* Typhi has previously been shown to be less invasive than *S.* Typhimurium during infection of cultured epithelial cells (Bishop et al. 2008) and this has been attributed to the expression of the Vi-antigen, as mutating genes involved in the synthesis of the Vi-antigen resulted in increased *S.* Typhi invasion (Bishop et al. 2008). Other work has shown that a gene involved in Vi-antigen regulation, *tviA*, also causes down-regulation of the *SPI-1* T3SS through repression of HilA expression in *S.* Typhi (Figure 1.5) (Winter et al. 2014). This suggests that the Vi-antigen may provide a physical barrier that reduces *S.* Typhi invasion, as well as being concomitantly regulated to the *SPI-1* T3SS, to reduce invasion at the transcriptional level, preventing the induction of a pro-inflammatory response in the intestine of infected individuals (Winter et al. 2014). It would therefore be interesting to investigate the inflammatory status of the intestine during infection with Vi-negative *S.* Typhi strains, such as CT18 and other Vi-negative clinical isolates to investigate if they do stimulate a pro-inflammatory response, or if not how they are repressing such a response. Recent work has shown that the H58 strains are more invasive compared to the Ty2 strain (Wong et al. 2015), therefore the basis for this hyperinvasive phenotype should also be investigated.

It was found that priming *S.* Typhi, via growth in a static overnight allowed the highest amount of intracellular replication, whereas, infection of THP-1 macrophages with bacteria that had been primed by subculture to late exponential phase showed the least amount of replication. Even though both the static overnight and subculture to late exponential phase priming methods have been shown to induce expression of the *SPI-1* operon, growth as a static overnight results in reduced expression of the *SPI-1* T3SS and its effector proteins, compared to subculturing to late exponential phase (Ibarra et al. 2010), this may therefore result in less

macrophage cell death (Brennan & Cookson 2000) and greater *S.* Typhi replication. The opsonisation methods also differed in their ability to facilitate intracellular bacterial replication. Opsonisation with human serum was relatively permissive to bacterial replication, however, it was variable, and cannot therefore be distinguished from opsonisation with an anti-Vi-antigen antibody. Opsonisation of *S.* Typhi may allow more efficient clearance of bacteria and hence less bacterial replication within macrophages was observed. Opsonisation-based methods of bacterial priming are often used with *S.* Typhimurium for infection of macrophages (Beuzón et al. 2000; Cardenal-Muñoz & Ramos-Morales 2011), however, there has not been a great amount of research into the optimal priming of *S.* Typhi for infection of macrophages. The finding that *S.* Typhi and *S.* Typhimurium require different priming methods for optimal replication in macrophages may just be a further difference that has occurred during the differentiation of these serovars.

It has been previously shown that the Vi-antigen in *S.* Typhi is capable of reducing the amount of protein secretion by the *SPI-1* T3SS and that its removal, by mutation, can increase *SPI-1* T3SS secretion (Arricau et al. 1998). Using this finding, a Δ*tviB* mutant of the Ty2 *S.* Typhi strain was generated and the finding that it does allow *SPI-1* T3SS secretion provides a means for assessing the secretion of putative effector proteins by the *SPI-1* T3SS.

To date, there has not been any work to characterise *SPI-2* T3SS secretion in *S.* Typhi. This may be due to the absence of many of the *SPI-2* T3SS effectors that are present in *S.* Typhimurium (Appendix 1) (Sabbagh et al. 2010). However, this study has shown that *S.* Typhi requires a longer incubation in *SPI-2*-inducing conditions before secretion from the *SPI-2* T3SS is observed. This may be a result of the adaptation *S.* Typhi has undergone to allow it to spread systemically throughout the body (Parry et al. 2002) rather than replicating within the mucosa of the intestine where *S.* Typhimurium colonises and causes gastroenteritis. Subsequent *SPI-2* secretion assays with *S.* Typhi, have shown that the second incubation step in MgMES media at neutral pH is dispensable and that secretion of effector proteins can be seen without it. This contradicts work with *S.* Typhimurium that shows that the second

incubation at pH 7.4 is required to cause dissociation of the gatekeeper complex and allow effector secretion (Yu, *et al.*, 2010). This may suggest that *S.* Typhi has a different means by which it regulates secretion from the assembled *SPI-2* T3SS.

In conclusion, this chapter has demonstrated the establishment of a CL3 laboratory, including the completion of all associated paperwork and adaptation of certain methods so that they were suitable for use in a CL3 laboratory. It has also shown some of the preliminary work to optimise protocols that were originally designed for use with *S.* Typhimurium, so that they were suitable for use with *S.* Typhi.

Chapter 4: Identification and Characterisation of Novel T3SS Effectors in S. Typhi

4.1. Introduction

Work to understand the role of T3SS effector proteins in *Salmonella* pathogenesis has been performed almost entirely using *S.* Typhimurium, and it has been assumed that these effectors perform the same roles in *S.* Typhi, despite differences in host range and disease outcome. These differences are thought to be due, in part, to the absence of many of the T3SS effectors in *S.* Typhi, that are present in *S.* Typhimurium (Spanò & Galán 2012). However, work from other research groups, as well as my own, has shown that effector function varies between *Salmonella* serovars. For example, the T3SS effectors SptP, SifA and SseF evolved differently between NTS and typhoidal *Salmonella* serovars (Eswarappa et al. 2008) and in the case of SptP, the biological function during *S.* Typhimurium infection is not retained by *S.* Typhi (Johnson et al. 2017). Also, previous work identified StoD, a putative T3SS effector, present in *S.* Typhi, but not *S.* Typhimurium (Fookes et al. 2011). These findings suggest that *S.* Typhi effectors may exhibit functions that differ from their *S.* Typhimurium homologues, and that *S.* Typhi may encode further T3SS effectors that are not present in *S.* Typhimurium. These factors may have also contributed to the differences in host range and disease outcome of *S.* Typhi compared to *S.* Typhimurium.

In this chapter, I will discuss work that was performed to identify and characterise novel T3SS effector proteins that are present in *S.* Typhi and to begin to understand how these proteins contribute to *S.* Typhi pathogenesis.

4.2. Identification of Putative T3SS effectors in *S.* Typhi using a Genome-Wide Machine-Learning Approach

In an attempt to identify novel T3SS effectors, a collaboration was established with Professor Tal Pupko of Tel Aviv University, Israel, who has developed a computational machine-learning approach that has been used to identify T4SS effectors in *L. pneumophila* (Burstein et al.

2009) and *C. burnettii* (Lifshitz et al. 2014), as well as T3SS effectors in *P. aeruginosa* (Burstein et al. 2015) and *X. euvesicatoria* (Teper et al. 2016). This technique works by computationally screening the genome of a particular bacterium and ranking each gene according to the likelihood of it encoding an effector protein based on a number of features including: a %GC content that differs to the surrounding genome, sequence similarity to known effectors or eukaryotic proteins, and the localisation of these genes compared to known effector genes within the genome (Burstein et al. 2009). Once ranked, genes can be selected for experimental confirmation.

To use this technique to identify novel T3SS effectors in Ty2 *S.* Typhi, a list of known *Salmonella* effectors and known non-effector genes (Table 4.1) were provided to Professor Pupko to act as a training set for the algorithm and to begin the screen. The list of effector proteins was based on those identified in other *Salmonella* serovars, but excluded those known to be absent, or pseudogenes in *S.* Typhi (Appendix 1). *StoD* was also included in this list as this represented the first putative effector that is present in *S.* Typhi and not *S.* Typhimurium (Fookes et al. 2011). The non-effector genes included known non-secreted genes were selected based on having either cytoplasmic or inner membrane localisation according to UniProt and included genes such as the transcriptional regulator, *sirC*, as well as genes encoding metabolic enzymes, such as *fbp*, and components of non-T3SS secretory systems, *tatA* and *yejM*. Using this list of genes, the machine-learning algorithm was used to screen the Ty2 *S.* Typhi genome.

Once the machine-learning algorithm had finished, all 4,352 Ty2 *S.* Typhi genes were ranked according to their likelihood of being a T3SS effector. The top 100 ranked genes (Table 4.2), were then assessed further. All but three of the known *Salmonella* T3SS effectors ranked inside of the top 100 ranked genes, *steA* was ranked at position 203, *srgE* was ranked at position 219 and *steD* was ranked at position 299 (Domingues et al. 2016; LaRock et al. 2015; Bayer-Santos et al. 2016). Within the top 20 genes, 18 out of the 22 known *S.* Typhi effector

Table 4.1. Table of known Salmonella T3SS effector and non-effector genes used in the machine-learning algorithm.

Known Effectors		Known Non-Effectors		
Protein	**Gene Locus**	**Protein**	**Gene Locus**	**Description**
SseL	*t0576*	DksA	*t0194*	RNA-polymerase-binding transcription factor
SspH2	*t0623*	RodZ	*t0332*	Cytoskeletal protein
SteD	*t0718*	CysZ	*t0428*	Sulfate transporter
SpiC	*t1261*	ZipA	*t0429*	Cell division protein
SseF	*t1272*	NuoA	*t0536*	NADH-quinolone oxidoreductase subunit A
SseG	*t1273*	YejM	*t0626*	Inner membrane protein
SrgE	*t1468*	YejK	*t0628*	Nucleoid-associated protein
SteA	*t1493*	MdtB	*t0745*	Multidrug resistance protein
SifB	*t1511*	Wzc	*t0756*	Tyrosine-protein kinase
SteC	*t1612*	CheZ	*t0962*	Protein phosphatase
SifA	*t1696*	HtpX	*t1034*	Protease
SopB	*t1828*	Rfc	*t1212*	O-antigen polymerase
PipB	*t1830*	YviB	*t1647*	Probable intracellular septation protein A
PipA	*t1831*	FtsK	*t1974*	DNA translocase
StoD	*t1865*	ClpP	*t2412*	ATP-dependent Clp protease proteolytic subunit
PipB2	*t2674*	DinB	*t2537*	DNA polymerase IV
SptP	*t2780*	NadK	*t2637*	NAD kinase
SipA	*t2784*	SirC	*t2769*	Transcriptional regulator
SipD	*t2785*	TatA	*t3324*	Sec-independent protein translocase protein
SipC	*t2786*	CyaA	*t3358*	Adenylate cyclase
SipB	*t2787*	ZraS	*t3458*	Sensor protein
SopD	*t2846*	Nfi	*t3463*	Endonuclease V
SopE	*t4303*	HslV	*t3526*	ATP-dependent protease subunit
		RbsA	*t3637*	Ribose import ATP-binding protein
		GyrB	*t3684*	DNA gyrase subunit B
		BcsB	*t3899*	Cyclic di-GMP-binding protein
		GlpE	*t3988*	Thiosulfate sulfurtransferase
		GroS	*t4381*	10 kDa chaperonin
		Fbp	*t4469*	Fructose-1,6-bisphosphate class 1

Table 4.2. Top 100 ranked genes from the machine-learning algorithm.

Rank	Gene Locus	Protein[1]	Rank	Gene Locus	Protein[1]
1	*t1830*	PipB	35	*t1276*	SsaI
2	*t1696*	SifA	36	*t1733*	YceQ
3	*t1511*	SifB	37	*t1265*	SseA
4	*t2846*	SopD	38	*t2680*	Uncharacterised protein[2]
5	*t2780*	SptP	39	*t4221*	AraC family regulatory protein
6	*t0576*	SseL	40	*t4196*	PhnA
7	*t2784*	SipA	41	*t4209*	Uncharacterised protein[2]
8	*t2674*	PipB2	42	*t0733*	Uncharacterised protein
9	*t1828*	SopB	43	*t1284*	SsaO
10	*t4303*	SopE	44	*t4219*	Uncharacterised protein[2]
11	*t2785*	SipD	45	*t1641*	Uncharacterised protein
12	*t1272*	SseF	46	*t04885*	Uncharacterised protein[2]
13	*t2786*	SipC	47	*t4235*	Uncharacterised protein
14	*t1273*	SseG	48	*t05880*	Uncharacterised protein
15	*t1261*	SpiC	49	*t1281*	SsaM
16	*t1831*	PipA	50	*t2620*	YfiA
17	*t0623*	SspH2	51	*t1440*	MarA
18	*t2787*	SipB	52	*t1875*	Putative bacteriophage protein
19	*t1827*	Uncharacterised protein[2]	53	*t1522*	Putative phosphotransferase protein[2]
20	*t1268*	SseC	54	*t1947*	YcaR
21	*t1829*	SigE	55	*t4247*	PilS
22	*t1865*	StoD	56	*t1205*	YdiZ
23	*t1509*	Uncharacterised protein[2]	57	*t1963*	Uncharacterised protein[2]
24	*t1274*	SsaG	58	*t4412*	Hfq
25	*t2863*	Uncharacterised protein	59	*t1266*	SseB
26	*t1264*	SsaE	60	*t3059*	Uncharacterised protein
27	*t05500*	IraM	61	*t4218*	Uncharacterised protein
28	*t0719*	SteD chaperone	62	*t0783*	RfbS
29	*t2064*	Uncharacterised protein[2]	63	*t1775*	CsgC
30	*t4294*	Positive regulator of late gene transcription	64	*t2710*	EmrR
31	*t1479*	Bdm	65	*t1903*	Putative bacteriophage protein[2]
32	*t2659*	Bacteriophage late gene regulator	66	*t0728*	Uncharacterised protein
33	*t1778*	CsgD	67	*t4220*	Putative GerE family regulatory protein
34	*t1744*	FlgD	68	*t1005*	Uncharacterised protein[2]

Rank	Gene Locus	Protein[1]	Rank	Gene Locus	Protein[1]
69	*t0635*	YejG	85	*t1171*	Uncharacterised protein[2]
70	*t0682*	Uncharacterised protein[2]	86	*t1018*	Uncharacterised protein[2]
71	*t1662*	HnsA	87	*t1612*	SteC
72	*t1477*	HlyE	88	*t2809*	Uncharacterised protein
73	*t0786*	RfbV	89	*t4202*	AdiY
74	*t1552*	Uncharacterised protein[2]	90	*t0647*	Putative membrane protein
75	*t4341*	YjhX1	91	*t2302*	Possible copper-binding protein
76	*t0620*	MsgA	92	*t2565*	Uncharacterised protein[2]
77	*t1737*	FlgK	93	*t4421*	YjfI
78	*t1467*	Putative isomerase	94	*t4145*	Uncharacterised protein[2]
79	*t1743*	FlgE	95	*t2145*	Uncharacterised protein[2]
80	*t0353*	Uncharacterised protein[2]	96	*t1244*	LppB
81	*t1570*	Uncharacterised protein	97	*t06460*	Annotation removed
82	*t1129*	Uncharacterised protein[2]	98	*t1826*	Uncharacterised protein[2]
83	*t1145*	Uncharacterised protein[2]	99	*t0589*	Uncharacterised protein
84	*t05010*	Uncharacterised protein[2]	100	*t2386*	YbaJ

[1]Protein name taken from UniProt. [2]Uncharacterised protein under 100 amino acids in length.

proteins used in the algorithm were present and no genes from the non-effector list were present within the top 100 ranked genes.

Several chaperones of the T3SS and effectors (*sigE*, *ssaE* and *sseA*), as well as components of the *SPI-2* T3SS, (*ssaG*, *ssaI*, *ssaO* and *ssaM*), were ranked within the top 100 genes. The flagellar genes, *flgK* and *flgE*, as well as the prepilin gene, *pilS*, and the *hlyE* gene which encodes a pore-forming toxin (Fuentes et al. 2008; Oscarsson et al. 2002) were also present. There were also several genes known not to be T3SS effectors, such as *yfiA*, *marA* and *rfbS* were also found within the top 100 ranked genes.

There were several hypothetical proteins within the top 100 genes. Many of these were under 100 amino acids in length and as such, were deemed too small for further characterisation, as the smallest *Salmonella* effector, SteD, is still 111 amino acids long. Five uncharacterised genes, *t0733*, *t1875*, *t2863*, *t4218* and *t05880*, as well as *stoD* were selected for experimental

validation as initial BLAST searches (Boratyn et al. 2013) suggested that these putative effectors were present in *S.* Typhi and not *S.* Typhimurium. (Table 4.3).

Table 4.3. Genes selected for further investigation based on the machine-learning algorithm results. Gene length is denoted in nucleotides (nt) and predicted molecular weight in kilodalton (kDa).

Gene	Ty2 Locus	Rank	Gene Length (nt)	Number of amino acids	Predicted Molecular Weight (kDa)
stoD	*t1865*	22	702	233	26.1
-	*t2863*	25	831	276	29.5
-	*t0733*	42	450	149	16.9
-	*t05880*	48	822	273	30.7
-	*t1875*	52	732	243	27.0
-	*t4218*	61	384	127	13.2

4.3. Assessing Secretion and Translocation of Putative T3SS Effectors

4.3.1. Assessing Secretion of Putative T3SS Effectors from *S*. Typhi

To assess whether *t0733*, *t1875*, *t2863*, *t4218*, *t05880* and *stoD* encoded T3SS effectors, these gene were cloned into a low copy number plasmid (pWSK29) with a C-terminal 4HA-tag, and transformed into Ty2 S. Typhi for secretion assays (Figure 4.1 and Figure 4.2).

4.3.1.1. *SPI-1* secretion assays

Preliminary *SPI-1* secretion assays were performed using *stoD* in a Ty2 *S.* Typhi strain that lacks the Vi-antigen (Δ*tviB*) (Figure 4.1A) as this had been demonstrated to improve secretion from the *SPI-1* T3SS in *S.* Typhi (Arricau et al. 1998). Under these conditions, SipD, was observed in the secreted fraction of all strains, demonstrating that the *SPI-1* T3SS is being expressed and is capable of secretion. Nevertheless, StoD-4HA was not found in the secreted fraction when it was cloned under the control of the T3 promoter within pWSK29 (StoD)

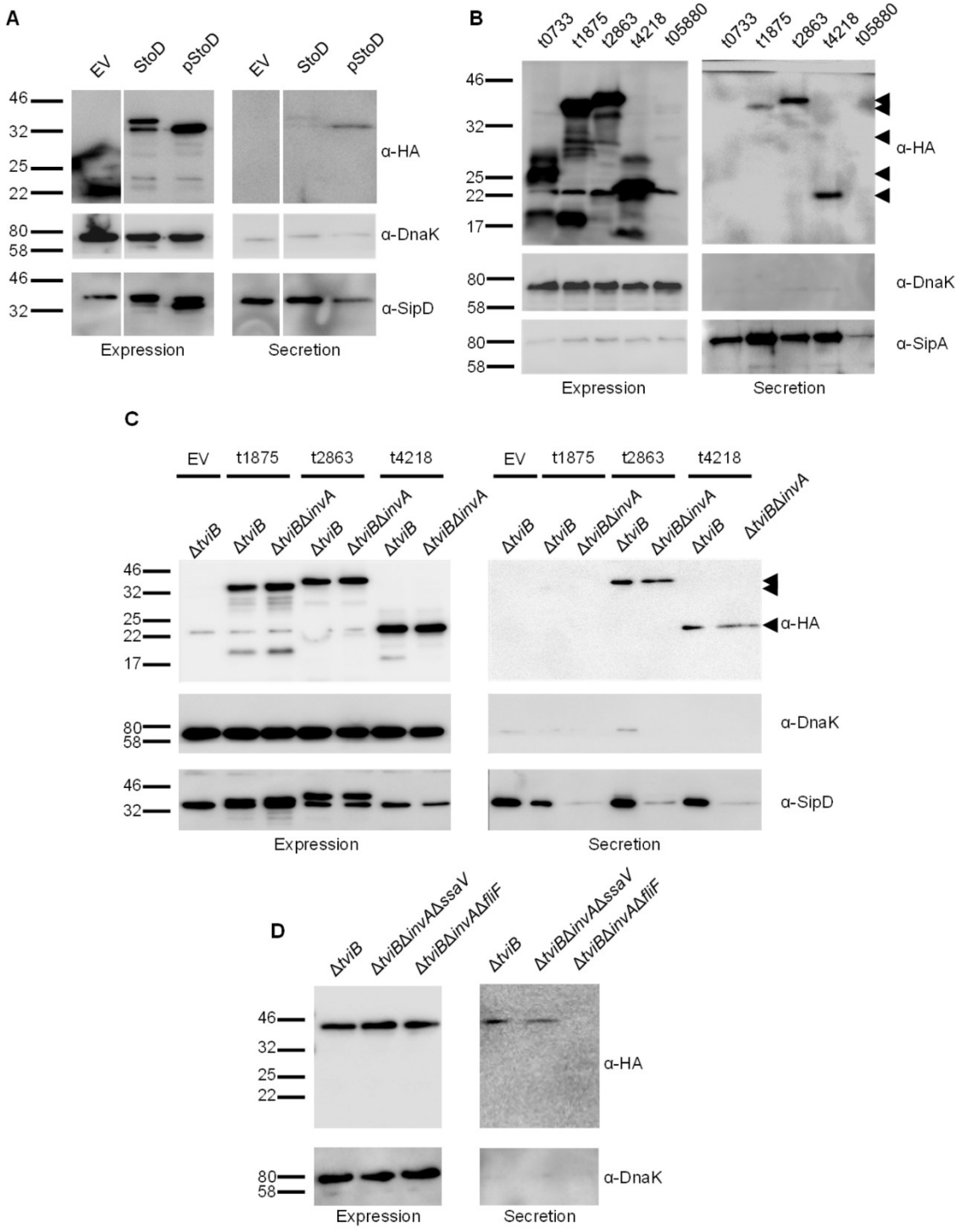


Figure 4.1. Assessing secretion of the putative effector proteins from the *SPI*-1 T3SS. (A) A strain of Ty2 *S.* Typhi lacking the Vi-antigen (Δ*tviB*) was transformed with empty pWSK29-Spec vector (EV), or this vector containing *stoD* or p*stoD*, with a C-terminal 4HA-tag. This image is representative of two independent repeats. **(B)** Δ*tviB* Ty2 *S.* Typhi was transformed with EV or pWSK29-Spec containing *t0733*, *t1875*, *t2863*, *t4218* or *t05880* with a C-terminal 4HA-tag. Protein bands representing the HA-tagged proteins are indicated, from top to bottom: t2863, t1875, t05880, t0733 and t4218. This secretion assay was performed by Rebecca Johnson. **(C)** Δ*tviB* or Δ*tviB*Δ*invA S.* Typhi Ty2 was transformed with EV, or pWSK29-Spec containing *t1875, t2863* or *t4218*, with a C-terminal 4HA-tag. The protein bands representing the HA-tagged proteins are indicated. **(D)** Δ*tviB*, Δ*tviB*Δ*invA*Δ*ssaV* or Δ*tviB*Δ*invA*Δ*fliF* Ty2 *S.* Typhi strains were transformed with pWSK29-Spec-*t2863*-4HA. All genes are under the control of the T3 promoter, except p*stoD*. All figures are from *SPI-1* secretion assays. Expression and secretion samples were taken and analysed by SDS-PAGE and western blotting. An anti-HA antibody was used to detect HA-tagged proteins. SipD, SipA and DnaK were detected using respective antibodies.

(Wang & Kushner 1991) and was only present in the secreted fraction when cloned with the 499 nt upstream of the *stoD* gene within the Ty2 genome (pStoD), which was chosen as it was thought to contain the endogenous promoter of this gene. There was a low DnaK signal in the secreted fractions, but since StoD-4HA signal was only observed in the secreted fraction of the strain containing pStoD, lysis is not thought to have contributed this signal.

The secretion of the remaining putative effector proteins; t0733, t1875, t2863, t4218 and t05880, was then assessed using the Δ*tviB* Ty2 *S.* Typhi strain (Figure 4.1B). Under *SPI-1* T3SS-inducing conditions, SipA, another protein shown to be secreted by the *SPI-1* T3SS (Kaniga et al. 1995) was present in the secreted fractions of all Δ*tviB* strains, indicating that the *SPI-1* T3SS is being expressed and capable of secretion. However, the amount of SipA secreted by the strain containing t05880-4HA was dramatically reduced, meaning that the amount of *SPI-1* T3SS secreted protein may also have been reduced. The expression of t05880-4HA was low in this strain, but was visible and it was therefore thought that if t05880-4HA was being secreted it would have been possible to observe this. DnaK was absent from the secreted fraction of all strains, indicating that no bacterial lysis had occurred. Despite all putative effectors being expressed, only three of the putative effectors were observed in the secreted fraction: t1875, t2863 and t4218 under *SPI-1* T3SS-inducing conditions. Therefore, of the six putative effectors assessed for secretion by the *SPI-1* T3SS, four in total were found to be secreted under *SPI-1*-inducing conditions.

The putative effectors t1875, t2863 and t4218 were then transformed into the double Δ*tviB*Δ*invA* Ty2 *S.* Typhi strain for further *SPI-1* secretion assays. This double mutant lacks both the ability to produce the Vi-antigen and a component of the *SPI-1* T3SS, which is essential for secretion (Galán et al. 1992), allowing the determination of whether these putative effectors are secreted in a *SPI-1*-dependent manner (Figure 4.1C). Under *SPI-1* T3SS-inducing conditions, SipD, was again seen in the secreted fraction of all Δ*tviB* Ty2 strains, but was reduced with the Δ*tviB*Δ*invA* Ty2 strains, as expected. DnaK was absent from all secreted fractions except that of the Δ*tviB* Ty2 strain expressing t2863, where a low DnaK signal was

observed. A HA signal was observed in the secreted fraction of both Δ*tviB* or Δ*tviB*Δ*invA* Ty2 strains expressing t2863-4HA and t4218-4HA, but not from either of the strains expressing t1875-4HA.

Since secretion of the putative effectors could be seen using the Δ*tviB*Δ*invA* Ty2 strains, further mutations were made in this strain to determine the source of this secretion. Strains containing triple mutations in the *tviB*, *invA* and either *ssaV* (Δ*tviB*Δ*invA*Δ*ssaV*), or *fliF* (Δ*tviB*Δ*invA*Δ*fliF*), a component of the flagellum basal body ring, required for flagellum assembly (Bergeron 2016) were generated, transformed with the vector containing *t2863*-4HA and *SPI-1* T3SS secretion was again assessed (Figure 4.1D). A Δ*ssaV* mutant was used as this is the other T3SS in *Salmonella* and may have therefore been the source of the secretion, whereas a Δ*fliF* mutant was used as the flagellum also contains a T3SS (Bergeron 2016) and is expressed under *SPI-1*-inducing conditions (Ibarra et al. 2010) and could also be the source of this secretion. Under *SPI-1*-inducing conditions, t2863-4HA was observed in the secreted fractions of the Δ*tviB* and Δ*tviB*Δ*invA*Δ*ssaV* strains, but not the Δ*tviB*Δ*invA*Δ*fliF* strain, suggesting that the secretion observed from the Δ*tviB*Δ*invA* strains previously, may be due to the flagellum ring complex. This meant that this assay was unsuitable to assess whether these putative effectors require the *SPI-1* T3SS for secretion, and therefore StoD secretion was not assessed using this assay.

4.3.1.2. *SPI-2* secretion assays

WT Ty2 strains were then used to assess the secretion of the putative effector proteins: t0733, t1875, t2863, t4218 and t05880, by *SPI-2* secretion assays (Figure 4.2A). The secretion of StoD was assessed using a Δ*stoD* strain; as a WT strain containing the pWSK29-Spec-p*stoD*-4HA vector, was not available at this time, and based on the above findings (Figure 4.1A), it was thought that secretion may only be observed when *stoD* was cloned with the upstream region. Under these conditions, SseB was present in the secreted fraction of all strains indicating that the *SPI-2* T3SS is expressed and capable of secretion. All putative effectors were expressed, but only four of six were observed in the secreted fraction:

t1875, t4218, t05880 and StoD. DnaK was absent from the secreted fractions of the majority of strains, except the strain expressing t05880-4HA.

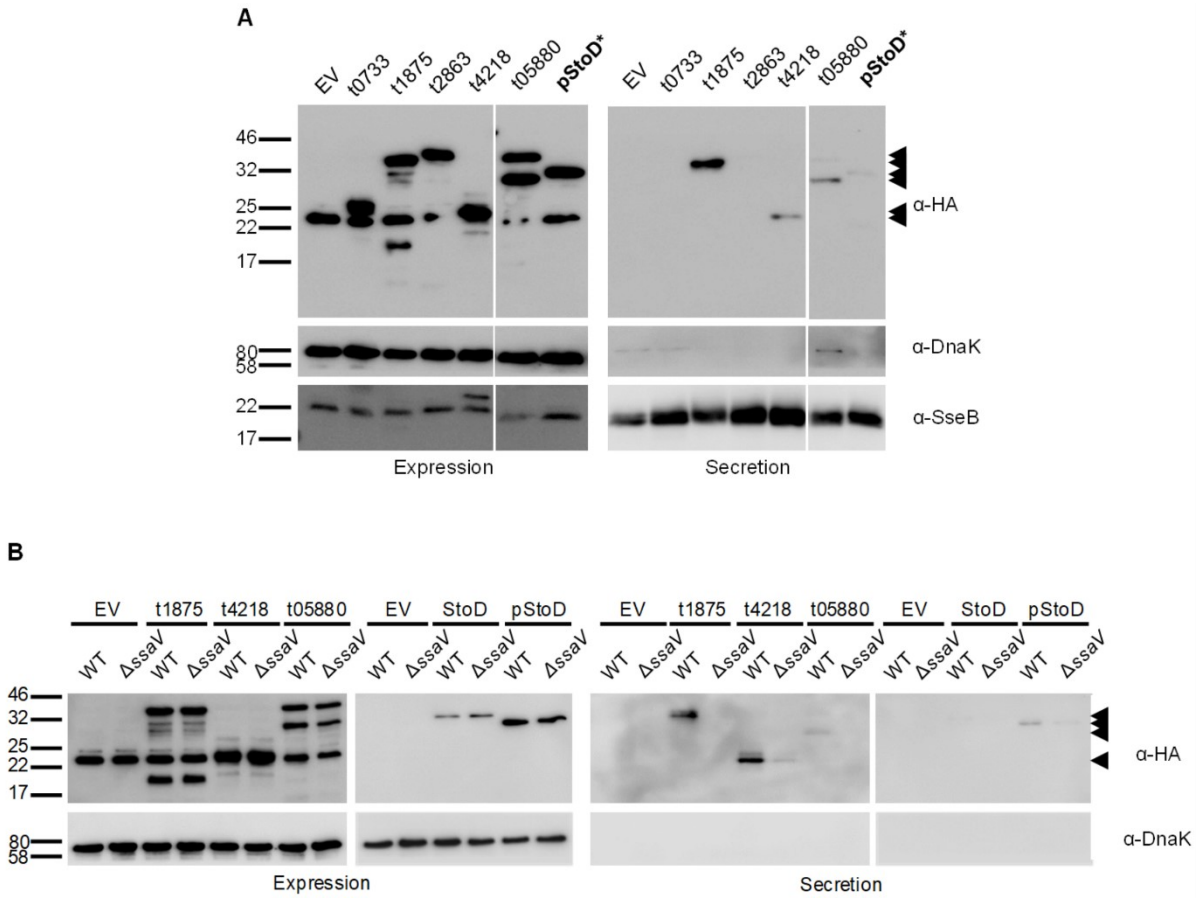


Figure 4.2. Assessing secretion of the putative effector proteins from the *SPI-2* T3SS. (A) WT or Δ*stoD* (*) Ty2 *S.* Typhi strains were transformed with the EV, or pWSK29-Spec containing *t0733*, *t1875*, *t2863*, *t4218*, *t05880* or p*stoD* with a C-terminal 4HA-tag. Protein bands representing the HA-tagged proteins are indicated, from top to bottom: t2863, t1875, StoD, t05880, t0733 and t4218.This image is representative of two independent repeats. **(B)** WT or Δ*ssaV* Ty2 *S.* Typhi strains were transformed with the EV or pWSK29-Spec *t1875*, *t4218*, *t05880*, *stoD* or p*stoD* with a C-terminal 4HA-tag. The protein bands representing the HA-tagged proteins are indicated. This image is representative of three independent repeats. All figures are from *SPI-2* secretion assays. Expression and secretion samples were taken and analysed by SDS-PAGE and western blotting. An anti-HA antibody was used to detect HA-tagged proteins. SseB and DnaK were detected using respective antibodies.

The putative effectors; t1875, t4218, t05880 and StoD were then transformed into a Δ*ssaV* Ty2 strain for further *SPI-2* secretion assays to determine whether the putative effectors were secreted in a *SPI-2* T3SS-dependent manner (Figure 4.2B). StoD was also transformed into WT Ty2 for these assays. Using this method, t1875, t4218, t05880 and StoD were all found in the secreted fraction of the WT, but not the Δ*ssaV* strain, indicating that they are being secreted in a *SPI-2* T3SS-dependent manner. Low levels of DnaK were observed in the

secreted fractions of some of the strains, such as both the WT and Δ*ssaV* Ty2 strains containing t05880-4HA. But since t05880-4HA was only be detected in the secreted fraction of the WT strain, this suggests that any bacterial lysis of this strain is not responsible for the presence of t05880-4HA in the secreted fraction, otherwise it would also be observed in the secreted fraction of the Δ*ssaV* strain. Both StoD and pStoD were used, and again StoD-4HA was only secreted when cloned with the region thought to contain the endogenous promoter, present in the pStoD vector.

It should be noted that some of the effectors did not run on the SDS-PAGE gels (Figure 4.1 and Figure 4.2) as according to their predicted size (Table 4.3). However, the bands that have been indicated were those that were observed upon secretion from *S.* Typhi on multiple occasions and were therefore taken to be the correct protein band. The reasons for the discrepancy between predicted and actual protein size may be due to many factors including modification of the proteins by the bacteria, as well as incorrect prediction and annotation of the translation start site.

Based on the results from the secretion assays, it was concluded that t1875, t2863, t4218, t05880 and StoD were T3SS effector proteins and were renamed as *Salmonella* Typhi Outer proteins (Sto) A (t1875), B (t4218), C (t2863) and E (t05880) according to the nomenclature established for StoD. These names will be used from here onwards.

4.3.2. Evaluating the Translocation of the Novel Effector Proteins

To determine if these secreted proteins were translocated into host cells during infection, the β-lactamase translocation assay (Charpentier & Oswald 2004) was used. The secreted effector proteins were cloned into pWSK29 with a C-terminal β-lactamase (TEM1) tag. Upon translocation, the TEM1 tag would degrade the CCF2/AM β-lactam-based fluorescent substrate loaded into host cells, resulting in a change in the fluorescence emission from green (520 nm) to blue (460 nm) (Charpentier & Oswald 2004). Due to the lack of a fluorescent plate reader in the CL3 laboratory, this assay could not be performed using *S.* Typhi and therefore

S. Typhimurium was used. However, *SPI-2* secretion assays in *S.* Typhimurium using the secreted proteins: StoA, StoB and StoE demonstrated that, unlike in *S.* Typhi, these proteins were found in the secreted fraction of both WT and Δ*ssaV S.* Typhimurium strains (Figure **4.3**). Although the secretion of StoA and StoB was reduced considerably from Δ*ssaV S.* Typhimurium, for StoE, no reduction was observed. Although, StoA and StoB had been shown to be secreted by the *SPI-1* T3SS in *S.* Typhi (Figure 4.1B), and this could account for the presence of StoA-4HA and StoB-4HA in the secreted fraction of Δ*ssaV*

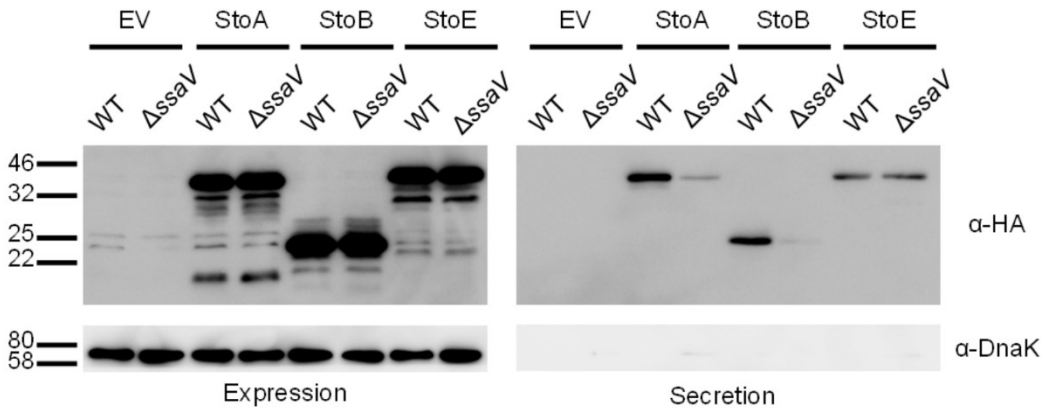


Figure 4.3. Novel effector proteins are secreted by a *SPI-2* mutant in *S.* Typhimurium. WT and Δ*ssaV* strains of ATCC 14028 *S.* Typhimurium were transformed with the EV, or pWSK29-Spec containing *stoA*, *stoB* or *stoC*, with a C-terminal 4HA-tag and used to perform *SPI-2* secretion assays. Expression and secretion samples were taken and analysed by SDS-PAGE and western blotting. An anti-HA antibody was used to detect HA-tagged proteins and DnaK was detected using an anti-DnaK antibody. This image is representative of three independent repeats. This experiment was performed by Elli Mylona.

S. Typhimurium, StoE-4HA was not. This suggests that there may be *S.* Typhi-specific factors which regulate the secretion of these proteins from their correct T3SS and therefore β-lactamase translocation assays in *S.* Typhimurium could not be used to determine which T3SS was required for translocation, but could be used to determine if the novel proteins were translocated in a T3SS-dependent manner.

The TEM1-tagged proteins were transformed into WT *S.* Typhimurium and a strain lacking components of both the *SPI-1* and *SPI-2* T3SSs (Δ*prgH*Δ*ssaV*). Expression of the TEM1-tagged proteins was assessed by sampling cultures of each strain and analysed by SDS-PAGE and western blot for the TEM1-tagged proteins (Figure 4.4A). A band was

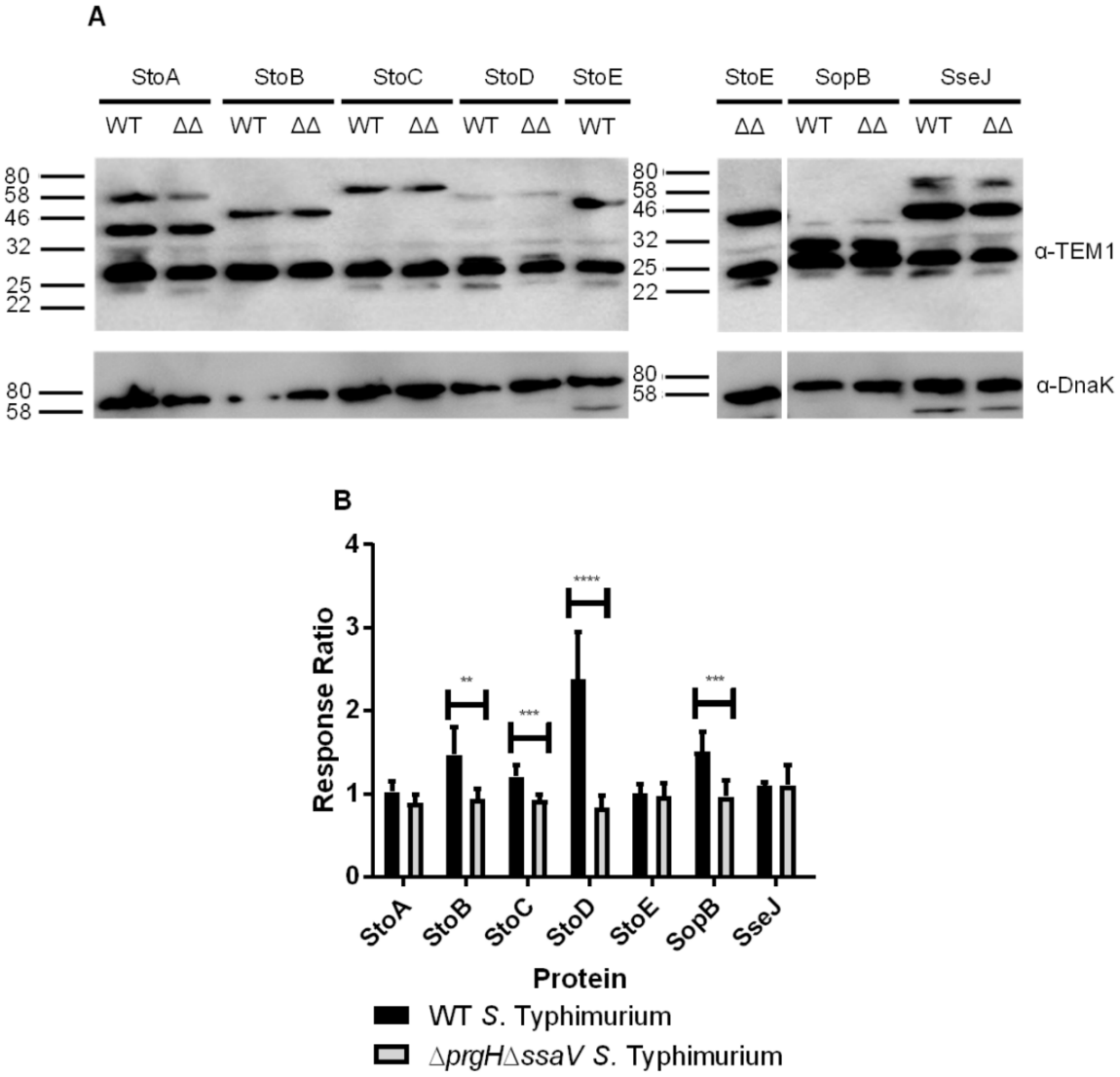


Figure 4.4. Assessing translocation of novel effector proteins. (A) Representative western blot assessing the expression of the pWSK29-TEM1 effector constructs in WT and Δ*prgH*Δ*ssaV* (ΔΔ) ATCC 14028 *S.* Typhimurium. This image is representative of two independent repeats. An anti-TEM1 antibody was used to detect TEM1-tagged proteins and an anti-DnaK antibody was used as a loading control. **(B)** Translocation of secreted proteins by either WT or Δ*prgH*Δ*ssaV* ATCC 14028 *S.* Typhimurium during infection of HeLa cells was assessed using the β-lactamase translocation assay. Graph shows mean + SD. Translocation of each protein was compared between the WT and Δ*prgH*Δ*ssaV* genetic backgrounds using a Multiple t-test with the Holm-Sidak correction for multiple comparisons (** = p<0.001, *** = p<0.001 and **** = p<0.0001). Graph represents an average of three independent repeats. Translocation assays were performed by Elli Mylona.

observed in all samples ~25 kDa, which corresponds to the TEM1 tag itself. All TEM1-tagged proteins were expressed, albeit at varying levels, and therefore these strains were then used to perform β-lactamase translocation assays during infection of HeLa cells (Figure 4.4B). For these assays, StoD-4HA was cloned under the control of the T3 promoter within pWSK29. At 3 h post-infection, SopB-TEM1, a known *SPI-1* T3SS-dependent effector (Galyov et al. 1997)

was translocated into HeLa cells, along with StoB-TEM1, StoC-TEM1 and StoD-TEM1 by WT *S.* Typhimurium, but not Δ*prgH*Δ*ssaV S.* Typhimurium, indicating that they are translocated in a T3SS-dependent manner. SseJ-TEM1, a known *SPI-2* T3SS-dependent effector (Freeman et al. 2003), was not translocated suggesting that the *SPI-2* T3SS is not active at 3 h post-infection in HeLa cells. Translocation of StoA-TEM1 and StoE-TEM1 was also not observed at 3 h post-infection and since, StoA and StoE were shown to be secreted in a *SPI-2* T3SS-dependent manner (Figure 4.2B) a later timepoint may be required to see translocation of these proteins, as well as, SseJ-TEM1. However, translocation at a later timepoint could not be assessed here as an appropriate protein that would control for lysis of intracellular bacteria, could not be identified. The protein that is commonly used in this assay, FabI-TEM1 (Fookes et al. 2011), was not expressed in the strains used here and therefore could not be used as a negative control for lysis and translocation. Nevertheless, three of the five novel effector proteins were found to be translocated by *S.* Typhimurium during infection of HeLa cells.

4.4. Characterisation of the Novel Effector Proteins

To gain a better understanding of these novel effector proteins, several bioinformatic resources were utilised, as well as the use of transient expression in HeLa cells to observe localisation within mammalian cells. The phenotypic consequences of deletion of these proteins on *Salmonella* invasion and replication within mammalian cells, were also assessed.

4.4.1. Bioinformatic Analysis of the Novel Effector Proteins

BLAST searches (Boratyn et al. 2013) found that these novel effectors were present in other species of Gram-negative pathogenic bacteria (Boratyn et al. 2013) (Table 4.4), and amino acid alignments are presented in Appendix 4. Homologues of StoA were found in *Y. enterolitica*, *Serratia marcescens*, *E. coli* and *Klebsiella pneumoniae*, whilst StoB and StoC were not found to have homologues in other bacterial species. StoD was already known to

Table 4.4. Putative homologues of the novel effectors in other species of Gram-negative pathogenic bacteria. Percentage identity to *S.* Typhi gene is shown in brackets.

Gene	*S.* Typhi Ty2	*Y. enterolitica*	*S. marcescens*	*E. coli*	*K. pneumoniae*	*V. cholerae* VC35
stoA	*t1875*	*WP_050876966*[1] (41.98%)	*WP_060452310*[3] (41.98%)	*WP_033883790*[5] (69.55%)	*WP_064161787*[8] (25.62%)	-
stoB	*t4218*	-	-	-	-	-
stoC	*t2863*	-	-	-	-	-
stoD	*t1865*	-	-	NleGs[6] (25.40%-34.50%)	-	-
stoE	*t05880*	*WP_050335604*[2] (58.3%)	*WP_06426800*[4] (50.18%)	*WP_000868916*[7] (99.63%)	*WP_064149086*[9] (43.75%)	*WP_000334978* (35.06%)

Strains: [1]YE04/02, [2]YE177/02, [3]2880STDY5682157, [4]2880STDY568999, [5]2010C-3325, [6]E2348/69, Sakai and EDL933, [7]S1191, [8]Kp757 and [9]K2746.

have NleG homologues in *E. coli*, which will be discussed in the subsequent chapter, but no further homologues were identified. Homologues of StoE were found in *Y. enterolitica*, *S. marcescens*, *E. coli*, *K. pneumoniae* and *Vibrio cholerae*. All homologues of StoA and StoE were hypothetical proteins and therefore provided no further insight into the possible function of these proteins during *S.* Typhi infection.

The distribution of the novel effector proteins was then investigated amongst *S. enterica* serovars (Table 4.5), and sequence alignments are presented in Appendix 5. StoA and StoE were found to only be present in *S.* Typhi, with StoE only being present in the Ty2 reference strain and no other *S.* Typhi strain, or any other *Salmonella* serovar. Homologues of StoB and StoC were identified in *S.* Paratyphi A, B and C, as well as *S.* Enteritidis. StoB was also the only novel effector that had a homologue in *S.* Typhimurium. As stated previously, initial BLAST searches did not identify any homologues for these proteins in *S.* Typhimurium, but further study identified this putative homologue of StoB with 88.0% sequence identity and was therefore named StoBTm. However, when this gene was cloned into pWSK29 with a TEM-1

Table 4.5. Putative homologues of the novel effectors in *S. enterica* serovars. Percentage identity to the *S.* Typhi gene is shown in brackets.

Gene	*S.* Typhi Ty2	*S.* Paratyphi A ATCC9150	*S.* Paratyphi B SPB7	*S.* Paratyphi C RKS4594	*S.* Typhimurium ATCC14028	*S.* Enteritidis EC20090135
stoA	*t1875*	-	-	-	-	-
stoB	*t4218*	*SPA4129* (99.14%)	*SPAB_05316* (86.67%)	*SPC_4375* (86.76%)	*STM14_5185* (88.00%)	*AU38_21090* (86.76%)
stoC	*t2863*	*SPA2819* (96.38%)	*SPAB_03676* (27.13%)	*SPC_3012* (27.52%)	-	*AU38_14220* (27.52%)
stoD	*t1865*	-	*SPAB_02256* (36.08%)	-	-	-
stoE	*t05880*	-	-	-	-	-

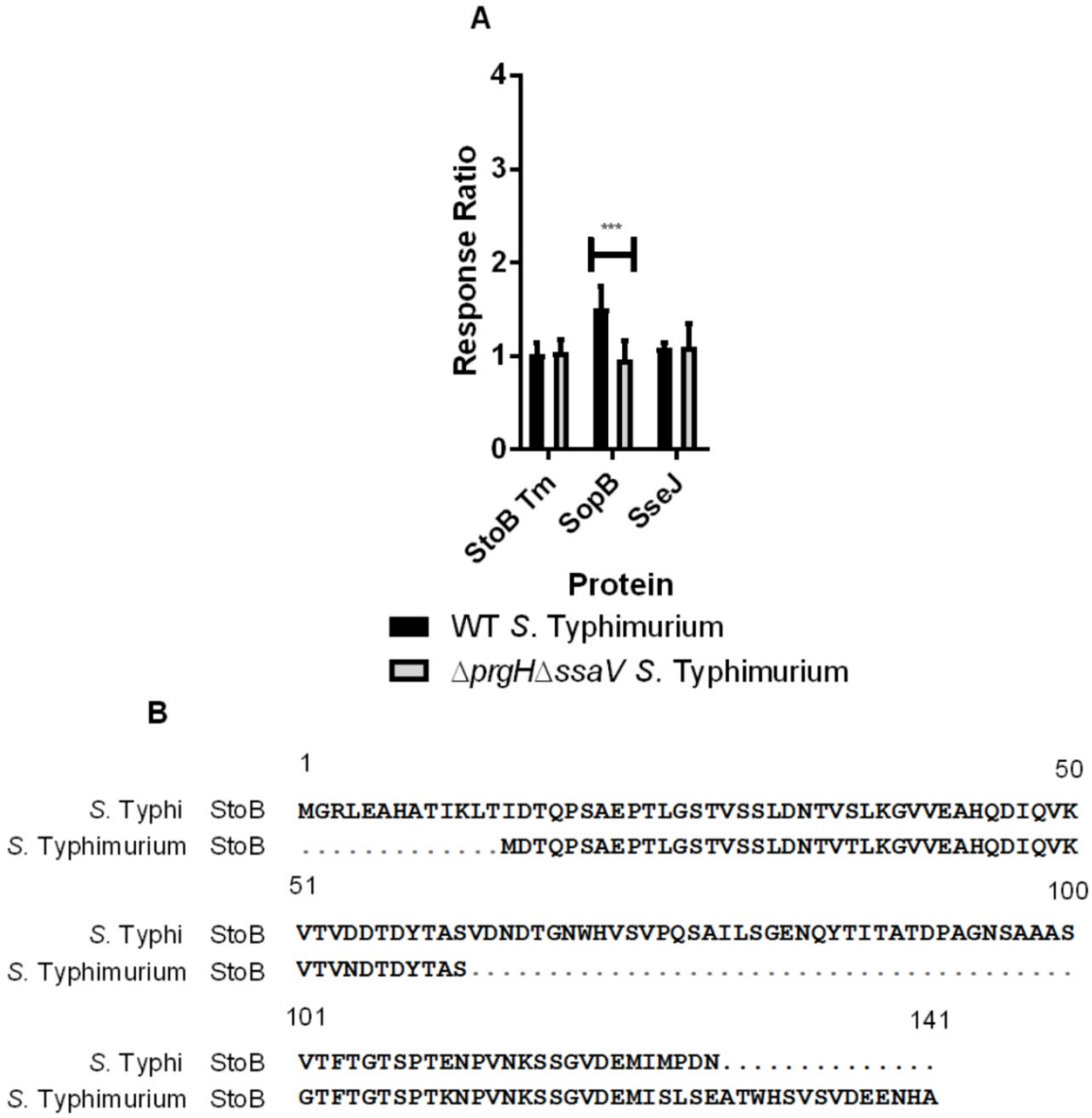


Figure 4.5. Assessing translocation of the *S.* Typhimurium homologue of StoB. (A) Translocation of the StoB homologue from *S.* Typhimurium (StoB Tm), SopB-TEM1 or SseJ-TEM1 by either WT or Δ*prgH*Δ*ssaV* ATCC 14028 *S.* Typhimurium was assessed during infection of HeLa cells using. Graph shows mean + SD. Translocation of each protein was compared between the WT and Δ*prgH*Δ*ssaV* genetic backgrounds using a Multiple t-test with the Holm-Sidak correction for multiple comparisons (*** = p<0.001). Graph represents an average of three independent repeats. Translocation assays were performed by Elli Mylona. **(B)** Alignment of the StoB genes from *S.* Typhi and *S.* Typhimurium. Alignment performed using Clustal Omega (Sievers et al. 2011) and formatted using Strap (Gille et al. 2014).

tag and translocation was assessed, it was not translocated (Figure 4.5A). This may be due to the 13-amino acid N-terminal amino acid truncation in this homologue (Figure 4.5B), which may have resulted in a loss of the translocation signal (Lloyd et al. 2001; Ehrbar et al. 2003). Another explanation is that the 39-amino acid deletion within StoBTm may have disrupted the interaction with the T3SS. Nevertheless, this is a non-translocated homologue of the *S.* Typhi

effector StoB. StoD was found to have a homologue in *S.* Paratyphi B only, which had not been previously identified.

The locations of these genes within the Ty2 *S.* Typhi genome was then assessed using SyntTax (Oberto 2013) (Figure 4.6). The *stoA* and *stoD* genes were found to be located amongst phage genes (Figure 4.6A) similar to other *Salmonella* effector proteins (Boyd & Brüssow 2002). The *stoB* gene was determined to be located downstream of the *rtsA* and *rtsB* regulatory genes (Figure 4.6B), which are involved in *SPI-1* T3SS expression (Ellermeier & Slauch 2003). The *stoB* gene was also found to be located upstream of the *S.* Typhi-specific *SPI-7* (Figure 4.6B) which encodes the operons required for Vi-antigen biosynthesis and export, as well as the T3SS effector *sopE* (Pickard et al. 2003). The *stoC* gene was identified to be located downstream of several putative fimbrial genes (Figure 4.6C), whilst *stoE* was

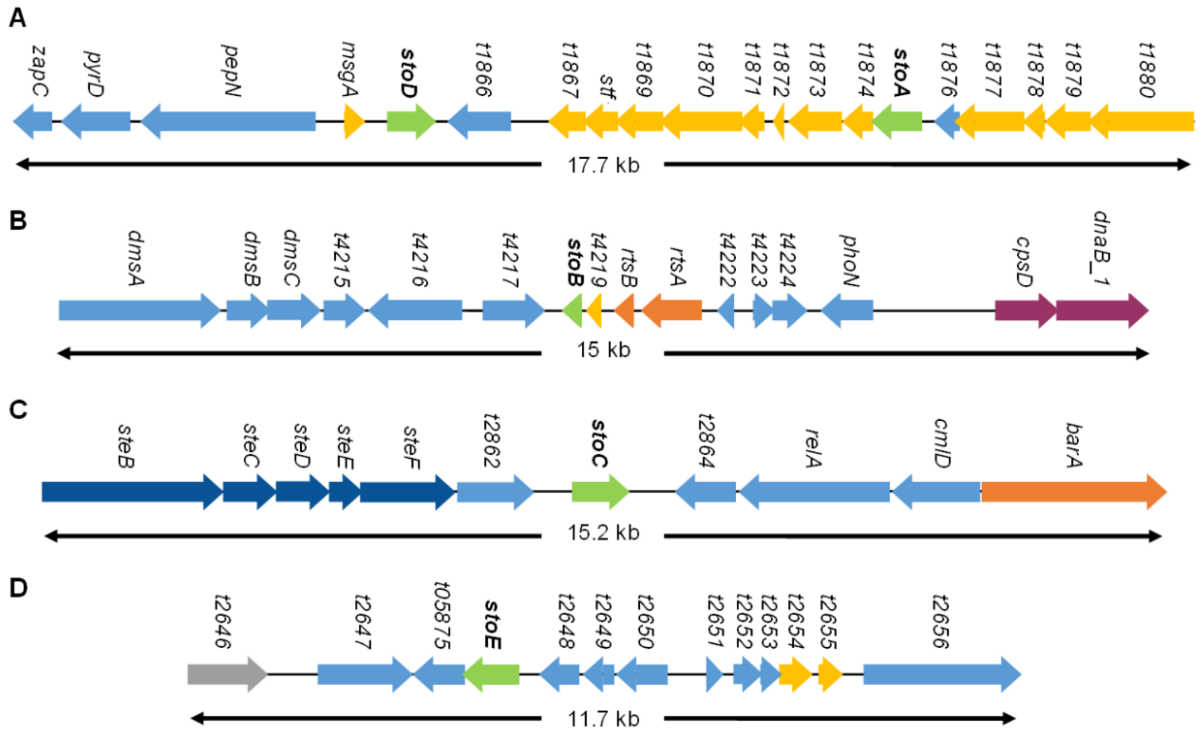


Figure 4.6. Genomic localisation of the novel effector proteins in *S.* Typhi A diagrammatic representation of the genomic localisation of the novel effector proteins (bold) within the Ty2 *S.* Typhi genome. Colours indicate different gene functions: virulence-associated genes (orange), phage genes (yellow), fimbrial genes (dark blue), secreted/*SPI-9* genes (grey), *SPI-7* genes (purple), novel T3SS effectors (green) and miscellaneous genes (light blue).

found to be located downstream of a putative, non-T3SS secreted gene, located at the end of *SPI-9* (Figure 4.6D).

The presence of any motifs or domains within the novel effectors was then determined using InterPro (Finn et al. 2017). StoA was predicted to contain a tetratricopeptide-like helical domain between amino acids 42-109, which are associated with protein-protein interactions in prokaryotes and eukaryotes with a variety of biological functions (Zeytuni & Zarivach 2012). StoD was predicted to contain a C-terminal putative RING-type E3 ubiquitin-ligase domain, which is found in other NleG proteins (Wu et al. 2010), as expected. StoE was predicted to contain a transmembrane domain, composed of an α-helix between amino acids 21-40. StoB and StoC were not predicted to contain any know domains or motifs.

Therefore, putative homologues of the novel effectors were identified in other pathogenic bacterial species as well as other *Salmonella* serovars, as well as their location within the Ty2 *S.* Typhi genome. The presence of putative functional domains was also determined.

4.4.2. Bioinformatic Analysis of the Promoter Region of *stoD*

Since StoD was only secreted in the *SPI-1* and *SPI-2* secretion assays when cloned with the upstream region in the Ty2 genome, it was investigated whether this region contained any transcriptional promoters (Figure 4.7). Using BPROM, an online bioinformatic resource that can predict bacterial promoter regions (Solovyev & Salamov 2011) the 499 nt upstream region of *stoD* used in the pStoD construct was found to contain two putative promoter regions. The first putative promoter region was located between 398 and 369 nt upstream of *stoD*, containing a -35 element, with sequence 5'-TTGGCT-3', and a -10 element, with sequence 5'-GGGTAGGAT-3', but was not predicted to contain any known transcription factor binding sites. The second putative promoter region was located between 74 and 45 nt upstream of *stoD* and contains a -35 element, with sequence 5'-TTGCTT-3', and a -10 element, with sequence 5'-CCTCAATAT-3'. This putative promoter was also predicted to contain binding

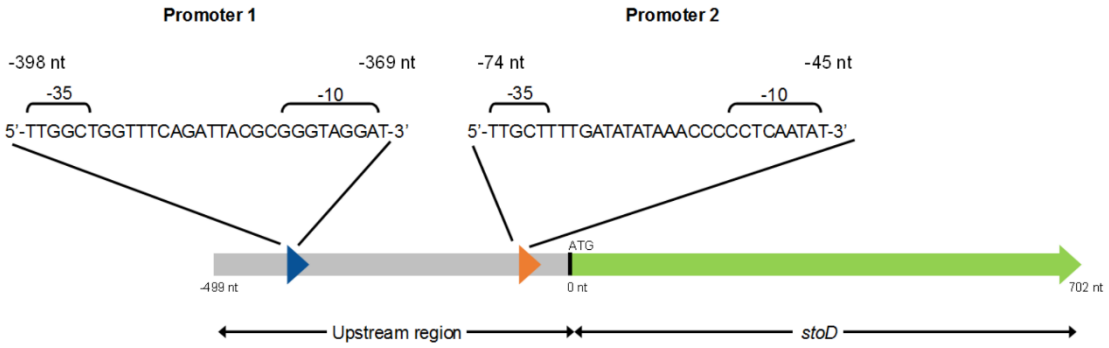


Figure 4.7. The upstream region of *stoD* contains two putative promoters. A diagrammatic representation of *stoD* and the upstream genomic region, with the two putative promoters displayed. For both promoters, the -35 and -10 regions are displayed. Promoter analysis performed using BPROM (Solovyev & Salamov 2011).

sites for the regulators PhoB (Lucas et al. 2000) and LexA (Bunny et al. 2002), as well as the RNA polymerase sigma factor, RpoD (Scaife et al. 1979). Therefore, it is likely that this second promoter is the promoter required for expression of *stoD* and intrinsic regulation of this promoter may be required for the correct expression of *stoD* that results in its secretion by the *SPI-1* and *SPI-2* T3SSs in *S.* Typhi.

4.4.3. Investigating the Localisation of the Novel Effectors in HeLa Cells

The novel effector proteins were cloned into the pRK5 vector with a HA-tag for transient expression in HeLa cells and their localisation was determined by immunofluorescence microscopy (Figure 4.8). HA-mCherry was used as a control, and was found to be localised throughout transfected cells with a diffuse staining pattern, as expected. HA-StoA, HA-StoB and HA-StoC were also found to have a diffuse localisation throughout transfected cells, similar to HA-mCherry. StoD-HA expression resulted in the formation of distinct puncta localised throughout transfected cells, whereas StoE-HA expression resulted in the formation of puncta of varying sizes that were enriched around the perinuclear region. As StoE was predicted to contain a transmembrane domain, it was investigated if this transmembrane domain was responsible for the formation of these puncta. Expression of HA-StoE without the transmembrane domain (HA-StoE [41-273]) in HeLa cells resulted in a loss of the punctate localisation, suggesting that this putative transmembrane domain is required for the punctate localisation.

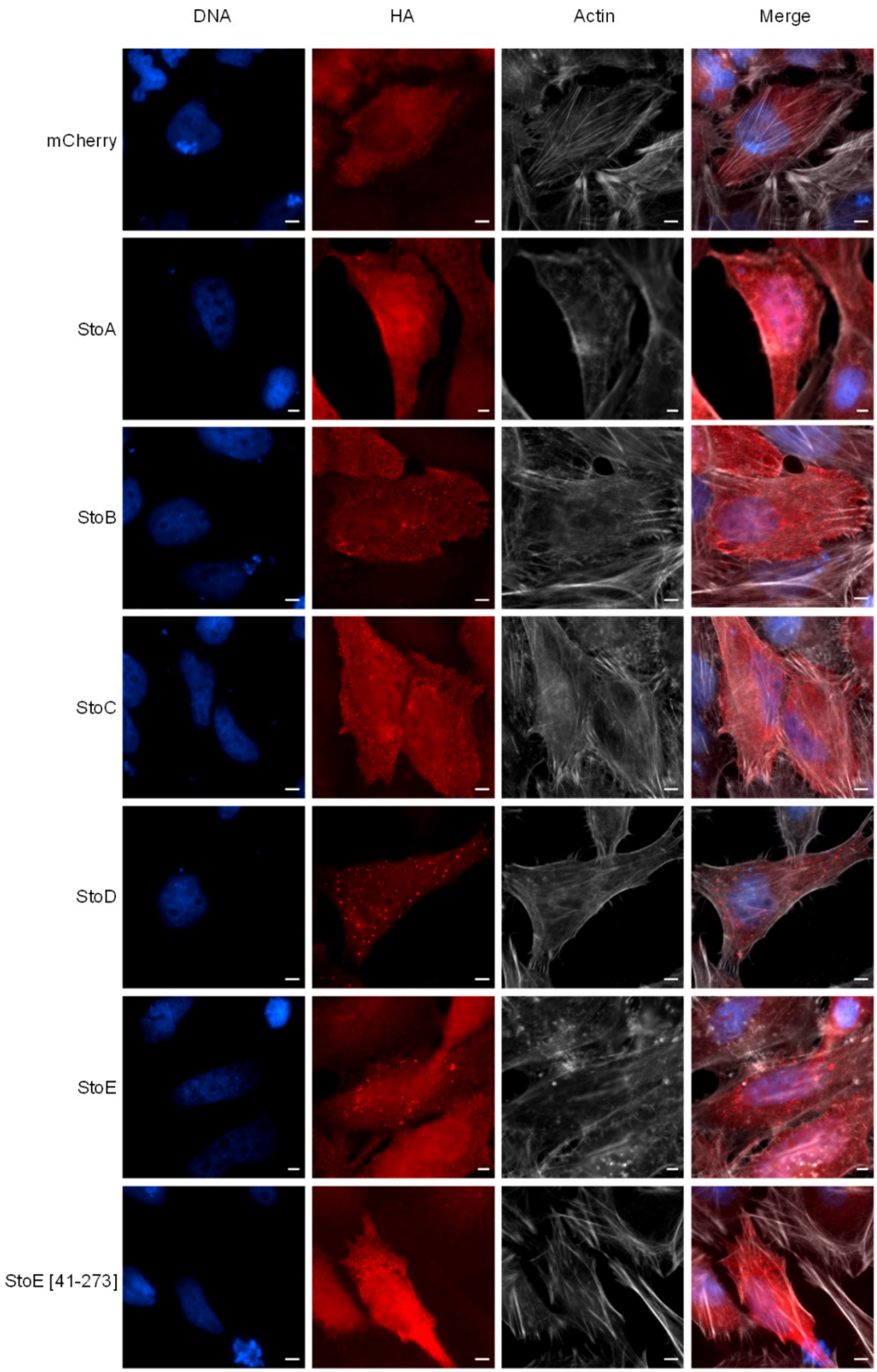


Figure 4.8. Localisation of the novel effectors during ectopic expression in HeLa cells. Representative immunofluorescence images of the novel effector proteins in HeLa cells 24 h post-transfection with pRK5 containing HA-tagged *mCherry*, *stoA*, *stoB*, *stoC*, *stoD*, *stoE* and *stoE* [41-273]. DNA and actin were visualised using Hoescht 33258 and Phalloidin-iFluor 647, respectively. Novel effector proteins were visualised by anti-HA antibodies. Scale bar, 5 μm. Images representative of three independent repeats.

Therefore, only two of the novel effectors were found to localise in a formation other than diffuse, and in the case of StoE, this was dependent on the putative N-terminal transmembrane domain predicted by InterPro analysis (Finn et al. 2017).

4.4.4. Assessing the Role of the Novel Effectors in *S.* Typhi Invasion and Replication

Genomic deletion mutations of the novel effector proteins were generated using the λ Red Recombinase system (Datsenko & Wanner 2000) in the Ty2 *S.* Typhi strain and used to infect HeLa and THP-1 macrophage cells lines to assess the role of these genes in *S.* Typhi invasion and replication (Figure 4.9).

To assess the role of these novel effectors in *S.* Typhi invasion, the Ty2 mutants were primed by two different methods both shown to induce *SPI-1* expression (Ibarra et al. 2010; Elhadad et al. 2016), as we had recently shown that *SPI-1* T3SS effectors are differentially required depending on how *S.* Typhi is primed prior to infection of HeLa cells (Johnson et al. 2017). Based on this work, bacteria were either grown as a static overnight (Figure 4.9A), or as a shaking overnight before sub-culturing and growth to OD_{600} ~1.8-2.0 (Figure 4.9B), before being used to infect HeLa cells. At 2 h post-infection, cells were lysed and the intracellular CFU enumerated and compared to the inoculum to calculate the percentage invasion. With both methods of bacterial priming, the Δ*invA* Ty2 strain (0.001% invasion for both methods) was significantly less invasive than WT Ty2. This was expected as the *SPI-1* T3SS is required for *Salmonella* invasion of non-phagocytic cells (Galán & Curtiss 1989). When primed using static overnight, WT Ty2 infection resulted in 1.1% invasion, compared to 0.7% when primed by sub-culture. There was no significant difference in invasion of any of the novel effector mutants compared to WT Ty2 when primed by either method.

To evaluate the role of the novel effectors in *S.* Typhi intracellular replication, these strains were also used to infect THP-1 macrophages. At 2 h and 24 h post-infection, cells were lysed and the number of intracellular bacteria was determined by CFU enumeration to determine

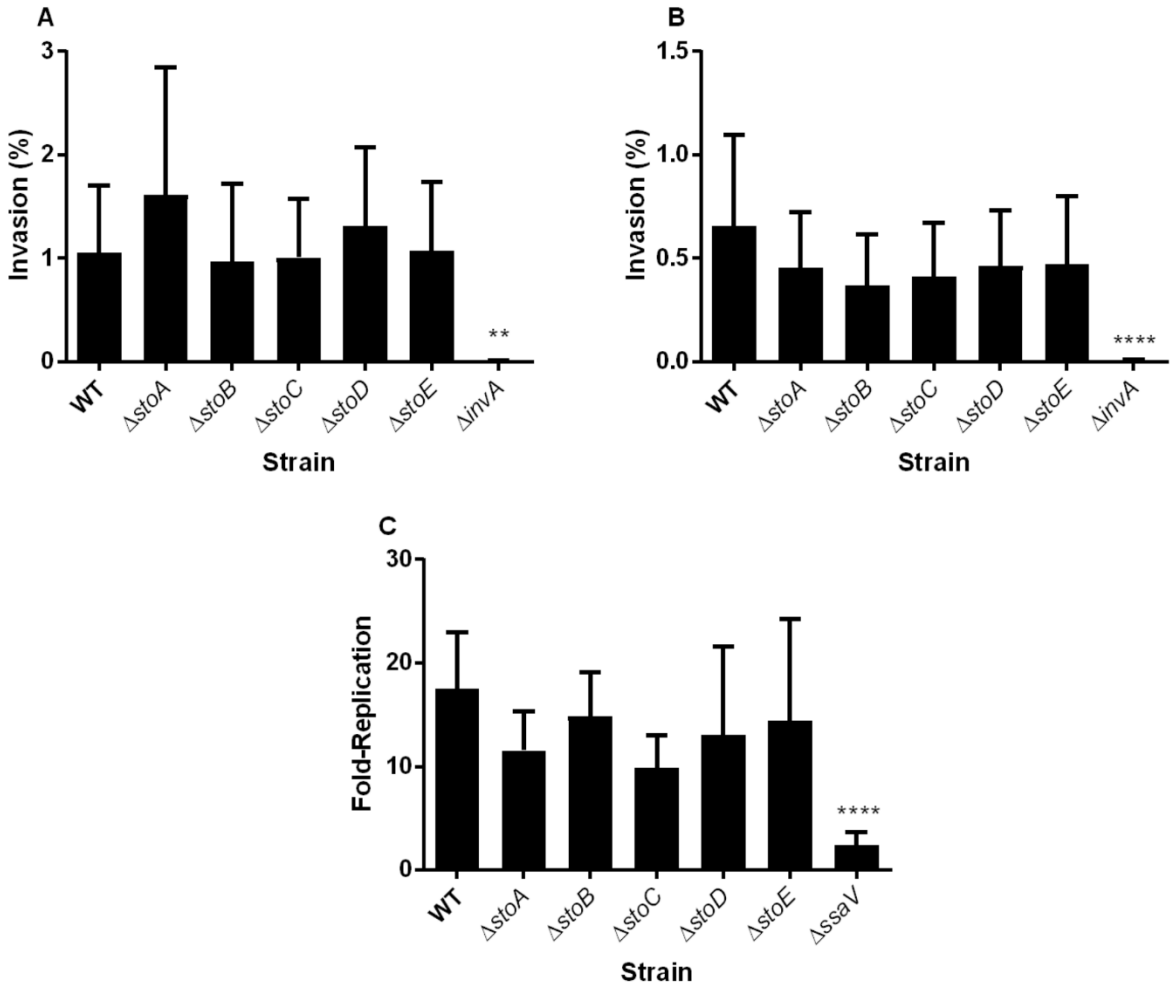


Figure 4.9. Assessing the role of the novel effectors in *S.* Typhi invasion and replication. (A) Invasion of HeLa cells by Ty2 *S.* Typhi mutant and WT strains was assessed after growth of these strains under static conditions overnight. **(B)** Invasion of HeLa cells by Ty2 *S.* Typhi mutant and WT strains was assessed after growth of these strains as shaking subcultures. **(C)** Replication of Ty2 *S.* Typhi mutant and WT strains was evaluated during infection of THP-1 cells. Graphs shows mean + SD. Mutant Ty2 strains were compared to WT in each infection using a Kruskal-Wallis test with a Dunn's multiple comparisons test (**= $p<0.01$, *** = $p<0.001$ and **** = $p<0.0001$). Each figure represents the average of three independent repeats.

the fold-replication (Figure 4.9C). The Δ*ssaV* Ty2 strain showed significantly less replication over the 24 h period (2.4-fold replication), compared to WT (17.6-fold replication), as expected, as the *SPI-2* T3SS is required for intracellular *Salmonella* replication and survival (Shea et al. 1996). There was no significant difference in replication between any of the novel effector mutants compared to WT Ty2.

Therefore, the novel effectors were found to not be required for *S.* Typhi invasion or replication using cell culture models.

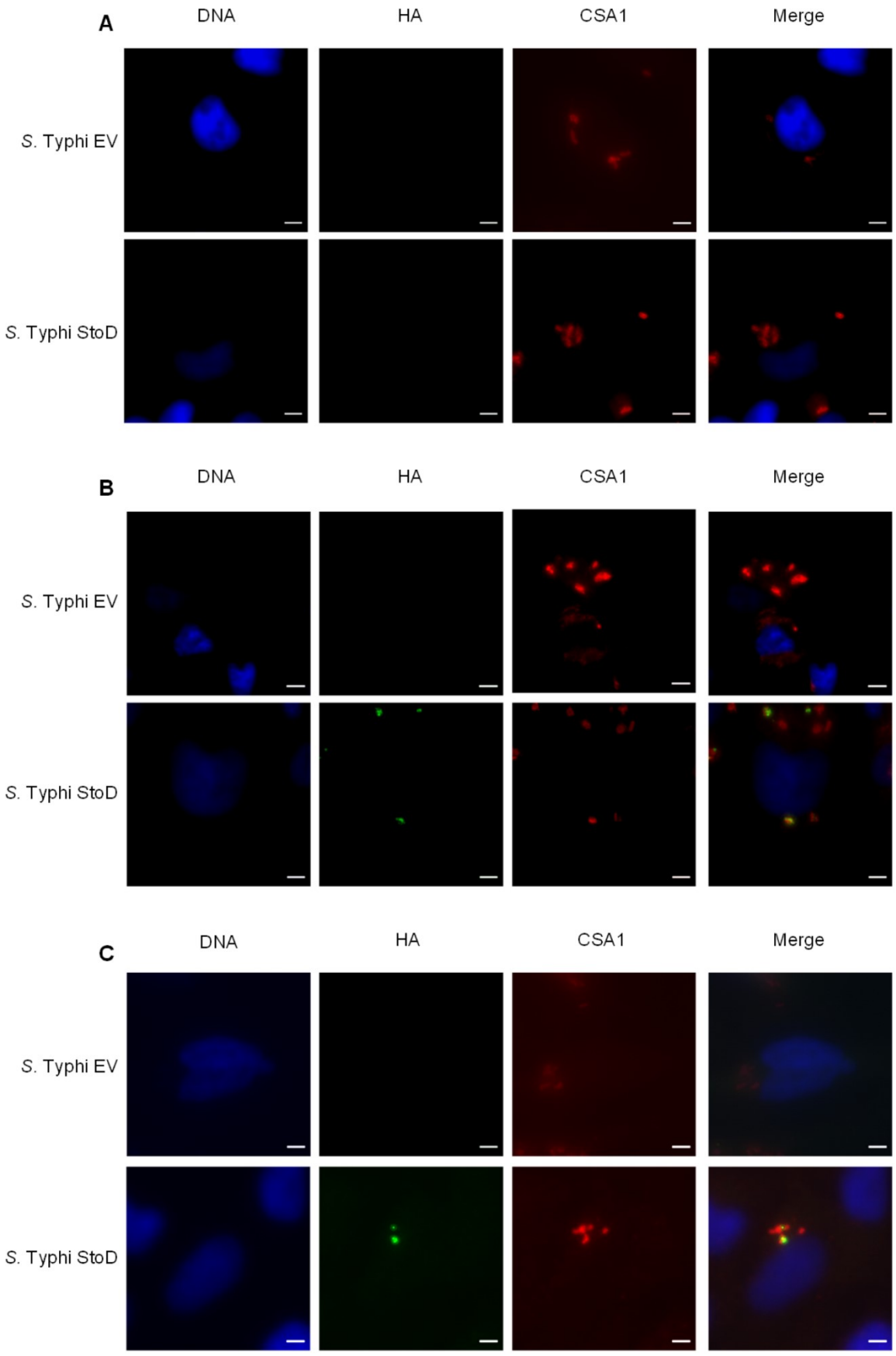
4.4.5. Investigating the Localisation of StoD and StoE during *S.* Typhi Infection

Since StoD and StoE were shown to assume punctate localisations upon ectopic expression in HeLa cells (Figure 4.8), it was therefore assessed whether these effectors localised in these puncta during *S.* Typhi infection. WT Ty2 strains containing either EV or pWSK29 encoding *stoD* or *stoE* with C-terminal 4HA-tags were used to infect HeLa cells. At 2, 4, 6 and 24 h post-infection, infected cells were fixed and stained for immunofluorescence microscopy (Figure 4.10). The pWSK29-Spec-p*stoD*-4HA construct was used in this experiment, to ensure that it would be secreted in the appropriate manner.

At 2 h post-infection, small clusters of bacteria were observed close to the nucleus (Figure **4.10**A) which did increase in size at 4 h (Figure 4.10B) and 6 h (Figure 4.10C) post-infection, until at 24 h post-infection when the bacterial clusters occupied the majority of the cell cytoplasm (Figure 4.10D). StoD-4HA could be observed in infected cells from 4 h post-infection infection (Figure 4.10B), where it appeared to localise with a minority of bacteria.

By 24 h post-infection however, StoD-4HA could be seen localised to a larger number of bacteria (Figure 4.10D). StoE-4HA was not observed in infected cells at 2, 4 or 6 h post-infection, but could be seen at 24 h post-infection, where it appeared to localise with the bacteria (Figure 4.10D), similar to StoD-4HA. Since both StoD-4HA and StoE-4HA appeared to localise in close association with bacteria during infection, it was investigated whether the HA staining for both effectors were inside the bacteria. To determine this, cells were permeabilised with saponin, a selective detergent that, unlike Triton X-100, does not permeabilise bacteria (Jamur & Oliver 2009) (Figure 4.10D). Saponin permeabilisation did not result in any StoD-4HA or StoE-4HA staining, suggesting that the staining observed previously had been from within the bacteria.

It was therefore not possible to observe the localisation of StoD or StoE during *S.* Typhi infection, and hence, no comparisons could be drawn with the localisations seen upon ectopic expression.


A
DNA
HA
CSA1
Merge
S. Typhi EV
S. Typhi StoD
B
DNA
HA
CSA1
Merge
S. Typhi EV
S. Typhi StoD
C
DNA
HA
CSA1
Merge
S. Typhi EV
S. Typhi StoD

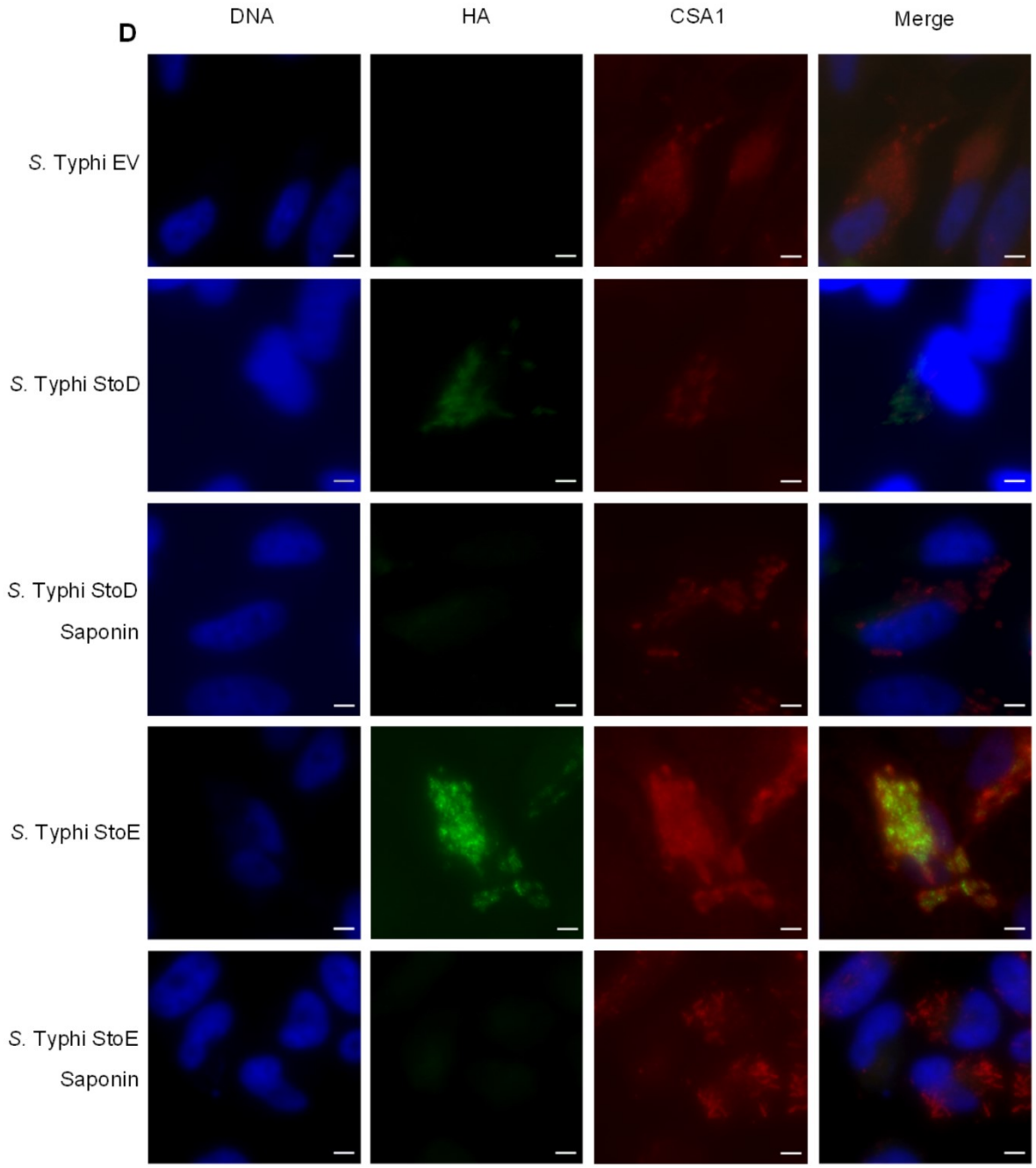


Figure 4.10. Investigating the localisation of StoD and StoE during *S.* Typhi infection. Representative images of HeLa cells infected with Ty2 *S.* Typhi containing either EV, pWSK29-Spec-p*stoD*-4HA (StoD) or pWSK29-Spec-*stoE*-4HA (StoE, 24 h post-infection only) at **(A)** 2 h post-infection, **(B)** 4 h post-infection, **(C)** 6 h post-infection or **(D)** 24 h post-infection. Cells were permeabilised with 0.2% Triton-X100 unless stated otherwise. DNA and actin were visualised using Hoescht 33258 and Phalloidin-iFluor 647, respectively. StoD-4HA and StoE-4HA proteins were visualised using an anti-HA antibody and *S.* Typhi were visualised using an anti-CSA1 antibody. Scale bar, 5 μm. Microscopy performed by Elli Mylona. Images representative of two independent repeats.

4.4.6. Evaluating StoD Expression during *S.* Typhi Infection of THP-1 Human Macrophages

As StoD was only secreted from S. Typhi when cloned under its endogenous promoter (Figure 4.1A, Figure 4.2A and Figure 4.2B), it was investigated if StoD was expressed from its own promoter during S. Typhi infection. Δ*stoD* Ty2 strains containing either EV or the pStoD construct were used to infect THP-1 macrophages and at 2, 4, 6, 8 and 24 h post-infection, infected cells were lysed and analysed by SDS-PAGE and western blot for the presence of StoD-4HA (Figure 4.11). A sample was also taken from the inoculum to examine if StoD was expressed here. As seen by western blot StoD-4HA was observed in the inoculum and from 2 h post-infection, and reached maximal expression at 24 h post-infection (Figure 4.11). However, since the number of intracellular bacteria would have increased during the infection, this may be responsible for the increase in HA signal in the western blot. Nevertheless, it was possible to observe the expression of StoD from its endogenous promoter during *S.* Typhi infection of THP-1 macrophages.

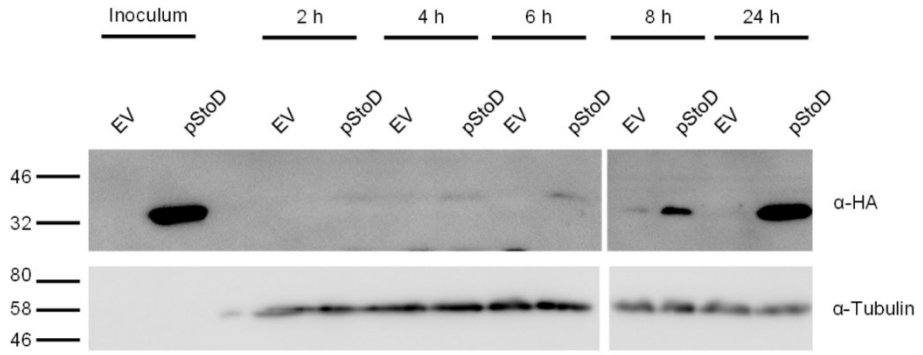


Figure 4.11. Investigating the expression of StoD during *S.* Typhi infection. Western blot of either the bacterial inoculum or cells infected with Δ*stoD* S. Typhi containing either EV or pWSK29-p*stoD*-4HA (pStoD). At 2, 4, 6, 8 and 24 h post-infection, infected cells were lysed and analysed by SDS-PAGE and western blot. HA-tagged proteins were detected using an anti-HA antibody and tubulin was detected using an anti-tubulin antibody. Image representative of two independent repeats.

4.4.7. Assessing the Effect of StoD on *S.* Typhimurium Invasion and Replication

As *S.* Typhimurium does not encode a homologue of StoD (Table 4.5), and StoD was translocated in abundance during *S.* Typhimurium infection (Figure 4.4B), it was investigated if ectopic expression of StoD in *S.* Typhimurium would have an effect on invasion or intracellular replication during infection (Figure 4.12).

WT and Δ*prgH S.* Typhimurium strains containing either EV or pWSK29-*stoD* were used to infect HeLa cells. At 2 h post-infection, cells were lysed and the intracellular CFU was enumerated and compared to the inoculum to calculate the percentage invasion (Figure **4.12**A). Both Δ*prgH S.* Typhimurium strains demonstrated 0.002% invasion, which was significantly less that WT strains (0.64% with the EV, and 0.56% with StoD, respectively). This was expected as the *SPI-1* T3SS is required for invasion (Galán & Curtiss 1989). There were no significant differences in invasion between EV and StoD strains in either WT or Δ*prgH* backgrounds.

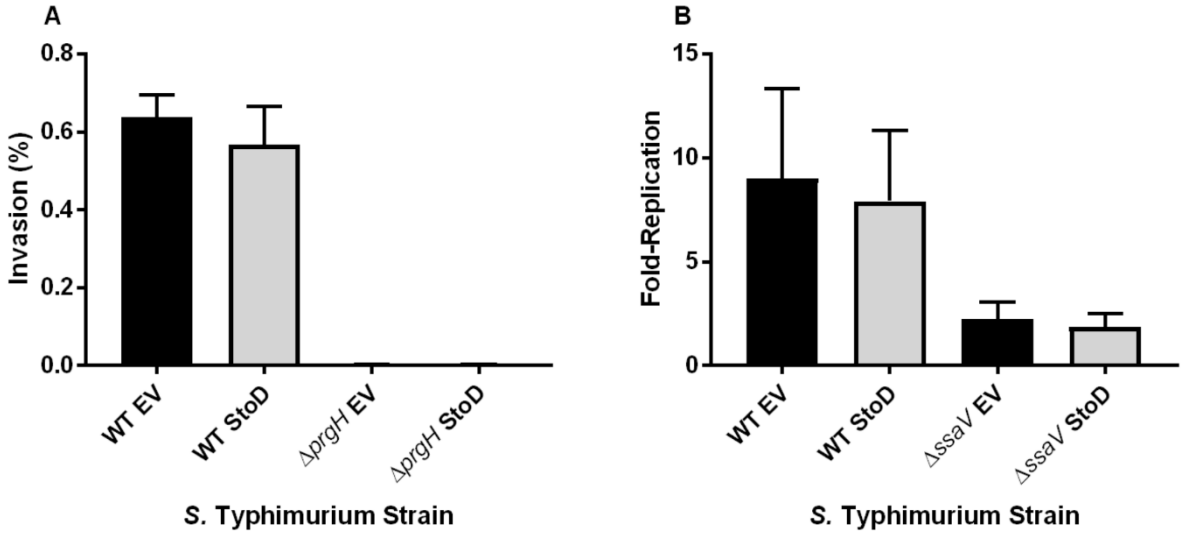


Figure 4.12. Assessing the effect of StoD on *S.* Typhimurium invasion and replication. (A) Invasion of HeLa cells with ATCC14028 *S.* Typhimurium WT and Δ*prgH* strains either with the EV or pWSK29-*stoD* (StoD). This graph represents the average of two independent repeats. **(B)** Replication of ATCC 14028 *S.* Typhimurium WT and Δ*ssaV* strains with either the EV or StoD at 24 h post-infection during infection of RAW264.7 cells compared to 2 h post-infection. This graph represents the average of four independent repeats. Graphs shows mean + SD. All strains were compared to each other using a Kruskal-Wallis test with a Dunn's multiple comparisons test.

WT and Δ*ssaV S.* Typhimurium strains containing either EV or pWSK29-*stoD* were used to infect RAW264.7 murine macrophages. Murine macrophages were used as opposed to the human macrophages used with *S.* Typhi as *S.* Typhimurium replication during infection is better characterised in murine macrophages (Freeman et al. 2003; Coombes et al. 2007), and if any phenotype was observed during *S.* Typhimurium infection, a comprehensive approach could be undertaken to investigate this phenotype. At 2 and 24 h post-infection, cells were lysed and CFU enumerated to determine the fold-replication of all strains (Figure 4.12B). Both Δ*ssaV* strains exhibited significantly less replication in RAW264.7 macrophages at 24 h post-infection (2.2-fold and 1.9-fold, with EV and StoD, respectively) compared to the WT strains (9.0-fold and 7.9-fold, with EV and StoD, respectively). This was expected as the *SPI-2* T3SS is required for intracellular replication of *Salmonella* (Shea et al. 1996). There were no significant differences in replication between EV and StoD strains in both WT and Δ*ssaV* genetic backgrounds.

Therefore, the addition of StoD to *S.* Typhimurium had no significant effect on *S.* Typhimurium invasion or replication within mammalian cells.

4.5. Discussion

Previous attempts to identify novel T3SS effector proteins in *Salmonella* have primarily been performed using *S.* Typhimurium (Miao et al. 1999; Geddes et al. 2005; Niemann et al. 2011). Whilst some of these proteins have been shown to be absent in *S.* Typhi (Appendix 1), no studies have attempted to identify additional T3SS effectors that are present in *S.* Typhi. To identify such effector proteins, a computational machine-learning approach was employed to identify putative T3SS effector proteins in *S.* Typhi. A list of known *Salmonella* T3SS effectors, and one putative *S.* Typhi effector was used to train the algorithm, and all but three of these were ranked within the top 100 genes most likely to be effector proteins. These effectors had been experimentally validated previously, and therefore it was expected that they would be highly ranked as possible effectors by the algorithm. However, three of these effectors were

ranked outside of the top 100 genes suggesting that there could be additional novel effector proteins also located outside of the top 100 ranked genes. Several genes known not to encode T3SS effectors were also present in the top 100 genes such as T3SS chaperones as well as components of the flagellum. T3SS chaperones have been shown to share structural motifs with T3SS effectors that enable them to maintain the effector in a secretion-competent confirmation (Lilic et al. 2006) and are usually localised close to effectors within the genome (Knodler et al. 2002; Miki et al. 2009). The T3SS and flagellar machinery are evolutionarily related and share many structural similarities (Kawamoto et al. 2013). It is therefore unsurprising that the algorithm identified some T3SS chaperones and flagellar components as possible T3SS effectors. Previous studies that have employed this machine-learning approach, have used successive rounds of putative effector identification and validation, each time adding the effector proteins identified and validated from the previous round (Burstein et al. 2009). In this study, it was intended that another round of putative effector identification would have been performed once the effectors identified here had been completely validated and could be used to further train the algorithm. However, the validation of these effectors took longer than anticipated, meaning that there was not sufficient time to repeat the machine-learning algorithm. Future work may seek to achieve this, but may also wish to use a larger database of known T3SS effectors from a wide range of pathogens, such as that used in previous work (Tobe et al. 2006) as this made aid in the improvement of the algorithm and enable the identification of additional effector proteins.

The putative homologues of *stoA* and *stoE* in other pathogenic bacterial species have not been investigated here as this was outside the scope of the project, but they have also not been studied elsewhere. However, such investigation may elucidate conserved biological activities or functions that could aid in the further understanding of *S.* Typhi infection. Only one of the predicted effector proteins investigated here, *stoB*, was found to have a putative homologue in *S.* Typhimurium. However, translocation assays demonstrated that this homologue was not translocated by *S.* Typhimurium, suggesting that this homologue is not an

effector protein. This should be considered by future work assessing further homologues of StoB, as well as those of StoC and StoD in other *Salmonella* serovars. However, the investigation of such genes in non-human restricted serovars such as *S.* Enteritidis and *S.* Gallinarum (Thomson et al. 2008; Feng et al. 2012) may enable the study of these effectors in an *in vivo* setting and therefore aid in furthering our understanding of the role of these proteins during infection.

Whilst it was found that by preventing production of the Vi-antigen by mutation of *tviB*, it was possible to observe secretion from the *SPI-1* T3SS in *S.* Typhi, it was also found that even upon mutation of the *SPI-1* T3SS, secretion was still observed under *SPI-1*-inducing conditions and further investigation found that the flagellar export apparatus was responsible for this secretion. This is unsurprising as the flagellum does use a T3SS to secrete the flagellar hook proteins during assembly (Bergeron 2016) and flagellar genes are induced under *SPI-1*-inducing conditions (Ibarra et al. 2010). However, this issue was not observed when assessing the secretion of endogenous proteins using specific antibodies, suggesting that constitutive expression of the novel effector from a vector may cause the effector proteins to 'leak out' from the flagellar ring complex (Ibarra et al. 2010). This therefore prevents the use of the current *SPI-1* secretion assays to determine if these novel effectors are secreted in a *SPI-1* T3SS-dependent manner. The use of a vector with an inducible promoter may remedy this, or the use of the β-lactamase translocation assay with *S.* Typhimurium may allow the determination of which T3SS is required for the translocation of these novel effectors. However, since three of the novel effectors were not secreted by the appropriate T3SS in *S.* Typhimurium, it could not be used for this purpose in this study. Therefore, if the β-lactamase translocation assay were to be used to determine the T3SS-dependency of the novel effectors, *S.* Typhi would have to be used. This was not possible in the current study, due to the lack of a fluorescent plate reader in the CL3 laboratory and although other methods are available for assessing the translocation of proteins, these are more susceptible to error (Charpentier & Oswald 2004). Nevertheless, the lack of an appropriate lysis control means

that longer infections to observe the translocation of *SPI-2* T3SS effectors such as SseJ, and potentially StoA and StoE, cannot be performed. A suitable lysis control is therefore required, but what protein to use requires careful consideration.

The finding that *stoD* was only secreted from *S.* Typhi when cloned under its endogenous promoter lead to the use of a bioinformatic approach to identify putative promoters. Of the two predicted promoters in this upstream region, only one of these promoters matched binding sites of known regulatory and RNA polymerase proteins (Lucas et al. 2000; Bunny et al. 2002; Scaife et al. 1979). One of the proteins predicted to bind to this promoter region, PhoB, regulates the expression of *hilA* and therefore expression of the *SPI-1* T3SS and associated effectors (Lucas et al. 2000; Bajaj et al. 1996), suggesting that *stoD* may be regulated in a similar manner to *SPI-1* in *S.* Typhi. A previous study investigating changes in the transcriptome of *S.* Typhi during infection of human macrophages found that whilst *stoD* was upregulated after phagocytosis, its expression decreased once *S.* Typhi was intracellular (Faucher et al. 2006). A similar expression profile was observed for many components of the *SPI-1* T3SS and the associated effector proteins (Faucher et al. 2006), corroborating with the idea that StoD is regulated in this way. However, expression of StoD from its endogenous promoter during *S.* Typhi infection of THP-1 macrophages showed that the amount of StoD protein increased during infection. Whilst this may be due to an increase in bacterial numbers, another explanation could be that whilst *stoD* expression decreases during infection (Faucher et al. 2006), the protein may remain throughout the infection. Interestingly, this upstream region was only required for secretion of *stoD* from *S.* Typhi and not for translocation by *S.* Typhimurium, suggesting that there are *S.* Typhi-specific regulatory processes that may control the secretion of StoD. One possibility for this finding may be that when *stoD* is expressed under the control of the T3 promoter, a doublet band is seen by western blot (Figure 4.1A), where the smaller protein corresponds to the band observed when *stoD* is cloned along with the upstream region. This larger, incorrect, protein of the doublet may sequester a *S.* Typhi protein required for StoD secretion, meaning that it cannot interact with StoD,

resulting in a lack of secretion. However, further experimentation is required to evaluate this hypothesis. This finding does raise the possibility that other proteins may be regulated in a similar way and their secretion may be missed in the current experimental setup. However, four other proteins have been demonstrated to be secreted when under the control of the T3 promoter, suggesting that this is not of significant concern. But, the regulation of these proteins during infection may be affected by the use of the T3 promoter and future investigation should take this into consideration.

StoE was predicted to contain a transmembrane domain which was then demonstrated to be required for a perinuclear vesicular localisation during ectopic expression in HeLa cells. SseF, another *Salmonella* effector, also localises to the perinuclear region upon transfection, where it colocalises with vesicles of the Golgi apparatus (Kuhle et al. 2004). However, it has been shown that upon translocation, the localisation of SseF is altered, and is no longer associated with the Golgi, but localises to the SCV (Kuhle et al. 2004). This highlights the importance of comparing the localisations of proteins during infection and upon ectopic expression, which has so far not been possible with the novel proteins identified here. However, this does suggest that further experiments should assess whether StoE localises to the SCV of *S.* Typhi and to elucidate its role during infection. Ectopic expression of StoD in HeLa cells also resulted in the formation of puncta indicating that it is being localised to a particular region within the cell, similar to StoE, and will be investigated further in the subsequent chapter.

Whilst none of the novel effectors were demonstrated to be required for *S.* Typhi invasion or replication, there were still some interesting findings.

During invasion of HeLa cells, it was found that bacteria primed by static overnight were more invasive than those that had been primed by shaking subculture, even though both are recognised as inducing expression of the *SPI-1* T3SS (Ibarra et al. 2010). It has been demonstrated that *sopE*, is expressed at higher levels when *S.* Paratyphi A is grown as a static overnight, where oxygen availability is limited, than when grown as a subculture, where oxygen availability is higher (Elhadad et al. 2016). We have also shown that *sopE* is essential

for invasion when *S.* Typhi is primed by growth as a static overnight, but not when grown as a subculture (Johnson et al. 2017). However, *sopE* is essential for invasion and its expression is unchanged when *S.* Typhimurium is primed by either of these growth conditions (Ibarra et al. 2010; Elhadad et al. 2016; Johnson et al. 2017). These differences in *sopE* expression between typhoidal and NTS serovars suggest that typhoidal serovars have an additional level of *sopE* regulation, based on environmental oxygen availability, that is absent in *S.* Typhimurium, and may account for the increased invasion of typhoidal bacteria grown under oxygen-limited conditions (Elhadad et al. 2016; Johnson et al. 2017). The exact mechanism of this regulation, and whether this extends to other T3SS effector proteins remains to be elucidated.

During infection of THP-1 macrophages it was demonstrated that the Δ*ssaV S.* Typhi mutant, lacking a functional *SPI-2* T3SS (Beuzón et al. 1999), replicated significantly less than WT *S.* Typhi. This was as expected as the *SPI-2* T3SS has been demonstrated to be required for replication of *S.* Typhimurium and *S.* Typhi within macrophages (Shea et al. 1996; Khan et al. 2003). However, one study previously found that deletion of the entire *SPI-2* T3SS operon, had no effect on the replication of *S.* Typhi in a human macrophage cell line (Forest et al. 2010). The latter report used the ISP1820 strain of *S.* Typhi (Forest et al. 2010), whereas our work and that of other previous studies used the Ty2 strain (Khan et al. 2003). These two *S.* Typhi strains do differ genetically, in particular Ty2 lacks the *rpoS* gene (Santander et al. 2007) which has been demonstrated to be involved cytotoxicity towards macrophages (Khan et al. 1998), which may have caused these differences in findings. Nevertheless, this disparity in results demonstrates that further work is required to investigate the role of the *SPI-2* T3SS in the pathogenesis of typhoidal *Salmonella* serovars and how this compares to NTS serovars.

Whilst assessing the roles of the novel effectors in *S.* Typhi invasion and replication does provide a means to determining if they are involved in these processes, *S.* Typhi infection in humans not only involves these processes (Parry et al. 2002), but also modulation of host immune responses (Winter et al. 2014; Wangdi et al. 2014). In *S.* Typhimurium, several

effectors are involved in the control of the host immune response, including SspH1 (Keszei et al. 2014; Haraga & Miller 2003; Haraga & Miller 2006), SpvC (Haneda et al. 2012) and SpvD (Rolhion et al. 2016). Future work should therefore seek to evaluate the roles of the novel effectors in modifying the host immune responses to *S.* Typhi infection.

Further to this, human infection with *S.* Typhi also involves systemic dissemination and colonisation of secondary infection sites such as the liver, spleen and gallbladder (Parry et al. 2002), which does not usually occur with NTS infection (de Jong et al. 2012). Although this is thought to involve effector proteins to some degree (Hernandez et al. 2003; Rytkönen et al. 2007; Fàbrega & Vila 2013) it is difficult to assess *S.* Typhi dissemination due to the lack of appropriate animal models. Whilst *S.* Typhi cannot survive in mice (Spanò & Galan 2012), humanised mice and non-human primates are both capable of sustaining *S.* Typhi infection (Firoz Mian et al. 2011; Edsall et al. 1960). However, since mice are not a natural host, this mean their use requires careful consideration (Darton et al. 2014), expense and ethical concerns limit the use of non-human primates (Gal-Mor et al. 2014). An obvious solution may be to use *S.* Typhimurium infection of mice, which does replicate some of the inflammatory and pathological responses seen in typhoid fever patients (Hurley et al. 2014), as well as being able to simulate colonisation of secondary infection sites (Gonzalez-Escobedo & Gunn 2013). However, *S.* Typhimurium is genetically distinct to *S.* Typhi and contains many genes, including T3SS effectors, that are absent in *S.* Typhi (Parkhill et al. 2001). This may somewhat explain why no effect on invasion or replication was seen when StoD was expressed in *S*. Typhimurium, and may therefore be inappropriate for the study of T3SS effectors that are present in *S.* Typhi, but absent in *S.* Typhimurium, such as those identified here. Therefore, to gain a better understanding of these processes and the potential role of T3SS effectors in this will require the development of new experimental models, preferably involving the use of *S.* Typhi itself.

Immunofluorescence microscopy demonstrated that *S.* Typhi localised into clusters close to the perinuclear region during infection and these clusters grew in size as the infection

progressed, which may indicate that these bacteria are residing inside SCVs. It has been demonstrated that during *S.* Typhimurium infection, host proteins such as, LAMP-1 (Madan et al. 2012) and various Rab GTPases (Smith et al. 2007) are recruited to the SCV to prevent fusion with lysosomes. It would therefore be of interest to investigate if this is conserved during *S.* Typhi infection. However, preliminary work attempting to observe the localisation of LAMP-1 during *S.* Typhi and *S.* Typhimurium infection using immunofluorescence microscopy was unsuccessful. It was also not possible to observe the localisation of StoD and StoE during *S.* Typhi infection, and both proteins could only be observed inside bacteria. One solution may be to transfect cells with vectors encoding *LAMP-1*, *stoD* or *stoE*, and then infect with *S.* Typhi, to observe where these effectors localise upon infection and how this compares to ectopic expression alone.

In conclusion, a genome-wide machine-learning approach was used to identify putative T3SS effector proteins in *S.* Typhi. Four out of the five predicted proteins were found to be secreted, along with a fifth, that had previously been predicted to be a T3SS effector. Whilst these effectors were found not to be required for *S.* Typhi invasion or replication, bioinformatic analyses found that putative homologues of these novel effectors were present in other pathogenic bacteria as well as other *Salmonella* serovars. Interestingly, only one of these effectors was found to have a homologue in *S.* Typhimurium, although this was later found not to be translocated into host cells. Therefore, these novel effectors represent the first demonstration of *Salmonella* T3SS effectors that are present in *S.* Typhi and not *S.* Typhimurium, increasing the known effector repertoire of *S.* Typhi from 22 to 27.

Chapter 5: Investigating the Biological Activity of StoD

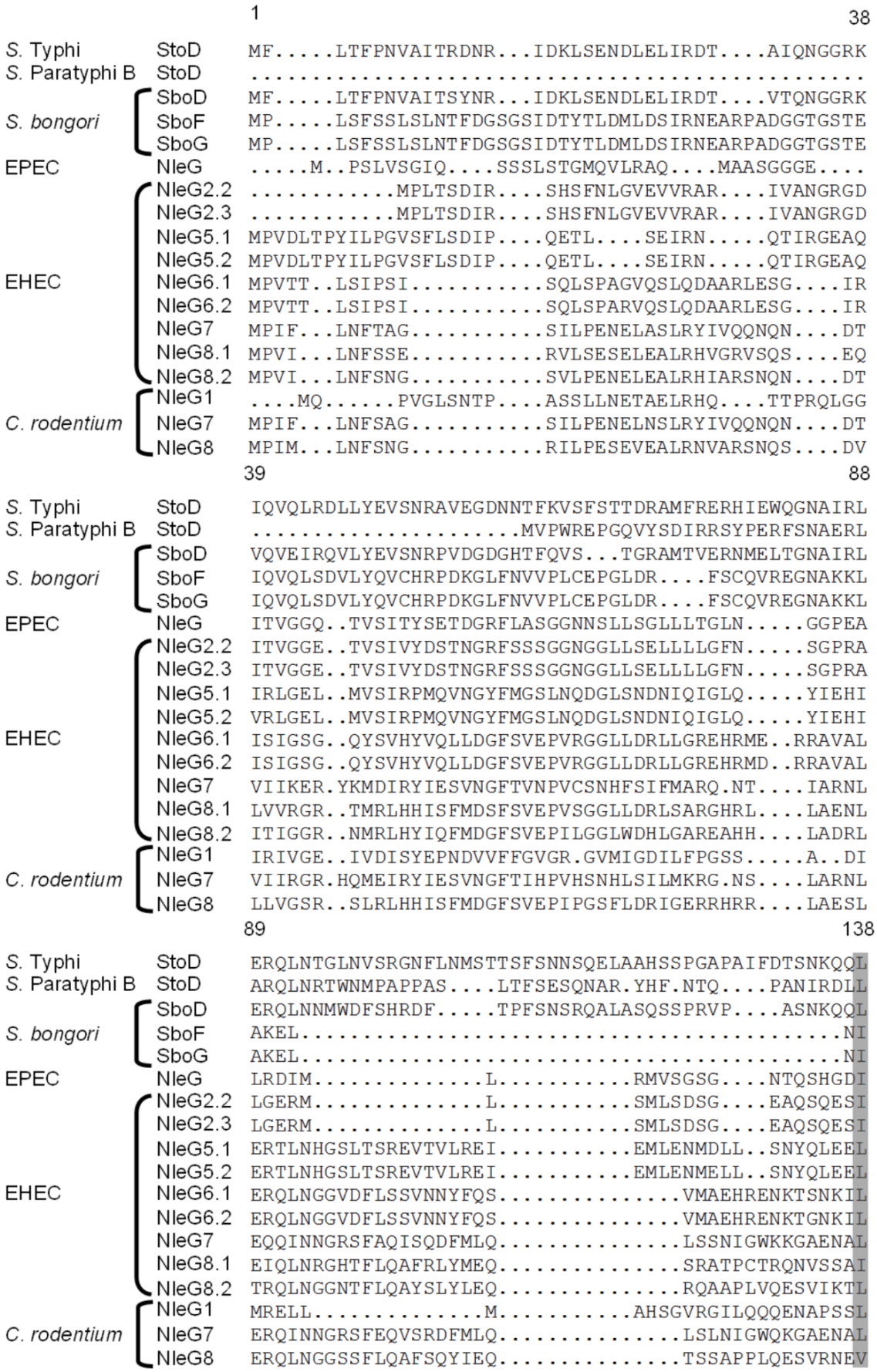
5.1. Introduction

In the previous chapters the establishment of a CL3 laboratory for the study of *S.* Typhi and the identification of novel T3SS effectors in *S.* Typhi have been described. In this chapter, the focus is on StoD, and the investigation into its biological activity as well as attempts to identify interacting partners that may be required for the function of StoD during *S.* Typhi infection.

5.2. StoD is a Putative Member of the NleG Family of T3SS Effectors

By performing BLAST analyses (Boratyn et al. 2013) and previous work (Fookes et al. 2011), it was found that StoD possessed sequence similarity to the NleG family of T3SS effectors (Table 4.4). InterPro prediction (Finn et al. 2017) also suggested that StoD contains a C-terminal RING-type domain as found in NleG proteins (Wu et al. 2010).

Since being identified as T3SS effector proteins in *C. rodentium* (Deng et al. 2004), NleG proteins have been identified in EPEC, EHEC, *S. bongori* and *S. enterica* (Tobe et al. 2006; Fookes et al. 2011). The overall sequence identity of these proteins, compared to StoD, range between 25.4% (EPEC NleG) to 74.66% (*S. bongori* SboD). The variability in sequence identity can be explained by looking at the aligned amino acid sequences of these proteins (Figure 5.1). The N-terminal region shows varying homology between proteins, ranging from 9.52% (*C. rodentium* NleG1) to 69.17% (*S. bongori* SboD) sequence identity compared to StoD. However, the C-termini are more homologous to each other with sequence identity ranging from 37.62% (EHEC NleG 2.2 and *C. rodentium* NleG8) to 82.18% (*S. bongori* SboD), compared to StoD. The C-terminus contains residues that have been identified to be involved in the formation of a RING-type E3 ubiquitin-ligase domain, in particular three residues shown to be involved in binding to E2 ubiquitin-conjugating enzymes: V165, L167 and P204 (Wu et al. 2010). It is therefore thought that the C-terminus of the NleG proteins contains the functional domain, whereas the N-terminus is thought to be required for substrate recognition


1
38
S. Typhi StoD MF.....LTFPNVAITRDNR...IDKLSENDLELIRDT....AIQNGGRK
S. Paratyphi B StoD .....
S. bongori SboD MF.....LTFPNVAITSYNR...IDKLSENDLELIRDT....VTQNGGRK
SboF MP.....LSFSSLSLNTFDGSGSIDTYTLDMLDSIRNEARPADGGTGSTE
SboG MP.....LSFSSLSLNTFDGSGSIDTYTLDMLDSIRNEARPADGGTGSTE
EPEC NleG .....M..PSLVSGIQ....SSSLSTGMQVLRAQ....MAASGGGE....
EHEC NleG2.2 .....MPLTSDIR....SHSFNLGVEVVRAR....IVANGRGD
NleG2.3 .....MPLTSDIR....SHSFNLGVEVVRAR....IVANGRGD
NleG5.1 MPVDLTPYILPGVSFLSDIP....QETL....SEIRN.....QTIRGEAQ
NleG5.2 MPVDLTPYILPGVSFLSDIP....QETL....SEIRN.....QTIRGEAQ
NleG6.1 MPVTT..LSIPSI.....SQLSPAGVQSLQDAARLESG....IR
NleG6.2 MPVTT..LSIPSI.....SQLSPARVQSLQDAARLESG....IR
NleG7 MPIF...LNFTAG.....SILPENELASLRYIVQQNQN....DT
NleG8.1 MPVI...LNFSSE.....RVLSESELEALRHVGRVSQS....EQ
NleG8.2 MPVI...LNFSNG.....SVLPENELEALRHIARSNQN....DT
C. rodentium NleG1 ....MQ.....PVGLSNTP....ASSLLNETAELRHQ....TTPRQLGG
NleG7 MPIF...LNFSAG.....SILPENELNSLRYIVQQNQN....DT
NleG8 MPIM...LNFSNG.....RILPESEVEALRNVARSNQS....DV
39
88
S. Typhi StoD IQVQLRDLLYEVSNRAVEGDNNTFKVSFSTTDRAMFRERHIEWQGNAIRL
S. Paratyphi B StoD .....MVPWREPGQVYSDIRRSYPERFSNAERL
S. bongori SboD VQVEIRQVLYEVSNRPVDGDGHTFQVS...TGRAMTVERNMELTGNAIRL
SboF IQVQLSDVLYQVCHRPDKGLFNVVPLCEPGLDR....FSCQVREGNAKKL
SboG IQVQLSDVLYQVCHRPDKGLFNVVPLCEPGLDR....FSCQVREGNAKKL
EPEC NleG ITVGGQ..TVSITYSETDGRFLASGGNNSLLSGLLLTGLN.....GGPEA
EHEC NleG2.2 ITVGGE..TVSIVYDSTNGRFSSSGGNGGLLSELLLLGFN.....SGPRA
NleG2.3 ITVGGE..TVSIVYDSTNGRFSSSGGNGGLLSELLLLGFN.....SGPRA
NleG5.1 IRLGEL..MVSIRPMQVNGYFMGSLNQDGLSNDNIQIGLQ.....YIEHI
NleG5.2 VRLGEL..MVSIRPMQVNGYFMGSLNQDGLSNDNIQIGLQ.....YIEHI
NleG6.1 ISIGSG..QYSVHYVQLLDGFSVEPVRGGLLDRLLGREHRME..RRAVAL
NleG6.2 ISIGSG..QYSVHYVQLLDGFSVEPVRGGLLDRLLGREHRMD..RRAVAL
NleG7 VIIKER.YKMDIRYIESVNGFTVNPVCSNHFSIFMARQ.NT....IARNL
NleG8.1 LVVRGR..TMRLHHISFMDSFSVEPVSGGLLDRLSARGHRL....LAENL
NleG8.2 ITIGGR..NMRLHYIQFMDGFSVEPILGGLWDHLGAREAHH....LADRL
C. rodentium NleG1 IRIVGE..IVDISYEPNDVVFFGVGR.GVMIGDILFPGSS.....A..DI
NleG7 VIIRGR.HQMEIRYIESVNGFTIHPVHSNHLSILMKRG.NS....LARNL
NleG8 LLVGSR..SLRLHHISFMDGFSVEPIPGSFLDRIGERRHRR....LAESL
89
138
S. Typhi StoD ERQLNTGLNVSRGNFLNMSTTSFSNNSQELAAHSSPGAPAIFDTSNKQQL
S. Paratyphi B StoD ARQLNRTWNMPAPPAS....LTFSESQNAR.YHF.NTQ....PANIRDLL
S. bongori SboD ERQLNNMWDFSHRDF.....TPFSNSRQALASQSSPRVP....ASNKQQL
SboF AKEL.....NI
SboG AKEL.....NI
EPEC NleG LRDIM.....L.....RMVSGSG....NTQSHGDI
EHEC NleG2.2 LGERM.....L.....SMLSDSG....EAQSQESI
NleG2.3 LGERM.....L.....SMLSDSG....EAQSQESI
NleG5.1 ERTLNHGSLTSREVTVLREI.....EMLENMDLL..SNYQLEEL
NleG5.2 ERTLNHGSLTSREVTVLREI.....EMLENMELL..SNYQLEEL
NleG6.1 ERQLNGGVDFLSSVNNYFQS.....VMAEHRENKTSNKIL
NleG6.2 ERQLNGGVDFLSSVNNYFQS.....VMAEHRENKTGNKIL
NleG7 EQQINNGRSFAQISQDFMLQ.....LSSNIGWKKGAENAL
NleG8.1 EIQLNRGHTFLQAFRLYMEQ.....SRATPCTRQNVSSAI
NleG8.2 TRQLNGGNTFLQAYSLYLEQ.....RQAAPLVQESVIKTL
C. rodentium NleG1 MRELL.....M.....AHSGVRGILQQQENAPSSL
NleG7 ERQINNGRSFEQVSRDFMLQ.....LSLNIGWQKGAENAL
NleG8 ERQLNGGSSFLQAFSQYIEQ.....TSSAPPLQESVRNEV

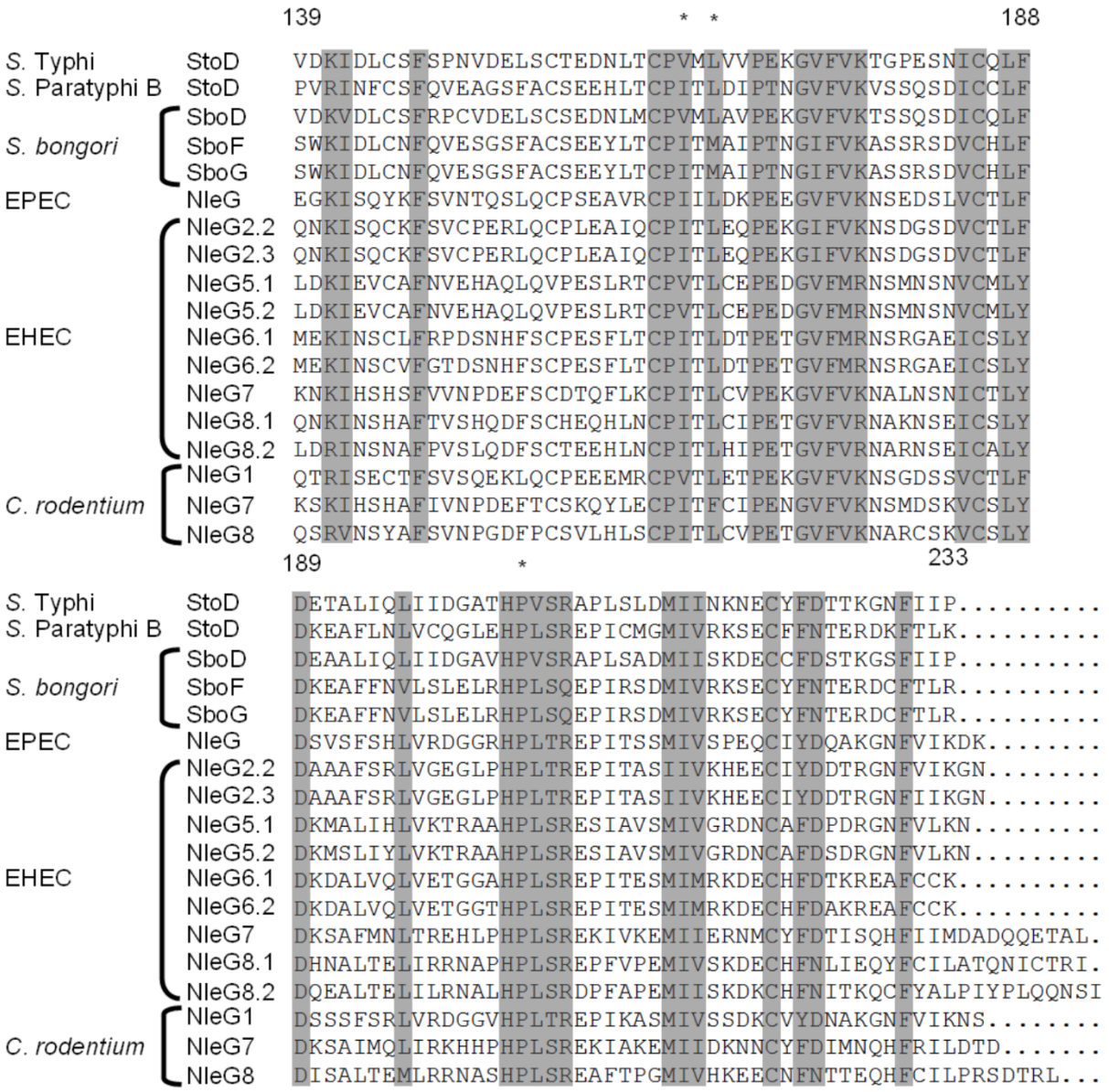


Figure 5.1. StoD is a member of the NleG family of effector proteins. Amino acid sequence alignments of StoD and NleG homologues from *S.* Paratyphi B, *S. bongori*, EPEC, EHEC and *C. rodentium.* Shaded residues are those shown to comprise the RING-type domain. * indicates residues that these residues have been shown to be involved in E2-binding (Wu et al. 2010). Sequences obtained from KEGG (Kanehisa et al. 2016), alignments performed using Clustal Omega (Sievers et al. 2011) and formatted using Strap (Gille et al. 2014).

(Wu et al. 2010), where the substrate for each NleG protein would differ, hence the lower homology for this region.

The structure of the StoD N-terminus was solved by collaborators based at the University of Oxford, Professor Susan Lea and Dr Melanie McDowell (Figure 5.2). Using X-ray crystallography, the structure of the N-terminus (StoD [1-95]) was determined at a resolution

of 2.5 Å and the C-terminus (StoD [134-233]) was modelled onto the structure of the NleG 2.3 C-terminus, which had been previously solved, using nuclear magnetic resonance (NMR) (Wu et al. 2010). While sequence identity between the C-termini of StoD and NleG 2.3 was only 38.61%, structural homology was retained, suggesting that StoD also contained the C-terminal E3 ubiquitin-ligase domain. StoD [1-95] exhibited a ubiquitin-like fold, which may be involved in targeting it towards its substrate.

Therefore, StoD shares C-terminal structural homology to the NleG family of T3SS effector proteins and is a putative member of this effector family.

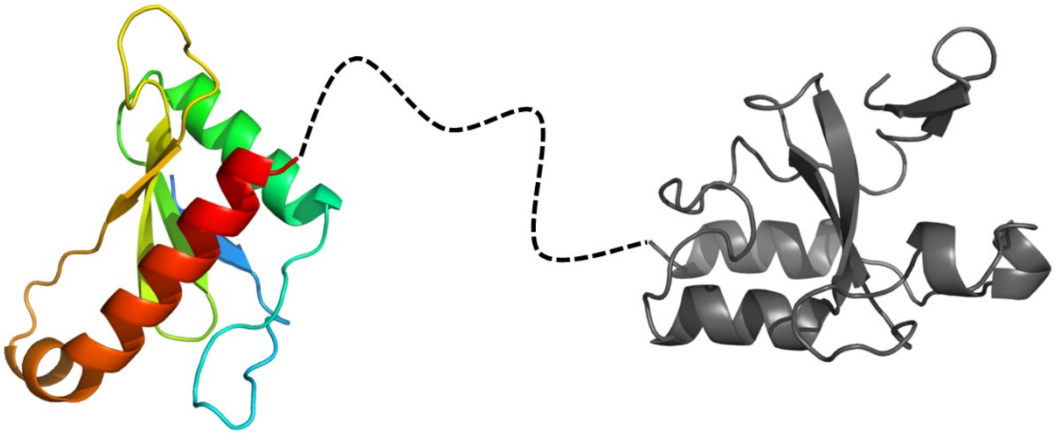


Figure 5.2. Structural model of StoD. A 2.5 Å resolution structure of the StoD [1-95] (coloured) was solved by X-ray crystallography and found to have a resemblance to a ubiquitin-like fold. The StoD [134-233] (greyscale) was modelled using the structure of NleG 2.3 (Wu et al. 2010) which has 38.61% sequence identity to the StoD [134-233]. A 30-amino acid unstructured linker connects the StoD N- and C-termini and is represented by a dashed line. Work performed by Dr Melanie McDowell and Prof. Susan Lea.

5.3. Assessing the Enzymatic Activity of StoD

5.3.1. Optimising the Expression and Purification of Recombinant StoD

Based on the sequence and structural homology to the NleG proteins, the first step in investigating the biological activity of StoD was to assess whether StoD is an E3 ubiquitin-ligase. To do this, vectors were generated encoding recombinant StoD, which would be used for *in vitro* autoubiquitination assays. However, the expression and purification of recombinant StoD had to be optimised.

Two variants of *E. coli* BL21, Star and pLysS (Table 2.1) were transformed with a pET28 construct containing StoD with a N-terminal 6His-tag, pET28-*stoD* (Table 2.2). BL21 Star contains a mutation in the RNase E gene that stabilises mRNAs produced by the T7 RNA polymerase found in BL21 *E. coli* strains (Lopez et al. 1999; Studier & Moffatt 1986). BL21 pLysS harbours a plasmid that encodes the lysozyme from the T7 bacteriophage that acts as an inhibitor of T7 RNA polymerase, therefore reducing accidental gene expression from T7 promoters, and aiding in the expression of toxic proteins (Studier & Moffatt 1986). The T7 lysozyme can also degrade the bacterial cell wall (Inouye et al. 1973) assisting in bacterial cell lysis.

Both BL21 variants were grown to an OD_{600} of 0.4-0.6 before induction with either 0.1 mM or 1 mM IPTG and incubation at 18°C overnight, or at 30°C or 37°C for 3 h. After induction, samples were taken from each condition and bacteria were collected by centrifugation. Bacterial cells were lysed by sonication to facilitate separation of soluble and insoluble fractions before being resuspended in 5x SDS loading buffer, according to the OD_{600} and analysed by SDS-PAGE with either Coomasie staining or western blot (Figure 5.3A). A protein of 30 kDa could be seen by Coomasie staining in the samples from several cultures, which was confirmed by western blot using an antibody raised against the 6His-tag, to be 6His-StoD. For BL21 Star, optimal 6His-StoD expression was observed at 37°C with either 0.1 mM or 1 mM IPTG, however the majority of this protein was found in the insoluble fraction. For BL21 pLysS, optimal 6His-StoD expression was observed at 30°C with 1 mM IPTG in which most of the 6His-StoD protein was seen in the soluble fraction.

Based on this screen, recombinant 6His-StoD was expressed using BL21 pLysS, induced with 1 mM IPTG at 30°C for 6 h. Using this method of expression followed by affinity chromatography yielded sufficient soluble 6His-StoD (Figure 5.3B).

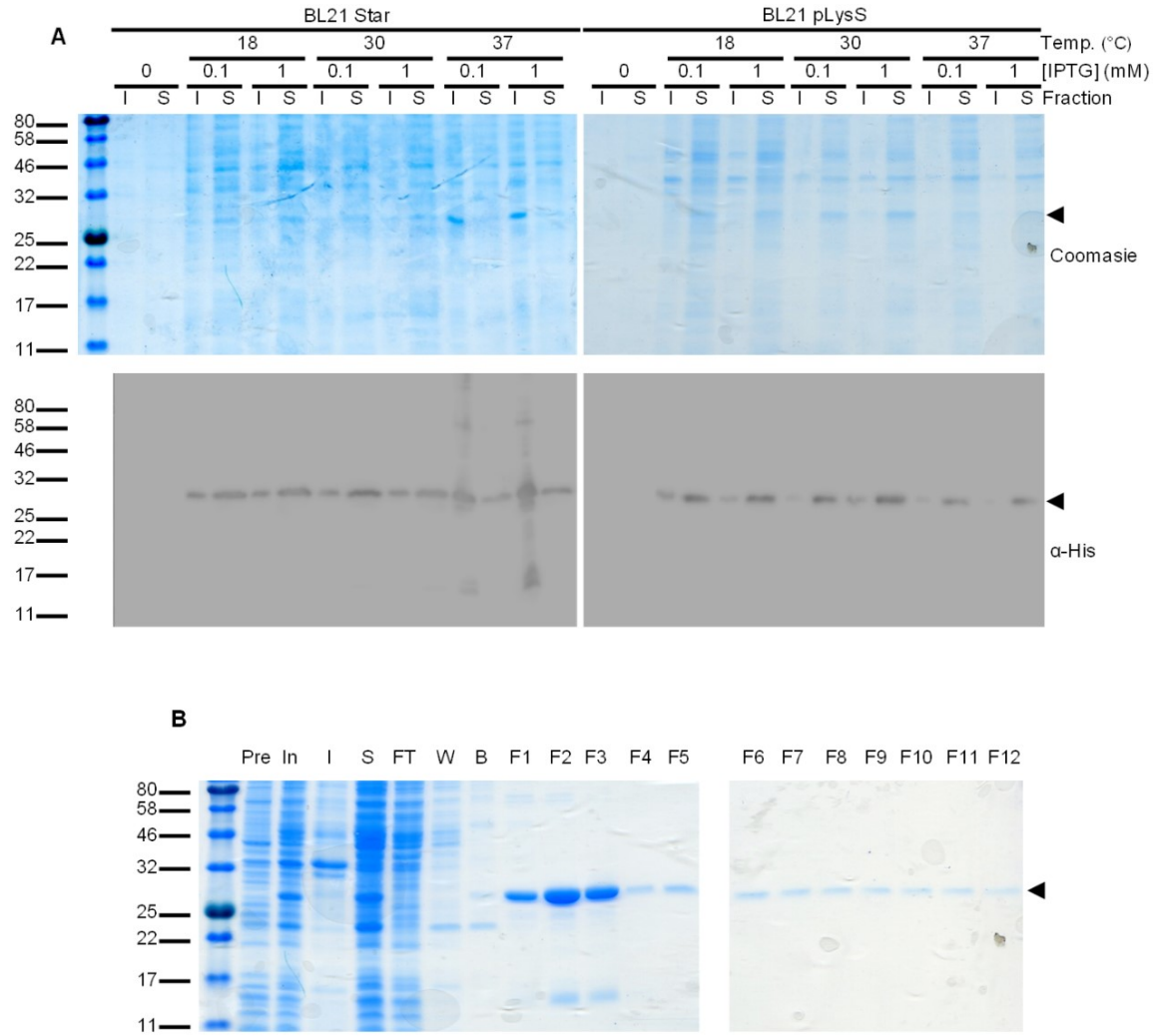


Figure 5.3. Optimising expression and purification of recombinant StoD. (A) BL21 Star and pLysS were transformed with the pET28-*stoD* construct and grown to OD_{600} 0.4-0.6. Cultures were then induced with the stated concentration of IPTG and grown at the given temperature either overnight (cultures grown at 18°C) or for 3 h (cultures grown at 30°C or 37°C). After induction, a culture sample was lysed by sonication and separated into insoluble (I) and soluble (S) fractions. These samples were then analysed by SDS-PAGE and Coomasie staining, for total protein staining, or western blot to detect 6His-StoD using an anti-His antibody. The protein band representing 6His-StoD is indicated. **(B)** An example purification of 6His-StoD showing pre-induced (Pre), induced (In), insoluble (I) and soluble (S) culture samples as well as, His purification samples: flow-through (FT), wash (W), bind (B) and elution fractions (F) 1 to 12. Samples were analysed by SDS-PAGE and Coomasie staining.

5.3.2. Assessing the Autoubiquitination Activity of StoD

Autoubiquitination, that is ubiquitination of an E3 ubiquitin-ligase by itself, is used to confirm that a protein is an E3 ubiquitin-ligase in the absence of a known substrate (Lorick et al. 1999; Wu et al. 2010). Several commercially available E2 ubiquitin-conjugating enzymes were used in combination with 6His-StoD in ubiquitination assays to assess which were capable of facilitating StoD autoubiquitination *in vitro* (Figure 5.4). In these assays, 6His-StoD was

combined with an E1 ubiquitin-activating enzyme (UBE1), biotinylated ubiquitin, ATP and an E2 ubiquitin-conjugating enzyme. Autoubiquitination was determined by western blot against tagged ubiquitin using a streptavidin antibody. If autoubiquitination occurs, a smear can be seen, indicating that multiple species of E3 ubiquitin-ligase, with varying molecular sizes due to differing numbers of conjugated ubiquitin molecules are present.

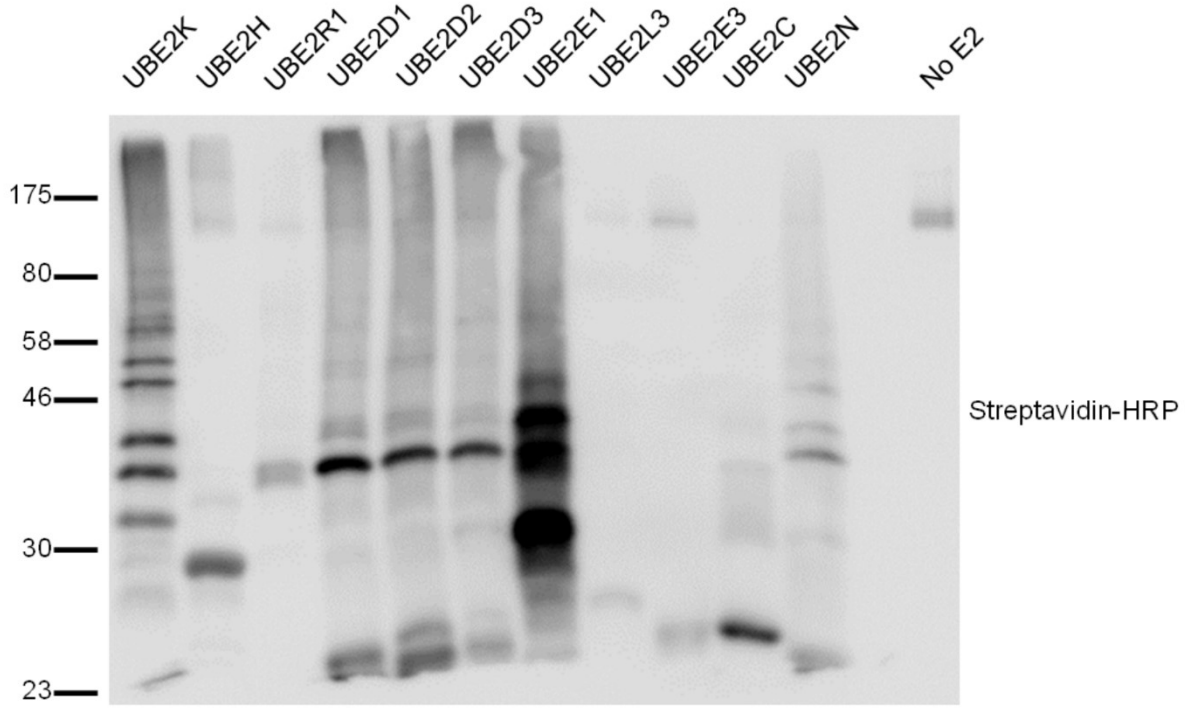


Figure 5.4. Screening E2 ubiquitin-conjugating enzymes with StoD. Recombinant 6His-StoD was used in autoubiquitination assays with several different E2 ubiquitin-conjugating enzymes to determine which were capable of facilitating StoD autoubiquitination. Biotinylated ubiquitin was used in these reactions. Samples were analysed by SDS-PAGE and western blot using streptavidin conjugated to HRP to detect ubiquitinated StoD. This experiment was performed by Dr Ranjani Ganji using the UbcH (E2) enzyme set from Boston Biochem.

Using this method, 6His-StoD was shown to perform autoubiquitination in the presence of UBE2K, UBE2H, UBE2D1, UBE2D2, UBE2D3 and UBE2E1, but not in combination with UBE2R1, UBE2L3, UBE2E3, UBE2C or UBE2N. In the absence of an E2 ubiquitin-conjugating enzyme, no autoubiquitination was seen either, indicating that an E2 is required for 6His-StoD to be able to perform autoubiquitination.

This confirmed that StoD does possess E3 ubiquitin-ligase activity similar to other NleG proteins, and that StoD can utilise several host E2 ubiquitin-conjugating enzymes *in vitro*.

5.3.3. Evaluating the Effect of the P204K Mutation on StoD Autoubiquitination

It has been shown that in NleG 2.3, three residues are required for binding to E2 ubiquitin-conjugating enzymes: I121, L152 and P160, and mutation of these residues to a lysine results in an inhibition of autoubiquitination activity (Wu et al. 2010). Further work with other NleG proteins in our research group showed that mutation of the proline residue (P160 and its equivalents) to a lysine was most effective at inhibiting autoubiquitination. Based on this data, it was hypothesised that mutation of the analogous proline residue in StoD, P204, to a lysine ($StoD_{P204K}$) would also inhibit autoubiquitination.

Based on the results from the screen of E2 ubiquitin-conjugating enzymes, UBE2E1 was selected and 6His-UBE2E1 was expressed using BL21 Star transformed with pET28-*UBE2E1* (Table 2.2) and purified by affinity chromatography in sufficient quantities (Figure 5.5A). This was then combined with 6His-UBE1, ubiquitin, and either 6His-StoD or 6His-$StoD_{P204K}$ in the presence or absence of ATP (Figure 5.5B). In the presence of ATP, 6His-StoD, but not 6His-$StoD_{P204K}$, performed autoubiquitination. UBE2E1 has been shown to be capable of autoubiquitination in the absence of an E3 ubiquitin-ligase (Ubiquigent 2013), but no autoubiquitination was seen in the absence of 6His-StoD indicating that the ubiquitin smear with 6His-StoD is due to StoD and not UBE2E1.

Therefore, inhibition of StoD binding to E2 ubiquitin-conjugating enzymes is sufficient to inhibit StoD autoubiquitination *in vitro*.

Further autoubiquitination assays were performed using recombinant 6His-StoD [1-95], 6His-StoD [134-233] and 6His-StoD [134-233] containing the P204K mutation (6His-$StoD_{P204K}$ [134-233]) to determine which domain was required for autoubiquitination (Figure 5.5B). Autoubiquitination was observed in the presence of 6His-StoD [134-233], but

not 6His-StoD [1-95] or 6His-StoD$_{P204K}$ [134-233]. This indicates that it is the C-terminal domain of StoD that is required for autoubiquitination.

Therefore, StoD is capable of autoubiquitination and this is dependent on the C-terminal E3 ubiquitin-ligase domain, similar to other NleG effector proteins.

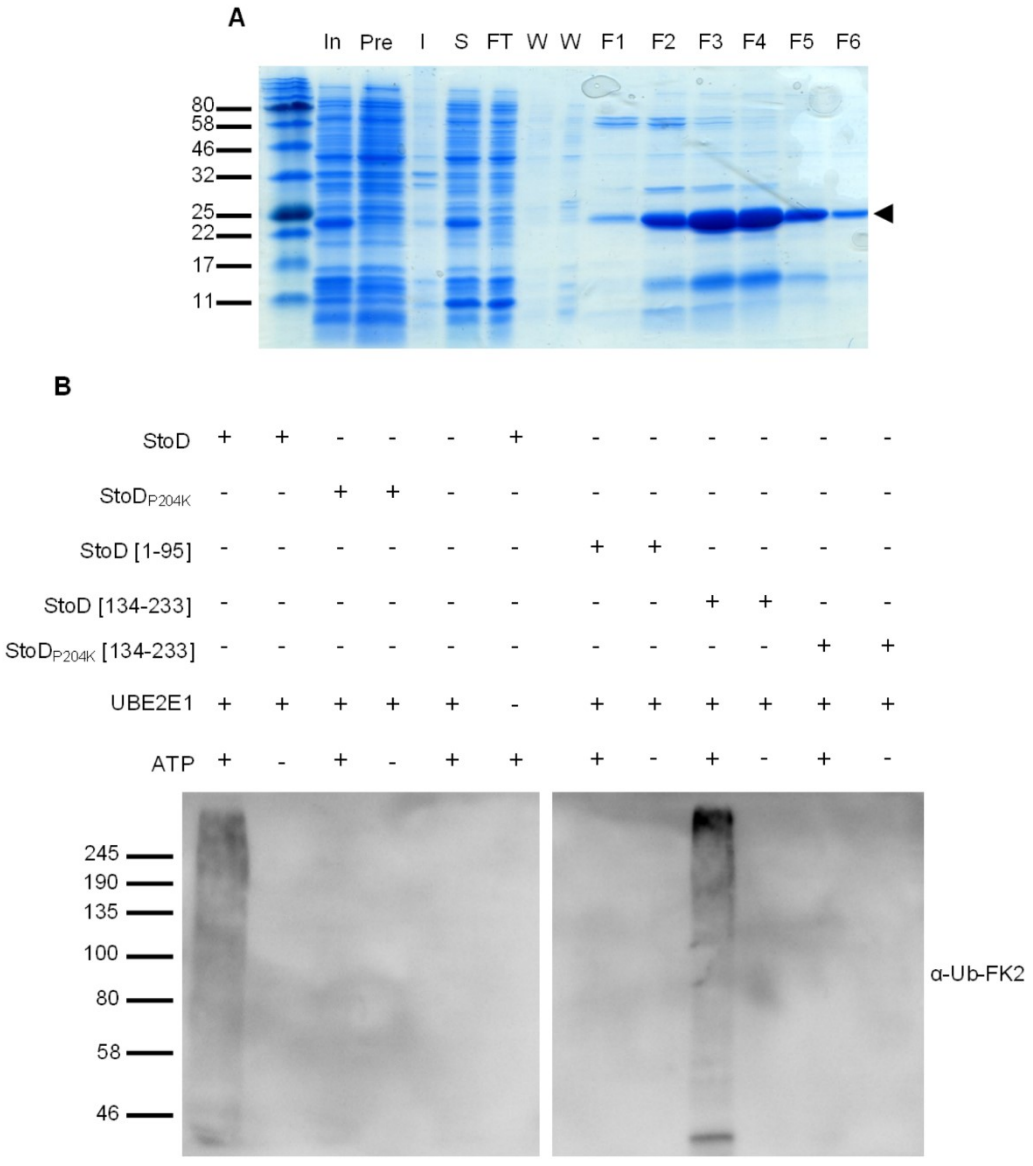


Figure 5.5. Purification of 6His-UBE2E1 and autoubiquitination assays with StoD. (A) Affinity purification of 6His-UBE2E1 showing induced (In), pre-induced (Pre), insoluble (I), soluble (S), flow-through (FT), wash (W) and elution fractions (F) 1 to 6. Samples were analysed by SDS-PAGE and Coomasie staining. The protein band representing 6His-UBE2E1 is indicated. **(B)** Autoubiquitination assay using StoD, StoD$_{P204K}$, StoD [1-95], StoD [134-233] or StoD$_{P204K}$ [134-233]. All reactions were analysed by SDS-PAGE and western blot, using an anti-Ub-FK2 antibody to detect ubiquitin conjugated to 6His-StoD and its variants. All reactions contain UBE1 and ubiquitin. Components that have been added or removed are depicted by crosses (+) or dashes (-), respectively. Image is representative of two independent repeats.

5.3.4. Investigating the Effect of StoD Expression on BY4741 *S. cerevisiae*

Expression of proteins from pYes2, a vector containing a GAL-1 galactose-inducible promoter, in the BY4741 *S. cerevisiae* strain can give an indication as to whether the enzymatic activity of a protein is toxic to *S. cerevisiae* and has been used previously to determine the activity of other T3SS effectors (Arbeloa et al. 2011; Lesser & Miller 2001). To investigate if the ubiquitination activity of StoD was toxic to BY4741 *S. cerevisiae*, StoD and $StoD_{P204K}$ were cloned into pYes2 and transformed into BY4741, along with the EV. These strains were then grown to stationary phase in liquid culture, before being diluted in sterile water and plated onto SD agar lacking uracil, to maintain the pYes2 vectors, and containing either glucose or galactose as a carbon source (Figure 5.6). Growth on glucose-containing media inhibits the expression of genes from pYes2, hence no effect on BY4741 growth was seen with any of the constructs. Growth on galactose-containing media induces expression of genes from pYes2 and resulted in approximately 100-fold less growth in BY4741 expressing StoD, compared to both the EV and expression of $StoD_{P204K}$. Therefore, the expression of StoD in BY4741 *S. cerevisiae*, was toxic, and this toxicity was relieved by inhibiting the ubiquitination activity of StoD.

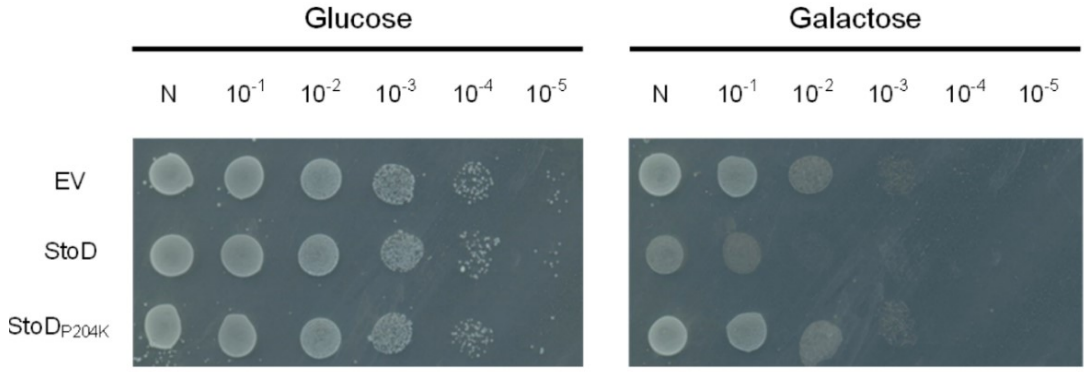


Figure 5.6. StoD is toxic to BY4741. BY4741 transformed with either the EV, pYes2-*stoD* or pYes2-$stoD_{P204K}$ were grown to stationary phase before serial dilution and plating onto SD agar lacking uracil and containing either glucose or galactose as a carbon source. Image is representative of three independent repeats.

5.4. Identifying Interacting Partners of StoD

Since StoD had been demonstrated to possess E3 ubiquitin-ligase activity, it was then sought to identify interacting partners and potential substrates of StoD using a yeast two-hybrid (Y2H) screen. Full-length $StoD_{P204K}$ was used as the bait protein, instead of StoD, as it was hypothesised that the lack of ubiquitination activity may stabilise any interaction with StoD substrates and therefore enable their identification using this system.

5.4.1. Assessing the Suitability of $StoD_{P204K}$ for use in a Y2H Screen

Before a Y2H screen could be performed, control experiments to determine the suitability of the pGBKT7-*stoD*$_{P204K}$ construct (Table 2.2) had to be conducted (Figure 5.7).

Firstly, the ability of $StoD_{P204K}$ to autoactivate; cause expression of the reporter genes *HIS3*, *ADE2* and *lacZ* in the absence of an interacting partner, was assessed. AH109 *S. cerevisiae* (Table 2.1), was transformed with pGBKT7-*stoD*$_{P204K}$ or the EV and grown on SD agar lacking tryptophan (SD/-Trp) or lacking adenine, histidine and tryptophan (SD/-Ade/-His/-Trp) (Figure **5.7**A). Growth on SD/-Trp is used to demonstrate successful transformation, as the pGBKT7 vector encodes the *TRP1* gene allowing growth in the absence of tryptophan. *S. cerevisiae* transformed with both the EV vector and pGBKT7-*stoD*$_{P204K}$ grew on SD/-Trp indicating successful transformation. Growth on SD/-Ade/-His/-Trp is used to assess autoactivation. If a protein is capable of autoactivation, the *ADE2* and *HIS3* genes would be expressed, and transformants would be able to grow in the absence of adenine and histidine. *S. cerevisiae* transformed with both the empty vector and pGBKT7-*stoD*$_{P204K}$ did not demonstrate growth on SD/-Ade/-His/-Trp indicating that neither construct induces autoactivation of the reporter genes.

The second control experiment was to determine if expression of $StoD_{P204K}$ caused a growth defect in *S. cerevisiae* that may affect the yeast mating efficiency, and therefore the ability of the Y2H screen to identify any interacting partners. AH109 *S. cerevisiae*, transformed with

either EV or pGBKT7-*stoD*$_{P204K}$ were grown in SD/-Trp broth, to maintain the pGBKT7 constructs, and the OD_{600} was recorded every 30 min for 30 h (Figure 5.7B).

S. cerevisiae containing either pGBKT7-*stoD*$_{P204K}$ or the EV demonstrated the same growth curves, indicating that expression of StoD$_{P204K}$ does not cause a growth defect in AH109 *S. cerevisiae*. Therefore, StoD$_{P204K}$ is suitable for use in a Y2H screen to identify potential StoD interacting partners.

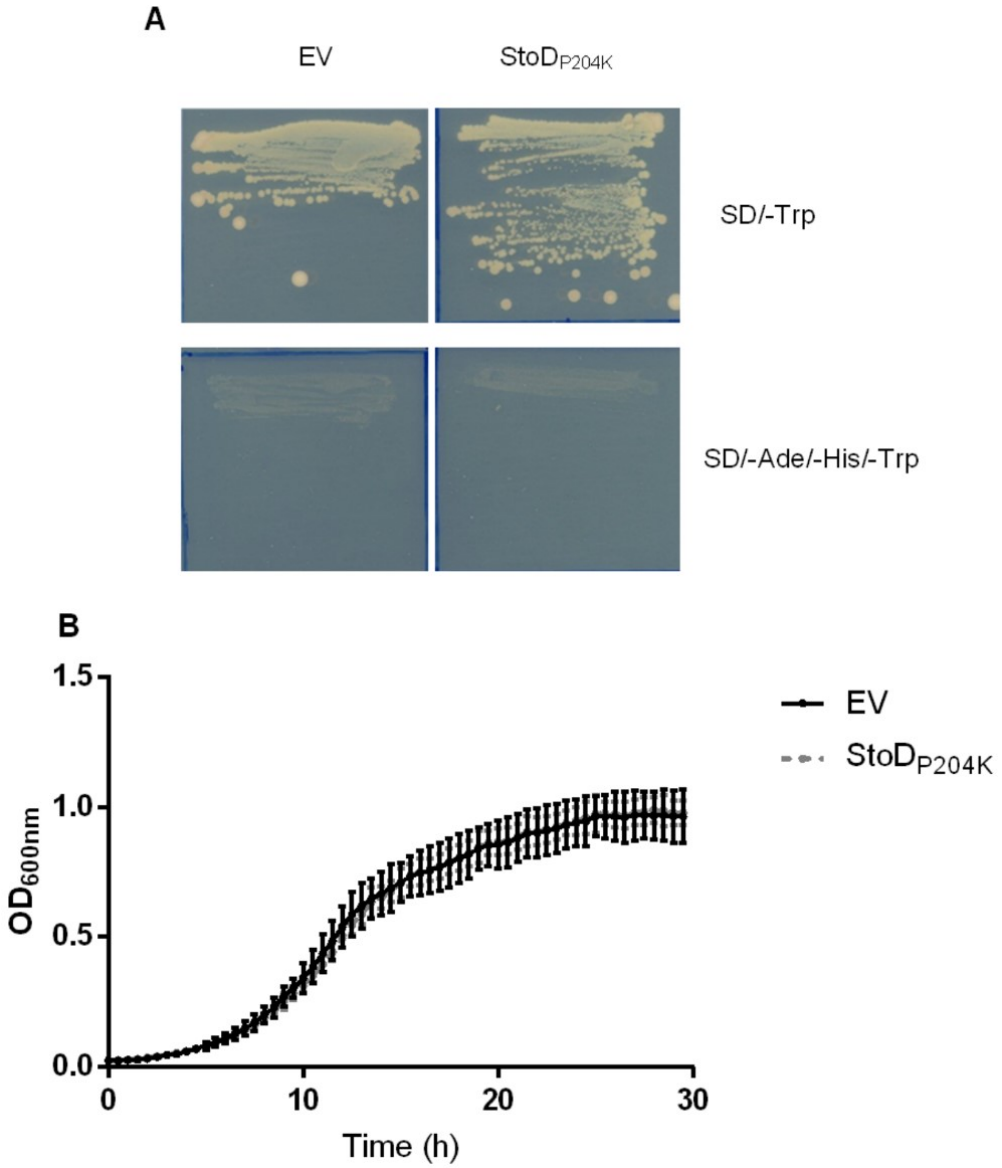


Figure 5.7. StoD$_{P204K}$ does not autoactivate or cause a growth defect in AH109 *S. cerevisiae*. (A) AH109 *S. cerevisiae* containing either EV or pGBKT7-*stoD*$_{P204K}$ (StoD$_{P204K}$) were plated onto SD/-Trp or SD/-Ade/-His/-Trp agar to assess autoactivation of the reporter genes. **(B)** AH109 *S. cerevisiae* containing either EV or StoD$_{P204K}$ were grown in SD/-Trp broth and the OD_{600} was recorded every 30 min to assess the growth of AH109 upon expression of StoD$_{P240K}$. Graph shows mean ± SD. This graph is an average of two independent repeats.

5.4.2. Y2H Screen with StoD$_{P204K}$

AH109 *S. cerevisiae* containing pGBKT7-*stoD*$_{P204K}$ was then used to screen 1.29x10^6 clones of a normalised HeLa S3 cDNA library, encoded within the pGADT7 vector, with a mating efficiency of 8.09%. After 14 days, 79 colonies had grown on SD agar plates containing X-α-Gal but lacking tryptophan, leucine, histidine and adenine (QDO).

The pGADT7 and pGBKT7 vectors encode the GAL4 transcription factor DNA-binding and activation domains, respectively. These are fused to the bait and prey proteins inserted into the vectors and if an interaction is observed between these proteins, the GAL4 DNA-binding and activation domains are brought into close enough proximity to induce expression of the *HIS3*, *ADE2* and *lacZ* reporter genes within the AH109 genome. Expression of the reporter genes allows growth of the colony in the absence of histidine and adenine, as found in QDO plates. The expression of the *lacZ* gene results in the expression of a β-galactosidase enzyme, which metabolises X-α-Gal resulting in the colonies developing a blue colouration.

These colonies were then re-streaked onto QDO plates three times, to remove any superficial interactions, reducing the number of colonies to 53. These colonies were screened for the presence of the pGADT7 vector by colony PCR using the pGADT7 FW and REV primer pair (Table 2.3) and the subsequent product or purified vector was sent for sequencing. Only 44 constructs returned usable sequencing results, including a known false positive, COP9 signalosome subunit 5, which yielded four clones. Of the remaining sequences, nine hits were chosen for further investigation (Table 5.1), including two E2 ubiquitin-conjugating enzymes.

The pGADT7 vectors containing these hits were isolated from their respective clones and used in direct Y2H assays with EV, pGBKT7-*stoD* or pGBKT7-*stoD*$_{P204K}$ to confirm if they were genuine interacting partners (Figure 5.8). In this assay, AH109 *S. cerevisiae* was co-transformed with a pGBKT7 bait vector, as well as a pGADT7 prey vector before being plated onto SD agar lacking tryptophan and leucine (DDO) as well as QDO plates. DDO plates select for co-transformants containing both the pGADT7 and pGBKT7 vectors, as these

Table 5.1. Shortlisted hits from Y2H screen with $StoD_{P204K}$ selected for further investigation.

Gene	Protein	Number of Clones	Function
FAM103A1	RNMT-activating mini protein	2	Involved in 5' mRNA cap methylation.
UBE2L3	UBE2L3	2	E2 ubiquitin-conjugating enzyme that specifically interacts with HECT and RBR E3 ubiquitin-ligases.
NPC2	Epididymal secretory protein E1	2	Lysosomal transporter involved in cholesterol export.
UBE2N	UBE2N	1	E2 ubiquitin-conjugating enzyme involved in NF-κB activation in response to HIV infection.
YES1	Protein tyrosine kinase Yes	1	Non-receptor tyrosine kinase involved in cell cycle progression.
BUD13	BUD13 homologue	1	RNA-binding protein.
IDI1	Isopentenyl-diphosphate Delta-isomerase 1	1	Involved in isoprenoid biosynthesis.
LAMTOR5	Ragulator complex protein LAMTOR5	1	Involved in inhibiting apoptosis during hepatitis B infection.
CAPN7	Calpain-7	1	Epidermal growth factor receptor degradation.

vectors encode the *TRP1* and *LEU2* genes, respectively, enabling co-transformants to grow in the absence of these amino acids. Based on this, all co- transformations were successful, as all co-transformants grew on DDO plates (Figure 5.8).

No interaction was observed between the StoD constructs and the empty pGADT7 vector, indicated by a lack of growth on QDO plates (Figure 5.8). All shortlisted hits interacted with $StoD_{P204K}$, but not StoD, as seen by growth on QDO plates. However, all hits, apart from UBE2L3, also interacted with the empty pGBKT7 vector, indicating that they are likely to be false positives.

Therefore, a Y2H screen using $StoD_{P204K}$ identified nine potential interacting partners of StoD. However, only one of these proteins was suitable for further investigation.

5.4.3. Evaluating the Interaction between StoD and UBE2L3

Since UBE2L3 was the only hit that did not interact with the empty pGBKT7 vector, it was decided to follow this up to see if it interacted with the various StoD constructs (Figure 5.9). An alignment of the amino acid sequence from one of the UBE2L3 hits that was in-frame, with the UBE2L3 sequence available on UniProt (Wasmuth & Lima 2016), showed that the Y2H hit protein contained an N-terminal extension that is not found in the annotated UBE2L3 sequence (Figure 5.9A). This N-terminal extension contained the partial sequence for a HA-

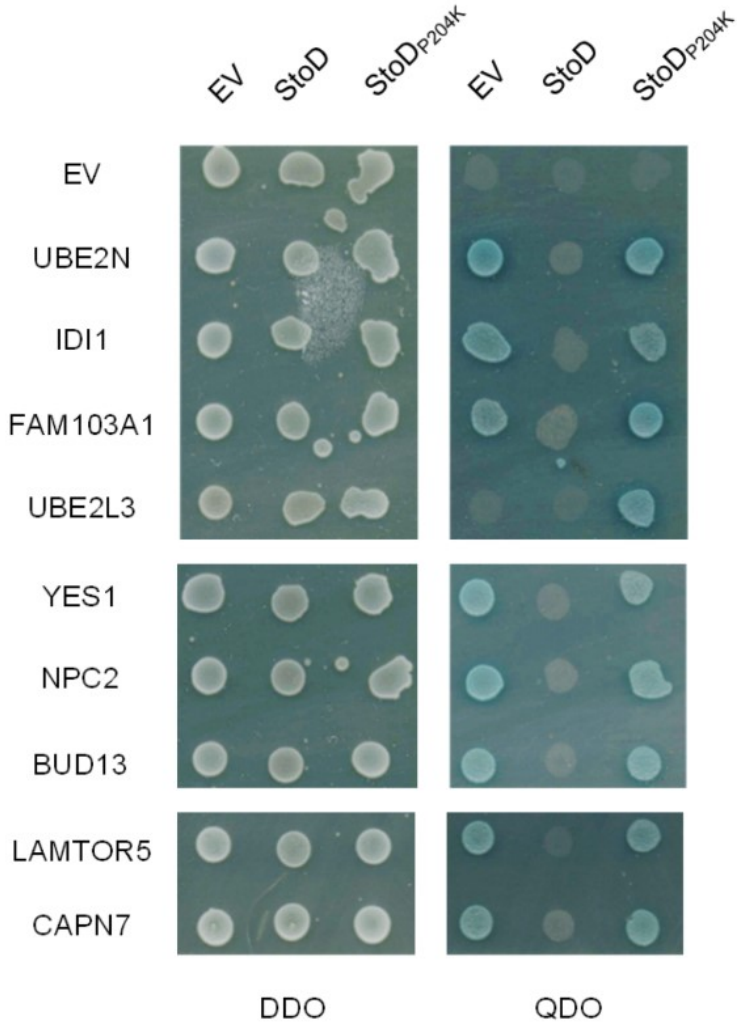


Figure 5.8. StoD$_{P204K}$ interacts with the UBE2L3 Hit. Direct Y2H assay co-transforming AH109 *S. cerevisiae* with either empty pGBKT7 vector (EV), pGBKT7-*stoD* or pGBKT7-*stoD*$_{P204K}$ constructs, and either empty pGADT7 vector (EV) or pGADT7 constructs from the Y2H screen. Co-transformants were then plated onto DDO and QDO plates to assess any protein-protein interactions.

tag, which is found within the pGADT7 vector (Table 2.2) as well as a linker region used in the construction of the cDNA library. The UBE2L3 hit also contained an alanine to threonine substitution at position 98 (A98T). Aside from these differences, the *UBE2L3* hit contained the entire UBE2L3 protein. To ensure that the N-terminal extension and the A98T substitution were not the cause for the interaction with StoD, *UBE2L3* was amplified from pGEX-*UBE2L3* (Table 2.2) and cloned into pGADT7. This construct, along with the empty pGADT7 vector and the pGADT7-*UBE2L3* Hit, were then co-transformed into AH109 *S. cerevisiae* with the various pGBKT7-*stoD* constructs and plated onto DDO and QDO plates (Figure 5.9B).

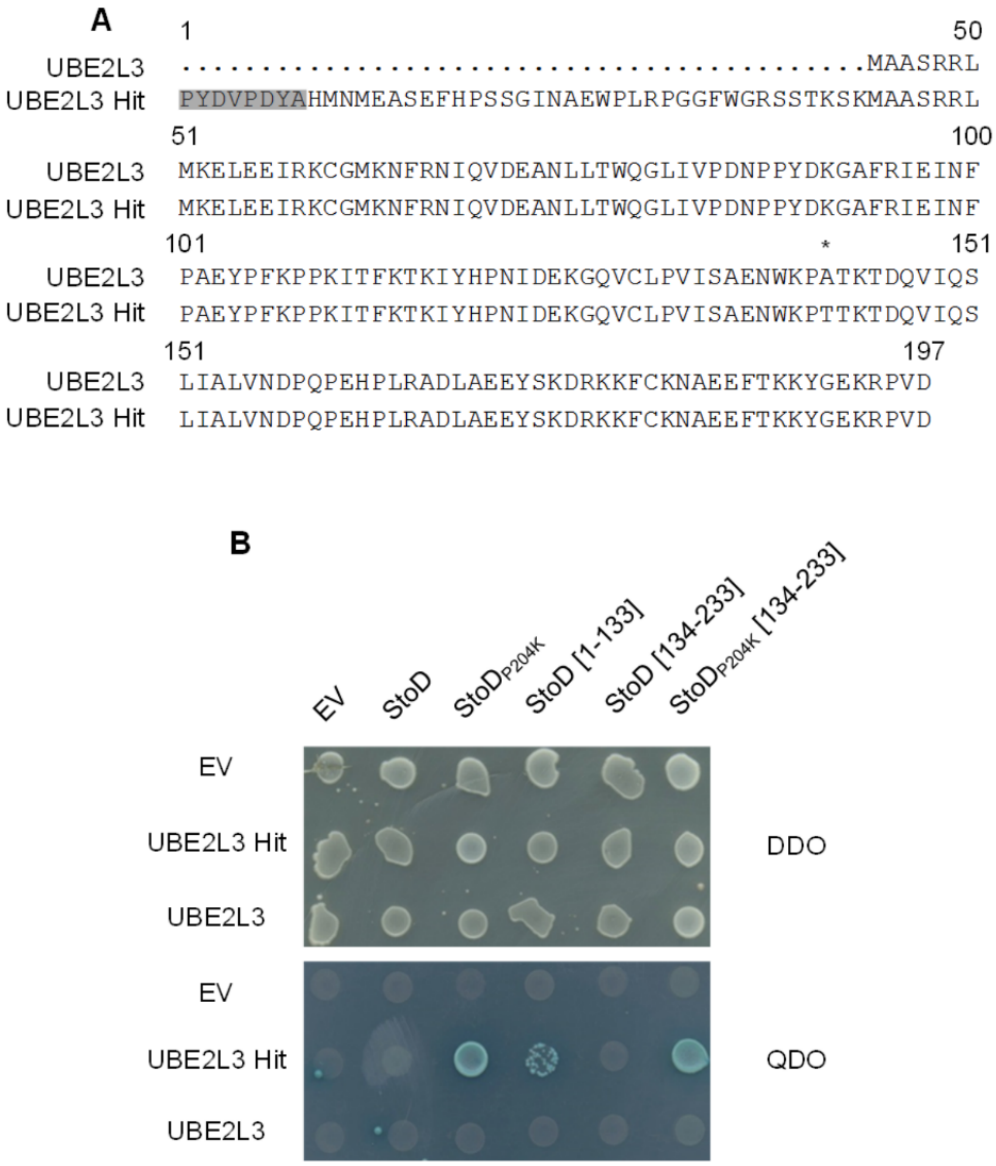


Figure 5.9. StoD does not interact with UBE2L3. Amino acid sequence alignment of the UBE2L3 sequence from UniProt (Wasmuth & Lima 2016) and the plasmid isolated from the AH109 *S. cerevisiae* clone (UBE2L3 Hit). The shaded region highlights the HA-tag in the pGADT7 vector. * indicates differences in amino acid sequence. Sequence alignments performed using Clustal Omega (Sievers et al. 2011) and formatted using Strap (Gille et al. 2014). **(B)** Direct Y2H assay co-transforming AH109 *S. cerevisiae* with either empty pGBKT7 (EV) or pGBKT7-*stoD* constructs, and either empty pGADT7 (EV), pGADT7-*UBE2L3* plasmid from yeast two-hybrid screen (UBE2L3 Hit) or pGADT7-*UBE2L3* (UBE2L3). Co-transformants were then plated onto DDO and QDO plates to assess any protein-protein interactions. Image representative of two independent repeats.

All co-transformations were successful, and no interactions were observed with either the empty pGADT7 or pGBKT7 vectors. Interactions were seen between the UBE2L3 hit and $StoD_{P204K}$, StoD [1-133] and $StoD_{P204K}$ [134-233], but not with StoD or StoD [134-233]. The UBE2L3 cloned from pGEX-*UBE2L3* was not found to interact with any of the StoD constructs. This suggests that the N-terminal extension or A98T mutation is required for interaction with

StoD and in their absence UBE2L3 is not capable of direct interaction with StoD. Therefore, UBE2L3 is not capable of a direct interaction with StoD in the direct Y2H system.

5.4.4. Assessing the Ability of StoD to Ubiquitinate UBE2L3 *in vitro*

Although a direct interaction between StoD and UBE2L3 could not be confirmed, and previous work had shown that UBE2L3 is unable to support StoD autoubiquitination (Figure 5.4), it was investigated if StoD was capable of ubiquitinating UBE2L3 *in vitro* (Figure 5.10). Recombinant 6His-StoD was combined with 6His-UBE1, 6His-UBE2E1 and either GST-UBE2L3 or GST in the presence of ATP and ubiquitination was assessed. In the reactions containing StoD along with GST and GST-UBE2L3, ubiquitination does occur, as shown by the high molecular weight smear when blotting using the anti-Ub-FK2 antibody. However, when blotting for GST, no increase in molecular weight is seen with GST or GST-UBE2L3 indicating that these proteins are not being ubiquitinated by StoD. Therefore, StoD is not capable of ubiquitinating UBE2L3 *in vitro.*

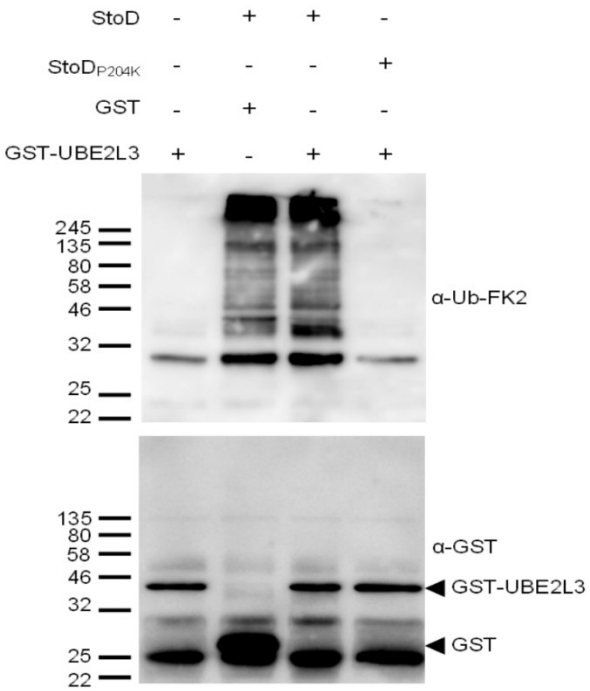


Figure 5.10. StoD does not ubiquitinate UBE2L3. Ubiquitination assay using 6His-StoD, 6His-StoD$_{P204K}$, GST and GST-UBE2L3. All reactions were analysed by SDS-PAGE and western blot using an anti-Ub-FK2 antibody to detect ubiquitinated proteins and anti-GST antibody to detect GST or GST-UBE2L3. All reactions contain 6His-UBE1, 6His-UBE2E1, ubiquitin and ATP. Components that have been added or removed are depicted by crosses (+) or dashes (-), respectively.

5.5. Investigating the Localisation of Vesicular Proteins upon StoD Expression in HeLa Cells

In the previous chapter, it was shown that upon expression in HeLa cells, StoD-HA formed discrete puncta throughout the cell (Figure 4.8), which is characteristic of proteins involved in vesicle formation and maturation. Since, modulation of the host vesicular system is a critical process for *Salmonella* to survive intracellularly (Bakowski et al. 2008), it was investigated if the localisation of known vesicular proteins was altered during ectopic expression of StoD. HeLa cells were co-transfected with pRK5 vectors encoding HA-*mCherry* or *stoD*-HA, as well as vectors encoding green fluorescent protein (GFP)-tagged vesicular proteins (Table 2.2) and visualised by immunofluorescence microscopy (Figure 5.11).

LC3 is a ubiquitin-like protein that is involved in the elongation of autophagosomal membranes (Weidberg et al. 2010). In HeLa cells, HA-mCherry and GFP-LC3 proteins were distributed throughout the cell (Figure 5.11A). HA-mCherry remained diffuse, whereas GFP-LC3 formed small puncta. GFP-LC3 and StoD-HA expression demonstrated the same StoD and LC3 localisations as seen previously. No colocalisation of LC3 puncta with StoD puncta was observed.

Rab11a is a small GTP-binding protein that localises to recycling vesicles within the cell (Hales et al. 2001). In HeLa cells, HA-mCherry was localised diffusely throughout the cell whilst GFP-Rab11a formed puncta throughout the cell (Figure 5.11B). StoD-HA and GFP-Rab11a expression resulted in the formation of puncta by both tagged proteins, however, no colocalisation was seen between these proteins.

Vamp3 is a vesicular SNARE protein involved in endosomal transport to the trans-Golgi network (Ganley et al. 2008). In HeLa cells, HA-mCherry and GFP-Vamp3 expression resulted in a diffuse HA-mCherry staining throughout the cell, whilst GFP-Vamp3 localised in discrete tubular structures throughout the cell, but particularly enriched within the perinuclear region

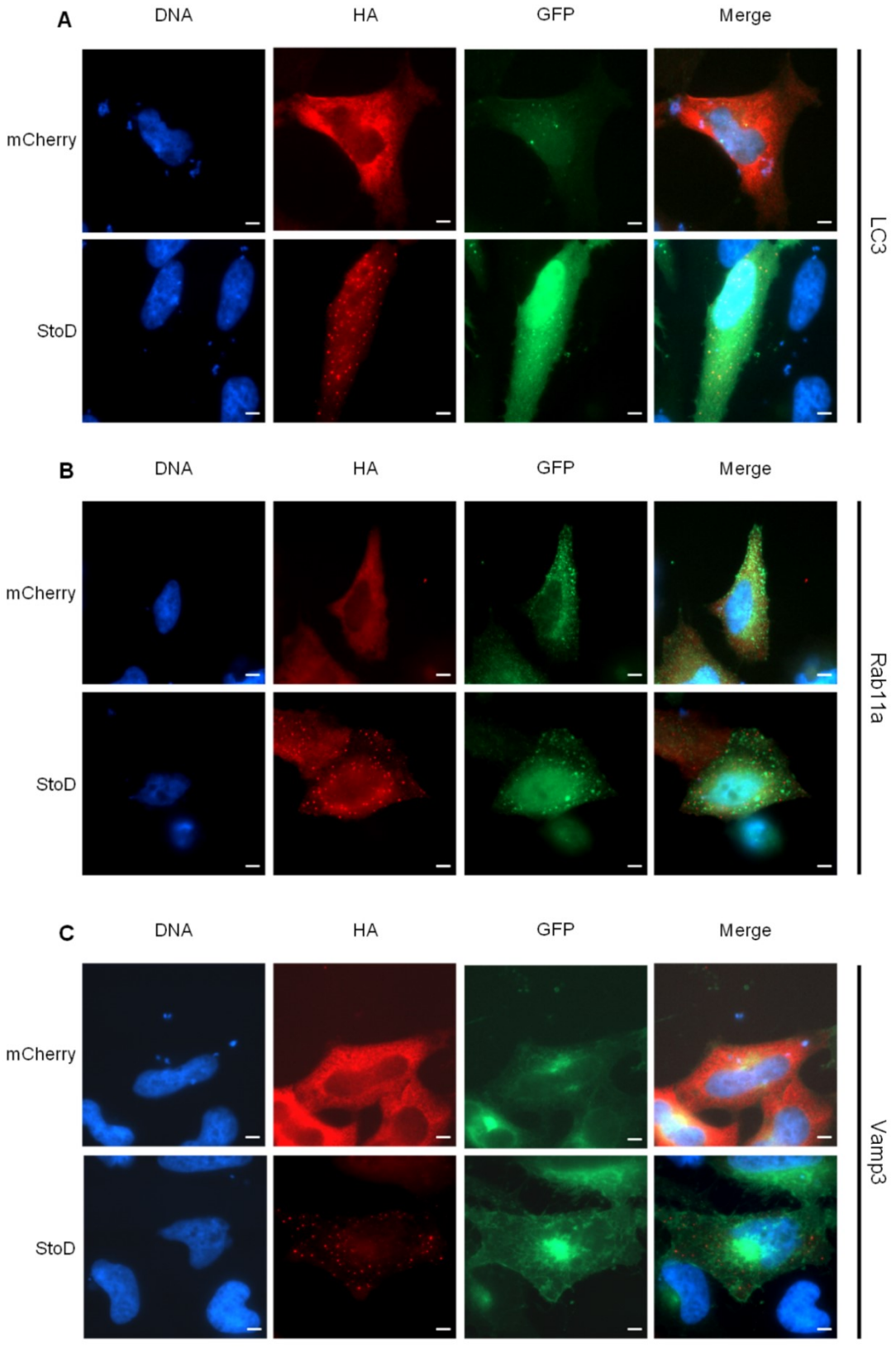


Figure 5.11. StoD does not colocalise with vesicular proteins. Immunofluorescence images of HeLa cells 24 h post-transfection with pRK5 containing HA-tagged *mCherry* or *stoD* and pGFP or pEGFP constructs containing GFP-tagged **(A)** *LC3*, **(B)** *Rab11a* or **(C)** *Vamp3*. DNA and actin were visualised using Hoescht 33258 and AlexaFluor 647-Phalloidin, respectively. StoD and mCherry were visualised using an anti-HA antibody, whilst LC3, Rab11a and Vamp3 were visualised using an anti–GFP antibody. Scale bar, 5 μm. Images representative of two independent repeats.

(Figure 5.11C). Expression of StoD-HA and GFP-Vamp3, resulted in the same StoD-HA puncta as seen previously and the localisation of the tubular GFP-Vamp3 structures was not altered. No colocalisation was seen between the StoD-HA puncta and the GFP-Vamp3 tubular structures.

Therefore, StoD expression in HeLa cells did not result in the relocalisation of LC3, Rab11a or Vamp3, and no colocalisation was observed between StoD and the cellular vesicles that are associated with these proteins.

5.6. Determining the Effect of StoD on Host Ubiquitin Localisation

Since StoD was found not to colocalise with any of the vesicular proteins tested, and the finding that StoD is an E3 ubiquitin-ligase (Figure 5.5), with an N-terminal domain that is structurally similar to ubiquitin, it was investigated if StoD colocalised with ubiquitin. HeLa cells were transfected with pRK5 constructs encoding either HA-*mCherry*, *stoD*-HA or *stoD*$_{P204K}$-HA and then visualised by immunofluorescence microscopy (Figure 5.12).

Upon expression of HA-mCherry in HeLa cells, a diffuse HA signal was observed, as expected and cellular ubiquitin was diffuse throughout the cell. In cells expressing StoD-HA, cellular ubiquitin was relocalised to a punctate signal that colocalised with the StoD puncta. However, in cells expressing StoD$_{P204K}$-HA, a diffuse HA staining pattern was observed and in these cells the ubiquitin localisation was again diffuse throughout the cell. This suggests that binding to E2 ubiquitin-conjugating enzymes, and therefore the ubiquitination activity of StoD is required to relocalise cellular ubiquitin upon ectopic expression in HeLa cells.

5.6.1. Assessing the Localisation of Ubiquitin-Like Proteins upon StoD Expression in HeLa Cells

Since ectopic expression of StoD-HA caused a relocalisation of cellular ubiquitin, it was investigated if StoD-HA could cause relocalisation of ubiquitin-like proteins. HeLa cells were

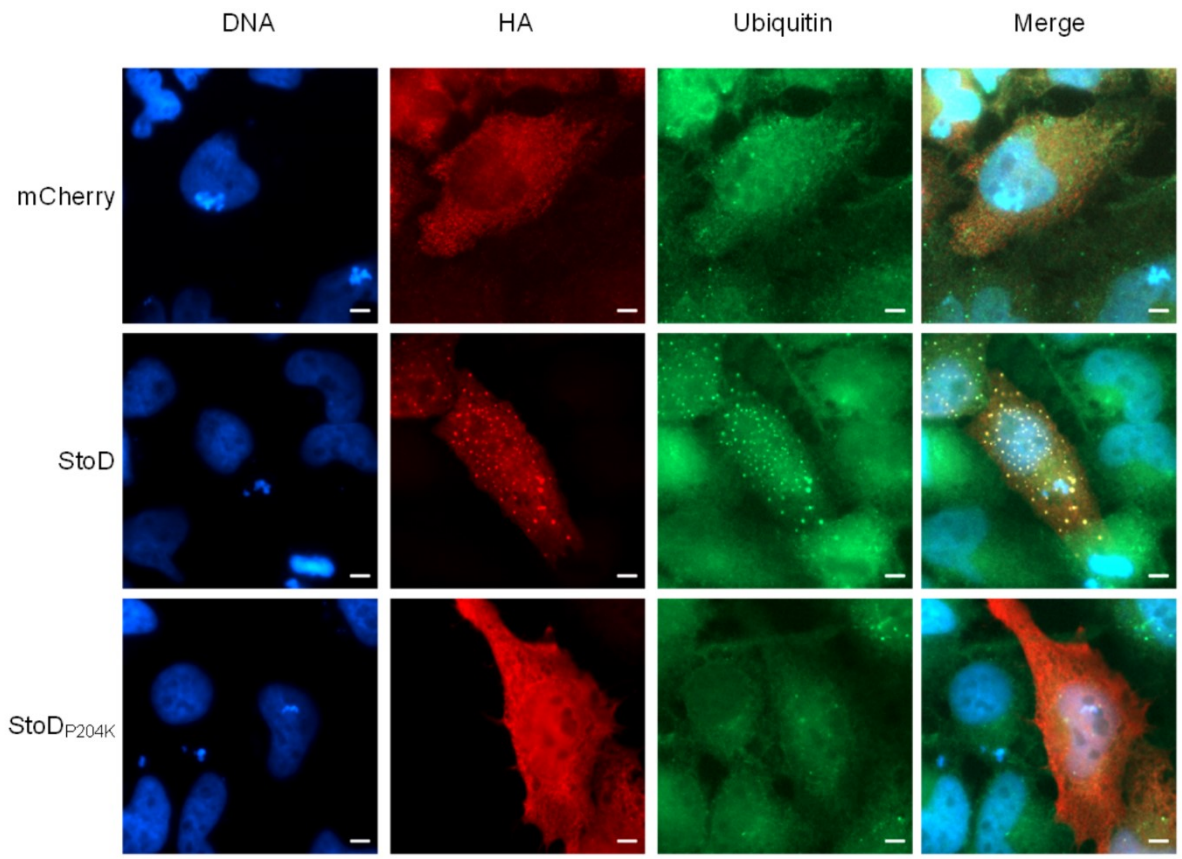


Figure 5.12 Ubiquitin is relocalised during ectopic expression of StoD. Immunofluorescence images of HeLa cells 24 h post-transfection with pRK5 constructs containing HA-tagged *mCherry*, *stoD* or *stoD*$_{P204K}$. DNA and actin were visualised using Hoescht 33258 and Phalloidin-iFluor 647, respectively. StoD, StoD$_{P204K}$ and mCherry were visualised using an anti-HA antibody, whilst ubiquitin was visualised using an anti-Ub-FK2 antibody. Scale bar, 5 µm. Images representative of three independent repeats.

transfected with pRK5 constructs encoding either HA-*mCherry* or *stoD*-HA and then visualised by immunofluorescence microscopy (Figure 5.13).

NEDD8 is an 81 amino acid protein with 60% sequence identity to ubiquitin (Kamitani et al. 1997), and has been demonstrated to be involved in the activation of host RING E3 ligases (Saha et al. 2008). Upon expression of HA-mCherry in HeLa cells, NEDD8 was diffuse throughout the cell with some enrichment in the nuclear region (Figure 5.13A). This localisation was also seen upon expression of StoD-HA and no colocalisation was seen between NEDD8 and StoD-HA.

SUMO-1 is a ubiquitin-like protein that was first identified as modifying the nuclear GTPase RanGAP1, and causing its relocalisation within the cell (Matunis et al. 1996). HA-mCherry

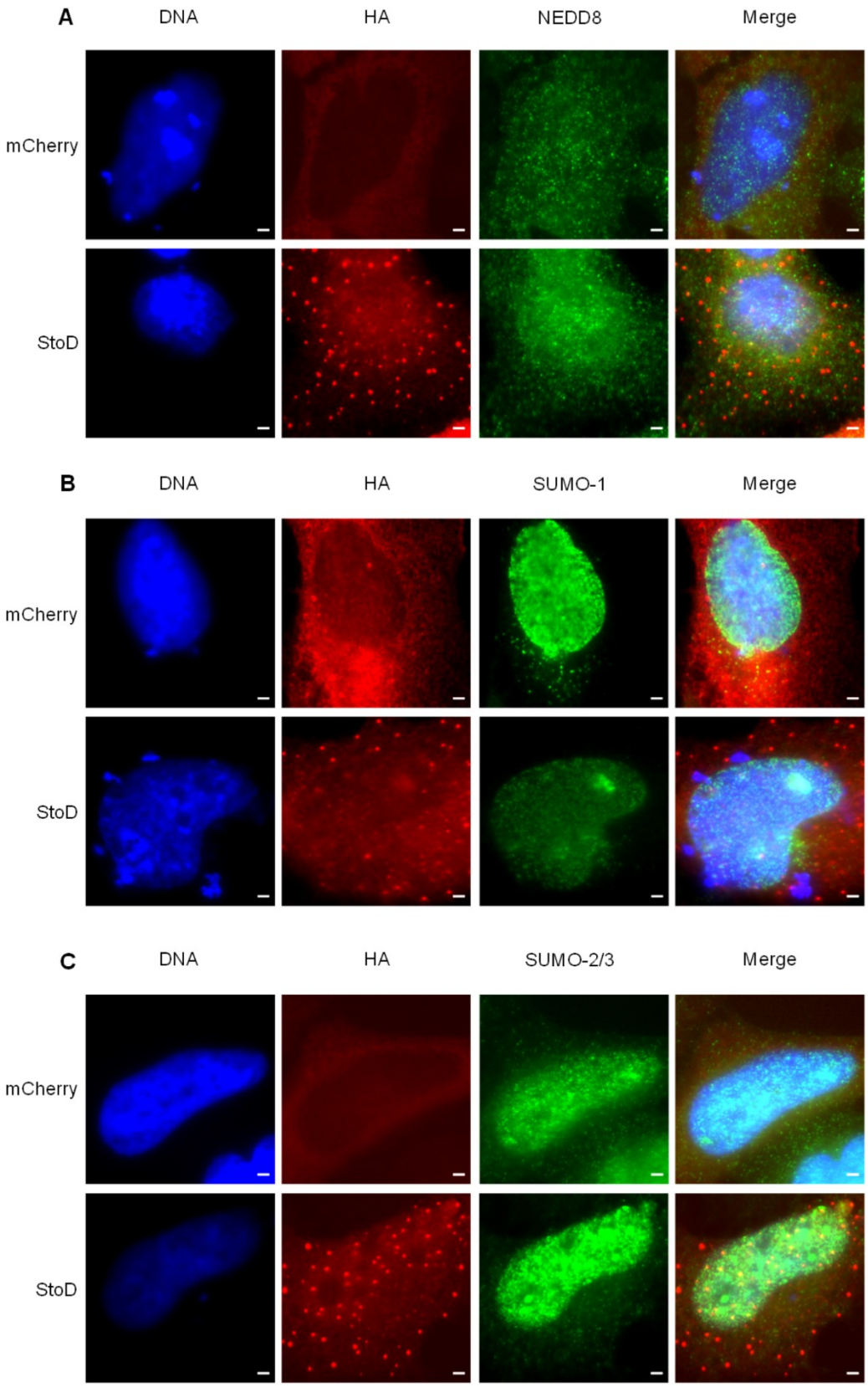


Figure 5.13. StoD does not cause relocalisation of ubiquitin-like proteins. Immunofluorescence images of HeLa cells 24 h post-transfection with pRK5 constructs containing HA-tagged *mCherry* or *stoD*. DNA and actin were visualised using Hoescht 33258 and Phalloidin-iFluor 647, respectively. StoD and mCherry were visualised using an anti-HA antibody, whilst **(A)** NEDD8, **(B)** SUMO-1 or **(C)** SUMO-2/3 were visualised using respective antibodies. Scale bar, 5 µm. Images representative of two independent repeats.

expression in HeLa cells, SUMO-1 was localised exclusively to the nucleus, where a diffuse staining was observed (Figure 5.13B). The expression of StoD-HA in HeLa cells did not alter the nuclear localisation of SUMO-1 and no colocalisation was seen with StoD-HA.

SUMO-2 and SUMO-3 are two distinct ubiquitin-like proteins that are 95% identical to each other (Tatham et al. 2001) and have been shown to form polymeric chains conjugated to substrate proteins, in response to environmental stresses (Saitoh & Hinchey 2000). Upon HA-mCherry expression in HeLa cells, SUMO-2/3 were localised to the nucleus (Figure **5.13**C). This nuclear localisation remained unchanged upon expression of StoD-HA and no colocalisation was seen between SUMO-2/3 and StoD-HA.

Therefore, StoD specifically causes the relocalisation of cellular ubiquitin, and none of the ubiquitin-like proteins tested here, into discrete puncta, with which StoD colocalises.

5.7. Investigating a Direct Interaction between StoD and Ubiquitin

Since StoD-HA expression in HeLa cells caused a relocalisation of cellular ubiquitin from a diffuse staining throughout the cell to discrete puncta that colocalise with StoD-HA, and that StoD had been demonstrated to possess autoubiquitination activity *in vitro* (Figure 5.4 and Figure 5.5B) the next step was to investigate if StoD can interact with ubiquitin directly.

To investigate if a direct interaction between StoD and ubiquitin existed, the direct Y2H system was used. In this assay, the AH109 *S. cerevisiae* strain was co-transformed with pGBKT7 vectors, both empty and those containing various *stoD* constructs, as well as pGADT7 vectors, both empty and containing *Ubiquitin* (Table 2.2), before being plated onto DDO and QDO agar plates (Figure 5.14A). Co-transformation of AH109 with all vector combinations resulted in growth on DDO, indicating successful co-transformation. No growth was seen on QDO upon co-transformation of AH109 with any StoD or ubiquitin construct in combination with the empty pGADT7 or pGBKT7 vectors. Growth was only observed in AH109 co-transformed with StoD

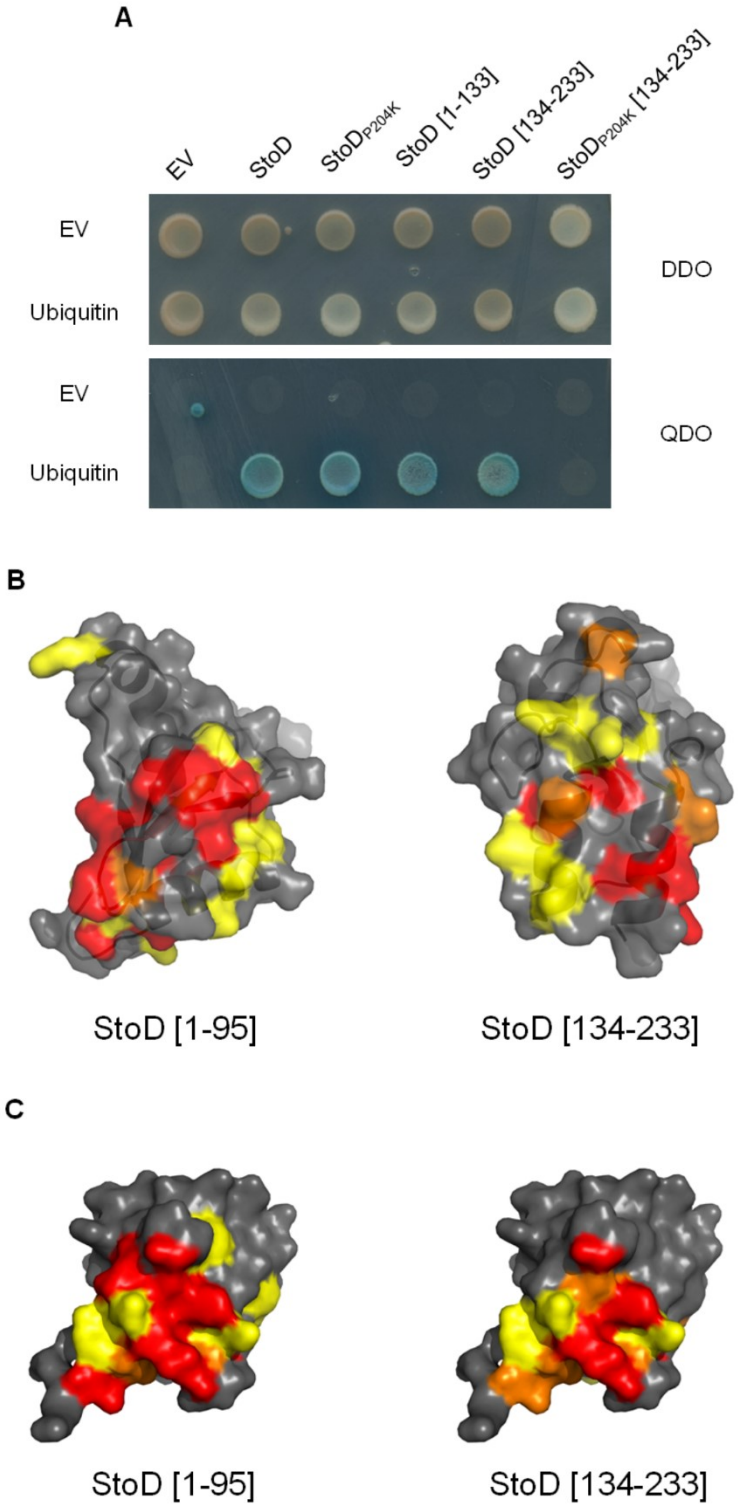


Figure 5.14. StoD directly interacts with ubiquitin. (A) Direct Y2H assay co-transforming AH109 *S. cerevisiae* with either empty pGBKT7 vector (EV) or pGBKT7-*stoD* constructs, and either empty pGADT7 vector (EV) or pGADT7-*Ubiquitin*. Co-transformants were the plated onto DDO and QDO plates to assess any protein-protein interactions. Image is representative of three independent repeats. **(B)** Chemical shift changes in StoD [1-95] or StoD [134-233] spectra upon ubiquitin binding were determined by NMR and mapped onto the surface structures of StoD [1-95] and StoD [134-233]. **(C)** Chemical shift changes in ubiquitin spectra upon either StoD [1-133] or StoD [134-233] binding were determined by NMR and mapped onto the surface structure of ubiquitin. Peak disappearances are shown in red, peak changes greater than 0.1 parts per million are shown in orange and peak changes between 0.05 and 0.1 parts per million are shown in yellow. NMR work performed by Dr Melanie McDowell.

$StoD_{P204K}$, StoD [1-133] and StoD [134-233], as well as ubiquitin. No growth was observed on QDO by AH109 co-transformed with ubiquitin and $StoD_{P204K}$ [134-233].

In parallel to this work, the interaction between StoD and ubiquitin was assessed by Professor Susan Lea and Dr Melanie McDowell using NMR. Firstly, 100 µM of ^{15}N-labelled StoD [1-95] and StoD [134-233] were titrated with increasing concentrations (0-100 µM) of unlabelled ubiquitin whilst chemical peak shifts were observed and mapped onto a surface model of each StoD domain (Figure 5.14B). Peak shifts in the spectra of both StoD [1-95] and StoD [134-233] indicate that both domains of StoD were interacting with ubiquitin. A reciprocal experiment was then performed where, 100 µM of ^{15}N-labelled ubiquitin was titrated with an equimolar amount of either StoD [1-95] or StoD [134-233], whilst chemical peak shifts were observed and mapped onto a surface model of ubiquitin (Figure 5.14C). Peak shifts were observed within the ubiquitin spectra indicating that both StoD [1-95] and StoD [134-233] were binding to ubiquitin. Interestingly, both StoD [1-95] and StoD [134-233] were interacting with the same region on the surface of ubiquitin (Figure 5.14C).

Therefore, using both direct Y2H and NMR methods, a direct interaction between StoD and ubiquitin was observed.

5.7.1. Evaluating the Binding of StoD and Di-Ubiquitin Moieties

StoD [1-95] and StoD [134-233] were both capable of interacting with ubiquitin (Figure 5.14B and Figure 5.14C), therefore suggesting that full-length StoD may be capable of interacting with two molecules of ubiquitin at the same time. Therefore, it was investigated if StoD had the ability to bind di-ubiquitin moieties, specifically, K48-linked and K63-linked di-ubiquitin (Figure 5.15).

To investigate any interaction between StoD and di-ubiquitin moieties, fluorescence polarisation was used. A ubiquitin variant that contained a C-terminal cysteine in place of the terminal glycine residue ($ubiquitin_{G76C}$) was generated, to allow fluorescent labelling of the recombinant ubiquitin proteins. This protein was then expressed, purified, labelled and used

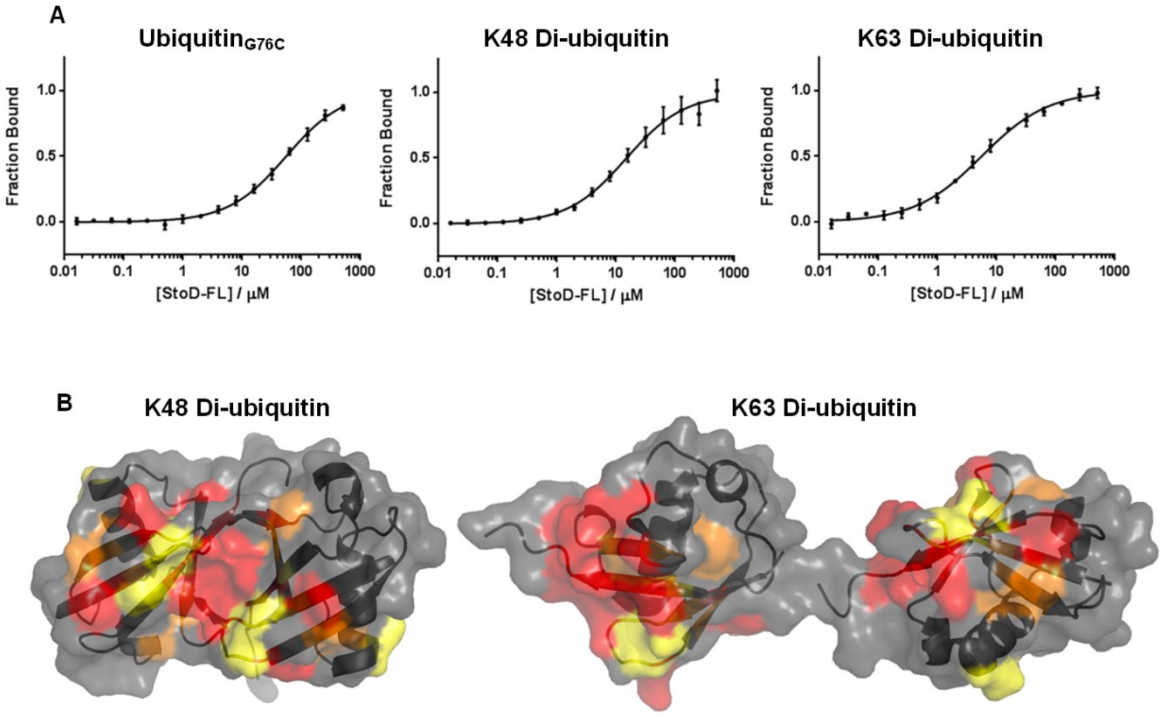


Figure 5.15. StoD binds to di-ubiquitin. (A) Increasing concentrations of recombinant StoD were added to fluorescently-labelled recombinant ubiquitin$_{G76C}$, K48-linked or K63-linked di-ubiquitin and changes in fluorescence were detected. Graphs are averages from three independent repeats and show the mean ± SD. **(B)** Chemical shift changes in ubiquitin spectra upon StoD binding were determined by NMR and mapped onto the structures of K48-linked and K63-linked di-ubiquitin. Peak disappearances are shown in red, peak changes greater than 0.1 parts per million are shown in orange and peak changes between 0.05 and 0.1 parts per million are shown in yellow. This work was performed by Dr Melanie McDowell.

to produce K48-linked or K63-linked di-ubiquitin *in vitro*. Recombinant StoD was titrated onto these fluorescently-labelled ubiquitin proteins and fluorescent changes, indicative of StoD-ubiquitin binding, were detected (Figure **5.15**A). Using this method, a dissociation constant (K_D) for the interaction between StoD and the ubiquitin moieties was calculated. The K_D for the interaction between StoD and ubiquitin$_{G76C}$ was found to be 55 ± 11 µM, whereas, the interaction between StoD and K48-linked di-ubiquitin had a K_D of 15 ± 4 µM and the interaction between StoD and K63-linked di-ubiquitin had a K_D of 5.6 ± 1 µM.

The peak shifts observed in the NMR spectra when ^{15}N-labelled ubiquitin was titrated with an equimolar amount of either StoD [1-95] or StoD [134-233] (Figure 5.14C) were then mapped onto the surface structures of K48-linked and K63-linked di-ubiquitin (Figure 5.15B). This showed that in K48-linked di-ubiquitin, the two ubiquitin molecules assume a ‘closed’

conformation, where the StoD-binding regions of both molecules are occluded between the two ubiquitin molecules. However, K63-linked di-ubiquitin assumes an 'open' conformation, where the StoD-binding regions of both ubiquitin molecules are exposed. This may explain why the K_D for StoD binding to K63-linked di-ubiquitin is lower than for K48-linked di-ubiquitin, as the ubiquitin surfaces required for StoD-binding are exposed, and therefore available for interaction in K63-linked di-ubiquitin, whereas, these surfaces are unavailable for interaction in K48-linked di-ubiquitin.

Therefore, StoD is capable of binding both K48-linked and K63-linked di-ubiquitin molecules, *in vitro*, with greater affinity than for monoubiquitin.

5.7.2. Assessing if StoD can Directly Interact with ISG15

Interferon-stimulated gene 15 (ISG15) is a ubiquitin-like protein, that, as its name suggests, is expressed in response to type I interferons (Blomstrom et al. 1986; Kunzi & Pitha 2003). Unlike SUMO and NEDD8 though, ISG15 contains two ubiquitin-like domains (Chang et al. 2008) and is therefore structurally similar to di-ubiquitin moieties. It was therefore investigated if StoD could interact with ISG15 using the direct Y2H system (Figure 5.16).

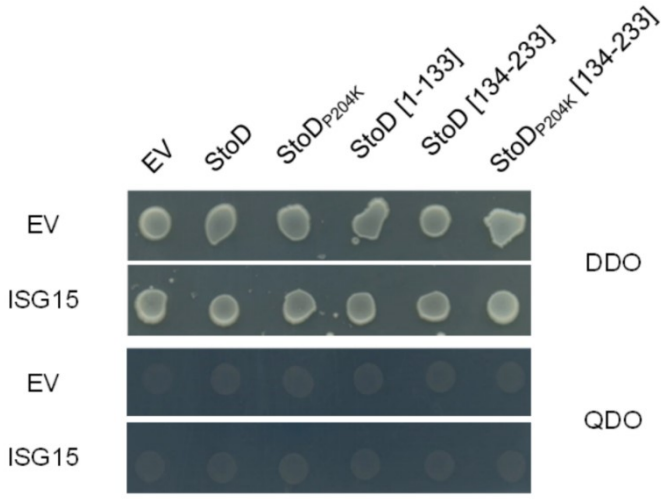


Figure 5.16. StoD does not interact with ISG15. Direct Y2H assay co-transforming AH109 *S. cerevisiae* with either empty pGBKT7 (EV) or pGBKT7-*stoD* constructs, and empty pGADT7 (EV) or pGADT7-*ISG15*. Co-transformants were then plated onto DDO and QDO plates to assess any protein-protein interactions. Image is representative of two independent repeats.

Co-transformation of AH109 *S. cerevisiae* with pGBKT7-*stoD* constructs or empty pGBKT7 vector along with either pGADT7 or pGADT7-*ISG15* (Table 2.2), resulted in growth on DDO, indicating successful co-transformation, however, no growth was seen on QDO (Figure 5.16). Therefore, StoD is not capable of interacting with ISG15 in the direct Y2H system.

5.8. Discussion

The NleG family of T3SS effectors are found in *C. rodentium*, EPEC, EHEC and *Salmonella* (Deng et al. 2004; Tobe et al. 2006; Fookes et al. 2011), but their enzymatic activity was unknown until the structure of the C-terminus of EHEC NleG 2.3 was determined, and found to contain a RING/U-box E3 ubiquitin-ligase domain (Wu et al. 2010). *Salmonella* encodes several T3SS effectors that are E3 ubiquitin-ligases, however, none of these are members of the NleG family and several, SopA, SlrP and SspH1, are absent or pseudogenes in *S.* Typhi (Appendix 1) (Parkhill et al. 2001; Deng et al. 2003; Sabbagh et al. 2010). Therefore, StoD is the first NleG protein family member to be identified in *S. enterica*, and is only present in two serovars, *S.* Typhi and *S.* Paratyphi B, both of which are typhoidal serovars.

Due to the diversity of the N-terminal domain of the NleG proteins it has been suggested that this is involved in substrate recognition (Wu et al. 2010) and would therefore direct different NleG proteins to different host targets. This is seen with the IpaH family of T3SS E3 ubiquitin-ligase effector proteins found in *S. flexneri*, *Salmonella* (SspH1, SspH2 and SlrP) and *P. aeruginosa* (Ashida & Sasakawa 2016). All IpaH proteins share the same overall topology: an N-terminal LRR domain, and a C-terminal NEL E3 ubiquitin-ligase domain, but it is differences in the LRR domain that determine substrate specificity (Ashida & Sasakawa 2016) and enable different IpaH proteins to ubiquitinate different host proteins. For example, the three IpaH proteins, IpaH 4.5, IpaH 9.8 and IpaH 0722 all inhibit the NF-κB pathway, but achieve this by ubiquitinating different substrates (Ashida & Sasakawa 2016). This may explain why EHEC, *C. rodentium* and *S. bongori* have multiple NleG proteins. However, this

theory cannot be substantiated as no substrates of NleG ubiquitination, have been confirmed to date. But, the presence of a ubiquitin-like fold in the N-terminus of StoD may suggest a role for StoD mimicking ubiquitin during *S.* Typhi infection. However, this remains to be evaluated.

StoD was able to perform autoubiquitination in the presence of a subset of E2 ubiquitin-conjugating enzymes, which has been demonstrated previously with other NleG proteins (Wu et al. 2010). The E2 enzymes UBE2D1, UBE2D2, UBE2D3 and UBE2E1 are closely related, and belong to the same family of E2 ubiquitin-conjugating enzymes and may therefore explain why all four were capable of facilitating StoD autoubiquitination, whereas, UBE2K and UBE2H are not related to each other or any of the other E2 ubiquitin-conjugating enzymes (Michelle et al. 2009). UBE2D1, UBE2D2 and UBE2D3 were previously shown to be able to facilitate autoubiquitination of both EHEC NleG 2.3 and NleG 5.1, suggesting that they may be capable of enabling autoubiquitination of different NleG proteins (Wu et al. 2010). These E2 ubiquitin-conjugating enzymes have been demonstrated to be involved in the ubiquitination of eukaryotic proteins, which may provide an insight into what proteins may be substrates of StoD. However, *in vitro* ubiquitination assays lack spatial and temporal regulation (Iconomou & Saunders 2016), meaning that *in vivo* these E2 ubiquitin-conjugating enzymes may not be available for StoD to use. Nevertheless, knowing which E2 ubiquitin-conjugating enzymes can be used by StoD *in vitro* for autoubiquitination does provide a method for identifying factors required by StoD for ubiquitination. As such, autoubiquitination assays were used to determine that StoD [134-233] as being required for autoubiquitination and that the P204K mutation abrogates this activity. The C-terminus has been demonstrated as being required for autoubiquitination of other NleG proteins (Wu et al. 2010) whilst C-terminus of these proteins is essential for autoubiquitination. P204 is analogous to P160, previously shown to be required for autoubiquitination of NleG 2.3 (Wu et al. 2010). This proline residue is present in the site used for interaction with E2 ubiquitin-conjugating enzymes and its mutation results in inhibition of this interaction (Wu et al. 2010). This in turn abrogates the ability of the NleG protein to conjugate ubiquitin to itself and substrates (Wu et al. 2010).

S. cerevisiae has been used as a model to study the activity of several T3SS effectors. SipA was found to be capable of directly interacting with actin and preventing depolymerisation of actin filaments in *S. cerevisiae* (Lesser & Miller 2001). EspV, a T3SS effector from pathogenic *E. coli* demonstrated that it was capable of inducing cell enlargement and cell cycle arrest in *S. cerevisiae* cells, although the actual target was not identified (Arbeloa et al. 2011). StoD expression using the galactose-inducible pYes2 vector, was toxic to BY4741 *S. cerevisiae*, whilst expression of $StoD_{P204K}$ was not, suggesting that the ubiquitination activity of StoD is required for toxicity in BY4741 *S. cerevisiae*. However, the toxicity seen upon StoD expression was not absolute, as growth was still observed albeit to a lesser extent, indicating that the substrate of StoD is not essential for *S. cerevisiae* survival. Identification of host substrates using *S. cerevisiae* is possible by screening different mutants and identifying any that suppress the toxicity induced by the T3SS effector (Arbeloa et al. 2011) or by immunoprecipitating the effector after expression in *S. cerevisiae* and analysis by LC-MS/MS. However, work using other effectors in our research group has shown that this can be problematic and was therefore not attempted with StoD.

Instead, a Y2H screen was utilised to identify interacting partners of StoD, but was unsuccessful. Of the 44 colonies that returned usable sequencing information, 35 were known false positives, whilst only one of the remaining nine sequences interacted specifically with $StoD_{P204K}$. This suggests that these eight proteins were most likely interacting with the Gal4 DNA-binding domain that was present in both the empty pGBKT7 vector and pGBKT7-$stoD_{P204K}$ vectors, which is common of known false positives (Nordgård et al. 2001; Tucker et al. 2009). Interestingly, these nine hits did not interact with StoD (Figure 5.8) and may suggest that StoD is ubiquitinating the prey protein causing it to be relocalised within the *S. cerevisiae* cell, so that a stable interaction, and therefore activation of the reporter genes is not possible. Alternatively, in the StoD-Gal4 DNA-binding domain fusion protein, the DNA binding domain may be obscured by StoD, which does not occur with $StoD_{P204K}$, making it unavailable for interaction.

Whilst the UBE2L3 hit from the Y2H screen did specifically interact with $StoD_{P204K}$, further investigation found that there was not a direct interaction between StoD and UBE2L3, and that UBE2L3 was not ubiquitinated by StoD, or capable of facilitating StoD autoubiquitination *in vitro*. This last finding is unsurprising as UBE2L3 has been demonstrated to be incapable of interaction with RING E3 ubiquitin-ligases (Wenzel et al. 2011). However, the findings that UBE2L3 can interact with SopA, a HECT E3 ubiquitin-ligase from *S.* Typhimurium (Lin et al. 2012) and is involved in modulating IL-1β secretion during pyroptosis (Eldridge et al. 2017) did make it an interesting target.

The high incidence of false positives, is known to be a limiting factor in the use of Y2H screens to identify interacting partners for a protein of interest (Brückner et al. 2009). However, Y2H screens have been used to identify interacting partners and substrates of E3 ubiquitin-ligases previously (Bex et al. 2007), but are limited by being dependent on a stable interaction between the E3 ubiquitin-ligase and the substrate, a factor which is unlikely due to the transient nature of this interaction (Iconomou & Saunders 2016). Therefore, other techniques have been developed to aid in the identification of substrates of E3 ubiquitin-ligases (Iconomou & Saunders 2016). One method, which was investigated to identify StoD substrates was the use of THP-1 and HeLa cell lines that had been transduced to express 6His-tagged ubiquitin which could be infected with WT or Δ*stoD* Ty2 *S.* Typhi, and ubiquitinated proteins could be enriched by purification using affinity-based purification and identified by LC-MS/MS. A similar approach has been used to identify proteins that are ubiquitinated upon infection with *L. pneumophila* (Ivanov & Roy 2013) and would not only identify substrates of StoD, but also aid in the understanding of how the host ubiquitiniome changes during infection with *S.* Typhi. However, it was found that the use of a His-tag resulted in the enrichment of many non-specific proteins, which meant that identification of any ubiquitinated proteins during *S.* Typhi infection would not be possible. Another method that follows the same principles is to use untagged ubiquitin and purifying ubiquitinated proteins using an antibody raised against the di-glycine motif that is produced when ubiquitinated proteins are trypsinised, which can then be identified

by LC-MS/MS (Xu et al. 2010). This approach was recently used to characterise the ubiquitiniome during *S.* Typhimurium infection and found that host components involved in actin remodelling, NF-κB signalling and autophagy were ubiquitinated during infection, as well as identifying substrates of the *Salmonella* E3 ubiquitin-ligase T3SS effectors, SlrP and SspH2 (Fiskin et al. 2016). A collaboration has now been established with this research group with the aim of using this method to determine the ubiquitiniome of *S.* Typhi infection and identify StoD substrates.

The lack of colocalisation between StoD and LC3, Rab11a or Vamp3, or relocalisation of these proteins in the presence of StoD, suggested that StoD does not interact with vesicles enriched with these proteins. LC3 is known to be recruited to SCVs containing replicating *Salmonellae*, through an interaction involving p62 and polyubiquitin chains that coat the SCV, resulting in autophagy and degradation of the bacteria (Mesquita et al. 2012). However, this is prevented by removal of the polyubiquitin chains from the surface of the SCV by the DUB, SseL (Mesquita et al. 2012). Rab11a, and other Rabs, are transiently recruited to the SCV as it matures and this is dependent on the *SPI-1* T3SS (Smith et al. 2007), although the effectors required for the recruitment of these proteins is unknown. In EHEC the T3SS effector, EspG has been demonstrated to abrogate the maturation of Rab11 vesicles, by preventing vesicle recycling during infection (Furniss et al. 2016). Vamp3 is enriched at the sites of *Salmonella* invasion of host cells (Coppolino et al. 2001) and is required for the fusion of Rab11 membrane vesicles in the formation of the autophagosome (Puri et al. 2013). Although, there is a multitude of vesicular proteins that are involved in *Salmonella* pathogenesis (Steele-Mortimer 2008), these three proteins represent key pathways that have been shown to be targeted by T3SS effectors and further work should seek to investigate their role in *S.* Typhi pathogenesis and how this compares to *S.* Typhimurium, even though they are not altered by StoD.

Relocalisation of ubiquitin into discrete puncta throughout the cell during ectopic expression of StoD, but not $StoD_{P204K}$ suggests that the ubiquitination activity of StoD is required for this colocalisation. A similar result was observed for the Herpes Simplex Virus protein, ICP0, which

is also an E3 ubiquitin-ligase, and causes relocalisation of ubiquitin into puncta upon ubiquitination of p53 (Boutell & Everett 2003). However, it was not possible to visualise StoD during *Salmonella* infection (Figure 4.10), and no relocalisation of ubiquitin was observed. This suggests that the relocalisation of ubiquitin during ectopic expression of StoD may be due to the large amount of StoD protein present, which would not occur during infection. Nevertheless, this phenotype was specific to ubiquitin, as it was not observed with ubiquitin-like proteins. Although less extensively studied, the ubiquitin-like proteins, SUMO-1, SUMO-2, SUMO-3 and NEDD8 are involved in eukaryotic cell signalling and bacteria have evolved methods of abrogating these pathways using the T3SS (Ashida et al. 2014). It has been demonstrated that *S. flexneri* causes a change in the localisation of and a decrease in the amount of SUMOylated proteins upon infection, in a T3SS-dependent manner (Sidik et al. 2015), although the effectors responsible have not been elucidated. The T3SS effector Cif, found in EPEC and *Yersinia* spp. has been shown to deamidate NEDD8, resulting in NEDD8 inactivation and cell cycle arrest in infected cells (Crow et al. 2012). Although these examples show that T3SS effectors are involved in interfering with the ubiquitin-like protein pathways within eukaryotic cells, as yet no effectors have been demonstrated to act as ubiquitin-ligase for ubiquitin-like proteins, and investigations into the activity of these proteins during *S.* Typhi infection may aid in further understanding *S.* Typhi pathogenesis.

Work from our research group has shown that other NleG proteins are capable of binding to ubiquitin using the direct Y2H system, however, StoD is the only NleG, capable of binding ubiquitin through both the N- and C-termini. The ubiquitin surface that both StoD termini bind to is commonly used by ubiquitin-binding domains (Dikic et al. 2009) and since the same binding surface is used by both StoD termini, this suggests that StoD binds to two separate molecules of ubiquitin. This hypothesis was corroborated by NMR data showing that StoD binds to di-ubiquitin moieties with higher affinity than monoubiquitin. Since binding between the N-terminus of StoD and ubiquitin was observed in the absence of the C-terminus by both direct Y2H and NMR, this suggests that this is not due to conjugation of a ubiquitin molecule

to the ubiquitin-like fold within the N-terminus. However, the lack of binding between $StoD_{P204K}$ [134-233] and ubiquitin may suggest that this mutation may abrogate the structure of the StoD C-terminus, in particular the ubiquitin-binding domain. But, in the absence of a NMR structure of $StoD_{P204K}$ [134-233] this cannot be confirmed. StoD is not the only E3 ubiquitin-ligase that has been shown to bind ubiquitin directly. HECT E3 ubiquitin-ligases, form a disulphide bond between an internal cysteine residue and a cysteine within ubiquitin which is essential for their activity (Foot et al. 2017) and a non-covalent interaction with ubiquitin is required for the activation of the RBR E3 ubiquitin-ligase, Parkin (Kumar et al. 2017). There are also over 150 different ubiquitin-binding domains (Dikic et al. 2009), many of which have affinities for monoubiquitin of greater than 100 μM (Hurley et al. 2006), whilst the concentration of ubiquitin within cells has been estimated to be 85 μM (Kaiser et al. 2011). This suggests that the binding affinities seen here for StoD towards both monoubiquitin and di-ubiquitin are within physiological limits, however, the residues required for binding should be investigated.

K48-linked polyubiquitin chains direct the conjugated substrate to the proteasome for degradation (Chau et al. 1989), whereas K63-linked polyubiquitin chains are associated with non-degradative cellular signalling (Chen & Sun 2009). The increased affinity of StoD for K63-linked di-ubiquitin over K48-linked di-ubiquitin, appears to be due to the availability of the binding region on the surface of the ubiquitin molecules, and suggests that StoD may be involved in altering non-degradative cellular signalling pathways, rather than those associated with proteasomal degradation. The ‘open’ configuration seen with K63-linked di-ubiquitin is also observed in linear di-ubiquitin, where two ubiquitin molecules are joined by an isopeptide bond between the carboxyl group of the terminal glycine from one molecule and the amine group present in the backbone of the methionine residue at amino acid position one (M1) in the second ubiquitin molecule (Figure 1.8) (Dikic et al. 2009). Such linkages have been found to be produced by the linear ubiquitin assembly complex (LUBAC) which contains two RING E3 ubiquitin-ligases, HOIL-1L and HOIP, and is involved in proteasomal degradation of substrates (Kirisako et al. 2006), as well as TNF receptor signalling (Gerlach et al. 2011).

Future studies may therefore seek to determine the binding affinity of StoD to linear di-ubiquitin amongst other di-ubiquitin linkages, as well as what the effect of StoD binding to K63-linked ubiquitin has on cellular signalling pathways.

ISG15 is a ubiquitin-like protein that utilises the E2 ubiquitin-conjugating enzymes UBE2L6 and UBE2E1 (Takeuchi et al. 2005), and has been demonstrated to be involved in a wide array of cellular pathways, including stress responses (Zhao et al. 2005). The binding between StoD and ISG15 was investigated based on the structural similarity of ISG15 to di-ubiquitin molecules, but this was not observed using the direct Y2H system. However, the fact that both StoD and ISG15 can utilise UBE2E1, may suggest that StoD may be capable of ligating ISG15 onto protein substrates, where a stable interactiono between StoD and ISG15 would not be necessary, and should be assessed by future investigation.

In conclusion, this chapter has shown that StoD is a member of the NleG family of T3SS effector proteins and that StoD is capable of autoubiquitination *in vitro*. It was also shown that StoD specifically causes the relocalisation of ubiquitin upon expression in HeLa cells and that StoD preferentially interacts with ubiquitin by direct Y2H and NMR studies. Further NMR experiments found that StoD preferentially bound to K63-linked di-ubiquitin. This may indicate that StoD is involved in interfering with cellular signalling during *S.* Typhi infection, although further work is needed to investigate this hypothesis.

Chapter 6: Conclusions

6.1. Overview

S. Typhi is a human-restricted bacterial pathogen that is the causative agent of typhoid fever (McClelland et al. 2004), a systemic, enteric fever that causes 200,000 deaths worldwide per year (WHO 2013). Another, closely related *Salmonella* serovar, *S.* Typhimurium, infects humans, as well as other mammals (Feasey et al. 2012), but causes a self-limiting diarrhoeal disease in immunocompetent individuals (Gal-Mor et al. 2014). Both pathogens, utilise two T3SSs to translocate effector proteins into the host cell, that allow the bacterium to invade and replicate, as well as modulating host immune responses (LaRock et al. 2015). Much of the work in identifying and characterising the T3SS effector repertoire of *Salmonella* has been performed in *S.* Typhimurium, and then extended to *S.* Typhi, where the function of these effectors has been assumed to be the same. However, many of these effectors are pseudogenes, or completely absent from the *S.* Typhi genome (Appendix 1), and no attempt has been made to identify effectors that are present in *S.* Typhi and not *S.* Typhimurium. The identification of one putative effector protein, StoD, that was present in *S.* Typhi but not *S.* Typhimurium (Fookes et al. 2011), raised the possibility that there may be more effectors that are present in *S.* Typhi, than had been previously found. This lead to the study described here, and three aims were set to accomplish such work. (I) To establish a CL3 laboratory at Imperial College London, so that *S.* Typhi could be studied. (II) To identify novel T3SS effector proteins in *S.* Typhi using a genome-wide machine-learning approach and assess the role of such proteins in *S.* Typhi pathogenesis. (III) To characterise the biochemical activity of one of these novel T3SS effectors, StoD.

6.2. Conclusions and Future Directions

The successful establishment of the CL3 laboratory and optimisation of protocols for the manipulation of *S.* Typhi, meant that it was possible to study aspects of *S.* Typhi pathogenesis without using *S.* Typhimurium as a proxy, as is common in much of the currently available

Salmonella literature. This process was a considerable undertaking, but was beneficial as it provided myself with a greater understanding of the regulatory elements that are involved in such work, as well as a better understanding of the fundamentals of *S.* Typhi biology. Now that it has been accomplished, it provides a basis for studying the differences in both disease outcome and host-range of *S.* Typhi compared to *S.* Typhimurium. On this note, it became quite evident during the optimisation of many of the methods, that *S.* Typhi and *S.* Typhimurium are fundamentally different pathogens, a point which is somewhat neglected by the current literature, and methods that were originally developed for use with *S.* Typhimurium, required further optimisation before they were suitable for use with *S.* Typhi. However, this now means that in future, more complex work can be undertaken and will benefit from this developed understanding.

The use of a genome-wide machine-learning approach enabled the successful identification of four novel T3SS effector proteins, from five candidates, which are present in *S.* Typhi and not *S.* Typhimurium. When combined with the confirmation of StoD as an effector protein, this increases the repertoire of known *S.* Typhi effectors from 22 proteins to 27 This is significant as the current dogma is that the host-restriction and disease outcome of *S.* Typhi is due to genome degradation (Spanò et al. 2011; McClelland et al. 2004). Genome degradation has been associated with host restriction and changes to the resultant disease in the definitive type (DT) 2 *S.* Typhimurium strain, which has become restricted to pigeons (Kingsley et al. 2013), and the ST313 *S.* Typhimurium strain, which is thought to be becoming human-restricted and causes a systemic bacteraemia that is more akin to typhoid fever than gastroenteritis (Kingsley et al. 2009; Okoro et al. 2015). However, the work presented here somewhat contradicts this, and suggests that *S.* Typhi could have undergone a process of genome addition, to some degree where these novel effectors were acquired from other pathogenic bacterial species, perhaps due to the different infection strategy of *S.* Typhi. For example, *S.* Typhimurium induces a pro-inflammatory response to enable it to colonise the intestine (Stecher et al. 2007), whereas, *S.* Typhi inhibits such an inflammatory response

(Winter et al. 2014). Although this has been largely attributed to the presence of the Vi-antigen (Winter et al. 2014), it is possible that *S.* Typhi-specific T3SS effectors, such as those identified here, could be involved in this process. Such phenotypic differences between *S.* Typhi and *S.* Typhimurium, along with the knowledge that *S.* Typhi possesses 600 genes that are absent in *S.* Typhimurium (Parkhill et al. 2001), suggests that there could well be more *S.* Typhi-specific effectors to be identified. This could be achieved by subjecting the *S.* Typhi genome to further rounds of identification and validation of novel effectors using the genome-wide machine-learning approach demonstrated here.

Whilst characterisation of the biochemical activity of StoD confirmed that it was an E3 ubiquitin-ligase, that could cause specific relocalisation of host ubiquitin during ectopic expression in mammalian cells, a substrate or interacting partner could not be identified using a Y2H screen. Whilst it is possible to identify substrates of E3 ubiquitin-ligases using a Y2H screen (Bex et al. 2007), an increasing number of researchers are using proteomic methods to identify such substrates (Ivanov & Roy 2013; Fiskin et al. 2016). Similar methods are now being used by our research group to identify substrates of the NleG proteins from *C. rodentium* and it is thought that this may be the most appropriate method to identify substrates of StoD and should be considered by future work. Aside from StoD, the biochemical activities of the remaining novel effectors were not characterised here. Since none of the novel effectors were essential for *S.* Typhi invasion and replication within mammalian cells, the determination of the biochemical activity and identification of interacting partners of the novel effectors may provide an insight into their role during *S.* Typhi infection.

Overall, the work presented here demonstrates the initial findings in a study into the biology of *S.* Typhi, showing how different it is to *S.* Typhimurium and highlighting the need to reassess the use of *S.* Typhimurium in the study of *S.* Typhi pathogenesis. This work also provides a basis for several lines of enquiry that should be investigated by future studies and will provide a greater understanding of *S.* Typhi and typhoid fever.

Bibliography

Agatep, R. et al., 1998. Transformation of Saccharomyces cerevisiae by the lithium acetate/single-stranded carrier DNA/polyethylene glycol protocol. *Technical Tips Online*, 3(1), pp.133–137.

Ahmer, B.M.M. et al., 1999. Salmonella SirA is a global regulator of genes mediating enteropathogenesis. *Molecular Microbiology*, 31(3), pp.971–982.

Alpuche-Aranda, B.C.M. et al., 1994. Salmonella Stimulate Macrophage Macropinocytosis and Persist within Spacious Phagosomes. *Journal of Experimental Medicine*, 179, pp.601–608.

Altier, C., Suyemoto, M. & Lawhon, S.D., 2000. Regulation of Salmonella enterica Serovar Typhimurium Invasion Genes by csrA Regulation of Salmonella enterica Serovar Typhimurium Invasion Genes by csrA. *Infection and Immunity*, 68(12), pp.6790–6797.

Andrews, J.R. & Ryan, E.T., 2015. Diagnostics for invasive Salmonella infections: Current challenges and future directions. *Vaccine*, 33(S3), pp.C8–C15. Available at: http://dx.doi.org/10.1016/j.vaccine.2015.02.030.

Arbeloa, A. et al., 2011. Enteropathogenic and Enterohemorrhagic Escherichia coli Type III Secretion Effector EspV Induces Radical Morphological Changes in Eukaryotic Cells. *Infection and Immunity*, 79(3), pp.1067–1076.

Arricau, N. et al., 1998. The RcsB-RcsC regulatory system of Salmonella typhi differentially modulates the expression of invasion proteins, flagellin and Vi antigen in response to osmolarity. *Molecular Microbiology*, 29(3), pp.835–850.

Ashida, H., Kim, M. & Sasakawa, C., 2014. Exploitation of the host ubiquitin system by human bacterial pathogens. *Nature Reviews Microbiology*, 12(6), pp.399–413.

Ashida, H. & Sasakawa, C., 2016. Shigella IpaH Family Effectors as a Versatile Model for Studying Pathogenic Bacteria. *Frontiers in Cellular and Infection Microbiology*, 5, pp.1–6.

Bajaj, V. et al., 1996. Co-ordinate regulation of Salmonella typhimurium invasion genes by environmental and regulatory factors is mediated by control of hilA expression. *Molecular Microbiology*, 22(4), pp.703–714.

Bajaj, V., Hwang, C. & Lee, C.A., 1995. hilA is a novel ompR/toxR family member that activates the expression of Salmonella typhimurium invasion genes. *Molecular Microbiology*, 18(4), pp.715–727.

Bakowski, M.A. et al., 2007. SopD acts cooperatively with SopB during Salmonella enterica serovar Typhimurium invasion. *Cellular Microbiology*, 9(12), pp.2839–2855.

Bakowski, M.A. et al., 2010. The phosphoinositide phosphatase SopB manipulates membrane surface charge and trafficking of the Salmonella-containing vacuole. *Cell Host and Microbe*, 7(6), pp.453–462.

Bakowski, M.A., Braun, V. & Brumell, J.H., 2008. Salmonella-containing vacuoles: directing traffic and nesting to grow. *Traffic*, 9(12), pp.2022–31.

Bayer-Santos, E. et al., 2016. The Salmonella Effector SteD Mediates MARCH8-Dependent Ubiquitination of MHC II Molecules and Inhibits T Cell Activation. *Cell Host and Microbe*, 20(5), pp.584–595.

Belden, W.J. & Miller, S.I., 1994. Further characterization of the PhoP regulon: Identification of new PhoP- activated virulence loci. *Infection and Immunity*, 62(11), pp.5095–5101.

Bergeron, J.R., 2016. Structural modeling of the flagellum MS ring protein FliF reveals similarities to the type III secretion system and sporulation complex. *PeerJ*, 4, p.e1718.

Berks, B.C., 1996. A common export pathway for proteins binding complex redox cofactors? *Molecular Microbiology*, 22(3), pp.393–404.

Bernal-Bayard, J., Cardenal-Muñoz, E. & Ramos-Morales, F., 2010. The Salmonella type III secretion effector, salmonella leucine-rich repeat protein (SlrP), targets the human chaperone ERdj3. *The Journal of Biological Chemistry*, 285(21), pp.16360–8.

Bernal-Bayard, J. & Ramos-Morales, F., 2009. Salmonella type III secretion effector SlrP is an E3 ubiquitin ligase for mammalian thioredoxin. *The Journal of Biological Chemistry*, 284(40), pp.27587–95.

Beuzon, C.R. et al., 2001. In Vivo Genetic Analysis Indicates That PhoP-PhoQ and the Salmonella Pathogenicity Island 2 Type III Secretion System Contribute Independently to Salmonella enterica Serovar Typhimurium Virulence. *Infection and Immunity*, 69(12), pp.7254–7261.

Beuzón, C.R. et al., 1999. pH-dependent secretion of SseB , a product of the SPI-2 type III secretion system of Salmonella typhimurium. *Molecular Microbiology*, 33(4), pp.806–816.

Beuzón, C.R. et al., 2000. Salmonella maintains the integrity of its intracellular vacuole through the action of SifA. *The EMBO journal*, 19(13), pp.3235–3249.

Bex, C. et al., 2007. A yeast two-hybrid system reconstituting substrate recognition of the von Hippel-Lindau tumor suppressor protein. *Nucleic Acids Research*, 35(21), p.e142.

Bhan, M.K., Bahl, R. & Bhatnagar, S., 2005. Typhoid and paratyphoid fever. *Lancet*, 366, pp.749–762.

Bhavsar, A.P. et al., 2013. The Salmonella type III effector SspH2 specifically exploits the NLR co-chaperone activity of SGT1 to subvert immunity. *PLoS Pathogens*, 9(7), p.e1003518.

Bijlsma, J.J.E. & Groisman, E.A., 2005. The PhoP/PhoQ system controls the intramacrophage type three secretion system of Salmonella enterica. *Molecular Microbiology*, 57(1), pp.85–96.

Bishop, A. et al., 2008. Interaction of Salmonella enterica serovar Typhi with cultured epithelial cells : roles of surface structures in adhesion and invasion Bacterial strains. *Microbiology*, 154(Pt 7), pp.1914–1926.

Blomstrom, D.C. et al., 1986. Molecular characterization of the interferon-induced 15-kDa protein. Molecular cloning and nucleotide and amino acid sequence. *Journal of Biological Chemistry*, 261(19), pp.8811–8816.

Boddicker, J.D., Knosp, B.M. & Jones, B.D., 2003. Transcription of the. *Microbiology*, 185(2), pp.525–533.

Boratyn, G.M. et al., 2013. BLAST: a more efficient report with usability improvements. *Nucleic Acids Research*, 41(Web Server issue), pp.W29-33.

Boucrot, E. et al., 2005. The intracellular fate of Salmonella depends on the recruitment of kinesin. *Science*, 308(5725), pp.1174–1178.

Boutell, C. & Everett, R.D., 2003. The herpes simplex virus type 1 (HSV-1) regulatory protein ICP0 interacts with and Ubiquitinates p53. *The Journal of Biological Chemistry*, 278(38), pp.36596–602.

Boyd, E.F. et al., 1996. Molecular genetic relationships of the salmonellae. *Applied and Environmental Microbiology*, 62(3), pp.804–8.

Boyd, E.F. & Brüssow, H., 2002. Common themes among bacteriophage-encoded virulence factors and diversity among the bacteriophages involved. *Trends in Microbiology*, 10(11), pp.521–529.

Brachmann, C.B. et al., 1998. Designer deletion strains derived from Saccharomyces cerevisiae S288C: A useful set of strains and plasmids for PCR-mediated gene disruption and other applications. *Yeast*, 14(2), pp.115–132.

Brawn, L.C., Hayward, R.D. & Koronakis, V., 2007. Salmonella SPI1 effector SipA persists after entry and cooperates with a SPI2 effector to regulate phagosome maturation and intracellular replication. *Cell Host and Microbe*, 1, pp.63–75.

Brennan, M.A. & Cookson, B.T., 2000. Salmonella induces macrophage death by caspase-1-dependent necrosis. *Molecular Microbiology*, 38(1), pp.31–40.

Brenner, F.W. et al., 2000. Salmonella Nomenclature. *Journal of Clinical Microbiology*, 38(7), pp.2465–2467.

Bronstein, P.A., Miao, E.A. & Miller, S.I., 2000. InvB Is a Type III Secretion Chaperone Specific for SspA InvB Is a Type III Secretion Chaperone Specific for SspA. *Journal of Bacteriology*, 182(23), pp.6638–6644.

Brückner, A. et al., 2009. Yeast two-hybrid, a powerful tool for systems biology. *International Journal of Molecular Sciences*, 10(6), pp.2763–2788.

Brumell, J.H., Goosney, D.L. & Finlay, B.B., 2002. SifA, a type III secreted effector of Salmonella typhimurium, directs Salmonella-induced filament (Sif) formation along microtubules. *Traffic*, 3(5), pp.407–415.

Brumell, J.H., Marcus, S.L. & Finlay, B.B., 2000. N-terminal conservation of putative type III secreted effectors of Salmonella typhimurium. *Molecular Microbiology*, 36(3), pp.773–774.

Buckle, G.C., Walker, C.L.F. & Black, R.E., 2012. Typhoid fever and paratyphoid fever: Systematic review to estimate global morbidity and mortality for 2010. *Journal of Global Health*, 2(1), p.10401.

Bunny, K., Liu, J. & Roth, J., 2002. Phenotypes of lexA mutations in Salmonella enterica: evidence for a lethal lexA null phenotype due to the Fels-2 prophage. *Journal of Bacteriology*, 184(22), pp.6235–6249.

Burkinshaw, B.J. & Strynadka, N.C.J., 2014. Assembly and structure of the T3SS. *Biochimica et Biophysica Acta*, 1843(8), pp.1648–1693.

Burstein, D. et al., 2009. Genome-scale identification of Legionella pneumophila effectors using a machine learning approach. *PLoS Pathogens*, 5(7), p.e1000508.

Burstein, D. et al., 2015. Novel Type III Effectors in Pseudomonas aeruginosa. *mBio*, 6(2), pp.e00161-15.

Cardenal-Muñoz, E. & Ramos-Morales, F., 2011. Analysis of the Expression, Secretion and Translocation of the Salmonella enterica Type III Secretion System Effector SteA. *PLoS ONE*, 6(10), p.e26930.

Chakravortty, D. et al., 2005. Formation of a novel surface structure encoded by Salmonella Pathogenicity Island 2. *The EMBO Journal*, 24(11), pp.2043–52.

Chang, Y.-G. et al., 2008. Different roles for two ubiquitin-like domains of ISG15 in protein modification. *The Journal of Biological Chemistry*, 283(19), pp.13370–7.

Charpentier, X. & Oswald, E., 2004. Identification of the secretion and translocation domain of the enteropathogenic and enterohemorrhagic Escherichia coli effector Cif , using TEM-1 β -

lactamase as a new fluorescence-based reporter. *Journal of Bacteriology*, 186(16), pp.5486–5495.

Chau, V. et al., 1989. A multiubiquitin chain is confined to specific lysine in a targeted short-lived protein. *Science*, 243(1982), pp.1576–1583.

Chavez, R.G. et al., 2010. The physiological stimulus for the BarA sensor kinase. *Journal of Bacteriology*, 192(7), pp.2009–2012.

Chen, Z.J. & Sun, L.J., 2009. Nonproteolytic functions of ubiquitin in cell signaling. *Molecular Cell*, 33(3), pp.275–86.

Christen, M. et al., 2009. Activation of a bacterial virulence protein by the GTPase RhoA. *Science Signaling*, 2(95), p.ra71.

Cirillo, D.M. et al., 1998. Macrophage-dependent induction of the Salmonella pathogenicity island 2 type III secretion system and its role in intracellular survival. *Molecular Microbiology*, 30(1), pp.175–188.

Clark, M.A. et al., 1994. Preferential interaction of Salmonella typhimurium with mouse Peyer's patch M cells. *Research in Microbiology*, 145(7), pp.543–552.

Clements, A. et al., 2014. Enterohaemorrhagic Escherichia coli inhibits recycling endosome function and trafficking of surface receptors. *Cellular Microbiology*, 16(11), pp.1693–1705.

Collazo, C.M. & Galán, J.E., 1997. The invasion-associated type III system of Salmonella typhimurium directs the translocation of Sip proteins into the host cell. *Molecular Microbiology*, 24(4), pp.747–756.

Collier-Hyams, L.S. et al., 2002. Cutting edge: Salmonella AvrA effector inhibits the key proinflammatory, anti-apoptotic NF-kappa B pathway. *Journal of Immunology*, 169(6), pp.2846–2850.

Coombes, B.K. et al., 2007. SseL is a Salmonella-specific translocated effector integrated into the SsrB-controlled Salmonella pathogenicity island 2 type III secretion system. *Infection and Immunity*, 75(2), pp.574–580.

Cooper, C.A. et al., 2010. Structural and biochemical characterization of SrcA, a multi-cargo type III secretion chaperone in Salmonella required for pathogenic association with a host. *PLoS Pathogens*, 6(2), p.e1000751.

Cooper, C.A. et al., 2013. The SseC translocon component in Salmonella enterica serovar Typhimurium is chaperoned by SscA. *BMC Microbiology*, 13(1), p.221.

Coppolino, M.G. et al., 2001. Requirement for N-Ethylmaleimide-sensitive Factor Activity at Different Stages of Bacterial Invasion and Phagocytosis. *Journal of Biological Chemistry*, 276(7), pp.4772–4780.

Cordero-Alba, M. et al., 2016. Proteomic insight into the effects of the Salmonella ubiquitin ligase SlrP on host cells. *Biochemical and Biophysical Research Communications*, 472(3), pp.539–544.

Cordero-Alba, M., Bernal-Bayard, J. & Ramos-Morales, F., 2012. SrfJ, a Salmonella Type III Secretion System Effector Regulated by PhoP, RcsB, and IolR. *Journal of Bacteriology*, 194(16), pp.4226–4236.

Costa, T.R.D. et al., 2015. Secretion systems in Gram-negative bacteria: structural and mechanistic insights. *Nature Reviews Microbiology*, 13(6), pp.343–359.

Cott Chubiz, J.E. et al., 2010. FliZ regulates expression of the Salmonella pathogenicity island 1 invasion locus by controlling HilD protein activity in Salmonella enterica serovar typhimurium.

Journal of Bacteriology, 192(23), pp.6261–6270.

Craig, M. et al., 2013. Twin-arginine translocation system (tat) mutants of Salmonella are attenuated due to envelope defects, not respiratory defects. *Molecular Microbiology*, 89(5), pp.887–902.

Crawford, R.W. et al., 2010. Gallstones play a significant role in Salmonella spp. gallbladder colonization and carriage. *Proceedings of the National Academy of Sciences of the United States of America*, 107(9), pp.4353–8.

Crow, A. et al., 2012. The molecular basis of ubiquitin-like protein NEDD8 deamidation by the bacterial effector protein Cif. *Proceedings of the National Academy of Sciences of the United States of America*, 109(27), pp.E1830-8.

Crown, 2001. *Anti-terrorism, Crime and Security Act 2001 - Part 7*, Available at: http://www.legislation.gov.uk/ukpga/2001/24/notes/division/4/7 [Accessed February 17, 2017].

Crump, J.A., Luby, S.P. & Mintz, E.D., 2004. The global burden of typhoid fever. *Bulletin of the World Health Organization*, 82(5), pp.346–353.

Daefler, S. & Russel, M., 1998. The Salmonella typhimurium InvH protein is an outer membrane lipoprotein required for the proper localization of InvG. *Molecular Microbiology*, 28(6), pp.1367–1380.

van Damme, P. et al., 2011. Safety, immunogenicity and dose ranging of a new Vi-CRM_{197} conjugate vaccine against typhoid fever: randomized clinical testing in healthy adults. *PLoS ONE*, 6(9), p.e25398.

Darton, T.C. et al., 2017. Blood culture-PCR to optimise typhoid fever diagnosis after controlled human infection identifies frequent asymptomatic cases and evidence of primary bacteraemia. *Journal of Infection*, 74(4), pp.358–366. Available at: http://dx.doi.org/10.1016/j.jinf.2017.01.006.

Darton, T.C., Blohmke, C.J. & Pollard, A.J., 2014. Typhoid epidemiology, diagnostics and the human challenge model. *Current Opinion in Gastroenterology*, 30(1), pp.7–17.

Darwin, H., Miller, V.L. & However, A., 1999. InvF Is Required for Expression of Genes Encoding Proteins Secreted by the SPI1 Type III Secretion Apparatus in. *Journal of Bacteriology*, 181(16), pp.4949–4954.

Datsenko, K.A. & Wanner, B.L., 2000. One-step inactivation of chromosomal genes in Escherichia coli K-12 using PCR products. *Proceedings of the National Academy of Sciences of the United States of America*, 97(12), pp.6640–6645.

Deiwick, J. et al., 2006. The translocated Salmonella effector proteins SseF and SseG interact and are required to establish an intracellular replication niche. *Infection and Immunity*, 74(12), pp.6965–6972.

Deng, L. et al., 2014. Host Adaptation of a Bacterial Toxin from the Human Pathogen Salmonella Typhi. *Cell*, 159(6), pp.1290–1299.

Deng, W. et al., 2003. Comparative Genomics of Salmonella enterica Serovar Typhi Strains Ty2 and CT18. *Journal of Bacteriology*, 185(7), pp.2330–2337.

Deng, W. et al., 2004. Dissecting virulence: Systematic and functional analyses of a pathogenicity island. *Proceedings of the National Academy of Sciences of the United States of America*, 101(10), pp.3597–3602.

Diao, J. et al., 2008. Crystal structure of SopA, a Salmonella effector protein mimicking a eukaryotic ubiquitin ligase. *Nature Structural and Molecular Biology*, 15(1), pp.65–70.

Diepold, A. & Wagner, S., 2014. Assembly of the bacterial type III secretion machinery. *FEMS Microbiology Reviews*, 38(4), pp.802–822.

Dikic, I., Wakatsuki, S. & Walters, K.J., 2009. Ubiquitin-binding domains - from structures to functions. *Nature Reviews Molecular Cell Biology*, 10(10), pp.659–671.

Domingues, L. et al., 2016. The Salmonella effector SteA binds phosphatidylinositol 4-phosphate for subcellular targeting within host cells. *Cellular Microbiology*, 18(7), pp.949–969.

Dorsey, C.W. et al., 2005. Salmonella enterica serotype Typhimurium MisL is an intestinal colonization factor that binds fibronectin. *Molecular Microbiology*, 57(1), pp.196–211.

Dougan, G. & Baker, S., 2014. Salmonella enterica serovar Typhi and the pathogenesis of typhoid fever. *Annual Review of Microbiology*, 68, pp.317–36.

Driessen, A.J.M., 2001. SecB, a molecular chaperone with two faces. *Trends in Microbiology*, 9(5), pp.193–196.

Dupont, N. et al., 2009. Shigella Phagocytic Vacuolar Membrane Remnants Participate in the Cellular Response to Pathogen Invasion and Are Regulated by Autophagy. *Cell Host and Microbe*, 6, pp.137–149.

Edsall, G. et al., 1960. Studies on infection and immunity in experimental typhoid fever. *Journal of Experimental Medicine*, 112(1), pp.143–166.

Ehrbar, K. et al., 2004. InvB is required for type III-dependent secretion of SopA in Salmonella enterica serovar Typhimurium. *Journal of Bacteriology*, 186(4), pp.1215–9.

Ehrbar, K. et al., 2003. Role of the Salmonella Pathogenicity Island 1 (SPI-1) Protein InvB in Type III Secretion of SopE and SopE2, Two Salmonella Effector Proteins Encoded Outside of SPI-1. *Journal of Bacteriology*, 185(23), pp.6950–6967.

Eldridge, M.J.G. et al., 2017. The Atypical Ubiquitin E2 Conjugase UBE2L3 Is an Indirect Caspase-1 Target and Controls IL-1β Secretion by Inflammasomes. *Cell Reports*, 18(31), pp.1285–1297.

Elhadad, D. et al., 2016. Differences in Host Cell Invasion and SPI-1 Expression between Salmonella enterica serovar Paratyphi A and the Non-Typhoidal Serovar Typhimurium. *Infection and Immunity*, 84(4), pp.1150–1165.

Ellermeier, C.D., Ellermeier, J.R. & Slauch, J.M., 2005. HilD, HilC and RtsA constitute a feed forward loop that controls expression of the SPI1 type three secretion system regulator hilA in Salmonella enterica serovar Typhimurium. *Molecular Microbiology*, 57(3), pp.691–705.

Ellermeier, C.D. & Slauch, J.M., 2003. RtsA and RtsB Coordinately Regulate Expression of the Invasion and Flagellar Genes in Salmonella enterica Serovar Typhimurium RtsA and RtsB Coordinately Regulate Expression of the Invasion and Flagellar Genes in Salmonella enterica Serovar Typhimurium. *Journal of Bacteriology*, 185(17), pp.5096–5108.

Eswarappa, S.M. et al., 2008. Differentially evolved genes of Salmonella pathogenicity islands: insights into the mechanism of host specificity in Salmonella. *PLoS ONE*, 3(12), p.e3829.

Fàbrega, A. & Vila, J., 2013. Salmonella enterica serovar Typhimurium skills to succeed in the host: Virulence and regulation. *Clinical Microbiology Reviews*, 26(2), pp.308–341.

Faucher, S.P. et al., 2006. Transcriptome of Salmonella enterica serovar Typhi within macrophages revealed through the selective capture of transcribed sequences. *Proceedings of the National Academy of Sciences of the United States of America*, 103(6), pp.1906–1911.

Feasey, N.A. et al., 2012. Invasive non-typhoidal salmonella disease: an emerging and

neglected tropical disease in Africa. *The Lancet*, 379(9835), pp.2489–2499.

Feng, X., Oropeza, R. & Kenney, L.J., 2003. Dual regulation by phospho-OmpR of ssrA/B gene expression in Salmonella pathogenicity island 2. *Molecular Microbiology*, 48(4), pp.1131–43.

Feng, Y. et al., 2012. Complete genome sequence of Salmonella enterica serovar pullorum RKS5078. *Journal of Bacteriology*, 194(3), p.744.

Figueira, R. et al., 2013. Identification of salmonella pathogenicity island-2 type III secretion system effectors involved in intramacrophage replication of S. enterica serovar typhimurium: implications for rational vaccine design. *mBio*, 4(2), p.e00065.

Figueira, R. & Holden, D.W., 2012. Functions of the Salmonella pathogenicity island 2 (SPI-2) type III secretion system effectors. *Microbiology*, 158, pp.1147–61.

Finn, R.D. et al., 2017. InterPro in 2017-beyond protein family and domain annotations. *Nucleic Acids Research*, 45, pp.D190–D199.

Firoz Mian, M. et al., 2011. Humanized mice are susceptible to Salmonella typhi infection. *Cellular and Molecular Immunology*, 8(1), pp.83–87.

Fiskin, E. et al., 2016. Global Analysis of Host and Bacterial Ubiquitinome in Response to Salmonella Typhimurium Infection. *Molecular Cell*, 62, pp.1–15.

Fiskin, E. et al., 2017. Structural basis for the recognition and degradation of host TRIM proteins by Salmonella effector SopA. *Nature Communications*, 8, p.14004.

Fookes, M. et al., 2011. Salmonella bongori Provides Insights into the Evolution of the Salmonellae. *PLoS Pathogens*, 7(8), p.e1002191.

Foot, N., Henshall, T. & Kumar, S., 2017. Ubiquitination and the Regulation of Membrane Proteins. *Physiological Reviews*, 97, pp.253–281.

Forest, C.G. et al., 2010. Intracellular survival of Salmonella enterica serovar Typhi in human macrophages is SPI-2 independent. *Microbiology*, 156, pp.3689–98.

Foster, J.W. & Hall, H.K., 1990. Adaptive acidification tolerance response of Salmonella typhimurium. *Journal of Bacteriology*, 172(2), pp.771–778.

Freeman, J.A. et al., 2002. SpiC Is Required for Translocation of Salmonella Pathogenicity Island 2 Effectors and Secretion of Translocon Proteins SseB and SseC. *Journal of Bacteriology*, 184(18), pp.4971–4980.

Freeman, J.A., Ohl, M.E. & Miller, S.I., 2003. The Salmonella enterica Serovar Typhimurium Translocated Effectors SseJ and SifB Are Targeted to the Salmonella-Containing Vacuole. *Infection and Immunity*, 71(1), pp.418–427.

Friebel, A. et al., 2001. SopE and SopE2 from Salmonella typhimurium Activate Different Sets of RhoGTPases of the Host Cell. *Journal of Biological Chemistry*, 276(36), pp.34035–34040.

Fu, Y. & Galán, J.E., 1999. A salmonella protein antagonizes Rac-1 and Cdc42 to mediate host-cell recovery after bacterial invasion. *Nature*, 401(6750), pp.293–297.

Fuentes, J. a et al., 2008. The Salmonella Typhi hlyE gene plays a role in invasion of cultured epithelial cells and its functional transfer to S. Typhimurium promotes deep organ infection in mice. *Research in Microbiology*, 159(4), pp.279–87.

Furniss, R.C.D. et al., 2016. Enterohaemorrhagic E. coli modulates an ARF6:Rab35 signaling axis to prevent recycling endosome maturation during infection. *Journal of Molecular Biology*, 428(17), pp.3399–3407.

Gal-Mor, O., Boyle, E.C. & Grassl, G.A., 2014. Same species, different diseases: how and why typhoidal and non-typhoidal Salmonella enterica serovars differ. *Frontiers in Microbiology*, 5, p.391.

Galán, J.E., 2016. Typhoid toxin provides a window into typhoid fever and the biology of Salmonella Typhi. *Proceedings of the National Academy of Sciences of the United States of America*, 113(23), pp.6338–6344.

Galán, J.E. & Curtiss, R., 1989. Cloning and molecular characterization of genes whose products allow Salmonella typhimurium to penetrate tissue culture cells. *Proceedings of the National Academy of Sciences of the United States of America*, 86, pp.6383–6387.

Galán, J.E., Ginocchio, C. & Costeas, P., 1992. Molecular and functional characterisation of the Salmonella invasion gene invA: Homology of InvA to members of a new protein family. *Journal of Bacteriology*, 174(13), pp.4338–4349.

Galyov, E.E. et al., 1997. A secreted effector protein of Salmonella dublin is translocated into eukaryotic cells and mediates inflammation and fluid secretion in infected ileal mucosa. *Molecular Microbiology*, 25(5), pp.903–912.

Ganley, I.G., Espinosa, E. & Pfeffer, S.R., 2008. A syntaxin 10-SNARE complex distinguishes two distinct transport routes from endosomes to the trans-Golgi in human cells. *Journal of Cell Biology*, 180(1), pp.159–172.

Garcia-del Portillo, F. et al., 1992. Characterization of the micro-environment of Salmonella typhimurium-containing vacuoles within MDCK epithelial cells. *Molecular Microbiology*, 6(22), pp.3289–97.

Garcia Vescovi, E., Soncini, F.C. & Groisman, E. a, 1996. Mg2+ as an Extracellular Signal: Environmental Regulation of Salmonella Virulence. *Cell*, 84, pp.165–174.

Garmendia, J. et al., 2003. The roles of SsrA-SsrB and OmpR-EnvZ in the regulation of genes encoding the Salmonella typhimurium SPI-2 type III secretion system. *Microbiology*, 149(9), pp.2385–2396.

Gat, O. et al., 2011. Cell-associated flagella enhance the protection conferred by mucosally-administered attenuated Salmonella paratyphi A vaccines. *PLoS Neglected Tropical Diseases*, 5(11), p.e1373.

Geddes, K. et al., 2005. Identification of New Secreted Effectors in Salmonella enterica Serovar Typhimurium. *Infection and Immunity*, 73(10), pp.6260–6271.

Gerlach, B. et al., 2011. Linear ubiquitination prevents inflammation and regulates immune signalling. *Nature*, 471(7340), pp.591–6.

Gerlach, R.G. et al., 2008. Cooperation of Salmonella pathogenicity islands 1 and 4 is required to breach epithelial barriers. *Cellular Microbiology*, 10(11), pp.2364–2376.

Germanier, R. & Fiirer, E., 1975. Isolation and Characterization of Gal E Mutant Ty 21a of Salmonella typhi: A Candidate Strain for a Live, Oral Typhoid Vaccine. *Journal of Infectious Diseases*, 131(5), pp.553–558. Available at: http://jid.oxfordjournals.org/content/131/5/553.abstract [Accessed February 21, 2015].

Gilchrist, J.J., MacLennan, C.A. & Hill, A.V.S., 2015. Genetic susceptibility to invasive Salmonella disease. *Nature Reviews Immunology*, 15(7), pp.452–463.

Gille, C. et al., 2014. Alignment-Annotator web server: Rendering and annotating sequence alignments. *Nucleic Acids Research*, 42, pp.W3–W6.

Ginocchio, C.C. et al., 1994. Contact with epithelial cells induces the formation of surface appendages on Salmonella typhimurium. *Cell*, 76(4), pp.717–724.

Gonzalez-Escobedo, G. & Gunn, J.S., 2013. Gallbladder epithelium as a niche for chronic salmonella carriage. *Infection and Immunity*, 81(8), pp.2920–2930.

Green, E.R. & Mecsas, J., 2016. Bacterial Secretion Systems – An overview. *Microbiology Spectrum*, 4(1), pp.1–32.

Greenwood, D. & O'Grady, F., 1978. The Response of Escherichia coli to Nalidixic Acid. *Chemotherapy*, 24, pp.249–258.

Grimont, P. & Weill, F.-X.F., 2007. Antigenic formulae of the Salmonella servovars. *WHO Collaborating Centre for Reference and Research on Salmonella*, pp.1–167. Available at: http://www.pasteur.fr/ip/portal/action/WebdriveActionEvent/oid/01s-000036-089%5Cnpapers2://publication/uuid/CA3447A0-61BF-4D62-9181-C9BA78AF0312.

Günster, R.A. et al., 2017. SseK1 and SseK3 T3SS effectors inhibit NF-κB signalling and necroptotic cell death in Salmonella- infected macrophages. *Infection and Immunity*, 85(3), pp.e00010-17.

Gupta, S.K. et al., 2008. Laboratory-based surveillance of paratyphoid fever in the United States: travel and antimicrobial resistance. *Clinical Infectious Diseases*, 46(11), pp.1656–1663.

Haghjoo, E. & Galán, J.E., 2004. Salmonella typhi encodes a functional cytolethal distending toxin that is delivered into host cells by a bacterial-internalization pathway. *Proceedings of the National Academy of Sciences of the United States of America*, 101(13), pp.4614–9.

Hales, C.M. et al., 2001. Identification and Characterization of a Family of Rab11-interacting Proteins. *The Journal of Biological Chemistry*, 276(42), pp.39067–39075.

Hall, M.N. & Silhavy, T.J., 1981. Genetic analysis of the ompB locus in Escherichia coli K-12. *Journal of Molecular Biology*, 151(1), pp.1–15.

Hallstrom, K.N. et al., 2015. PERP, a host tetraspanning membrane protein, is required for Salmonella-induced inflammation. *Cellular Microbiology*, 17(6), pp.843–59.

Haneda, T. et al., 2012. Salmonella type III effector SpvC, a phosphothreonine lyase, contributes to reduction in inflammatory response during intestinal phase of infection. *Cellular Microbiology*, 14(4), pp.485–499.

Haraga, A. & Miller, S.I., 2003. A Salmonella enterica serovar typhimurium translocated leucine-rich repeat effector protein inhibits NF-kappa B-dependent gene expression. *Infection and Immunity*, 71(7), pp.4052–4058.

Haraga, A. & Miller, S.I., 2006. A Salmonella type III secretion effector interacts with the mammalian serine/threonine protein kinase PKN1. *Cellular Microbiology*, 8(5), pp.837–46.

Harding, C.R. et al., 2013. LtpD is a novel legionella pneumophila effector that binds phosphatidylinositol 3-phosphate and inositol monophosphatase IMPA1. *Infection and Immunity*, 81(11), pp.4261–4270.

Hardt, W.D. et al., 1998. S. typhimurium Encodes an activator of Rho GTPases that induces membrane ruffling and nuclear responses in host cells. *Cell*, 93, pp.815–826.

Hardt, W.D. & Galán, J.E., 1997. A secreted Salmonella protein with homology to an avirulence determinant of plant pathogenic bacteria. *Proceedings of the National Academy of Sciences of the United States of America*, 94(18), pp.9887–92.

Hayashi, F. et al., 2001. The innate immune response to bacterial flagellin is mediated by Toll-like receptor 5. *Nature*, 410(6832), p.1099–103.

Hayward, R.D. et al., 2005. Cholesterol binding by the bacterial type III translocon is essential

for virulence effector delivery into mammalian cells. *Molecular Microbiology*, 56(3), pp.590–603.

Hayward, R.D. & Koronakis, V., 1999. Direct nucleation and bundling of actin by the SipC protein of invasive Salmonella. *The EMBO Journal*, 18(18), pp.4926–4934.

Henry, T. et al., 2006. The Salmonella effector protein PipB2 is a linker for kinesin-1. *Proceedings of the National Academy of Sciences of the United States of America*, 103(36), pp.13497–13502.

Hensel, M. et al., 1995. Simultaneous Identification of Bacterial Virulence Genes by Negative Selection. *Science*, 269(5222), pp.400–403.

Hernandez, L.D. et al., 2003. A Salmonella protein causes macrophage cell death by inducing autophagy. *Journal of Cell Biology*, 163(5), pp.1123–1131.

Hernandez, L.D. et al., 2004. Salmonella modulates vesicular traffic by altering phosphoinositide metabolism. *Science*, 304, pp.1805–1807.

Hersh, D. et al., 1999. The Salmonella invasin SipB induces macrophage apoptosis by binding to caspase-1. *Proceedings of the National Academy of Sciences of the United States of America*, 96(5), pp.2396–401.

Hicks, S.W. et al., 2011. Subcellular Targeting of Salmonella Virulence Proteins by Host-Mediated S-Palmitoylation. *Cell Host and Microbe*, 10(1), pp.9–20.

Hodak, H. & Galán, J.E., 2013. A Salmonella Typhi homologue of bacteriophage muramidases controls typhoid toxin secretion. *EMBO reports*, 14(1), pp.95–102.

Holt, K.E. et al., 2009. Pseudogene accumulation in the evolutionary histories of Salmonella enterica serovars Paratyphi A and Typhi. *BMC Genomics*, 10(36), p.36.

HSE, 2005. Biological agents: Managing the risks in laboratories and healthcare premises. , pp.1–80. Available at: http://www.hse.gov.uk/biosafety/biologagents.pdf [Accessed August 13, 2017].

HSE, 2013. The Approved List of biological agents. , pp.1–32. Available at: http://www.hse.gov.uk/biosafety/information.htm#a2 [Accessed June 14, 2015].

Hurley, D. et al., 2014. Salmonella – host interactions – modulation of the host innate immune system. *Frontiers in Immunology*, 5, p.481.

Hurley, J.H., Lee, S. & Prag, G., 2006. Ubiquitin-binding domains. *The Biochemical Journal*, 399(3), pp.361–72.

Ibarra, J.A. et al., 2010. Induction of Salmonella pathogenicity island 1 under different growth conditions can affect Salmonella–host cell interactions in vitro. *Microbiology*, 156, pp.1120–1133.

Iconomou, M. & Saunders, D.N., 2016. Systematic approaches to identify E3 ligase substrates. *The Biochemical Journal*, 473(22), pp.4083–4101.

Inouye, M., Arnheim, N. & Sternglanz, R., 1973. Bacteriophage T7 Lysozyme Is an N-Acetylmuramyl- L-alanine Amidase. *The Journal of Biological Chemistry*, 248(20), pp.7247–7252.

Ivanov, S.S. & Roy, C.R., 2013. Pathogen signatures activate a ubiquitination pathway that modulates the function of the metabolic checkpoint kinase mTOR. *Nature Immunology*, 14(12), pp.1219–1228.

Iwobi, A. et al., 2003. Novel virulence-associated type II secretion system unique to high-

pathogenicity Yersinia enterocolitica. *Infection and Immunity*, 71(4), pp.1872–1879.

Jamur, C. & Oliver, C., 2009. Permeabilization of cell membranes. In *Immunocytochemical Methods and Protocols*. Springer, pp. 63–66.

Johnson, R. et al., 2017. The type III secretion system effector SptP of Salmonella enterica serovar Typhi. *Journal of Bacteriology*, 199(4), pp.e00647-16.

Jones, R.M. et al., 2008. Salmonella AvrA Coordinates Suppression of Host Immune and Apoptotic Defenses via JNK Pathway Blockade. *Cell Host and Microbe*, 3(4), pp.233–44.

de Jong, H.K. et al., 2012. Host – pathogen interaction in invasive salmonellosis. *PLoS Pathogens*, 8(10), pp.1–9.

Journet, L. et al., 2003. The Needle Length of Bacterial Injectisomes Is Determined by a Molecular Ruler. *Science*, 302(5651), pp.1757–1760.

Juhas, M. et al., 2007. Novel type IV secretion system involved in propagation of genomic islands. *Journal of Bacteriology*, 189(3), pp.761–771.

Jung, T., Catalgol, B. & Grune, T., 2009. The proteasomal system. *Molecular Aspects of Medicine*, 30(4), pp.191–296.

Kaiser, S. et al., 2011. Protein standard absolute quantification (PSAQ) method for the measurement of cellular ubiquitin pools. *Nature Methods*, 8(8), pp.691–696.

Kamitani, T. et al., 1997. Characterization of NEDD8, a Developmentally Down-regulated Ubiquitin-like Protein. *The Journal of Biological Chemistry*, 272(45), pp.28557–28562.

Kanehisa, M. et al., 2016. KEGG as a reference resource for gene and protein annotation. *Nucleic Acids Research*, 44(D1), pp.D457–D462.

Kaniga, K., Tucker, S., et al., 1995. Homologs of the Shigella IpaB and IpaC invasins are required for Salmonella typhimurium entry into cultured epithelial cells. *Journal of Bacteriology*, 177(14), pp.3965–3971.

Kaniga, K., Trollinger, D. & Galan, J.E., 1995. Identification of Two Targets of the Type III Protein Secretion System Encoded by the inv and spa Loci of Salmonella typhimurium That Have Homology to the Shigella IpaD and IpaA Proteins. *Journal of Bacteriology*, 177(24), pp.7078–7085.

Kass, E.H., 1987. A Brief Perspective on the Early History of American Infectious Disease Epidemiology. *The Yale Journal of Biology and Medicine*, 60, pp.341–348.

Kaur, J. & Jain, S.K., 2012. Vi antigen of Salmonella enetrica serovar Typhi - biosynthesis, regulation and its use as vaccine candidate. *Central European Journal of Biology*, 7(5), pp.825–838.

Kawamoto, A. et al., 2013. Common and distinct structural features of Salmonella injectisome and flagellar basal body. *Scientific Reports*, 3, p.3369.

Keestra-Gounder, A.M., Tsolis, R.M. & Bäumler, A.J., 2015. Now you see me, now you don't: the interaction of Salmonella with innate immune receptors. *Nature Reviews Microbiology*, 13(4), pp.206–216.

Keestra, A.M. et al., 2013. Manipulation of small Rho GTPases is a pathogen-induced process detected by NOD1. *Nature*, 496(7444), pp.233–7.

Keszei, A.F. a et al., 2014. Structure of an SspH1-PKN1 complex reveals the basis for host substrate recognition and mechanism of activation for a bacterial E3 ubiquitin ligase. *Molecular and Cellular Biology*, 34(3), pp.362–73.

Khan, A.Q. et al., 1998. Salmonella typhi rpoS mutant is less cytotoxic than the parent strain but survives inside resting THP-1 macrophages. *FEMS Microbiology Letters*, 161(1), pp.201–208.

Khan, S.A. et al., 2003. Salmonella typhi and S. typhimurium derivatives harbouring deletions in aromatic biosynthesis and Salmonella Pathogenicity Island-2 (SPI-2) genes as vaccines and vectors. *Vaccine*, 21(5–6), pp.538–548.

Khatri, N.S. et al., 2009. Annals of Internal Medicine. *Annals of Internal Medicine*, 150(8), pp.567–568.

Kim, K. Il et al., 2004. Interferon-inducible ubiquitin E2, Ubc8, is a conjugating enzyme for protein ISGylation. *Molecular and Cellular Biology*, 24(21), pp.9592–600.

Kim, Y.-G., Kim, J.-H. & Kim, K.-J., 2009. Crystal structure of the Salmonella enterica serovar typhimurium virulence factor SrfJ, a glycoside hydrolase family enzyme. *Journal of Bacteriology*, 191(21), pp.6550–6554.

Kingsley, R.A. et al., 2009. Epidemic multiple drug resistant Salmonella Typhimurium causing invasive disease in sub-Saharan Africa have a distinct genotype. *Genome Research*, 19(12), pp.2279–2287.

Kingsley, R.A. et al., 2013. Genome and transcriptome adaptation accompanying emergence of the definitive type 2 host-restricted salmonella enterica Serovar Typhimurium pathovar. *mBio*, 4(5), pp.1–14.

Kingsley, R.A. et al., 2003. Molecular and phenotypic analysis of the CS54 island of Salmonella enterica serotype typhimurium: identification of intestinal colonization and persistence determinants. *Infection and Immunity*, 71(2), pp.629–40.

Kirisako, T. et al., 2006. A ubiquitin ligase complex assembles linear polyubiquitin chains. *The EMBO Journal*, 25(20), pp.4877–87.

Knodler, L.A. & Steele-Mortimer, O., 2005. The Salmonella effector PipB2 affects late endosome/lysosome distribution to mediate Sif extension. *Molecular Biology of the Cell*, 16, pp.4108–4123.

Knodler, L. a. et al., 2002. Salmonella effectors within a single pathogenicity island are differentially expressed and translocated by separate type III secretion systems. *Molecular Microbiology*, 43(5), pp.1089–1103.

Komander, D., 2009. The emerging complexity of protein ubiquitination. *Biochemical Society Transactions*, 37(5), pp.937–953.

Korotkov, K. V, Sandkvist, M. & Hol, W.G.J., 2012. The type II secretion system: biogenesis, molecular architecture and mechanism. *Nature Reviews Microbiology*, 10(5), pp.336–51.

Kubori, T. et al., 1998. Supramolecular Structure of the Salmonella typhimurium Type III Protein Secretion System. *Science*, 280(5363), pp.602–605.

Kubori, T. et al., 2003. Temporal regulation of Salmonella virulence effector function by proteasome-dependent protein degradation. *Cell*, 115(3), pp.333–342.

Kuhle, V., Abrahams, G.L. & Hensel, M., 2006. Intracellular Salmonella enterica redirect exocytic transport processes in a Salmonella pathogenicity island 2-dependent manner. *Traffic*, 7(6), pp.716–730.

Kuhle, V., Jäckel, D. & Hensel, M., 2004. Effector proteins encoded by Salmonella Pathogenicity Island 2 interfere with the microtubule cytoskeleton after translocation into host cells. *Traffic*, 5(5), pp.356–370.

Kumar, A. et al., 2017. Parkin–phosphoubiquitin complex reveals cryptic ubiquitin-binding site required for RBR ligase activity. *Nature Structural & Molecular Biology*, 24, pp.475–483.

Kunzi, M.S. & Pitha, P.M., 2003. Interferon targeted genes in host defense. *Autoimmunity*, 36(8), pp.457–461.

Lan, R., Reeves, P.R. & Octavia, S., 2009. Population structure, origins and evolution of major Salmonella enterica clones. *Infection, Genetics and Evolution*, 9(5), pp.996–1005.

Lara-Tejero, M. et al., 2011. A sorting platform determines the order of protein secretion in bacterial type III systems. *Science*, 331(6021), pp.1188–91.

LaRock, D.L., Chaudhary, A. & Miller, S.I., 2015. Salmonellae interactions with host processes. *Nature Reviews Microbiology*, 13(4), pp.191–205.

Lawhon, S.D. et al., 2002. Intestinal short-chain fatty acids alter Salmonella typhimurium invasion gene expression and virulence through BarA / SirA. *Molecular Microbiology*, 46(5), pp.1451–1464.

Lee, S.H. & Galán, J.E., 2003. InvB is a type III secretion-associated chaperone for the Salmonella enterica effector protein SopE. *Journal of Bacteriology*, 185(24), pp.7279–84.

Lesnick, M.L. et al., 2001. The Salmonella spvB virulence gene encodes an enzyme that ADP-ribosylates actin and destabilizes the cytoskeleton of eukaryotic cells. *Molecular Microbiology*, 39(6), pp.1464–1470.

Lesser, C.F. & Miller, S.I., 2001. Expression of microbial virulence proteins in Saccharomyces cerevisiae models mammalian infection. *The EMBO Journal*, 20(8), pp.1840–1849.

Levy, H. et al., 2008. PCR method to identify Salmonella enterica serovars Typhi, Paratyphi A, and Paratyphi B among Salmonella isolates from the blood of patients with clinical enteric fever. *Journal of Clinical Microbiology*, 46(5), pp.1861–1866.

Lhocine, N. et al., 2015. Apical invasion of intestinal epithelial cells by salmonella typhimurium requires villin to remodel the brush border actin cytoskeleton. *Cell Host and Microbe*, 17(2), pp.164–177.

Li, S. et al., 2013. Pathogen blocks host death receptor signalling by arginine GlcNAcylation of death domains. *Nature*, 501(7466), pp.242–6.

Liao, A.P. et al., 2008. Salmonella type III effector AvrA stabilizes cell tight junctions to inhibit inflammation in intestinal epithelial cells. *PLoS ONE*, 3(6), p.e2369.

Lifshitz, Z. et al., 2014. Identification of novel Coxiella burnetii Icm/Dot effectors and genetic analysis of their involvement in modulating a mitogen-activated protein kinase pathway. *Infection and Immunity*, 82(9), pp.3740–3752.

Lilic, M., Vujanac, M. & Stebbins, C.E., 2006. A common structural motif in the binding of virulence factors to bacterial secretion chaperones. *Molecular Cell*, 21(5), pp.653–664.

Lin, D.Y. et al., 2011. Biochemical and structural studies of a HECT-like ubiquitin ligase from Escherichia coli O157:H7. *The Journal of Biological Chemistry*, 286(1), pp.441–449.

Lin, D.Y. -w., Diao, J. & Chen, J., 2012. Crystal structures of two bacterial HECT-like E3 ligases in complex with a human E2 reveal atomic details of pathogen-host interactions. *Proceedings of the National Academy of Sciences of the United States of America*, 109(6), pp.1925–1930.

Lin, S.L., Le, T.X. & Cowen, D.S., 2003. SptP, a Salmonella typhimurium type III-secreted protein, inhibits the mitogen-activated protein kinase pathway by inhibiting Raf activation. *Cellular Microbiology*, 5(4), pp.267–275.

Ling, J. & Chau, P., 1984. Plasmids Mediating Resistance to Chloramphenicol, Trimethoprim, and Ampicillin in Salmonella typhi Strains Isolated in the Southeast Asian Region. *Journal of Infectious Diseases*, 149(4).

Liu, J. et al., 2013. The type VI secretion system gene cluster of Salmonella typhimurium: required for full virulence in mice. *Journal of Basic Microbiology*, 53, pp.600–607.

Lloyd, S.A. et al., 2001. Yersinia YopE is targeted for type III secretion by N-terminal, not mRNA, signals. *Molecular Microbiology*, 39(2), pp.520–531.

Lohou, D. et al., 2013. Type III chaperones & Co in bacterial plant pathogens: a set of specialized bodyguards mediating effector delivery. *Frontiers in Plant Science*, 4, p.435.

Lopez, P.J. et al., 1999. The C-terminal half of RNase E, which organizes the Escherichia coli degradosome, participates in mRNA degradation but not rRNA processing in vivo. *Molecular Microbiology*, 33(1), pp.188–199.

Lorick, K.L. et al., 1999. RING fingers mediate ubiquitin-conjugating enzyme (E2) -dependent ubiquitination. *Proceedings of the National Academy of Sciences of the United States of America*, 96, pp.11364–11369.

Lu, R. et al., 2012. Consistent activation of the β-catenin pathway by Salmonella type-three secretion effector protein AvrA in chronically infected intestine. *American journal of physiology Gastrointestinal and Liver Physiology*, 303(10), pp.G1113-25.

Lu, R. et al., 2016. Salmonella Protein AvrA Activates the STAT3 Signaling Pathway in Colon Cancer 1. *Neoplasia*, 18(5), pp.307–316.

Lucas, R.L. et al., 2000. Multiple factors independently regulate hilA and invasion gene expression in Salmonella enterica serovar typhimurium. *Journal of Bacteriology*, 182(7), pp.1872–82.

Luo, Y. et al., 2001. Structural and biochemical characterization of the type III secretion chaperones CesT and SigE. *Nature Structural Biology*, 8(12), pp.1031–1036.

Madan, R. et al., 2012. Salmonella acquires lysosome-associated membrane protein 1 (LAMP1) on phagosomes from golgi via SipC protein-mediated recruitment of host syntaxin6. *Journal of Biological Chemistry*, 287(8), pp.5574–5587.

Marineli, F. et al., 2013. Mary Mallon (1869-1938) and the history of typhoid fever. *Annals of Gastroenterology*, 26(2), pp.132–134.

Marlovits, T.C. et al., 2006. Assembly of the inner rod determines needle length in the type III secretion injectisome. *Nature*, 441(7093), pp.637–40.

Marlovits, T.C. et al., 2004. Structural Insights into the Assembly of the Type III Secretion Needle Complex. *Science*, 306(5698), pp.1040–1042.

Martin, L.B. et al., 2016. Status of paratyphoid fever vaccine research and development. *Vaccine*, 34(26), pp.2900–2902.

Matunis, M.J., Coutavas, E. & Blobel, G., 1996. A Novel Ubiquitin-like Modification Modulates the Partitioning of the Ran-GTPase-activating Protein RanGAP1 between the Cytosol and the Nuclear Pore Complex. *The Journal of Cell Biology*, 135(6), pp.1457–1470.

Mayor, A. et al., 2007. A crucial function of SGT1 and HSP90 in inflammasome activity links mammalian and plant innate immune responses. *Nature Immunology*, 8(5), pp.497–503.

McCann, J.R. & St. Geme, J.W., 2014. The HMW1C-Like Glycosyltransferases-An Enzyme Family with a Sweet Tooth for Simple Sugars. *PLoS Pathogens*, 10(4), pp.2–5.

McClelland, M. et al., 2004. Comparison of genome degradation in Paratyphi A and Typhi, human-restricted serovars of Salmonella enterica that cause typhoid. *Nature genetics*, 36(12), pp.1268–74.

McCormick, B. a et al., 1993. Salmonella typhimurium attachment to human intestinal monolayers; transcellular signaling to subepithelial neutrophils. *The Journal of Cell Biology*, 123(4), pp.895–907.

McGregor, A.C., Waddington, C.S. & Pollard, A.J., 2013. Prospects for prevention of Salmonella infection in children through vaccination. *Current Opinion in Infectious Diseases*, 26(3), pp.254–62.

McLaughlin, L.M. et al., 2009. The Salmonella SPI2 effector SseI mediates long-term systemic infection by modulating host cell migration. *PLoS Pathogens*, 5(11), p.e1000671.

McQuiston, J.R. et al., 2008. Do Salmonella carry spare tyres? *Trends in Microbiology*, 16(4), pp.142–148.

Meltzer, E., Sadik, C. & Schwartz, E., 2005. Enteric Fever in Israeli Travelers: A Nationwide Study. *Journal of Travel Medicine*, 12, pp.275–281.

Méresse, S. et al., 2001. Remodelling of the actin cytoskeleton is essential for replication of intravacuolar Salmonella. *Cellular Microbiology*, 3(8), pp.567–577.

Mesquita, F.S. et al., 2012. The Salmonella Deubiquitinase SseL Inhibits Selective Autophagy of Cytosolic Aggregates. *PLoS Pathogens*, 8(6), p.e1002743.

Mesquita, F.S., Holden, D.W. & Rolhion, N., 2013. Lack of Effect of the Salmonella Deubiquitinase SseL on the NF-KB Pathway. *PLoS ONE*, 8(1), pp.1–9.

Miao, E.A. et al., 2003. Salmonella effectors translocated across the vacuolar membrane interact with the actin cytoskeleton. *Molecular Microbiology*, 48(2), pp.401–415.

Miao, E.A. et al., 1999. Salmonella typhimurium leucine-rich repeat proteins are targeted to the SPI1 and SPI2 type III secretion systems. *Molecular Microbiology*, 34(4), pp.850–64.

Miao, E.A. & Miller, S.I., 2000. A conserved amino acid sequence directing intracellular type III secretion by Salmonella typhimurium. *Proceedings of the National Academy of Sciences of the United States of America*, 97(13), pp.7539–7544.

Michelle, C. et al., 2009. What Was the Set of Ubiquitin and Ubiquitin-Like Conjugating Enzymes in the Eukaryote Common Ancestor? *Journal of Molecular Evolution*, 68, pp.616–628.

Michiels, T. et al., 1991. Analysis of virC, an operon involved in the secretion of Yop proteins by Yersinia enterocolitica. *Journal of Bacteriology*, 173(16), pp.4994–5009.

Micoli, F. et al., 2011. Vi-CRM197 as a new conjugate vaccine against Salmonella Typhi. *Vaccine*, 29(4), pp.712–720.

Miki, T. et al., 2009. Functional characterization of SsaE, a novel chaperone protein of the type III secretion system encoded by Salmonella pathogenicity island 2. *Journal of Bacteriology*, 191(22), pp.6843–54.

Miller, R.A. & Wiedmann, M., 2016. The Cytolethal Distending Toxin Produced by Nontyphoidal Salmonella Serotypes Javiana, Montevideo, Oranienburg, and Mississippi Induces DNA Damage in a Manner Similar to That of Serotype Typhi. *mBio*, 7(6), pp.e02109-16.

Murli, S., Watson, R.O. & Galan, J.E., 2001. Role of tyrosine kinases and the tyrosine phosphatase SptP in the interaction of Salmonella with host cells. *Cellular Microbiology*, 3(12),

pp.795–810.

Myeni, S.K. & Zhou, D., 2010. The C terminus of SipC binds and bundles F-actin to promote Salmonella invasion. *Journal of Biological Chemistry*, 285(18), pp.13357–13363.

Natale, P., Brüser, T. & Driessen, A.J.M., 2008. Sec- and Tat-mediated protein secretion across the bacterial cytoplasmic membrane-Distinct translocases and mechanisms. *Biochimica et Biophysica Acta*, 1778(9), pp.1735–1756.

Negrate, G. Le et al., 2008. Salmonella Secreted Factor L Deubiquitinase of Salmonella typhimurium Inhibits NF- B , Suppresses I kBa Ubiquitination. *The Journal of Immunology*, 180, pp.5045–5056.

Nga, T.V.T. et al., 2010. The sensitivity of real-time PCR amplification targeting invasive Salmonellaserovars in biological specimens. *BMC Infectious Diseases*, 10(1), p.125. Available at: http://bmcinfectdis.biomedcentral.com/articles/10.1186/1471-2334-10-125.

NHS, 2016. Typhoid fever. Available at: http://www.nhs.uk/Conditions/Typhoid-fever/Pages/Introduction.aspx [Accessed December 16, 2016].

Niemann, G.S. et al., 2011. Discovery of novel secreted virulence factors from salmonella enterica serovar typhimurium by proteomic analysis of culture supernatants. *Infection and Immunity*, 79(1), pp.33–43.

Nikolaus, T. et al., 2001. SseBCD proteins are secreted by the type III secretion system of Salmonella pathogenicity island 2 and function as a translocon. *Journal of Bacteriology*, 183(20), pp.6036–6045.

Nordgård, O. et al., 2001. JAB1/CSN5 interacts with the GAL4 DNA binding domain: A note of caution about two-hybrid interactions. *Biochimie*, 83(10), pp.969–971.

Notti, R.Q. & Stebbins, C.E., 2016. The Structure and Function of Type III Secretion Systems. *Microbiology Spectrum*, 4(1), pp.1–30.

Oberto, J., 2013. SyntTax: a web server linking synteny to prokaryotic taxonomy. *BMC Bioinformatics*, 14(4), pp.1–10.

Ochman, H. et al., 1996. Identification of a pathogenicity island required for Salmonella survival in host cells. *Proceedings of the National Academy of Sciences of the United States of America*, 93, pp.7800–7804.

Ochsner, U. a et al., 2002. Effects of the twin-arginine translocase on secretion of virulence factors, stress response, and pathogenesis. *Proceedings of the National Academy of Sciences of the United States of America*, 99(12), pp.8312–8317.

Odendall, C. et al., 2012. The salmonella kinase SteC targets the MAP kinase MEK to regulate the host actin cytoskeleton. *Cell Host and Microbe*, 12, pp.657–668.

Ohlson, M.B. et al., 2008. Structure and Function of Salmonella SifA Indicate that Its Interactions with SKIP, SseJ, and RhoA Family GTPases Induce Endosomal Tubulation. *Cell Host and Microbe*, 4(5), pp.434–446.

Okoro, C.K. et al., 2015. Signatures of Adaptation in Human Invasive Salmonella Typhimurium ST313 Populations from Sub-Saharan Africa. *PLoS Neglected Tropical Diseases*, 9(3), pp.1–18.

Oscarsson, J. et al., 2002. Characterization of a pore-forming cytotoxin expressed by Salmonella enterica serovars Typhi and Paratyphi A. *Infection and Immunity*, 70(10), pp.5759–5769.

Parkhill, J. et al., 2001. Complete genome sequence of a multiple drug resistant Salmonella

enterica serovar Typhi CT18. *Nature*, 413, pp.848–852.

Parry, C. et al., 1998. Quinolone-resistant Salmonella typhi in Vietnam. *The Lancet*, 351(9111), p.1289.

Parry, C.M. et al., 2002. Typhoid Fever. *The New England Journal of Medicine*, 347(22), pp.1770–1782.

Patel, J.C. et al., 2009. Diversification of a Salmonella Virulence Protein Function by Ubiquitin-Dependent Differential Localization. *Cell*, 137(2), pp.283–294.

Pearce, M.J. et al., 2008. Ubiquitin-Like Protein Involved in the Proteasome Pathway of Mycobacterium tuberculosis. *Science*, 322(14), pp.1104–1107.

Pegues, D. et al., 1995. PhoP / PhoQ transcriptional repression of Salmonella typhimurium invasion protein secretion genes: evidence for a role in protein secretion. *Molecular Microbiology*, 17(1), pp.169–181.

Phu Huong Lan, N. et al., 2016. Invasive Non-typhoidal Salmonella Infections in Asia: Clinical Observations, Disease Outcome and Dominant Serovars from an Infectious Disease Hospital in Vietnam. *PLoS Neglected Tropical Diseases*, 10(8), pp.1–13.

Phung, L. Van, Ryo, H. & Nomura, T., 2002. Specific gyrA mutation at codon 83 in nalidixic acid-resistant Salmonella enterica serovar Typhi strains isolated from Vietnamese patients. *Antimicrobial Agents and Chemotherapy*, 46(6), pp.2052–3.

Pickard, D. et al., 2003. Composition, acquisition, and distribution of the Vi exopolysaccharide-encoding Salmonella enterica pathogenicity island SPI-7. *Journal of Bacteriology*, 185(17), pp.5055–5065.

Pilar, A.V.C. et al., 2012. GogB is an anti-inflammatory effector that limits tissue damage during Salmonella infection through interaction with human FBXO22 and Skp1. *PLoS Pathogens*, 8(6), p.e1002773.

Porwollik, S., Wong, R.M.-Y. & McClelland, M., 2002. Evolutionary genomics of Salmonella: Gene acquisitions revealed by microarray analysis. *Proceedings of the National Academy of Sciences of the United States of America*, 99(13), pp.8956–8961.

Pradel, N. et al., 2003. Contribution of the twin arginine translocation system to the virulence of enterohemorrhagic Escherichia coli O157:H7. *Infection and Immunity*, 71(9), pp.4908–4916.

Puri, C. et al., 2013. Diverse autophagosome membrane sources coalesce in recycling endosomes. *Cell*, 154(6), pp.1285–1299.

Quezada, C.M. et al., 2009. A family of Salmonella virulence factors functions as a distinct class of autoregulated E3 ubiquitin ligases. *Proceedings of the National Academy of Sciences of the United States of America*.

Raffatellu, M. et al., 2008. Clinical pathogenesis of typhoid fever. *Journal of Infection in Developing Countries*, 2(4), pp.260–266.

Raffatellu, M. et al., 2005. The Vi capsular antigen of Salmonella enterica serotype Typhi reduces toll-like receptor-dependent interleukin-8 expression in the intestinal mucosa. *Infection and Immunity*, 73(6), pp.3367–3374.

Raghunathan, D. et al., 2011. SadA, a trimeric autotransporter from Salmonella enterica serovar Typhimurium, can promote biofilm formation and provides limited protection against infection. *Infection and Immunity*, 79(11), pp.4342–4352.

Ramsden, A.E., Holden, D.W. & Mota, L.J., 2007. Membrane dynamics and spatial distribution

of Salmonella-containing vacuoles. *Trends in Microbiology*, 15(11), pp.516–524.

Rathman, M. & Sjaastad, M.D., 1996. Acidification of phagosomes containing Salmonella typhimurium in murine macrophages . Acidification of Phagosomes Containing Salmonella typhimurium in Murine Macrophages. *Infection and Immunity*, 64(7), pp.2765–2773.

Rayamajhi, M. et al., 2013. Cutting Edge: Mouse NAIP1 Detects the Type III Secretion System Needle Protein. *Journal of Immunology*, 191, pp.3986–3989.

Reeves, M.W. et al., 1989. Clonal nature of Salmonella typhi and its genetic relatedness to other salmonellae as shown by multilocus enzyme electrophoresis and proposal of Salmonella bongori comb. nov. *Journal of Clinical Microbiology*, 27(2), pp.313–320.

Rehman, M.A. et al., 2015. Complete Genome and Plasmid Sequences of Three Canadian Strains of Salmonella enterica subsp . enterica Serovar Enteritidis Belonging to Phage Types 8, 13 and 13a. *Genome Announcements*, 3(5), pp.8–9.

Rohde, J.R. et al., 2007. Type III Secretion Effectors of the IpaH Family Are E3 Ubiquitin Ligases. *Cell Host and Microbe*, 1(1), pp.77–83.

Rolhion, N. et al., 2016. Inhibition of Nuclear Transport of NF-κB p65 by the Salmonella Type III Secretion System Effector SpvD. *PLoS Pathogens*, 12(5), p.e1005653.

Rossier, O., Starkenburg, S.R. & Cianciotto, N.P., 2004. Legionella pneumophila type II protein secretion promotes virulence in the A/J mouse model of Legionnaires' disease pneumonia. *Infection and Immunity*, 72(1), pp.310–321.

Royle, M.C.J. et al., 2003. Stimulation of Toll-like receptor 4 by lipopolysaccharide during cellular invasion by live Salmonella typhimurium is a critical but not exclusive event leading to macrophage responses. *Journal of Immunology*, 170(22), pp.5445–5454.

Russell, A.B., Peterson, S.B. & Mougous, J.D., 2014. Type VI secretion system effectors: poisons with a purpose. *Nature Reviews Microbiology*, 12(2), pp.137–48.

Rytkönen, A. et al., 2007. SseL, a Salmonella deubiquitinase required for macrophage killing and virulence. *Proceedings of the National Academy of Sciences of the United States of America*, 104(9), pp.3502–3507.

Sabbagh, S.C. et al., 2010. So similar, yet so different: uncovering distinctive features in the genomes of Salmonella enterica serovars Typhimurium and Typhi. *FEMS Microbiology Letters*, 305(1), pp.1–13.

Saha, A. et al., 2008. Multimodal activation of the ubiquitin ligase SCF by Nedd8 conjugation. *Molecular Cell*, 32(1), pp.21–31.

Saitoh, H. & Hinchey, J., 2000. Functional Heterogeneity of Small Ubiquitin-related Protein Modifiers SUMO-1 versus SUMO-2/3. *The Journal of Biological Chemistry*, 275(9), pp.6252–6258.

Sansonetti, P.J., 2004. War and peace at mucosal surfaces. *Nature Reviews Immunology*, 4, pp.953–964.

Santander, J. et al., 2007. Role of RpoS in fine-tuning the synthesis of Vi capsular polysaccharide in Salmonella enterica serotype Typhi. *Infection and Immunity*, 75(3), pp.1382–1392.

Scaife, J.G. et al., 1979. Gene for the RNA polymerase sigma subunit mapped in Salmonella typhimurium and Escherichia coli by cloning and deletion. *Proceedings of the National Academy of Sciences of the United States of America*, 76(12), pp.6510–6514.

Schechter, L.M., Damrauer, S.M. & Lee, C.A., 1999. Two AraC/XylS family members can

independently counteract the effect of repressing sequences upstream of the hilA promoter. *Molecular Microbiology*, 32(3), pp.629–642.

Scherer, C.A., Cooper, E. & Miller, S.I., 2000. The Salmonella type III secretion translocon protein SspC is inserted into the epithelial cell plasma membrane upon infection. *Molecular Microbiology*, 37(5), pp.1133–1145.

Schroeder, N. et al., 2010. The virulence protein SopD2 regulates membrane dynamics of Salmonella-containing vacuoles. *PLoS Pathogens*, 6(7), p.e1001002.

Seth-Smith, H.M.B., 2008. SPI-7: Salmonella's Vi-Encoding Pathogenicity Island. *The Journal of Infection in Developing Countries*, 2(4), pp.267–271.

Shea, J.E. et al., 1996. Identification of a virulence locus encoding a second type III secretion system in Salmonella typhimurium. *Proceedings of the National Academy of Sciences of the United States of America*, 93(6), pp.2593–2597.

Shotland, Y., Krämer, H. & Groisman, E.A., 2003. The Salmonella SpiC protein targets the mammalian Hook3 protein function to alter cellular trafficking. *Molecular Microbiology*, 49(6), pp.1565–1576.

Sidik, S.M. et al., 2015. Shigella Infection Interferes with SUMOylation and Increases PML-NB Number. *PLoS ONE*, 10(4), p.e0122585.

Sievers, F. et al., 2011. Fast, scalable generation of high-quality protein multiple sequence alignments using Clustal Omega. *Molecular Systems Biology*, 7(1), p.539.

Sigma, 2017. Sigma Aldrich website. Available at: http://www.sigmaaldrich.com/catalog/product/sigma/cls430320?lang=en&region=GB [Accessed March 17, 2017].

da Silva Correia, J. et al., 2007. SGT1 is essential for Nod1 activation. *Proceedings of the National Academy of Sciences of the United States of America*, 104(16), pp.6764–9.

Silverman, J. & Brunet, Y., 2012. Structure and regulation of the type VI secretion system. *Annual Review of Microbiology*, 66, pp.453–472.

Smith, A.C. et al., 2007. A network of Rab GTPases controls phagosome maturation and is modulated by Salmonella enterica serovar Typhimurium. *Journal of Cell Biology*, 176(3), pp.263–268.

Solovyev, V. & Salamov, A., 2011. Automatic Annotation of Microbial Genomes and Metagenomic Sequences. In *Metagenomics and its Applications in Agriculture, Biomedicine and Environmental Studies*. pp. 61–78.

Song, J., Gao, X. & Galan, J.E., 2013. Structure and function of the Salmonella Typhi chimaeric A2B5 typhoid toxin. *Nature*, 499, pp.350–354.

Sontag, R.L. et al., 2016. Identification of Novel Host Interactors of Effectors Secreted by Salmonella and Citrobacter. *mSystems*, 1(4), pp.e00032-15.

Sory, M.-P. & Cornelis, G.R., 1994. Translocation of a hybrid YopE-adenylate cyclase from Yersinia enterocolitica into HeLa cells. *Molecular Microbiology*, 14(3), pp.583–594.

Spanò, S. et al., 2016. A Bacterial Pathogen Targets a Host Rab-Family GTPase Defense Pathway with a GAP. *Cell Host and Microbe*, 19, pp.216–226.

Spanò, S. & Galan, J.E., 2012. A Rab32-dependent pathway contributes to Salmonella Typhi host restriction. *Science*, 338(6109), pp.960–963.

Spanò, S. & Galán, J.E., 2012. A Rab32-dependent pathway contributes to Salmonella typhi

host restriction. *Science*, 338(6109), pp.960–963.

Spanò, S., Liu, X. & Galán, J.E., 2011. Proteolytic targeting of Rab29 by an effector protein distinguishes the intracellular compartments of human-adapted and broad-host Salmonella. *Proceedings of the National Academy of Sciences of the United States of America*, 108(45), pp.18418–18423.

Stebbins, C.E. & Galán, J.E., 2001. Maintenance of an unfolded polypeptide by a cognate chaperone in bacterial type III secretion. *Nature*, 414(6859), pp.77–81.

Stecher, B. et al., 2007. Salmonella enterica serovar typhimurium exploits inflammation to compete with the intestinal microbiota. *PLoS Biology*, 5(10), pp.2177–2189.

Steele-Mortimer, O., 2008. The Salmonella-containing vacuole: moving with the times. *Current Opinion in Microbiology*, 11(1), pp.38–45.

Steele, A.D. et al., 2016. Challenges and Opportunities for Typhoid Fever Control: A Call for Coordinated Action. *Clinical Infectious Diseases*, 62(Suppl 1), pp.s4–s8.

Studier, F.W. & Moffatt, B.A., 1986. Use of bacteriophage T7 RNA polymerase to direct selective high-level expression of cloned genes. *Journal of Molecular Biology*, 189(1), pp.113–130.

Sun, H. et al., 2016. A Family of Salmonella Type III Secretion Effector Proteins Selectively Targets the NF-κB Signaling Pathway to Preserve Host Homeostasis. *PLoS Pathogens*, 12(3), p.e1005484.

Swatek, K.N. & Komander, D., 2016. Ubiquitin modifications. *Cell Research*, 26(4), pp.399–422.

Tacket, C.O. & Levine, M.M., 2007. CVD 908, CVD 908-htrA, and CVD 909 live oral typhoid vaccines: a logical progression. *Clinical Infectious Diseases*, 45 Suppl 1(Suppl 1), pp.S20–S23.

Takeuchi, T. et al., 2005. Link between the ubiquitin conjugation system and the ISG15 conjugation system: ISG15 conjugation to the UbcH6 ubiquitin E2 enzyme. *Journal of Biochemistry*, 138(6), pp.711–719.

Tatavarthy, A., Luna, V. a & Amuso, P.T., 2014. How multidrug resistance in typhoid fever affects treatment options. *Annals of the New York Academy of Sciences*, 1323, pp.1–15.

Tatham, M.H. et al., 2001. Polymeric chains of SUMO-2 and SUMO-3 are conjugated to protein substrates by SAE1/SAE2 and Ubc9. *The Journal of Biological Chemistry*, 276(38), pp.35368–74.

Teper, D. et al., 2016. Identification of novel Xanthomonas euvesicatoria type III effector proteins by a machine-learning approach. *Molecular Plant Pathology*, 17(3), pp.398–411.

Thiem, V.D. et al., 2011. The Vi conjugate typhoid vaccine is safe, elicits protective levels of IgG anti-Vi, and is compatible with routine infant vaccines. *Clinical and Vaccine Immunology*, 18(5), pp.730–5.

Thijs, I.M. V et al., 2007. Delineation of the Salmonella enterica serovar Typhimurium HilA regulon through genome-wide location and transcript analysis. *Journal of Bacteriology*, 189(13), pp.4587–4596.

Thomas, N.A. et al., 2012. Expanded roles for multicargo and class 1B effector chaperones in type III secretion. *Journal of Bacteriology*, 194(15), pp.3767–3773.

Thomas, S., Holland, I.B. & Schmitt, L., 2014. The Type 1 secretion pathway - The hemolysin system and beyond. *Biochimica et Biophysica Acta*, 1843(8), pp.1629–1641.

Thomson, N.R. et al., 2008. Comparative genome analysis of Salmonella Enteritidis PT4 and Salmonella Gallinarum 287/91 provides insights into evolutionary and host adaptation pathways. *Genome Research*, 18, pp.1624–1637.

Tobe, T. et al., 2006. An extensive repertoire of type III secretion effectors in Escherichia coli O157 and the role of lambdoid phages in their dissemination. *Proceedings of the National Academy of Sciences of the United States of America*, 103(40), pp.14941–14946.

Tran, T.H. et al., 2010. A randomised trial evaluating the safety and immunogenicity of the novel single oral dose typhoid vaccine M01ZH09 in healthy Vietnamese children. *PLoS ONE*, 5(7), p.e11778.

Tseng, T.-T., Tyler, B.M. & Setubal, J.C., 2009. Protein secretion systems in bacterial-host associations, and their description in the Gene Ontology. *BMC Microbiology*, 9(Suppl 1), p.S2.

Tsolis, R.M. et al., 1999. Identification of a putative Salmonella enterica serotype typhimurium host range factor with homology to IpaH and YopM by signature-tagged mutagenesis. *Infection and Immunity*, 67(12), pp.6385–93.

Tucker, C.L. et al., 2009. A genetic test for yeast two-hybrid bait competency using RanBPM. *Genetics*, 182(4), pp.1377–1379.

Tucker, S.C. & Galán, J.E., 2000. Complex Function for SicA , a Salmonella enterica Serovar Typhimurium Type III Secretion-Associated Chaperone Complex Function for SicA , a Salmonella enterica Serovar Typhimurium Type III Secretion-Associated Chaperone. *Journal of Bacteriology*, 182(8), pp.2262–2268.

Ubiquigent, 2013. E2 Scan Kit Version 2 User Protocol Manual.

Uchiya, K. et al., 1999. A Salmonella virulence protein that inhibits cellular trafficking. *The EMBO Journal*, 18(14), pp.3924–3933.

Velasquez, J.C. et al., 2016. SPI-9 of Salmonella enterica serovar typhi is constituted by an operon positively regulated by RpoS and contributes to adherence to epithelial cells in culture. *Microbiology*, 162(8), pp.1367–1378.

Virlogeux, I. et al., 1996. Characterization of the rcsA and rcsB genes from Salmonella typhi: RcsB through tviA is involved in regulation of Vi antigen synthesis. *Journal of Bacteriology*, 178(6), pp.1691–1698.

Virlogeux, I. et al., 1995. Role of the viaB locus in synthesis, transport and expression of Salmonella typhi Vi antigen. *Microbiology*, 141(12), pp.3039–3047.

Waddington, C.S. et al., 2014. An outpatient, ambulant-design, controlled human infection model using escalating doses of salmonella typhi challenge delivered in sodium bicarbonate solution. *Clinical Infectious Diseases*, 58(9), pp.1230–1240.

Wagner, S. et al., 2010. Organization and coordinated assembly of the type III secretion export apparatus. *Proceedings of the National Academy of Sciences of the United States of America*, 107(41), pp.17745–17750.

Wain, J. et al., 1997. Quinolone-resistant Salmonella typhi in Viet Nam: molecular basis of resistance and clinical response to treatment. *Clinical Infectious Diseases*, 25, pp.1404–1410.

Wain, J. et al., 2014. Typhoid fever. *The Lancet*, 6736, pp.1–10.

Wallden, K., Rivera-calzada, A. & Waksman, G., 2010. Type IV secretion systems: Versatility and diversity in function. *Cellular Microbiology*, 12(9), pp.1203–1212.

Wang, J.I.N.Y. et al., 2000. Constitutive Expression of the Vi Polysaccharide Capsular Antigen in Attenuated Salmonella enterica Serovar Typhi Oral Vaccine Strain CVD 909. *Infection and*

Immunity, 68(8), pp.4647–4652.

Wang, R.F. & Kushner, S.R., 1991. Construction of versatile low-copy-number vectors for cloning, sequencing and gene expression in Escherichia coli. *Gene*, 100, pp.195–199.

Wang, S. et al., 2014. A Role of Rab29 in the Integrity of the Trans-Golgi Network and Retrograde Trafficking of Mannose-6-Phosphate Receptor. *PLoS ONE*, 9(5), p.e96242.

Wangdi, T. et al., 2014. The Vi capsular polysaccharide enables Salmonella enterica serovar typhi to evade microbe-guided neutrophil chemotaxis. *PLoS Pathogens*, 10(8), p.e1004306.

Ward, C.L., Omura, S. & Kopito, R.R., 1995. Degradation of CFTR by the Ubiquitin-Proteasome Pathway. *Cell*, 83(1), pp.121–127.

Wasmuth, E. V & Lima, C.D., 2016. UniProt: the universal protein knowledgebase. *Nucleic Acids Research*, 45, pp.1–12.

Wasylnka, J.A. et al., 2008. Role for myosin II in regulating positioning of Salmonella-containing vacuoles and intracellular replication. *Infection and Immunity*, 76(6), pp.2722–2735.

Weidberg, H. et al., 2010. LC3 and GATE-16/GABARAP subfamilies are both essential yet act differently in autophagosome biogenesis. *The EMBO Journal*, 29, pp.1792–1802.

Weinstein, D.L. et al., 1998. Differential early interactions between Salmonella enterica serovar Typhi and two other pathogenic Salmonella serovars with intestinal epithelial cells. *Infection and Immunity*, 66(5), pp.2310–8.

Wenzel, D.M. et al., 2011. UBCH7 reactivity profile reveals parkin and HHARI to be RING/HECT hybrids. *Nature*, 474(7349), pp.105–8.

Wetter, M. et al., 2012. Molecular Characterization of the viaB Locus Encoding the Biosynthetic Machinery for Vi Capsule Formation in Salmonella Typhi. *PLoS ONE*, 7(9).

WHO, 2003. Background document : The diagnosis, treatment and prevention of typhoid fever. , pp.2–48. Available at: www.who.int/vaccines-documents/.

WHO, 2013. Immunization, Vaccines and Biologicals - Typhoid. Available at: http://www.who.int/immunization/diseases/typhoid/en/ [Accessed April 23, 2014].

WHO, 2008. Typhoid vaccines: WHO position paper. , 83(6), pp.49–59.

Wille, T. et al., 2014. SiiA and siib are novel type I secretion system subunits controlling SPI4-mediated adhesion of salmonella enterica. *Cellular Microbiology*, 16(2), pp.161–178.

Williams, S.G. et al., 1996. Vibrio cholerae Hcp , a secreted protein coregulated with HlyA . These include : Vibrio cholerae Hcp , a Secreted Protein Coregulated with HlyA. *Microbiology*, 64(1), pp.283–289.

Wilson, R.P. et al., 2008. The Vi-capsule prevents Toll-like receptor 4 recognition of Salmonella. *Cellular Microbiology*, 10(4), pp.876–90.

Wilson, R.P. et al., 2011. The Vi capsular polysaccharide prevents complement receptor 3-mediated clearance of Salmonella enterica serotype Typhi. *Infection and Immunity*, 79(2), pp.830–7.

Winter, S.E. et al., 2014. Salmonella enterica Serovar Typhi conceals the invasion-associated type three secretion system from the innate immune system by gene regulation. *PLoS Pathogens*, 10(7), p.e1004207.

Winter, S.E. et al., 2008. The Salmonella enterica serotype Typhi regulator TviA reduces interleukin-8 production in intestinal epithelial cells by repressing flagellin secretion. *Cellular*

Microbiology, 10(1), pp.247–261.

Winter, S.E. et al., 2009. The TviA auxiliary protein renders the Samonella enterica serotype Typhi RcsB regulon responsive to changes in osmolarity. *Molecular Microbiology*, 74(1), pp.175–193.

Wong, V.K. et al., 2016. An extended genotyping framework for Salmonella enterica serovar Typhi, the cause of human typhoid. *Nature Communications*, 7, p.12827.

Wong, V.K. et al., 2015. Phylogeographical analysis of the dominant multidrug-resistant H58 clade of Salmonella Typhi identifies inter- and intracontinental transmission events. *Nature Genetics*, 47, pp.632–639.

Wood, M.W. et al., 2000. The secreted effector protein of Salmonella dublin, SopA, is translocated into eukaryotic cells and influences the induction of enteritis. *Cellular Microbiology*, 2(4), pp.293–303.

Woodward, D.L., Khakhria, R. & Johnson, W.M., 1997. Human salmonellosis associated with exotic pets. *Journal of Clinical Microbiology*, 35(11), pp.2786–90.

Wu, B. et al., 2010. NleG Type 3 effectors from enterohaemorrhagic Escherichia coli are U-Box E3 ubiquitin ligases. *PLoS Pathogens*, 6(6), p.e1000960.

Xu, G., Paige, J. & Jaffrey, S., 2010. Global analysis of lysine ubiquitination by ubiquitin remnant immunoaffinty profiling. *Natural Biotechnology*, 28(8), pp.868–873.

Ye, Z. et al., 2007. Salmonella effector AvrA regulation of colonic epithelial cell inflammation by deubiquitination. *The American Journal of Pathology*, 171(3), pp.882–892.

Yu, X.J. et al., 2010. pH sensing by intracellular Salmonella induces effector translocation. *Science*, 328(5981), pp.1040–1043.

Zaki, S.A. & Karande, S., 2011. Multidrug-resistant typhoid fever: a review. *Journal of Infection in Developing Countries*, 5(5), pp.324–337.

Zeytuni, N. & Zarivach, R., 2012. Structural and Functional Discussion of the Tetra-Trico-Peptide Repeat, a Protein Interaction Module. *Structure*, 20(3), pp.397–405.

Zhang, S. et al., 2002. The Salmonella enterica serotype typhimurium effector proteins SipA, SopA, SopB, SopD, and SopE2 act in concert to induce diarrhea in calves. *Infection and Immunity*, 70(7), pp.3843–55.

Zhang, Y. et al., 2015. Bacterial protein AvrA stabilizes intestinal epithelial tight junctions via blockage of the C-Jun N-terminal kinase pathway. *Tissue Barriers*, 3(1–2), p.e972849.

Zhang, Y. et al., 2005. Recognition and ubiquitination of Salmonella type III effector SopA by a ubiquitin E3 ligase, HsRMA1. *The Journal of Biological Chemistry*, 280(46), pp.38682–8.

Zhang, Y. et al., 2006. The inflammation-associated Salmonella SopA is a HECT-like E3 ubiquitin ligase. *Molecular Microbiology*, 62(3), pp.786–93.

Zhao, C. et al., 2005. Human ISG15 conjugation targets both IFN-induced and constitutively expressed proteins functioning in diverse cellular pathways. *Proceedings of the National Academy of Sciences of the United States of America*, 102(29), pp.10200–5.

Zhou, D. et al., 2001. A Salmonella inositol polyphosphatase acts in conjunction with other bacterial effectors to promote host cell actin cytoskeleton rearrangements and bacterial internalization. *Molecular Microbiology*, 39, pp.248–259.

Zhou, D., Mooseker, M.S. & Galán, J.E., 1999. Role of the S. typhimurium actin-binding protein SipA in bacterial internalization. *Science*, 283, pp.2092–2095.

Zhou, L. & Pollard, A.J., 2010. A fast and highly sensitive blood culture PCR method for clinical detection of Salmonella enterica serovar Typhi. *Annals of Clinical Microbiology and Antimicrobials*, 9 (no pagi(14), pp.1–7. Available at: http://www.ann-clinmicrob.com/content/9/1/14%5Cnhttp://ovidsp.ovid.com/ovidweb.cgi?T=JS&CSC=Y&NEWS=N&PAGE=fulltext&D=emed9&AN=2010328919%5Cnhttp://wa4py6yj8t.search.serialssolutions.com/?url_ver=Z39.88-2004&rft_val_fmt=info:ofi/fmt:kev:mtx:journal&rfr_id=.

Zouhir, S. et al., 2014. The Structure of the SlrP-hTrx1 Complex Sheds Light on the Autoinhibition Mechanism of the Type III Secretion System Effectors of the NEL Family. *Biochemical Journal*, 464, pp.135–144.

Appendices

Appendix 1

Comparison of the T3SS effector protein repertoire of LT2 *S.* Typhimurium and the CT18 and Ty2 *S.* Typhi strains.

Effector Protein	Gene Locus			Function
	LT2 *S.* Typhimurium	CT18 *S.* Typhi	Ty2 *S.* Typhi	
				***SPI-1* T3SS**
SipA (SspA)	*STM2882*	*STY3005*	*t2784*	Actin-binding protein that promotes the entry of *Salmonellae* into host cells as well as stimulating bacterial replication with SifA and polymorphonuclear neutrophil migration (Zhou et al. 1999; Brawn et al. 2007; Hallstrom et al. 2015).
SipB (SspB)	*STM2885*	*STY3008*	*t2787*	Cholesterol-binding component of the *SPI-1* T3SS translocon that induces cell death in macrophages (Hayward et al. 2005; Hernandez et al. 2003).
SipC (SspC)	*STM2884*	*STY3007*	*t2786*	Actin-binding protein component of the *SPI-1* T3SS translocon that bundles and nucleates actin polymerisation promoting bacterial internalisation (Scherer et al. 2000; Myeni & Zhou 2010).
SipD (SspD)	*STM2883*	*STY3006*	*t2785*	Regulates translocation of SipA, SipB and SipC (Kaniga et al. 1995).
SopA	*STM2066*	*STY2275*	*t0808*	E3 ubiquitin-ligase involved in polymorphonuclear neutrophil migration and bacterial escape from the SCV (Zhang et al. 2005; Zhang et al. 2006).
SopB (SigD)	*STM1091*	*STY1121*	*t1828*	Inositol phosphatase that induces Cdc42-dependent actin rearrangement resulting in membrane ruffling and bacterial internalisation as well as beginning the formation of the SCV, inhibiting fusion with lysosomes and activating myosin (Zhou et al. 2001; Hernandez et al. 2004; Wasylnka et al. 2008).
SopE	A[1]	*STY4609*	*t4303*	Guanine nucleotide exchange factor for Cdc42 and Rac-1 involved in the formation of membrane ruffles for bacterial internalisation (Friebel et al. 2001).
SopE2	*STM1855*	*STY1987*	*t1023*	Guanine nucleotide exchange factor for Cdc42 involved in the formation of membrane ruffles for bacterial internalisation (Friebel et al. 2001).
SptP	*STM2878*	*STY3001*	*t2780*	GTPase-activating protein for Cdc42 and Rac-1 which results in the reformation of the host cell membrane after bacterial internalisation (Fu & Galán 1999).
StoC	A	*STY3092*	*t2863*	Unknown function.
				***SPI-2* T3SS**
GogA	*STM2614*	A	A	Protease that cleaves RelA and RelB to reduce NF-κB induction during infection (Sun et al. 2016).
GogB	*STM2584*	A	A	F-box-like protein that interacts with the host SCF E3 ubiquitin-ligase resulting in reduced NF-κB activation (Pilar et al. 2012).
PipA	*STM1087*	*STY1115*	*t1831*	Protease that cleaves RelA and RelB to reduce NF-κB induction during infection (Sun et al. 2016).
PipB	*STM1088*	*STY1117*	*t1830*	Localises to SCV and Sifs (Knodler et al. 2002).
PipB2	*STM2780*	*STY2897*	*t2674*	Recruits kinesin-1 to the SCV and is involved in the elongation of Sifs (Henry et al. 2006; Knodler & Steele-Mortimer 2005).

Effector Protein	Gene Locus			Function
	LT2 *S.* Typhimurium	CT18 *S.* Typhi	Ty2 *S.* Typhi	
SifA	*STM1224*	*STY1264*	*t1696*	Localises to SCV and Sifs, interacts with kinesin and directs Sif elongation required for *Salmonella* replication (Boucrot et al. 2005; Brumell et al. 2002).
SifB	*STM1602*	*STY1462*	*t1511*	Localises to SCV and is moved along Sifs away from the SCV (Freeman et al. 2003).
SopD2	*STM0972*	*STY0971*	*t1962*	Antagonist of Sif formation in regulating the stability of the SCV and membrane tubule formation and prevents Rab32 recruitment to the SCV (Schroeder et al. 2010; Spanò et al. 2016).
SpiC (SsaB)	*STM1393*	*STY1727*	*t1261*	Required for the secretion of the *SPI-2* T3SS translocon proteins SseB and SseC, and prevents fusion of the SCV with lysosomes (Freeman et al. 2002; Uchiya et al. 1999; Shotland et al. 2003).
SseF	*STM1404*	*STY1716*	*t1272*	Interacts with SseG and is required for the localisation of the SCV during infection (Deiwick et al. 2006).
SseG	*STM1405*	*STY1715*	*t1273*	Interacts with SseF and is required for the localisation of the SCV during infection, redirection of host vesicles towards the SCV (Deiwick et al. 2006; Kuhle et al. 2006).
SseI (SrfH)	*STM1051*	A	A	Inhibits migration of macrophages and dendritic cells and involved in long-term systemic infection of mice (McLaughlin et al. 2009).
SseJ	*STM1631*	*STY1439a*	*t1534*	Glycrophospholipid:cholesterol acetyl transferase that recruits SifA to the SCV and induces formation of Sifs (Figueira & Holden 2012; LaRock et al. 2015; Ohlson et al. 2008).
SseK1	*STM4157*	A	A	Glycosyltransferase of TRADD and FADD and inhibits TNFα-dependent NF-κB activation and necroptotic macrophage cell death (Li et al. 2013; Günster et al. 2017).
SseK2	*STM2137*	A	A	Glycosyltransferase which can inhibit TNFα-dependent NF-κB activation (Günster et al. 2017).
SseK3	A[2]	A	A	Glycosyltransferase of TRADD and inhibits TNFα-dependent NF-κB activation and necroptotic macrophage cell death (Günster et al. 2017).
SseL	*STM2287*	*STY2517*	*t0576*	Deubiquitinase involved in preventing the accumulation of ubiquitin chains, and therefore autophagy markers, around the SCV (Rytkönen et al. 2007; Mesquita et al. 2012).
SspH2	*STM2241*	*STY2467*	*t0623*	E3 ubiquitin-ligase that is involved in inhibiting the accumulation of actin around the SCV as well as ubiquitinating NOD1 resulting in increased IL-8 secretion (Miao et al. 2003; Bhavsar et al. 2013).
SteC	*STM1698*	*STY1353*	*t1612*	Kinase that phosphorylates host MAP kinases resulting in the accumulation of actin around the SCV (Odendall et al. 2012).
SteD	*STM2139*	*STY2367*	*t0718*	Causes depletion of MHC Class II at the cell surface and supresses T cell activation (Bayer-Santos et al. 2016).
SpvB	pSLT039	A	A	ADP-ribosyltransferase that causes actin depolymerisation and reduces actin deposition around the SCV (Lesnick et al. 2001).
SrgE	*STM1554*	*STY1509*	*t1468*	Unknown function (LaRock et al. 2015).
GtgA	A[3]	A	A	Protease that cleaves RelA and RelB to reduce NF-κB induction during infection (Sun et al. 2016).
CigR	*STM3762*	*STY4024*	*t3756*	Involved in replication within murine macrophages (Figueira et al. 2013).
SrfJ	*STM4426*	A	A	Glycoside hydrolase with unknown function (Cordero-Alba et al. 2012; Kim et al. 2009).
StoE	A	A	*t05880*	Unknown function.
Translocated by both *SPI-1* and *SPI-2* T3SS				
SopD	*STM2945*	*STY3073*	*t2846*	Involved in initial formation of the SCV along with SopB (Bakowski et al. 2007).

Effector Protein	Gene Locus			Function
	LT2 *S.* Typhimurium	CT18 *S.* Typhi	Ty2 *S.* Typhi	
SlrP	*STM0800*	*STY0833*	*t2087*	E3 ubiquitin-ligase that ubiquitinates thioredoxin resulting in cell death (Bernal-Bayard & Ramos-Morales 2009).
AvrA	*STM2865*	A	A	An effector with both deubiquitinase and acetyl transferase activities that regulates *Salmonella*-induced inflammation and maintenance of cellular tight junctions (Ye et al. 2007; Jones et al. 2008; Zhang et al. 2015).
SspH1	A[4]	A	A	E3 ubiquitin-ligase that ubiquitinates PKN1 resulting in abrogated neutrophil and macrophage activation. Also reduces the level of NF-κB-dependent gene expression (Keszei et al. 2014; Haraga & Miller 2003; Haraga & Miller 2006).
SteA	*STM1583*	*STY1482*	*t1493*	Binds to phosphatidylinositol 4-phosphate and localises to the SCV surface (Domingues et al. 2016).
SteB	*STM1629*	A	A	Unknown function (Figueira & Holden 2012).
SteE	*STM2585*	A	A	Unknown function (Figueira & Holden 2012).
StoA	A	*STY2021*	*t1875*	Unknown function.
StoB	*STM4312*[5]	*STY4512*	*t4218*	Unknown function.
StoD	A	*STY1076*	*t1865*	E3 ubiquitin-ligase with unknown function.
SpvC	*pSLT038*	A	A	Phosphothreonine lyase that inhibits pro-inflammatory cytokine expression (Haneda et al. 2012).
SpvD	*pSLT037*	A	A	Interacts with Xpo2 to prevent accumulation of p65 in the nucleus and therefore reduces NF-κB-dependent gene expression (Rolhion et al. 2016).
GtgE	*STM1055*	A	A	Protease involved in the degradation of Rab29 and Rab32, preventing their recruitment to the SCV and therefore allows *Salmonella* replication within murine macrophages (Spanò et al. 2011; Spanò & Galan 2012).

A; absent from chromosome, grey highlighting; pseudogene, 1; only present in ATCC14028 *S.* Typhimurium on Gifsy-3 prophage, 2; present on ST64B prophage, 3; absent in LT2 *S.* Typhimurium but present in strain ATCC 14028, 4; only present in ATCC 14028 *S.* Typhimurium strain and 5; not translocated by ATCC14028 *S.* Typhimurium. Table adapted from (Sabbagh et al. 2010; Niemann et al. 2011; Figueira & Holden 2012; LaRock et al. 2015) .

Appendix 2

Permission to republish the article: "The Type III Secretion System Effector SptP of *Salmonella enterica* Serovar Typhi" of which I was an author, along with the entire article.

Copyright Clearance Center

Confirmation Number: 11666622
Order Date: 08/29/2017

Customer Information

Customer: Alexander Byrne
Account Number: 3001189325
Organization: Alexander Byrne
Email: abyrne@live.co.uk
Phone: +44 7903215612
Payment Method: Invoice

This is not an invoice

Order Details

Journal of bacteriology : JB

Billing Status: N/A

Order detail ID: 70657963
ISSN: 1098-5530
Publication Type: e-Journal
Volume:
Issue:
Start page:
Publisher: AMERICAN SOCIETY FOR MICROBIOLOGY
Author/Editor: American Society for Microbiology

Permission Status: Granted
Permission type: Republish or display content
Type of use: Thesis/Dissertation
Order License Id: 4178370046940

Requestor type	Author of requested content
Format	Print, Electronic
Portion	chapter/article
Title or numeric reference of the portion(s)	Entire article
Title of the article or chapter the portion is from	The Type III Secretion System Effector SptP of Salmonella enterica Serovar Typhi.
Editor of portion(s)	N/A
Author of portion(s)	Johnson R, Byrne A, Berger CN, Klemm E, Crepin VF, Dougan G, Frankel G.
Volume of serial or monograph	199
Issue, if republishing an article from a serial	4
Page range of portion	
Publication date of portion	Jan 30 2017
Rights for	Main product
Duration of use	Current edition and up to 5 years
Creation of copies for the disabled	no
With minor editing privileges	no
For distribution to	Worldwide

In the following language(s)	Original language of publication
With incidental promotional use	no
Lifetime unit quantity of new product	Up to 499
Made available in the following markets	Open access
The requesting person/organization	Alexander Byrne
Order reference number	
Author/Editor	Alexander Byrne
The standard identifier of New Work	thesis
Title of New Work	Identification and Characterisation of Novel T3SS Effector Proteins of Salmonella enterica serovar Typhi
Publisher of New Work	Imperial College London
Expected publication date	Aug 2017
Estimated size (pages)	236

Note: This item was invoiced separately through our RightsLink service. More info $ 0.00

Total order items: 1 Order Total: $0.00

About Us | Privacy Policy | Terms & Conditions | Pay an Invoice

Copyright 2017 Copyright Clearance Center

AMERICAN SOCIETY FOR MICROBIOLOGY | Journal of Bacteriology®

RESEARCH ARTICLE

The Type III Secretion System Effector SptP of *Salmonella enterica* Serovar Typhi

Rebecca Johnson,[a] Alexander Byrne,[a] Cedric N. Berger,[a] Elizabeth Klemm,[b] Valerie F. Crepin,[a] Gordon Dougan,[b] Gad Frankel[a]

MRC Centre for Molecular Bacteriology and Infection, Department of Life Sciences, Imperial College London, London, United Kingdom[a]; Wellcome Trust Sanger Institute, Wellcome Trust Genome Campus, Hinxton, Cambridge, United Kingdom[b]

ABSTRACT Strains of the various *Salmonella enterica* serovars cause gastroenteritis or typhoid fever in humans, with virulence depending on the action of two type III secretion systems (*Salmonella* pathogenicity island 1 [SPI-1] and SPI-2). SptP is a *Salmonella* SPI-1 effector, involved in mediating recovery of the host cytoskeleton postinfection. SptP requires a chaperone, SicP, for stability and secretion. SptP has 94% identity between *S. enterica* serovar Typhimurium and *S.* Typhi; direct comparison of the protein sequences revealed that *S.* Typhi SptP has numerous amino acid changes within its chaperone-binding domain. Subsequent comparison of *sptP S.* Typhi and *S.* Typhimurium strains demonstrated that, unlike SptP in *S.* Typhimurium, SptP in *S.* Typhi was not involved in invasion or cytoskeletal recovery postinfection. Investigation of whether the observed amino acid changes within SptP of *S.* Typhi affected its function revealed that *S.* Typhi SptP was unable to complement *S.* Typhimurium *sptP* due to an absence of secretion. We further demonstrated that while *S.* Typhimurium SptP is stable intracellularly within *S.* Typhi, *S.* Typhi SptP is unsta-ble, although stability could be recovered following replacement of the chaperone-binding domain with that of *S.* Typhimurium. Direct assessment of the strength of the interaction between SptP and SicP of both serovars via bacterial two-hybrid analysis demonstrated that *S.* Typhi SptP has a significantly weaker interaction with SicP than the equivalent proteins in *S.* Typhimurium. Taken together, our results suggest that changes within the chaperone-binding domain of SptP in *S.* Typhi hin-der binding to its chaperone, resulting in instability, preventing translocation, and therefore restricting the intracellular activity of this effector.

IMPORTANCE Studies investigating *Salmonella* pathogenesis typically rely on *Salmo-nella* Typhimurium, even though *Salmonella* Typhi causes the more severe disease in humans. As such, an understanding of *S.* Typhi pathogenesis is lacking. Differences within the type III secretion system effector SptP between typhoidal and nontyphoi-dal serovars led us to characterize this effector within *S.* Typhi. Our results suggest that SptP is not translocated from typhoidal serovars, even though the loss of *sptP* results in virulence defects in *S.* Typhimurium. Although SptP is just one effector, our results exemplify that the behavior of these serovars is significantly different and genes identified to be important for *S.* Typhimurium virulence may not translate to *S.* Typhi.

KEYWORDS *Salmonella enterica* serovar Typhi, SptP, type III secretion system

Received 30 August 2016
Accepted 19 November 2016
Accepted manuscript posted online 5 December 2016
Citation Johnson R, Byrne A, Berger CN, Klemm E, Crepin VF, Dougan G, Frankel G. 2017. The type III secretion system effector SptP of *Salmonella enterica* serovar Typhi. J Bacteriol 199:e00647-16. https://doi.org/10.1128/ JB.00647-16.
Editor Thomas J. Silhavy, Princeton University

Copyright © 2017 Johnson et al. This is an open-access article distributed under the terms of the Creative Commons Attribution 4.0 International license.

Address correspondence to Gad Frankel, g.frankel@imperial.ac.uk.

Downloaded from http://jb.asm.org/ on August 29, 2017 by guest

Salmonella species are diverse Gram-negative intracellular pathogens responsible for a range of diseases resulting in significant morbidity and mortality among both animals and humans worldwide (1). In humans, the outcome of infection with *Salmonella* primarily depends on the infecting serovar; while nontyphoidal serovars, such as

Salmonella enterica serovar Typhimurium, typically cause self-limiting gastroenteritis, typhoidal serovars, such as *Salmonella enterica* serovar Typhi and *Salmonella enterica* serovar Paratyphi, result in the invasive systemic disease typhoid fever (1).

Central to *Salmonella* virulence is the action of two type III secretion systems (T3SS), encoded on *Salmonella* pathogenicity island 1 (SPI-1) and SPI-2, which secrete over 40 effectors to subvert host cell processes during infection (2–4). The SPI-1 T3SS is active when *Salmonella* is extracellular, where it functions to permit the invasion of nonphagocytic host cells (4), while the SPI-2 T3SS is activated upon internalization, where it functions to create a stable and permissive intracellular niche, termed the *Salmonella*-containing vacuole (SCV) (3, 4).

Although *S*. Typhi causes a more serious disease in humans, *S*. Typhimurium is often used as the model for understanding *Salmonella* pathogenesis, owing to biosafety concerns and, most importantly, the availability of viable *in vivo* models, since *S*. Typhi and other typhoidal serovars are strictly restricted to humans (5). Despite the wide-spread acceptance of *S*. Typhimurium as the *Salmonella* model organism, significant genomic differences exist between *S*. Typhimurium and *S*. Typhi. Comparison of *S*. Typhimurium strain LT2 to *S*. Typhi reference strain CT18 revealed that 89% of genes were shared; approximately 480 genes were unique to LT2 and approximately 600 genes were unique to CT18 (6). Significant variations in prophage, pathogenicity island, and plasmid elements were observed between the two serovars (6).

Importantly, many known SPI-1 and SPI-2 T3SS effectors are absent or pseudogenes in *S*. Typhi, and this may be associated with genome degradation linked with host restriction (6) and could contribute to the differences in pathogenicity observed between typhoidal and nontyphoidal serovars. A notable example is the *S*. Typhimu-rium effector GtgE, which is absent in *S*. Typhi (6); the introduction of GtgE into *S*. Typhi permits its growth in nonpermissive mouse cells, strongly linking the absence of this effector to typhoidal host restriction (7). Another example which highlights the limita-tions of using *S*. Typhimurium to investigate *Salmonella* pathogenesis is the fact that the *Salmonella* virulence plasmid (pSLT), encoding the effectors SpvB and SpvC, is required for full *S*. Typhimurium virulence in mice (8) but absent in *S*. Typhi and other typhoidal serovars (5, 9). Additional effectors that are either absent or pseudogenes in *S*. Typhi (CT18) include SopA, CigR, SopE2, SlrP, SseJ, SopD2, AvrA, SteB, GogB, SseI/SrfH, SseK1, SseK2, SseK3, and SspH1 (6, 10). Other effectors appear to be differentially evolved between human-restricted and generalist serovars, including SipD, SseC, SseD, SseF, SifA, and SptP (11), which could reflect functional differences. Further evidence of the degradation of the T3SS effector repertoire has been reported within the highly successful and globally dominant *S*. Typhi haplotype 58 (H58), which, owing to a premature stop codon at position 185, lacks both the GTPase-activating phosphatase (GAP) and tyrosine phosphatase domains of SptP and therefore lacks a functional copy of this effector (12).

SptP is an SPI-1 effector encoded within the SPI-1 pathogenicity island immediately downstream of its chaperone, SicP (13). Like other effectors, SptP requires its chaperone for stability within the bacterial cytosol and to direct secretion (13, 14). SptP is a modular protein consisting of three distinct domains: a chaperone-binding domain, a GAP domain, and a tyrosine phosphatase domain. SptP is best characterized in its role as a GTPase-activating protein, acting antagonistically to another SPI-1 effector, SopE/ SopE2, a guanine nucleotide exchange factor (GEF) which manipulates the host cyto-skeleton to permit membrane ruffle formation and *Salmonella* internalization (2, 15). SptP deactivates the Rho GTPases Rac1 and Cdc42 to reverse cytoskeletal changes and return the host membrane to a steady-state condition (16). Importantly, extended activation of Rho GTPases by SopE can be sensed by host cells by NOD1, resulting in NF-*k*B activation and proinflammatory signaling (17); antagonism of SopE by SptP therefore represents an important mechanism to prevent the activation of host im-mune defenses. SptP has also been reported to directly inhibit the activation of the mitogen-activated protein kinase pathway and subsequently downregulate tumor necrosis factor alpha secretion from infected J774A.1 macrophages (18). The less well

Downloaded from http://jb.asm.org/ on August 29, 2017 by guest

characterized tyrosine phosphatase domain of SptP has been shown to be involved in SCV biogenesis and bacterial replication up to 8 h postinfection (19). SptP is also important for virulence *in vivo*, as a *sptP S*. Typhimurium SL1344 strain demonstrates attenuated virulence in BALB/c mice (20) and disruption of *sptP* in *S*. Typhimurium ST4/74 also results in reduced intestinal colonization of chicks, pigs, and cattle (21).

Most of the characterization of SptP has been performed with *S*. Typhimurium (16, 22–24), with the underlying assumption being that *S*. Typhi behaves similarly. The phenotypes attributed to SptP in *S*. Typhimurium, in particular, the virulence defects reported during *in vivo* infection, would seemingly contradict the global success of H58 *S*. Typhi strains, which lack a functional copy of SptP (12). This suggests that the function of this effector in *S*. Typhi may be different from that reported in *S*. Typhimu-rium.

RESULTS

Comparison of SptP from different serovars. SptP is relatively conserved between *S*. Typhimurium and *S*. Typhi, sharing 94% amino acid sequence identity between the two serovars. Alignment of the amino acid sequences of SptP from *S*. Typhi Ty2 and SptP from *S*. Typhimurium 14028 revealed that a large number of amino acid changes (10/31) are concentrated within the chaperone-binding domain of SptP (residues 35 to 139 [25]) (Fig. 1A), despite SicP being highly conserved between serovars (97% identity). Direct comparison of the chaperone-binding domains of SptP from various *Salmonella* serovars shows that these amino acid changes are conserved between *S*. Typhi and *S*. Paratyphi A and that these amino acids are distinct from those in nontyphoidal serovars, including *S*. Typhimurium, *S*. Enteritidis, and *S*. Choleraesuis (Fig. 1B).

Further differences between *sptP* of *S*. Typhimurium and *S*. Typhi can be found outside the protein-coding sequence. It has previously been demonstrated in *S*. Typhimurium that efficient translation of SptP following transcription from its endogenous locus depends on disruption of a stem-loop approximately 20 nucleotides upstream of the start codon of SptP, which is mediated by the upstream translation of SicP (23). Elongation of this stem-loop by just 3 nucleotides decreases the level of translation of SptP by approximately 80% (23). Comparison of the predicted RNA structure (by use of the Mfold server) (26) of this region between the two serovars reveals that *S*. Typhi possesses an elongated stem-loop structure relative to the sequence of *S*. Typhimurium (40 bp and 27 bp, respectively) (Fig. 1C), suggesting that the expression of SptP at the level of translation may differ between the two serovars. Given these differences, we investigated if SptP in *S*. Typhi has the same functions reported during *S*. Typhimurium infection.

The role of SptP in *Salmonella* invasion and cytoskeletal recovery. In *S*. Typhimurium, the loss of *sptP* abolishes the ability of infected cells to recover the host cytoskeleton, with cells displaying extended actin disruption up to 3 h postinfection; conversely, cells infected with wild-type (WT) *S*. Typhimurium regain a normal cytoskeletal structure as soon as 80 min postinfection (16). To assess if the same phenotype was seen during *S*. Typhi infection, we compared the ability of HeLa cells to regain a normal actin cytoskeleton following infection with WT and *sptP S*. Typhi strains. The equivalent *S*. Typhimurium strains were used as controls.

During epithelial cell infection, both *S*. Typhimurium and *S*. Typhi manipulate the host cytoskeleton, with membrane ruffles associated with invasion events clearly being visible at 15 min postinfection (Fig. 2A). By 2 h, cells infected with WT *Salmonella* display an actin architecture similar to that seen for uninfected cells, visible as the formation of stress fibers (Fig. 2A). In line with previous findings (16), cells infected with *S*. Typhi-murium *sptP* did not demonstrate cytoskeletal recovery and continued to exhibit membrane ruffling and an absence of stress fibers. In contrast, cells infected with *S*. Typhi *sptP* displayed a recovered cytoskeleton at 2 h postinfection. To quantify this phenotype, we determined the proportion of infected cells displaying an actin architecture akin to that of uninfected cells at 2 h postinfection. While 76% of cells infected with WT *S*. Typhimurium (*n* 309) demonstrated cytoskeletal recovery, only 27% of

Downloaded from http://jb.asm.org/ on August 29, 2017 by guest

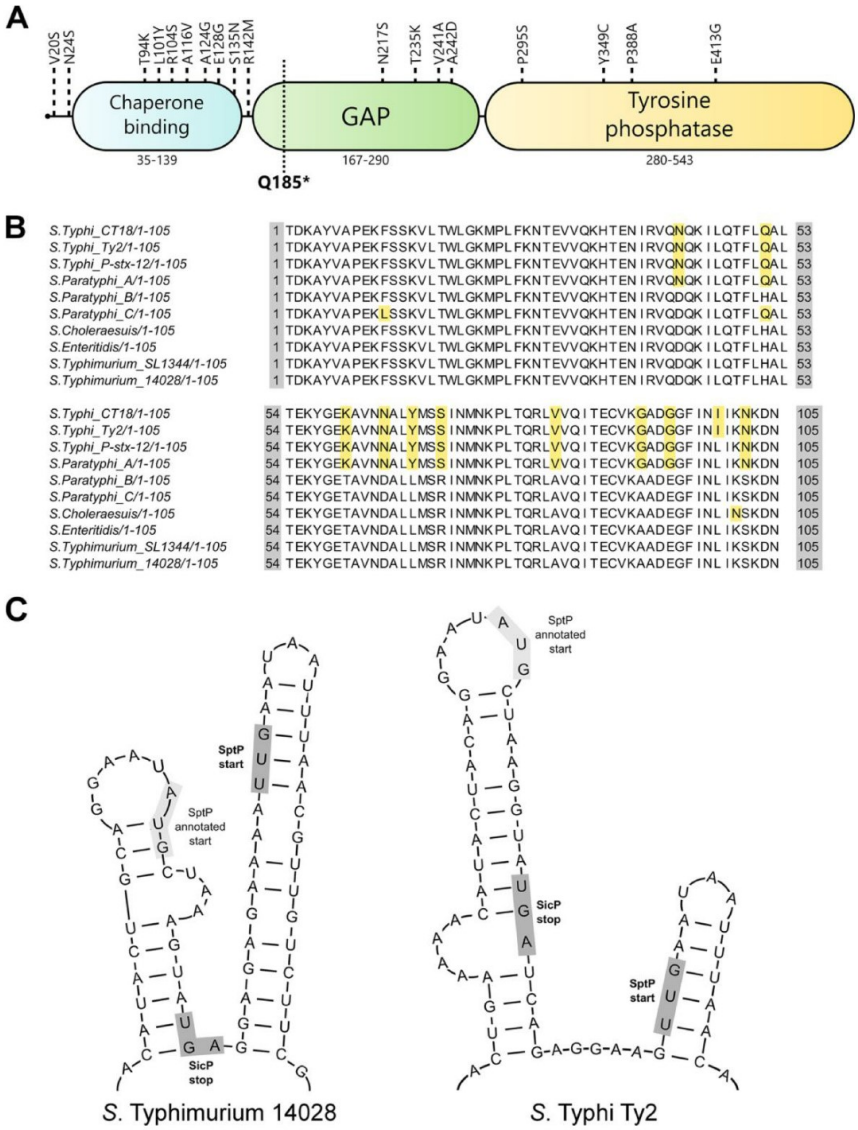


FIG 1 SptP of *Salmonella* Typhi. (A) Schematic of SptP showing amino acid changes (weakly similar or dissimilar amino acids) between *S.* Typhimurium 14028 and *S.* Typhi Ty2. The location of the single nucleotide polymorphism (Q185*) which generates a premature stop codon in H58 isolates is also shown. (B) Alignment of the sequence of the chaperone-binding domain (positions 35 to 139) of SptP from various *Salmonella* serovars. Nonconserved amino acids are highlighted. (C) Comparison of the mRNA structures upstream of the start codon of SptP present in *S.* Typhimurium and *S.* Typhi, predicted by use of the Mfold server. Both the annotated ATG (AUG) start codon and the proposed TTG (UUG) start codon of SptP are highlighted.

cells infected with *S.* Typhimurium *sptP* (*n* 315) demonstrated a recovered actin cytoskeleton. In comparison, 70% of cells infected with either WT *S.* Typhi (*n* 294) or *S.* Typhi *sptP* (*n* 301) exhibited cytoskeletal recovery (Fig. 2B).

Although SptP has not previously been linked with invasion in *S.* Typhimurium (20, 27), SptP, via its antagonism of SopE, should directly govern the size and duration of membrane ruffling and therefore influence the efficiency of invasion. As such, we

Downloaded from http://jb.asm.org/ on August 29, 2017 by guest

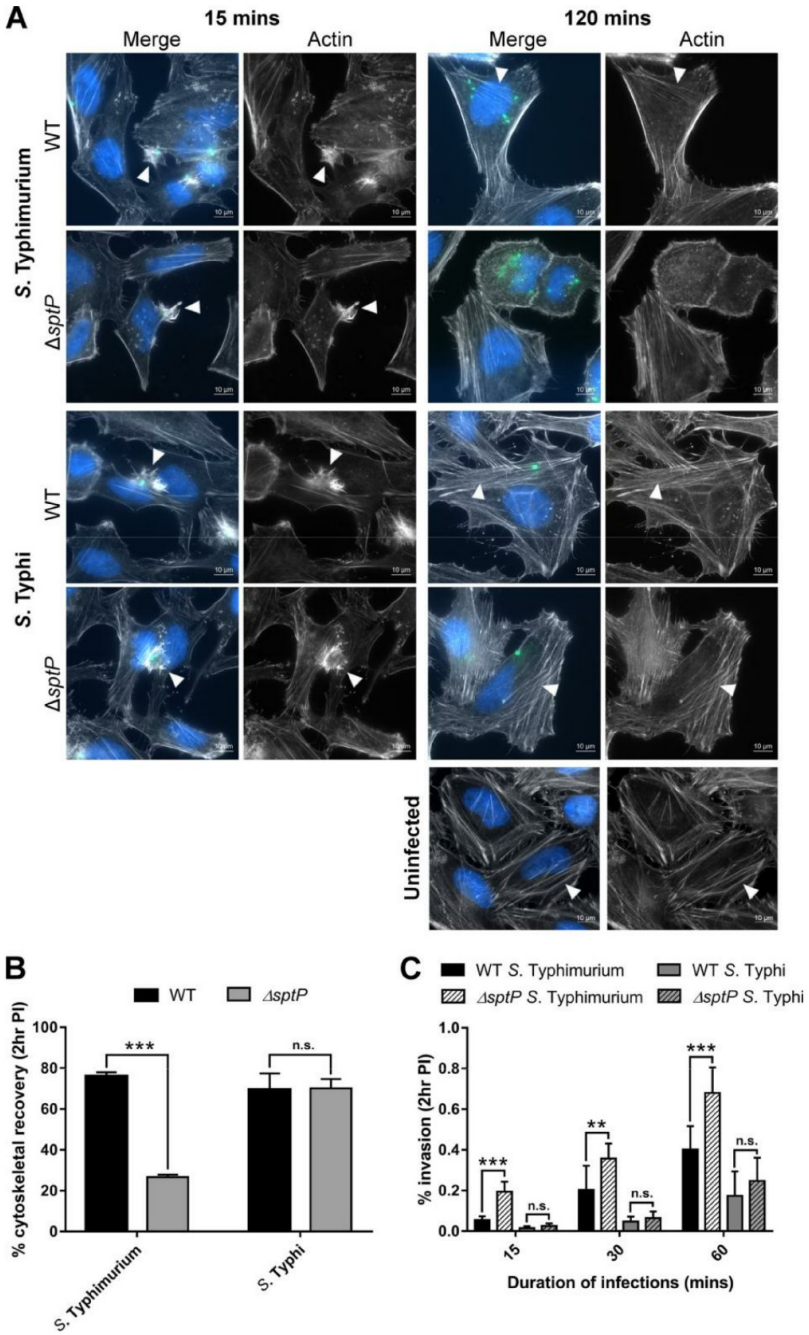


FIG 2 Role of SptP in invasion and cytoskeletal recovery following exponential growth. *Salmonella* strains, grown aerobically to late exponential phase, were used to infect HeLa cells at an MOI of 100. (A) Representative images of HeLa cells infected with WT or *sptP* S. Typhimurium or *S.* Typhi at 15 min and 2 h postinfection. Actin was stained with phalloidin (white), bacteria were stained with the CSA-1 antibody (green), and nuclei were stained with Hoechst (blue). Arrowheads, invasion-associated membrane ruffles (15 min) or stress fibers (120 min). (B) HeLa cells infected with *Salmonella* strains were fixed at 2 h postinfection (PI) and stained with phalloidin to determine the

(Continued on next page)

Downloaded from http://jb.asm.org/ on August 29, 2017 by guest

compared the levels of invasion of WT and *sptP S.* Typhimurium and *S.* Typhi strains into HeLa cells. While deletion of *sptP* from *S.* Typhimurium resulted in a significantly increased level of invasion relative to that of the WT strain, deletion of *sptP* from *S.* Typhi did not affect the invasion efficiency (Fig. 2C). Increasing the length of time that *Salmonella* was incubated with host cells improved the invasion efficiency of all strains but did not alter the trends observed (Fig. 2C). SPI-1-deficient *S.* Typhimurium (Δ*prgH*) and *S.* Typhi (Δ*invA*) strains, used as controls, failed to invade HeLa cells, as expected (see Fig. S1 in the supplemental material).

Growth under different SPI-1-inducing conditions influences SopE activity in *S.* Typhi. A recent study comparing *S.* Paratyphi A and *S.* Typhimurium following growth under different SPI-1-inducing conditions demonstrated that *S.* Paratyphi was signifi-cantly less invasive, had reduced levels of SPI-1 expression, and had reduced levels of SptP and SopE2 following aerobic growth to late exponential phase compared to the results obtained by microaerobic growth to stationary phase (28). Since our initial comparisons between WT and *sptP Salmonella* strains were performed following aerobic exponential growth (Fig. 2), we were interested in whether SopE, the guanine exchange factor which SptP antagonizes (16), was active during *S.* Typhi infection after growth under these conditions.

To determine if environmental conditions impact SopE activity, we assessed the invasiveness of WT or *sopE S.* Typhi and *S.* Typhimurium strains following aerobic growth to late exponential phase or microaerobic growth to stationary phase. Since *S.* Typhimurium 14028 expresses SopE2 but lacks SopE (29), while *S.* Typhi Ty2 expresses SopE but not SopE2 (6, 30), we instead used the *S.* Typhimurium strain SL1344, which has both SopE and SopE2 (31), for the comparisons in order to account for any differences in activity or regulation between SopE and SopE2 (31). Following growth to late exponential phase, deletion of *sopE* in *S.* Typhi resulted in a modest decrease in the rate of invasion into HeLa cells, with a relative invasion rate of 84.4% of that of the WT (Fig. 3A). When grown to stationary phase, however, invasion of the *S.* Typhi *sopE* strain was significantly attenuated (0.002% invasion efficiency, with a relative invasion rate of 0.5% of that of the WT) (Fig. 3A). A *invA S.* Typhi strain was unable to invade HeLa cells following growth to either exponential phase or stationary phase, demon-strating that invasion under both conditions is SPI-1 dependent (Fig. S1). In contrast, *S.* Typhimurium SL1344 did not demonstrate this marked phenotypic difference between growth conditions, as the *sopE* (Fig. 3B) and *sopE sopE2* (Fig. 3C) strains demon-strated similar reductions in the rates of invasion following growth to either late exponential or stationary phase.

Since these results suggest that SopE is nonessential for *S.* Typhi invasion following aerobic subculture to late exponential phase, it follows that SptP would also be dispensable, potentially explaining the lack of phenotypes previously observed for *S.* Typhi *sptP* compared to *S.* Typhimurium *sptP* (Fig. 2). The role of SptP in invasion and cytoskeletal recovery postinfection was therefore reassessed as before, but with strains instead being grown under microaerobic conditions to stationary phase. While signif-icant differences in invasion and cytoskeletal recovery were observed between the WT and *sptP S.* Typhimurium strains, no significant differences between the WT and *sptP S.* Typhi strains were observed (Fig. 4).

Complementation of *S.* Typhimurium *sptP* with S. Typhi *sptP*. Since the loss of SptP does not result in phenotypes during *S.* Typhi infection the same as those observed during *S.* Typhimurium infection, it suggests that functional differences exist

FIG 2 Legend (Continued)
proportion of infected cells displaying a normal actin cytoskeleton. At least 100 infected cells were counted per strain and per biological repeat. Error bars show SDs (*n* 3). The levels of cytoskeletal recovery of WT and *sptP* strains were compared by *t* test (***, *P* 0.001; n.s., no significant difference). (C) HeLa cells were infected with WT or *sptP S.* Typhimurium 14028 or *S.* Typhi Ty2 for 15, 30, or 60 min. The percentage of intracellular bacteria at 2 h postinfection relative to the number of bacteria added in the inoculum is shown. Error bars show SDs (*n* 3). The invasion rates of the strains were compared by *t* test (**, *P* 0.01; ***, *P* 0.001).

Downloaded from http://jb.asm.org/ on August 29, 2017 by guest

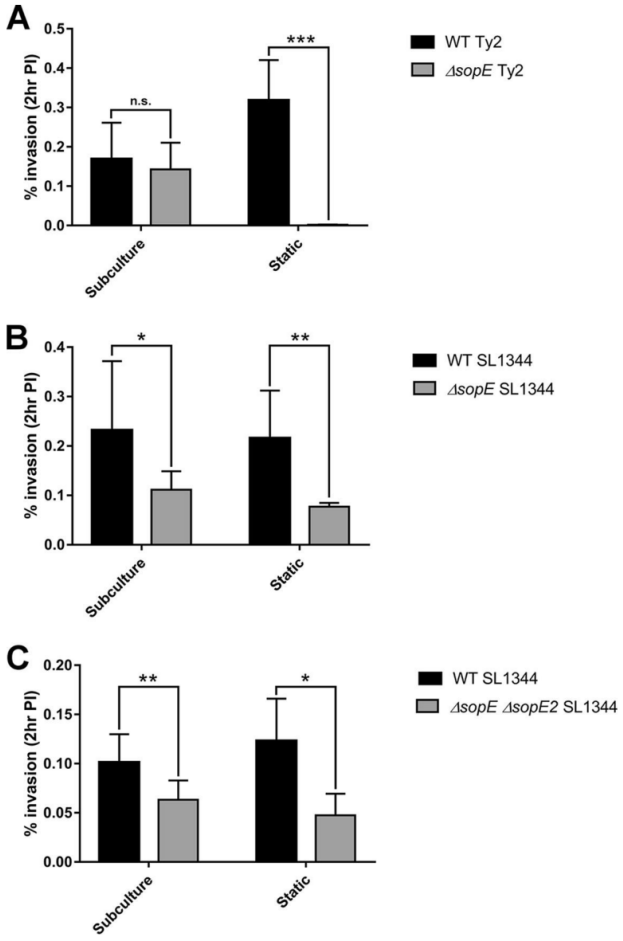


FIG 3 Growth conditions alter the dependency on SopE for invasion in *S*. Typhi. *Salmonella* strains were grown either aerobically to late exponential phase (subculture) or to stationary phase under microaero-bic conditions (static overnight culture) and added to HeLa cells at an MOI of 100. Cells were infected for 1 h with WT and *sopE S*. Typhi (A) and 15 min for WT, *sopE*, and *sopE sopE2 S*. Typhimurium SL1344 (B and C). The percentage of intracellular bacteria at 2 h postinfection relative to the number of bacteria added in the inoculum is shown. Error bars show SDs (*n* 3). The invasion rates of the strains were compared by *t* test (*, *P* 0.05; **, *P* 0.01; ***, *P* 0.001; n.s., no significant difference).

between the SptP proteins from these serovars. SptP was one of several *Salmonella* T3SS proteins identified as being differentially evolved between typhoidal and nonty-phoidal serovars (11). We therefore investigated if expression of *S*. Typhi SptP would be able to cross complement *S*. Typhimurium *sptP*. As shown above (Fig. 2 and 4), deletion of *sptP* from *S*. Typhimurium results in a significant increase in the level of invasion of HeLa cells. While complementation with *S*. Typhimurium *sptP* restored the level of invasion back to WT levels, *S*. Typhimurium *sptP* expressing *sptP* from *S*. Typhi

was as invasive as both the *sptP* strain and the *sptP* strain carrying the empty pWSK29 vector (Fig. 5). Furthermore, a *sptP S*. Typhimurium strain expressing the truncated SptP present within H58 strains was as invasive as the strain expressing Ty2 SptP (Fig. 5).

The inability of *S*. Typhi SptP to complement *S*. Typhimurium *sptP* could be due to either the amino acid changes within the GAP and tyrosine phosphatase domains

Downloaded from http://jb.asm.org/ on August 29, 2017 by guest

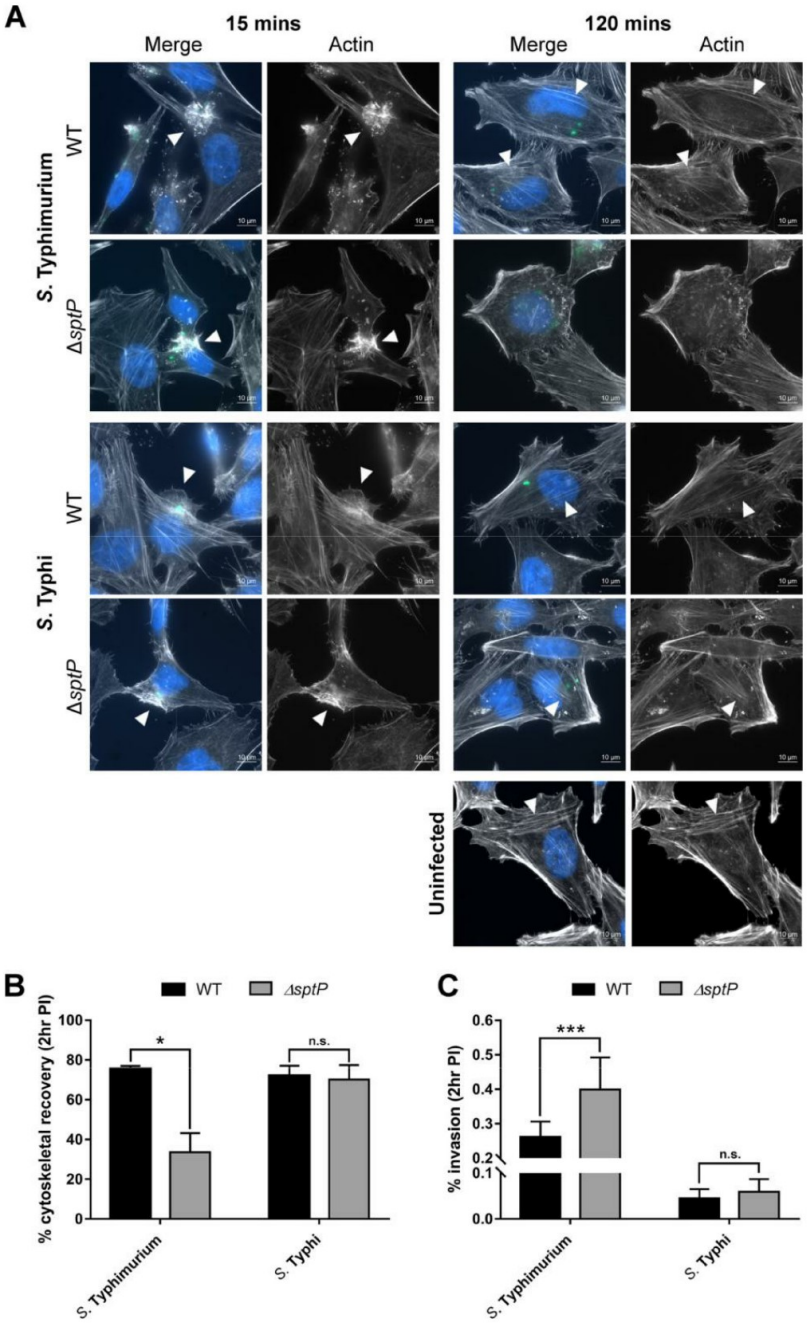


FIG 4 Role of SptP in invasion and cytoskeletal recovery following growth to stationary phase. *Salmonella* strains, grown under microaerobic conditions to stationary phase, were used to infect HeLa cells at an MOI of 100. (A) Representative images of HeLa cells infected with WT *or sptP S.* Typhimurium 14028 or *S.* Typhi Ty2 at 15 min and 2 h postinfection. Actin was stained with phalloidin (white), bacteria were stained with the CSA-1 antibody (green), and nuclei were stained with Hoechst (blue). Arrowheads, invasion-associated membrane ruffles (15 min) or stress fibers (120 min). (B) HeLa cells infected with *Salmonella* strains were fixed at 2 h postinfection and stained with phalloidin to determine the proportion of infected cells displaying a normal actin cytoskeleton. At least 100

(Continued on next page)

Downloaded from http://jb.asm.org/ on August 29, 2017 by guest

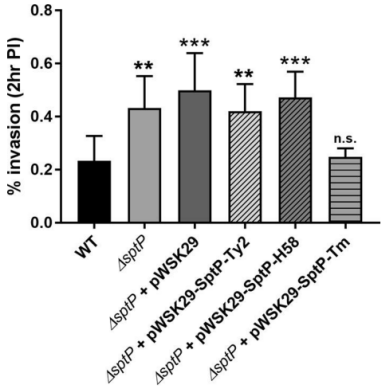


FIG 5 Expression of *S*. Typhi SptP fails to complement the deletion in *S*. Typhimurium. WT and *sptP S*. Typhimurium strains complemented with either empty pWSK29-Spec or plasmids expressing *S*. Typhimurium (Tm) or *S*. Typhi Ty2 SptP from a constitutive promoter were grown aerobically to late exponential phase and added to HeLa cells at an MOI of 100. Strains were left to infect the cells for 15 min, and the number of intracellular bacteria was determined at 2 h postinfection. The percentage of intracellular bacteria relative to the number of bacteria added in the inoculum is shown. Error bars show SDs (*n* 3). The invasion rates of the strains were compared to the rate for the WT by one-way ANOVA, followed by Tukey's *post hoc* test (**, *P* 0.01; ***, *P* 0.001; n.s., no significant difference).

rendering it functionally inactive or the numerous substitutions within the chaperone-binding region compromising the ability of *S*. Typhi SptP to bind the SicP chaperone, therefore destabilizing SptP intracellularly and preventing its secretion by the SPI-1 T3SS (13, 14) (Fig. 1). We tested these two possibilities by performing an SPI-1 secretion assay with hemagglutinin (HA)-tagged SptP expressed in *S*. Typhimurium. While SptP from both *S*. Typhimurium and *S*. Typhi was detected intracellularly in WT *S*. Typhimu-rium, *S*. Typhi SptP was observed at lower levels and only *S*. Typhimurium SptP was detected in culture supernatants, with secretion being dependent on the presence of a functional SPI-1 T3SS (Fig. 6). Similar levels of the SPI-1 translocon component SipD were secreted by the WT strains, suggesting that the lack of *S*. Typhi SptP secretion relates specifically to differences between the two SptP variants, likely from changes within the chaperone-binding domain.

The chaperone-binding domain of SptP is essential for stability. Although SicP is highly similar between *S*. Typhimurium and *S*. Typhi (97% identity), the inability of *S*. Typhi SptP to function within *S*. Typhimurium might reflect its inability to efficiently bind *S*. Typhimurium SicP, rather than indicating a general inability to bind its chap-erone. As SicP binding of SptP also prevents the degradation of SptP within the bacterial cytosol prior to secretion (13), the ability of SptP to bind SicP can be assessed by detecting the total levels of HA-tagged *S*. Typhi and *S*. Typhimurium SptP in an *S*. Typhi SPI-1 mutant background (Δ*invA*), where secretion of effectors is prevented. Two constructs were used to assess SptP stability for both *S*. Typhimurium and *S*. Typhi SptP: one constitutively expressing SptP from the T3 promoter of pWSK29 and one express-ing SptP from the endogenous promoter of each serovar, taken to be 700 bp upstream from the SptP start codon, on the basis of the predicted transcriptional start site from *S*. Typhimurium transcriptome sequencing data (32). While the T3 promoter accounts for any regulatory differences between *S*. Typhi and *S*. Typhimurium, expression from

FIG 4 Legend (Continued)
infected cells were counted per strain and per biological repeat. Error bars show SDs (*n* 3). The levels of cytoskeletal recovery of WT and *sptP* strains were compared by *t* test (*, *P* 0.05; n.s., no significant difference).
(C) HeLa cells were infected with WT *or sptP S*. Typhimurium 14028 or *S*. Typhi Ty2 for 30 min. The percentage of intracellular bacteria at 2 h postinfection relative to the number of bacteria added in the inoculum is shown. Error bars show SDs (*n* 3). The invasion rates of the strains were compared by *t* test (***, *P* 0.001).

Downloaded from http://jb.asm.org/ on August 29, 2017 by guest

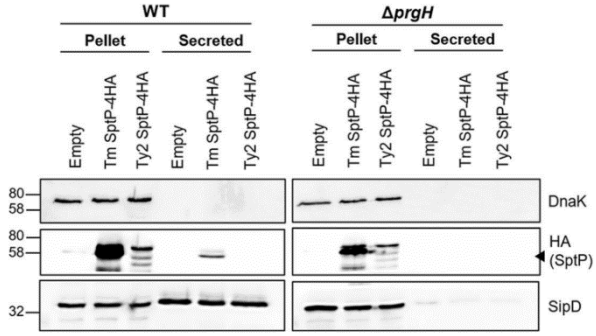


FIG 6 *S.* Typhimurium cannot secrete S. Typhi SptP. WT and SPI-1 mutant *S.* Typhimurium (Δ*prgH*) strains expressing C-terminally 4HA-tagged SptP were grown to late exponential phase. The presence of S. Typhi Ty2 or *S.* Typhimurium (Tm) SptP in bacterial pellets and the supernatant was detected using an anti-HA antibody; the cytoplasmic protein DnaK was used to control for bacterial lysis, and the SPI-1 translocon component SipD was used as a positive control for SPI-1 secretion. A representative blot of three independent repeats is shown. The numbers on the left are molecular masses (in kilodaltons). Arrowhead, the band which corresponds to SptP.

the endogenous promoter, which also encodes SicP, ensures the correct coregulation of SicP and SptP at both the transcriptional and translational levels (23).

S. Typhi SptP-4HA was not detectable within bacteria following expression from either the constitutive or endogenous promoter, while SptP-4HA from *S.* Typhimurium was readily detectable following expression from either construct (Fig. 7). The stability of *S.* Typhimurium SptP-4HA within *S.* Typhi indicates that SicP is still functional in this serovar, suggesting that the instability of *S.* Typhi SptP results from changes within SptP alone. It is worth highlighting that the doublet produced from the constitutive SptP-4HA construct likely arises from forced expression from the current annotated ATG start codon of SptP, as well as expression from a downstream TTG codon, reported to be the true start site for SptP (23). Given that only the lower band was secreted (Fig. 6) and the size of the *S.* Typhimurium product expressed by the endogenous promoter also corresponds to that of the lower band, it is probable that the smaller band represents the correct form of SptP.

In order to further confirm that the instability of SptP in *S.* Typhi results from changes within the chaperone-binding domain, constitutive HA-tagged SptP chimeras were constructed in which the first 139 residues of *S.* Typhimurium SptP were swapped with those of *S.* Typhi and vice versa, and the proteins were again expressed in an *S.*

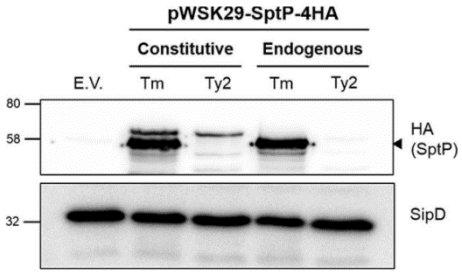


FIG 7 SptP is unstable within *S.* Typhi. SPI-1 mutant (Δ*invA*) *S.* Typhi bacteria expressing *S.* Typhimurium (Tm) or *S.* Typhi Ty2 SptP-4HA from either a constitutive T3 promoter or the endogenous promoter of *sptP* were grown aerobically to late exponential phase. The presence of intracellular SptP was detected using an anti-HA antibody. SipD was used as both a loading control and a positive control for SPI-1 expression. A representative blot of three independent repeats is shown. The numbers on the left are molecular masses (in kilodaltons). Arrowhead, the band which corresponds to SptP; E.V., empty vector.

Downloaded from http://jb.asm.org/ on August 29, 2017 by guest

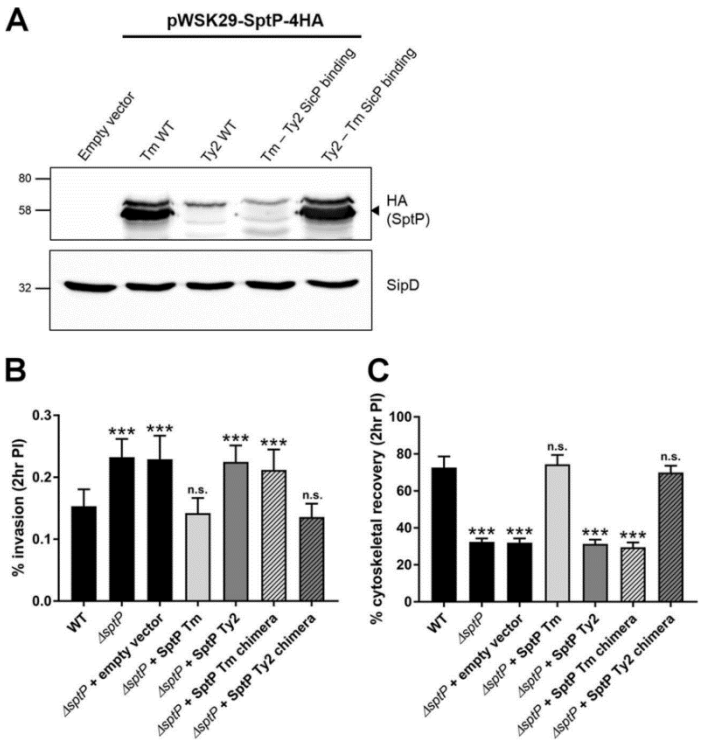


FIG 8 The chaperone-binding domain of *S.* Typhi SptP is responsible for its instability. (A) SPI-1 mutant (Δ*invA*) *S.* Typhi bacteria constitutively expressing either WT SptP-4HA from *S.* Typhimurium (Tm) or *S.* Typhi Ty2 or SptP-4HA chimeras with the SicP binding domain switched with that of the other serovar were grown aerobically to late exponential phase. The presence of SptP was determined using an antibody against the HA tag. SipD was used as both a loading control and a positive control for SPI-1 expression. A representative blot of three independent repeats is shown. The numbers on the left are molecular masses (in kilodaltons). Arrowhead, the band which corresponds to SptP. (B and C) HeLa cells were infected with WT or *sptP S.* Typhimurium strains constitutively expressing either WT SptP-4HA from *S.* Typhimurium (Tm) and *S.* Typhi (Ty2) or the SptP-4HA chimeras for 15 min. The percentage of intracellular bacteria at 2 h postinfection relative to the number of bacteria added in the inoculum is shown (B), and the proportion of infected cells displaying normal actin cytoskeleton was enumerated (C). At least 100 infected cells were counted per strain and per biological repeat. Error bars show SDs (n 3). The invasion rates of the strains and cytoskeletal recovery were compared to those for the WT by one-way ANOVA, followed by Tukey's *post hoc* test (***, P 0.001; n.s., no significant difference).

Typhi SPI-1 null background (Δ*invA*). As before, WT *S.* Typhi SptP was undetectable within bacteria; however, when the SicP binding domain of *S.* Typhi SptP was replaced with that of *S.* Typhimurium, *S.* Typhi SptP could be detected intracellularly (Fig. 8A). In contrast, *S.* Typhimurium SptP was destabilized when given the *S.* Typhi SicP binding domain, while the WT SptP remained readily detectable (Fig. 8A).

Since replacement of the chaperone-binding domain of SptP confers stability to *S.* Typhi SptP, we were interested to see if these changes would also influence the activity of *S.* Typhi SptP. Therefore, *sptP S.* Typhimurium was transformed with both WT and chimera *S.* Typhimurium and *S.* Typhi HA-tagged SptP, and invasion and cytoskeletal recovery assays were performed. While expression of *S.* Typhimurium SptP-4HA decreased the level of invasion back to WT levels, a strain expressing *S.* Typhi SptP-4HA was found to be as invasive as both the *sptP* strain and the *sptP* strain carrying the empty pWSK29 vector (Fig. 8B), in line with our previous findings (Fig. 5). The same pattern was observed with cytoskeletal recovery, with the *S.* Typhimurium SptP complemented strain achieving recovery rates akin to those achieved with WT infection,

Downloaded from http://jb.asm.org/ on August 29, 2017 by guest

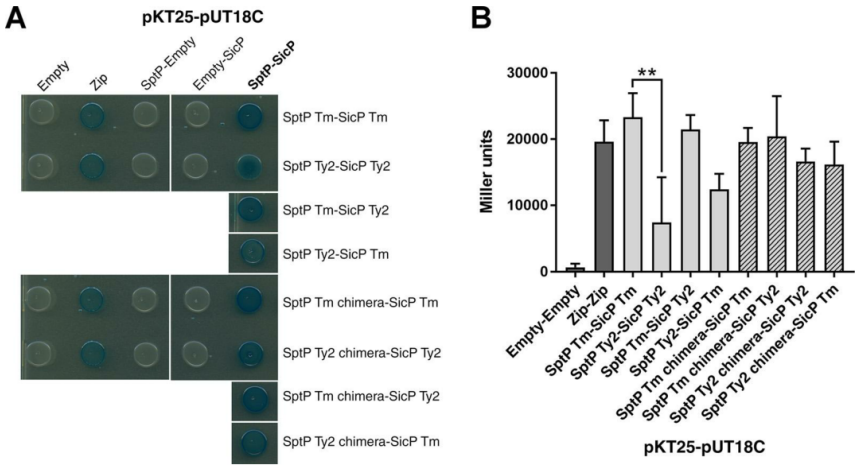


FIG 9 *S.* Typhi SptP interacts weakly with its chaperone, SicP. The interaction of SptP with its chaperone was assessed via a bacterial two-hybrid assay. The adenylate cyclase T25 and T18 fragments were fused to the N terminus of SptP and SicP of *S.* Typhimurium (Tm) and *S.* Typhi Ty2, respectively, and cotransformed into a *cyaA* mutant, *E. coli* DHM1. The levels of coexpression of the T25 and T18 fragments alone (Empty) or fused to leucine zipper motifs (Zip) were used as negative and positive controls, respectively. (A) Ten microliters of an overnight culture was spotted in triplicate on LB–X-Gal plates and incubated at 30°C for 24 h. Blue colonies indicate restored adenylate cyclase activity. A representative plate is shown. (B) Colonies were resuspended, and a *b*-galactosidase assay was performed in order to quantify the strength of the interaction between SptP and its chaperone, SicP (Miller units). Error bars show SDs (*n* 3). The levels of *b*-galactosidase expression induced by *S.* Typhimurium SptP and *S.* Typhi SptP were compared by *t* test (**, *P* 0.01).

while the strain expressing *S.* Typhi SptP demonstrated significantly impaired cytoskeletal recovery at 2 h postinfection (Fig. 8C). However, *sptP S.* Typhimurium expressing the *S.* Typhimurium SptP chimera displayed significantly increased invasion and significantly reduced cytoskeletal recovery compared to WT *S.* Typhimurium (Fig. 8), demonstrating that the *S.* Typhi chaperone-binding domain abolishes the ability of *S.* Typhimurium SptP to complement *sptP* deletion. Conversely, the *sptP S.* Typhimurium strain was fully complemented by expression of the *S.* Typhi SptP chimera, indicating that the GAP domain of *S.* Typhi SptP is still functional.

Binding of SptP to SicP. Assessment of the secretion and stability of SptP within *S.* Typhimurium and *S.* Typhi represents only an indirect way to measure SptP-SicP binding. In order to directly determine the strength of the interaction between SptP and SicP of both serovars, a bacterial two-hybrid assay was performed. SptP from *S.* Typhimurium and *S.* Typhi was found to interact with SicP of both serovars, indicated by the blue coloration of the colonies on Lennox broth (LB)–5-bromo-4-chloro-3-indolyl-*b*-D-galactopyranoside (X-Gal) indicator plates arising from the reconstitution of adenylate cyclase activity and subsequent induction of *b*-galactosidase expression (33). However, SptP-SicP interactions involving *S.* Typhi SptP resulted in a color change weaker than that in the equivalent cotransformations involving *S.* Typhimurium SptP (Fig. 9A). Since *b*-galactosidase expression is correlated with the strength of the interaction, a *b*-galactosidase assay was performed on the resuspended colonies in order to quantify the ability of SptP and SicP to interact between serovars. While *S.* Typhimurium SptP could interact strongly with SicP from *S.* Typhimurium, the equivalent interaction involving SptP and SicP from *S.* Typhi was significantly weaker (Fig. 9B). Interestingly, the strength of the interaction between *S.* Typhimurium SptP and *S.* Typhi SicP was equivalent to that of the interaction between *S.* Typhimurium SptP and its endogenous chaperone (Fig. 9B), further validating that SicP in *S.* Typhi is still functional.

Although replacement of the *S.* Typhimurium chaperone-binding domain with that of *S.* Typhi does not significantly decrease its interaction with SicP compared to that of

Downloaded from http://jb.asm.org/ on August 29, 2017 by guest

WT SptP, replacement of the chaperone-binding domain of *S*. Typhi SptP with that of *S*. Typhimurium increased the ability of *S*. Typhi SptP to bind both *S*. Typhi and *S*. Typhimurium SicP (Fig. 9B), reiterating that the reduced chaperone binding observed within *S*. Typhi SptP likely arises through changes within its SicP binding domain.

DISCUSSION

The presence of a premature stop codon within the SPI-1 effector SptP in H58 strains (12) led us to characterize the function of this effector during *S*. Typhi infection and compare it to that of this effector during *S*. Typhimurium infection. To date, there has been very limited characterization of SptP or, indeed, any *Salmonella* T3SS effector using WT *S*. Typhi, with studies instead tending to use *S*. Typhimurium or attenuated *S*. Typhi strains.

Our data demonstrate that SptP of *S*. Typhi has reduced chaperone binding, resulting in intracellular instability and preventing secretion. Unsurprisingly, given the instability of SptP within the *Salmonella* cytosol, deletion of *sptP* from *S*. Typhi Ty2 did not affect the efficiency of invasion into HeLa cells, in line with the findings of a previous study (24), and did not affect cytoskeletal recovery postinfection. Conversely, *S*. Typhimurium SptP demonstrates strong binding to its chaperone, SicP, ensuring its stability and secretion; as such, deletion of *sptP* from *S*. Typhimurium resulted in significant phenotypic differences, including increased invasion and a failure to recover the host cytoskeleton postinfection, as previously reported (13, 16).

Although significant differences between the ability of *S*. Typhimurium and *S*. Typhi SptP to bind SicP were observed in our bacterial two-hybrid assay, this technique failed to discern any significant differences between the WT and chaperone-binding chimeras of SptP, even though marked phenotypes with the SptP chimera constructs were seen in *Salmonella* (Fig. 8). The use of *Escherichia coli* as a host, incubation at a lower temperature (30°C), and overexpression of both SptP and SicP likely promoted protein-protein interactions and reduced the overall sensitivity of the assay. However, experiments conducted in both *S*. Typhimurium and *S*. Typhi demonstrate that changes within the first 139 amino acids of *S*. Typhi SptP, corresponding to the SicP binding domain, are sufficient to compromise its activity.

Our results strongly suggest that SptP is nonfunctional in *S*. Typhi. Interestingly, *S*. Paratyphi A shares the same amino acid changes within the chaperone-binding domain, and SptP failed to be detected intracellularly by Western blotting from *S*. Paratyphi A grown to late exponential phase (28), suggesting that the instability of SptP may be a common feature of typhoidal serovars. This apparent loss of function may explain how a premature stop codon within SptP within strains belonging to the globally dominant *S*. Typhi H58 haplotype is tolerated (12), despite evidence from *in vivo S*. Typhimurium infections demonstrating attenuated virulence when *sptP* is de-leted (20, 21). This suggests that *S*. Typhimurium is not always an appropriate model for typhoidal disease and that SptP, like the *spv* locus (8), may be required for systemic disease in mice or other hosts but not humans.

Although pseudogenization or the loss of known SPI-1 and SPI-2 effectors within *S*. Typhi has previously been reported (6, 10), the mechanism by which the function of SptP has been lost—via multiple amino acid changes, reducing its interaction with its chaperone—is unusual. A premature stop codon, such as that found in *S*. Typhi H58 strains (12), or even deletion of the gene would achieve the same end, without expending the energy invested in the transcription or translation of SptP. This could suggest that the loss of SptP function occurred gradually, maybe in conjunction with the acquisition and assimilation of a new effector with a similar function that was better suited to the induction of typhoidal disease; the presence of *S*. Typhi-specific effectors is not unlikely, given that *S*. Typhi CT18 has almost 600 genes not found in *S*. Typhimurium LT2 and effectors found only in *S*. Typhimurium and not *S*. Typhi are common (6). Alternatively, SptP is relatively unique among SPI-1 effectors, in that it is encoded within the SPI-1 pathogenicity island itself (4). Its central location within SPI-1 may not permit deletion or truncation without having deleterious effects on the

Downloaded from http://jb.asm.org/ on August 29, 2017 by guest

transcription or translation of neighboring genes, such as *hilA*, thereby driving the loss of function at the protein level.

If SptP is indeed not functional in *S.* Typhi, several key questions remain. Given that extended Rho GTPase activation mediated by SopE during infection would lead to proinflammatory signaling uncharacteristic of *S.* Typhi infection (17, 34), is another effector responsible for antagonizing SopE in *S.* Typhi? Perhaps most intriguingly, the question as to what function SicP, the chaperone of SptP, is performing in *S.* Typhi remains. SicP is relatively conserved between serovars (97% identity); since *S.* Typhimurium SptP is stable within *S.* Typhi and is able to strongly interact with *S.* Typhi SicP in a direct bacterial two-hybrid assay, we can be confident that SicP itself is still functional in *S.* Typhi. It is currently thought that SicP acts as a chaperone for SptP only (35); however, if it is not required to bind SptP in *S.* Typhi, it is unclear why its activity has been preserved. Although SicP is better conserved between serovars than SptP, there are amino acid changes. It is possible that, given time, these changes will accumulate and decrease the activity of SicP. An alternative explanation could be that SicP is simply acting as a chaperone for another, currently unknown effector.

Although the finding is not directly related to the function of SptP, we have also observed that different environmental conditions induced *S.* Typhi-specific regulation of the SPI-1 effector SopE. At present there are two accepted methods to induce SPI-1 expression, achieved either via aerobic growth to late exponential phase (subculture) or through growth to stationary phase under microaerobic conditions (static overnight culture) (28, 36). Our findings suggest that in comparison to *S.* Typhimurium, *S.* Typhi has additional regulatory mechanisms to control SPI-1 activity, likely in response to oxygen tension, acting at least at the level of SopE. Interestingly, a study comparing global SPI-1 expression in *S.* Paratyphi A between the different SPI-1-inducing conditions reported significant differences in SPI-1 expression between aerobic and microaerobic growth (28), while a similar study using *S.* Typhimurium SL1344 did not (36). Overall, this suggests that typhoidal serovars additionally use oxygen availability to tightly control virulence gene expression, an observation that may help explain the different diseases induced by typhoidal and nontyphoidal serovars.

Overall, this study demonstrates that the behavior of *S.* Typhi is significantly different from that of *S.* Typhimurium; the potential loss of function of SptP within *S.* Typhi exemplifies just how different these serovars are, even at the level of a single effector. This indicates that the findings of work performed in one serovar may not directly translate to the other, highlighting the need for further studies to elucidate the role of T3SS effectors in the context of *S.* Typhi infection.

MATERIALS AND METHODS

Bacterial strains, growth conditions, and cell culture. The strains and plasmids used in this study are listed in Table 1. *Salmonella* strains were routinely grown in Lennox broth (LB; Sigma-Aldrich). Kanamycin (50 μg/ml), ampicillin (100 μg/ml), and spectinomycin (100 μg/ml) were supplemented as required.

HeLa cells (ATCC) were maintained in Dulbecco's modified Eagle medium (DMEM) supplemented with 10% fetal bovine serum (FBS) (Sigma-Aldrich) in a 5% CO_2 incubator at 37°C. Cells were maintained at a maximum density of 1 10^6 cells/ml. The HeLa cells used in this study were authenticated via short tandem repeat profiling in February 2016 (Microsynth).

Construction of plasmids and strains. A full list of the oligonucleotides used in this study can be found in Table S1 in the supplemental material.

To permit the use of pWSK29 in ampicillin-resistant *S.* Typhi strains, pWSK29-Spec and pWSK29-Spec-4HA were constructed by amplifying the backbone of pWSK29 (37) and pWSK29-4HA, without the ampicillin resistance cassette, with primers containing NcoI and AvrII restriction sites (primer pair 1 and 2); the *aadA* gene, which confers resistance to spectinomycin, was amplified with primers containing the same restriction sites (primer pair 3 and 4). In addition to digestion with NcoI and AvrII, both products were digested with DpnI prior to ligation.

To create SptP complementation plasmids, SptP from *S.* Typhimurium 14028 (STM14_3477) and *S.* Typhi Ty2 (t2780) and H58 were amplified with primers containing BamHI and KpnI restriction sites (primer pair 5 and 6 and primer pair 7 and 8, respectively) and then cloned into these sites of pWSK29-Spec, generating constructs which constitutively express untagged SptP.

To create HA-tagged SptP, pWSK29-Spec-4HA was amplified with a reverse primer containing the PacI digestion site (primer pair 9 and 10). SptP was again amplified from both *S.* Typhimurium and *S.* Typhi with primers containing BamHI and PacI restriction sites (primer pair 11 and 13 and primer pair 12 and

Downloaded from http://jb.asm.org/ on August 29, 2017 by guest

TABLE 1 Strains and plasmids used in this study

Strain or plasmid	Identifier	Genotype or comments	Source or reference
Strains			
S. Typhimurium			
14028	ICC797	WT	This study
14028	ICC1373	*sptP*::Kan^r	This study
14028	ICC796	*prgH*::Tn*5*	This study
SL1344	ICC314	WT	This study
SL1344	ICC1374	*sopE*::Kan^r	This study
SL1344	ICC1376	*sopE*::FRT *sopE2*::Kan^r	This study
S. Typhi			
Ty2	ICC1500	WT	
Ty2	ICC1522	*sptP*::Kan^r	This study
Ty2	ICC1556	*invA*::Kan^r	This study
Ty2	ICC1555	*sopE*::Kan^r	This study
Plasmids			
pWSK29-Amp			37
pWSK29-4HA			This study
pWSK29-Spec	pICC2489	Empty vector	This study
pWSK29-Spec	pICC2491	*S*. Typhimurium SptP, T3 promoter	This study
pWSK29-Spec	pICC2490	Ty2 SptP, T3 promoter	This study
pWSK29-Spec	pICC2535	H58 SptP, T3 promoter	This study
pWSK29-Spec-4HA	pICC2493	*S*. Typhimurium SptP-4HA, T3 promoter	This study
pWSK29-Spec-4HA	pICC2492	Ty2 SptP-4HA, T3 promoter	This study
pWSK29-Spec-4HA	pICC2494	*S*. Typhimurium SptP-4HA, endogenous promoter	This study
pWSK29-Spec-4HA	pICC2495	Ty2 SptP-4HA, endogenous promoter	This study
pWSK29-Spec-4HA	pICC2520	*S*. Typhimurium SptP-Ty2 SicP binding 4HA, T3 promoter	This study
pWSK29-Spec-4HA	pICC2521	Ty2 SptP-*S*. Typhimurium SicP binding 4HA, T3 promoter	This study
pKT25	pICC2531	Empty vector	Euromedex
pKT25	pICC2533	Zip	Euromedex
pKT25	pICC2498	*S*. Typhimurium SptP	This study
pKT25	pICC2499	Ty2 SptP	This study
pUT18C	pICC2532	Empty vector	Euromedex
pUT18C	pICC2534	Zip	Euromedex
pUT18C	pICC2504	*S*. Typhimurium SicP	This study
pUT18C	pICC2505	Ty2 SicP	This study
pKD4	pICC893	Kanamycin resistance cassette template plasmid	38
pKD46	pICC1298	Bacteriophage lambda red recombinase plasmid	38
pCP20	pICC1303	FLP recombinase plasmid	38

13, respectively). Both products were digested, and SptP was cloned into the existing BamHI site and the introduced PacI site of pWSK29-Spec-4HA, resulting in constitutively expressed C-terminally tagged SptP-4HA. SptP-4HA expressed from its endogenous promoter was constructed in the same way, with the exception that SptP was amplified from both *S*. Typhimurium and *S*. Typhi with an additional 700 bp upstream from the annotated start codon (primer pair 14 and 13) and ligated into pWSK29-Spec-4HA as described above.

To create SptP-4HA chimeras in which the chaperone-binding domain was switched with that of the other serovar, the first 417 bp of SptP, encompassing the SicP binding domain (amino acid positions 35 to 139), was amplified from the *S*. Typhimurium (primer pair 15 and 16) and *S*. Typhi (primer pair 17 and 18) chromosomes. The *S*. Typhimurium and *S*. Typhi/pWSK29-SptP-4HA plasmids were then amplified without the SicP binding domain (primer pair 19 and 21 and primer pair 20 and 21, respectively), and the two products (an *S*. Typhimurium/pWSK29-SptP-4HA backbone with *S*. Typhi SicP binding and vice versa) were assembled via Gibson assembly (50°C, 30 min) (New England BioLabs).

To determine protein interactions by a bacterial two-hybrid assay, SptP (primer pair 22 and 24 and primer pair 23 and 24 for *S*. Typhimurium and *S*. Typhi SptP, respectively) and SicP (primer pair 25 and 26 and primer pair 25 and 27 for *S*. Typhimurium and *S*. Typhi SicP, respectively) were amplified from both *S*. Typhimurium 14028 and *S*. Typhi Ty2 and cloned into the BamHI and KpnI sites of pKT25 and pUT18C, generating SptP and SicP fused to the C terminus of the T25 and T18 adenylate cyclase fragments.

Gene deletions were constructed via bacteriophage *l* red recombination as previously described (38). Primers 28 and 30 were used to amplify the kanamycin resistance cassette of pKD4 with regions of homology to *S*. Typhimurium *sptP*, and primer pair 29 and 30 was used to amplify the kanamycin resistance cassette of pKD4 with regions of homology to *S*. Typhi *sptP*; primers 30 and 31 were used to create a kanamycin resistance cassette with *sopE* flanking regions; primer pair 32 and 33 was used to create the *sopE2* kanamycin resistance cassette product; and primers 41 and 42 were used to create the kanamycin resistance cassette with regions of *invA* homology. Correct deletion of the gene via insertion of the kanamycin resistance cassette was screened using primers 31 and 32 (*sptP*), 35 and 36 (*sopE*), 39

Downloaded from http://jb.asm.org/ on August 29, 2017 by guest

and 40 (*sopE2*), and 43 and 44 (*invA*). To create the SL1344 *sopE sopE2* double mutant strain, the FLP recognition target (FRT)-flanked kanamycin resistance cassette within *sopE* was excised via FLP-mediated recombination (pCP20), generating SL1344 *sopE*::FRT, prior to transformation with the *sopE2* pKD4 PCR product.

HeLa cell invasion assays. The invasiveness of the *sptP* and *sopE* strains relative to that of WT *Salmonella* was determined by gentamicin protection assays. At 24 h prior to infection, HeLa cells were seeded in a 24-well plate at a density of 7 10^4 cells/well. To induce expression of the SPI-1 T3SS, *Salmonella* strains were either cultured overnight at 37°C and 200 rpm before they were subcultured 1:33 in LB until late exponential phase (optical density at 600 nm [OD_{600}], 1.8) or cultured overnight at 37°C without shaking. *Salmonella* was added to the cells at a multiplicity of infection (MOI) of 100:1, and the cells and bacteria were incubated for 15 min for *S.* Typhimurium infections or for 30 min for infections involving both *S.* Typhimurium and *S.* Typhi. The cells were then washed three times with phosphate-buffered saline (PBS), before the addition of DMEM supplemented with 100 *m*g/ml gentamicin. The cells were further incubated for 1 h and washed with PBS, and the gentamicin concentration was reduced to 20 *m*g/ml. At the required time points, the cells were again washed three times in PBS before the addition of 0.1% Triton X-100. The cells were incubated for 5 min at room temperature (RT), before serial dilution and plating onto LB agar plates to enumerate the intracellular bacteria.

Immunofluorescence staining and microscopy. To compare the ability of the strains to recover the host cytoskeleton postinfection, cells were seeded onto glass coverslips and infected as outlined above. At the required time point, the cells were washed three times in PBS, before fixation with 4% paraformaldehyde for 15 min at room temperature, and were then washed a further three times in PBS. The cells were then quenched in 50 mM ammonium chloride for 10 min at RT, prior to permeabilization in 0.2% Triton X-100 for 4 min. Coverslips were blocked in 0.2% bovine serum albumin (BSA) for 5 min before addition of the primary antibody diluted in 0.2% BSA for 1 h. Intracellular *Salmonella* bacteria were detected using the CSA-1 antibody (1:200; Insight Biotechnology). The cells were again washed and blocked, prior to addition of the appropriate secondary antibody (1:200 donkey anti-goat immunoglob-ulin–Cy2; Jackson ImmunoResearch), Hoechst (1:1,000; Sigma), and phalloidin-tetramethyl rhodamine isocyanate (1:100; Invitrogen) for 30 min at room temperature. The coverslips were washed in PBS before they were mounted with ProLong Gold antifade reagent (Invitrogen) and visualized using a Zeiss Axio Observer Z1 microscope at 100 magnification.

SPI-1 secretion assays and Western blotting. To determine the secretion of SptP, *Salmonella* strains were grown aerobically to late exponential phase in 50 ml LB. The OD_{600} was recorded, and 1 ml bacteria was pelleted and resuspended in 2 SDS loading buffer (1 M Tris, pH 6.8, 2% SDS, 20% glycerol, 5% *b*-mercaptoethanol, bromophenol blue) in proportion to the OD_{600} reached to normalize bacterial numbers (10 *m*l of loading buffer per 0.1 OD_{600} unit). The remaining culture was centrifuged for 20 min at 3,300 *g* before syringe filtering (pore size, 0.2 *m*m). Five milliliters of the cleared supernatant was precipitated overnight at 4°C following the addition of 10% trichloroacetic acid (TCA). Precipitated proteins were recovered by centrifugation at 20,000 *g*, followed by two acetone washes. The pellets were left to air dry before the addition of 2 SDS loading buffer in the same volume used for the pellet fractions. To determine SptP stability or intracellular protein levels, the strains were grown aerobically to late exponential phase in 5 ml LB, before the OD_{600} was recorded and 1 ml was pelleted and resuspended in 2 SDS loading buffer. Samples were then heated at 95°C for 10 min. Proteins were separated on 12% acrylamide SDS-polyacrylamide gels, followed by semidry or wet transfer onto a polyvinylidene difluoride membrane (GE Healthcare). The membranes were blocked in 5% milk in PBS– 0.05% Tween 20 and blotted with either anti-DnaK 8E2/2 (1:10,000; Enzo Life Sciences), anti-HA (1:1,000; Sigma), or anti-SipD (1:5,000) primary antibodies, followed by the addition of horseradish peroxidase-conjugated secondary antibody (1:10,000; Jackson ImmunoResearch). Following the addition of the EZ-ECL reagent (Geneflow), chemiluminescence was detected using a LAS-3000 imager (Fuji).

Bacterial two-hybrid and -galactosidase assays. *E. coli* DHM1 was cotransformed with pKT25 and pUT18C constructs in various combinations, and transformants were selected on LB agar plates supplemented with kanamycin and ampicillin. Three colonies from each transformation were subsequently grown overnight with antibiotic selection at 37°C. Ten microliters of these cultures was spotted onto LB agar plates supplemented with kanamycin, ampicillin, 1 mM isopropyl-*b*-D-thiogalactopyranoside (IPTG), and 0.1 mg/ml of 5-bromo-4-chloro-3-indolyl-*b*-D-galactopyranoside (X-Gal) and incubated at 30°C for 24 h. Colonies with reconstituted adenylate cyclase activity mediated by interaction of the fused proteins were distinguished by their ability to metabolize X-Gal and subsequent blue coloration (33).

For quantitative analysis, colonies were resuspended in 1.2 ml LB. The OD_{600} was recorded, and the bacteria were pelleted and resuspended in Z buffer (0.06 M Na_2HPO_4, 0.04 M NaH_2PO_4, 0.01 M KCl, 0.001 M $MgSO_4$, 0.05 M *b*-mercaptoethanol, pH 7). *b*-Galactosidase assays were then performed as previously described (39).

Statistical analysis. Statistical tests were performed using GraphPad Prism (version 7.00) software for Windows (GraphPad Software, San Diego, CA, USA). All data are expressed as the mean standard deviation (SD). Significance (*P* 0.05) was determined either by unpaired *t* test or by one-way analysis of variance (ANOVA) followed by Tukey's *post hoc* test.

SUPPLEMENTAL MATERIAL

Supplemental material for this article may be found at https://doi.org/10.1128/JB.00647-16.

TEXT S1, PDF file, 0.2 MB.

Downloaded from http://jb.asm.org/ on August 29, 2017 by guest

ACKNOWLEDGMENTS

We are grateful to V. Koronakis for providing the anti-SipD antibody and to P. Pissaridou and A. Filloux for providing the DHM1 strain, the pKT25 and pUT18C vectors, *o*-nitrophenyl-*b*-D-galactopyranoside (ONPG), and the assistance required for the bac-terial two-hybrid assay.

REFERENCES

1. Coburn B, Grassl GA, Finlay BB. 2006. Salmonella, the host and disease: a brief review. Immunol Cell Biol 85:112–118.
2. McGhie EJ, Brawn LC, Hume PJ, Humphreys D, Koronakis V. 2009. Salmonella takes control: effector-driven manipulation of the host. Curr Opin Microbiol 12:117–124. https://doi.org/10.1016/j.mib.2008.12.001.
3. Figueira R, Holden DW. 2012. Functions of the Salmonella pathogenicity island 2 (SPI-2) type III secretion system effectors. Microbiology 158: 1147–1161. https://doi.org/10.1099/mic.0.058115-0.
4. Fàbrega A, Vila J. 2013. Salmonella enterica serovar Typhimurium skills to succeed in the host: virulence and regulation. Clin Microbiol Rev 26:308 –341. https://doi.org/10.1128/CMR.00066-12.
5. Santos RL, Zhang S, Tsolis RM, Kingsley RA, Garry Adams L, Bäumler AJ. 2001. Animal models of Salmonella infections: enteritis versus typhoid fever. Microbes Infect 3:1335–1344. https://doi.org/10.1016/S1286 -4579(01)01495-2.
6. Sabbagh SC, Forest CG, Lepage C, Leclerc J-M, Daigle F. 2010. So similar, yet so different: uncovering distinctive features in the genomes of Salmonella enterica serovars Typhimurium and Typhi. FEMS Microbiol Lett 305:1–13. https://doi.org/10.1111/j.1574-6968.2010.01904.x.
7. Spanò S, Galán JE. 2012. A Rab32-dependent pathway contributes to Salmonella typhi host restriction. Science 338:960 –963. https://doi.org/ 10.1126/science.1229224.
8. Matsui H, Bacot CM, Garlington WA, Doyle TJ, Roberts S, Gulig PA. 2001. Virulence plasmid-borne spvB and spvC genes can replace the 90-kilobase plasmid in conferring virulence to Salmonella enterica serovar Typhimurium in subcutaneously inoculated mice. J Bacteriol 183: 4652–4658. https://doi.org/10.1128/JB.183.15.4652-4658.2001.
9. Rotger R, Casadesus J. 1999. The virulence plasmids of Salmonella. Int Microbiol 2:177–184.
10. Parkhill J, Dougan G, James KD, Thomson NR, Pickard D, Wain J, Churcher C, Mungall KL, Bentley SD, Holden MT, Sebaihia M, Baker S, Basham D, Brooks K, Chillingworth T, Connerton P, Cronin A, Davis P, Davies RM, Dowd L, White N, Farrar J, Feltwell T, Hamlin N, Haque A, Hien TT, Holroyd S, Jagels K, Krogh A, Larsen TS, Leather S, Moule S, O'Gaora P, Parry C, Quail M, Rutherford K, Simmonds M, Skelton J, Stevens K, Whitehead S, Barrell BG. 2001. Complete genome sequence of a multiple drug resistant Salmonella enterica serovar Typhi CT18. Nature 413: 848 – 852. https://doi.org/10.1038/35101607.
11. Eswarappa SM, Janice J, Nagarajan AG, Balasundaram SV, Karnam G, Dixit NM, Chakravortty D. 2008. Differentially evolved genes of Salmo-nella pathogenicity islands: insights into the mechanism of host speci-ficity in Salmonella. PLoS One 3:e3829. https://doi.org/10.1371/ journal.pone.0003829.
12. Wong VK, Baker S, Pickard DJ, Parkhill J, Page AJ, Feasey NA, Kingsley RA, Thomson NR, Keane JA, Weill F-X, Edwards DJ, Hawkey J, Harris SR, Mather AE, Cain AK, Hadfield J, Hart PJ, Thieu NTV, Klemm EJ, Glinos DA, Breiman RF, Watson CH, Kariuki S, Gordon MA, Heyderman RS, Okoro C, Jacobs J, Lunguya O, Edmunds WJ, Msefula C, Chabalgoity JA, Kama M, Jenkins K, Dutta S, Marks F, Campos J, Thompson C, Obaro S, MacLennan CA, Dolecek C, Keddy KH, Smith AM, Parry CM, Karkey A, Mulholland EK, Campbell JI, Dongol S, Basnyat B, Dufour M, Bandaranayake D, et al. 2015. Phylogeographical analysis of the dominant multidrug-resistant H58 clade of Salmonella Typhi identifies inter- and intracontinental transmission events. Nat Genet 47:632– 639. https://doi.org/10.1038/ ng.3281.
13. Fu Y, Galan JE. 1998. Identification of a specific chaperone for SptP, a substrate of the centisome 63 type III secretion system of Salmonella typhimurium. J Bacteriol 180:3393–3399.
14. Lee SH, Galán JE. 2004. Salmonella type III secretion-associated chaper-ones confer secretion-pathway specificity. Mol Microbiol 51:483– 495. https://doi.org/10.1046/j.1365-2958.2003.03840.x.
15. Kubori T, Galán JE. 2003. Temporal regulation of Salmonella virulence effector function by proteasome-dependent protein degradation. Cell 115:333–342. https://doi.org/10.1016/S0092-8674(03)00849-3.
16. Fu Y, Galán JE. 1999. A Salmonella protein antagonizes Rac-1 and Cdc42 to mediate host-cell recovery after bacterial invasion. Nature 401: 293–297. https://doi.org/10.1038/45829.
17. Keestra AM, Winter MG, Auburger JJ, Fräßle SP, Xavier MN, Winter SE, Kim A, Poon V, Ravesloot MM, Waldenmaier JFT, Tsolis RM, Eigenheer RA, Bäumler AJ. 2013. Manipulation of small Rho GTPases is a pathogen-induced process detected by NOD1. Nature 496:233–237. https:// doi.org/10.1038/nature12025.
18. Lin SL, Le TX, Cowen DS. 2003. SptP, a Salmonella typhimurium type III-secreted protein, inhibits the mitogen-activated protein kinase path-way by inhibiting Raf activation. Cell Microbiol 5:267–275. https:// doi.org/10.1046/j.1462-5822.2003.t01-1-00274.x.
19. Humphreys D, Hume PJ, Koronakis V. 2009. The Salmonella effector SptP dephosphorylates host AAA ATPase VCP to promote development of its intracellular replicative niche. Cell Host Microbe 5:225–233. https:// doi.org/10.1016/j.chom.2009.01.010.
20. Kaniga K, Uralil J, Bliska JB, Galan JE. 1996. A secreted protein tyrosine phosphatase with modular effector domains in the bacterial pathogen Salmonella typhimurium. Mol Microbiol 21:633– 641. https://doi.org/ 10.1111/j.1365-2958.1996.tb02571.x.
21. Chaudhuri RR, Morgan E, Peters SE, Pleasance SJ, Hudson DL, Davies HM, Wang J, van Diemen PM, Buckley AM, Bowen AJ, Pullinger GD, Turner DJ, Langridge GC, Turner AK, Parkhill J, Charles IG, Maskell DJ, Stevens MP. 2013. Comprehensive assignment of roles for Salmonella typhimurium genes in intestinal colonization of food-producing animals. PLoS Genet 9:e1003456. https://doi.org/10.1371/journal.pgen.1003456.
22. Fu Y, Galan JE. 1998. The Salmonella typhimurium tyrosine phosphatase SptP is translocated into host cells and disrupts the actin cytoskeleton. Mol Microbiol 27:359 –368. https://doi.org/10.1046/j.1365-2958.1998.00684.x.
23. Button JE, Galan JE. 2011. Regulation of chaperone/effector complex synthesis in a bacterial type III secretion system. Mol Microbiol 81: 1474 –1483. https://doi.org/10.1111/j.1365-2958.2011.07784.x.
24. Arricau N, Hermant D, Waxin H, Popoff M. 1997. Molecular characteriza-tion of the Salmonella typhi StpA protein that is related to both Yersinia YopE cytotoxin and YopH tyrosine phosphatase. Res Microbiol 148: 21–26. https://doi.org/10.1016/S0923-2508(97)81896-7.
25. Stebbins CE, Galán JE. 2001. Maintenance of an unfolded polypeptide by a cognate chaperone in bacterial type III secretion. Nature 414:77– 81. https://doi.org/10.1038/35102073.
26. Zuker M. 2003. Mfold web server for nucleic acid folding and hybridiza-tion prediction. Nucleic Acids Res 31:3406 –3415. https://doi.org/ 10.1093/nar/gkg595.
27. Cain RJ, Hayward RD, Koronakis V. 2008. Deciphering interplay between Salmonella invasion effectors. PLoS Pathog 4:e1000037. https://doi.org/ 10.1371/journal.ppat.1000037.
28. Elhadad D, Desai P, Grassl GA, McClelland M, Rahav G, Gal-Mor O. 2016. Differences in host cell invasion and Salmonella pathogenicity island 1 expression between Salmonella enterica serovar Paratyphi A and non-typhoidal S. Typhimurium. Infect Immun 84:1150 –1165. https://doi.org/ 10.1128/IAI.01461-15.
29. Clark L, Perrett CA, Malt L, Harward C, Humphrey S, Jepson KA, Martinez-Argudo I, Carney LJ, La Ragione RM, Humphrey TJ, Jepson MA. 2011. Differences in Salmonella enterica serovar Typhimurium strain invasive-ness are associated with heterogeneity in SPI-1 gene expression. Micro-biology 157:2072–2083. https://doi.org/10.1099/mic.0.048496-0.
30. McClelland M, Sanderson KE, Clifton SW, Latreille P, Porwollik S, Sabo A, Meyer R, Bieri T, Ozersky P, McLellan M, Harkins CR, Wang C, Nguyen C, Berghoff A, Elliott G, Kohlberg S, Strong C, Du F, Carter J, Kremizki C, Layman D, Leonard S, Sun H, Fulton L, Nash W, Miner T, Minx P, Delehaunty K, Fronick C, Magrini V, Nhan M, Warren W, Florea L, Spieth J, Wilson RK. 2004. Comparison of genome degradation in Paratyphi A

Downloaded from http://jb.asm.org/ on August 29, 2017 by guest

and Typhi, human-restricted serovars of Salmonella enterica that cause typhoid. Nat Genet 36:1268 –1274. https://doi.org/10.1038/ng1470.
31. Friebel A, Ilchmann H, Aepfelbacher M, Ehrbar K, Machleidt W, Hardt WD. 2001. SopE and SopE2 from Salmonella typhimurium activate different sets of RhoGTPases of the host cell. J Biol Chem 276:34035–34040. https://doi.org/10.1074/jbc.M100609200.
32. Kröger C, Colgan A, Srikumar S, Händler K, Sivasankaran SK, Hammarlöf DL, Canals R, Grissom JE, Conway T, Hokamp K, Hinton JC. 2013. An infection-relevant transcriptomic compendium for Salmonella enterica serovar Typhimurium. Cell Host Microbe 14:683– 695. https://doi.org/ 10.1016/j.chom.2013.11.010.
33. Karimova G, Pidoux J, Ullmann A, Ladant D. 1998. A bacterial two-hybrid system based on a reconstituted signal transduction pathway. Proc Natl Acad Sci U S A 95:5752–5756. https://doi.org/10.1073/pnas.95.10.5752.
34. Gal-Mor O, Boyle EC, Grassl GA. 2014. Same species, different diseases: how and why typhoidal and non-typhoidal Salmonella enterica serovars differ. Front Microbiol 5:391. https://doi.org/10.3389/fmicb.2014.00391.
35. Parsot C, Hamiaux C, Page A-L. 2003. The various and varying roles of specific chaperones in type III secretion systems. Curr Opin Microbiol 6:7–14. https://doi.org/10.1016/S1369-5274(02)00002-4.
36. Ibarra JA, Knodler LA, Sturdevant DE, Virtaneva K, Carmody AB, Fischer ER, Porcella SF, Steele-Mortimer O. 2010. Induction of Salmonella patho-genicity island 1 under different growth conditions can affect Salmonella-host cell interactions in vitro. Microbiology 156:1120 –1133. https://doi.org/10.1099/mic.0.032896-0.
37. Wang RF, Kushner SR. 1991. Construction of versatile low-copy-number vectors for cloning, sequencing and gene expression in Escherichia coli. Gene 100:195–199. https://doi.org/10.1016/0378-1119 (91)90366-J.
38. Datsenko KA, Wanner BL. 2000. One-step inactivation of chromosomal genes in Escherichia coli K-12 using PCR products. Proc Natl Acad Sci U S A 97:6640 – 6645. https://doi.org/10.1073/pnas.120163297.
39. Miller J. 1972. Experiments in molecular genetics. Cold Spring Harbor Laboratory, Cold Spring Harbor, NY.

Downloaded from http://jb.asm.org/ on August 29, 2017 by guest

Appendix 3

Equipment obtained for the *S.* Typhi CL3 laboratory.

Piece of Equipment	Health and Safety/Security Requirement(s)
Benchtop centrifuge	Centrifuge buckets with lids and O-rings to prevent the release of aerosols in the event of a failure of the primary containment vessel during centrifugation.
Bio-bins	To store any solid waste generated inside MSCs that can then be sealed before removal from the MSC.
Centrifugal 0.2 µm filters	To enable the filtration of small (<0.5 mL) volumes of liquid to remove any bacteria and prevent the removal of infectious material from the CL3 laboratory.
Electroporation cuvettes	Cuvettes with lids to prevent the release of aerosols during electroporation of bacteria.
PCR thermocycler	Demonstration that a PCR using *S.* Typhi colonies was sufficient to kill any bacteria and therefore avoid removal of live bacteria from the CL3 laboratory.
Pipettes	Two sets of pipettes that are kept inside the MSCs and only removed after fumigation to prevent the removal of any infectious material from inside the MSC.
Refrigerated shaking incubator	Capable of housing large secondary containers.
Secondary containers	O-rings that enable the containers to be sealed to prevent the release of aerosols in the event of a failure of the primary containment vessel during use.
Spark-free electroporator	Spark-free electroporator with a separate cuvette chamber that could be taken inside the MSC to prevent the formation and escape of aerosols from the MSC during electroporation.
Ultra-low temperature freezer	Lockable door to prevent access to unauthorised personnel.
Vacuum pump system	To maintain the waste bottle, containing Virkon at all times, within the MSC and to have a 0.2 µm filter on the tubing that leaves the MSC and connects to the vacuum pump to prevent the release of any aerosol from the MSC.
Vacuum-based 0.2 µm filters	To enable the filtration of large (>0.5 mL) volumes of liquid to remove any bacteria and prevent the removal of infectious material from the CL3 laboratory.

Appendix 4

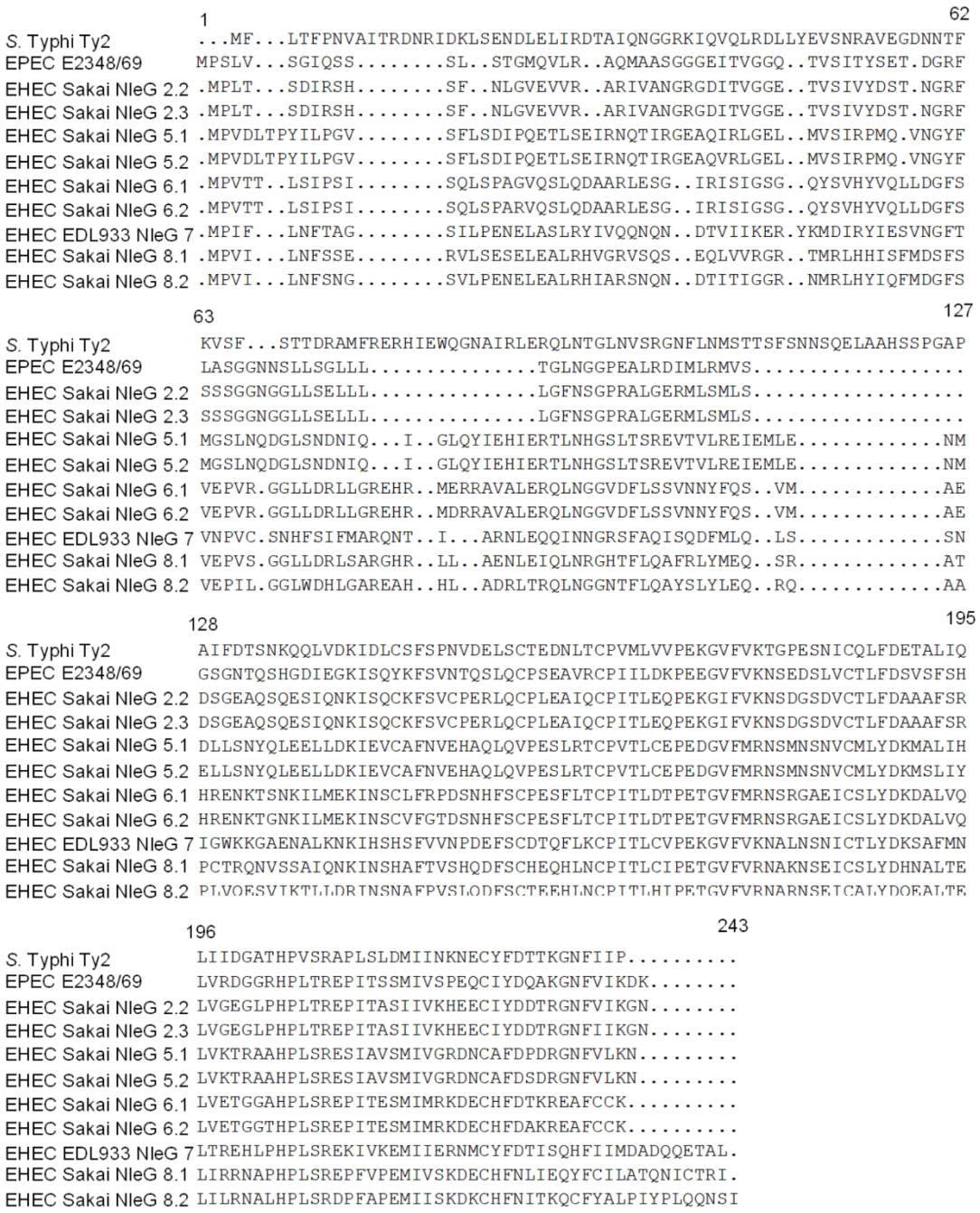
Amino acid sequence alignments of the novel effectors with homologues from other Gram-negative bacterial pathogens.

Sequences obtained from NCBI website (https://blast.ncbi.nlm.nih.gov/Blast.cgi), aligned using Clustal Omega (Sievers et al. 2011) and formatted using Strap (Gille et al. 2014).

StoA

```
                                  1                                                                  68
S. Typhi Ty2                      MSLAQPKSGELLEILGPSLTQGENLLSEFEIHAVIRDARNVPEYYQGLSIEGLAKLVLGEVEEGCALC
Y. enterolitica YE04/02           MIAPKPKSAELIELLTPSLIEGKNFLSEFEARRVIACAKQLPDRYQGICIEGLVKIICGDIEEGSSLC
S. marcescens 2880STDY5682957     MRVPQPKSGELLDILTPSLIKGENLLSEIEVRRVIVEARKLPDRYQGLSIEGLVRIVGDDLEEGYSLL
E. coli O146:H21 2010C-3325       MSLAQPKSGELLDLLTPSLTKGENLLSEFEVHQIIREAKKIPERYQGLSIEGLAKLVLGEIEEGCSLC
K. pneumoniae K2746               MAAPKLKTNDIIRDLKPSLEAGRLLMSDFEKQTMLRQVRSIPSRYQSLALEGMIHFLDGKNRLGTESL
                                      69                                                             135
S. Typhi Ty2                      EKSLAIAPDDSVSFCNYTIALRNKGYHVKQYEIIKRAI.NSRNPRILSEVAINAAYWVDLDLLKKVMP
Y. enterolitica YE04/02           ERSLLLAPHESVTWANYALALANKGLHSKQIEILKRAIEVIRNPVLISDILVIATFWVDVDLLNKVAP
S. marcescens 2880STDY5682957     EKALALAPYDAVSWGNFSRVVGNKALHSKQLEILKRSL.VVREPALLVEALIIGAFWADMELLDKVVP
E. coli O146:H21 2010C-3325       EQGLRLAPNDSVSFCNYTIALRNLGLHARQYAMIQNSA.NSLNPTILAEVATISAYWADIDLLEKVMP
K. pneumoniae K2746               ERSLELCPSDDVTWTNYAAILNQKGLYTQAEGLFQRAI.LQCVPRMFEQALLFGAFWGDMEMMTKALT
                                     136                                                             202
S. Typhi Ty2                      MLNAMEVAKADDLLKCNESLDYLIDHEN.HSHDLKAIGQLMMTIAEKYRLRLAGAHAFYVMNELNTFF
Y. enterolitica YE04/02           MFAAMEIKPNDSCEAALRNLDKILNLGE.RAKDVEDVAKAVMKVAEKHNLPAISSQLGDDGYGMIAFS
S. marcescens 2880STDY5682957     MVRAMEIQLSEPATQAIAMYERMLGYGD.KAKQVSAVAKVVMSVAERHRLPSDISRVDDDDEGLMGFC
E. coli O146:H21 2010C-3325       MLTAMEVPRPEEMAKWCHTLDYLHTHQE.HAQDLKTIGQLMMNVADKYRVRLAGAHAFYVLSELDTLF
K. pneumoniae K2746               MIEKYDCEITFG.ESALNTFKNMKNFDEKLRQDIKNAASVVRNIAEEFGLVCTRSHVEDDGFGELAFT
                                     203                                                  249
S. Typhi Ty2                      VEIKTDDPALLSKVNNDLANELIAAGLENSECVGCFQAGDF...
Y. enterolitica YE04/02           FTVDTDDINFISTLNDELYEEMIEHGLETSNCIGYFEPKGE...
S. marcescens 2880STDY5682957     LFVNTDDADYIQALNNELLDEMIDAGLETGCCVGFFEPGGKECL
E. coli O146:H21 2010C-3325       VEVKTDDPALLSQMNNDLADEIINAGLADSECVGCFEAGDF...
K. pneumoniae K2746               CEICVDDVDTLMNLNSRVIEDMVSQGYESSRCVAYFESAGDL..
```

StoD


1 62
S. Typhi Ty2 ...MF...LTFPNVAITRDNRIDKLSENDLELIRDTAIQNGGRKIQVQLRDLLYEVSNRAVEGDNNTF
EPEC E2348/69 MPSLV...SGIQSS.....SL..STGMQVLR..AQMAASGGGEITVGGQ..TVSITYSET.DGRF
EHEC Sakai NleG 2.2 .MPLT...SDIRSH.....SF..NLGVEVVR..ARIVANGRGDITVGGE..TVSIVYDST.NGRF
EHEC Sakai NleG 2.3 .MPLT...SDIRSH.....SF..NLGVEVVR..ARIVANGRGDITVGGE..TVSIVYDST.NGRF
EHEC Sakai NleG 5.1 .MPVDLTPYILPGV.....SFLSDIPQETLSEIRNQTIRGEAQIRLGEL..MVSIRPMQ.VNGYF
EHEC Sakai NleG 5.2 .MPVDLTPYILPGV.....SFLSDIPQETLSEIRNQTIRGEAQVRLGEL..MVSIRPMQ.VNGYF
EHEC Sakai NleG 6.1 .MPVTT..LSIPSI.....SQLSPAGVQSLQDAARLESG..IRISIGSG..QYSVHYVQLLDGFS
EHEC Sakai NleG 6.2 .MPVTT..LSIPSI.....SQLSPARVQSLQDAARLESG..IRISIGSG..QYSVHYVQLLDGFS
EHEC EDL933 NleG 7 .MPIF...LNFTAG.....SILPENELASLRYIVQQNQN..DTVIIKER.YKMDIRYIESVNGFT
EHEC Sakai NleG 8.1 .MPVI...LNFSSE.....RVLSESELEALRHVGRVSQS..EQLVVRGR..TMRLHHISFMDSFS
EHEC Sakai NleG 8.2 .MPVI...LNFSNG.....SVLPENELEALRHIARSNQN..DTITIGGR..NMRLHYIQFMDGFS
63 127
S. Typhi Ty2 KVSF...STTDRAMFRERHIEWQGNAIRLERQLNTGLNVSRGNFLNMSTTSFSNNSQELAAHSSPGAP
EPEC E2348/69 LASGGNNSLLSGLLL.....TGLNGGPEALRDIMLRMVS.....
EHEC Sakai NleG 2.2 SSSGGNGGLLSELLL.....LGFNSGPRALGERMLSMLS.....
EHEC Sakai NleG 2.3 SSSGGNGGLLSELLL.....LGFNSGPRALGERMLSMLS.....
EHEC Sakai NleG 5.1 MGSLNQDGLSNDNIQ...I..GLQYIEHIERTLNHGSLTSREVTVLREIEMLE.....NM
EHEC Sakai NleG 5.2 MGSLNQDGLSNDNIQ...I..GLQYIEHIERTLNHGSLTSREVTVLREIEMLE.....NM
EHEC Sakai NleG 6.1 VEPVR.GGLLDRLLGREHR..MERRAVALERQLNGGVDFLSSVNNYFQS..VM.....AE
EHEC Sakai NleG 6.2 VEPVR.GGLLDRLLGREHR..MDRRAVALERQLNGGVDFLSSVNNYFQS..VM.....AE
EHEC EDL933 NleG 7 VNPVC.SNHFSIFMARQNT..I...ARNLEQQINNGRSFAQISQDFMLQ..LS.....SN
EHEC Sakai NleG 8.1 VEPVS.GGLLDRLSARGHR..LL..AENLEIQLNRGHTFLQAFRLYMEQ..SR.....AT
EHEC Sakai NleG 8.2 VEPIL.GGLWDHLGAREAH..HL..ADRLTRQLNGGNTFLQAYSLYLEQ..RQ.....AA
128 195
S. Typhi Ty2 AIFDTSNKQQLVDKIDLCSFSPNVDELSCTEDNLTCPVMLVVPEKGVFVKTGPESNICQLFDETALIQ
EPEC E2348/69 GSGNTQSHGDIEGKISQYKFSVNTQSLQCPSEAVRCPIILDKPEEGVFVKNSEDSLVCTLFDSVSFSH
EHEC Sakai NleG 2.2 DSGEAQSQESIQNKISQCKFSVCPERLQCPLEAIQCPITLEQPEKGIFVKNSDGSDVCTLFDAAAFSR
EHEC Sakai NleG 2.3 DSGEAQSQESIQNKISQCKFSVCPERLQCPLEAIQCPITLEQPEKGIFVKNSDGSDVCTLFDAAAFSR
EHEC Sakai NleG 5.1 DLLSNYQLEELLDKIEVCAFNVEHAQLQVPESLRTCPVTLCEPEDGVFMRNSMNSNVCMLYDKMALIH
EHEC Sakai NleG 5.2 ELLSNYQLEELLDKIEVCAFNVEHAQLQVPESLRTCPVTLCEPEDGVFMRNSMNSNVCMLYDKMSLIY
EHEC Sakai NleG 6.1 HRENKTSNKILMEKINSCLFRPDSNHFSCPESFLTCPITLDTPETGVFMRNSRGAEICSLYDKDALVQ
EHEC Sakai NleG 6.2 HRENKTGNKILMEKINSCVFGTDSNHFSCPESFLTCPITLDTPETGVFMRNSRGAEICSLYDKDALVQ
EHEC EDL933 NleG 7 IGWKKGAENALKNKIHSHSFVVNPDEFSCDTQFLKCPITLCVPEKGVFVKNALNSNICTLYDKSAFMN
EHEC Sakai NleG 8.1 PCTRQNVSSAIQNKINSHAFTVSHQDFSCHEQHLNCPITLCIPETGVFVRNAKNSEICSLYDHNALTE
EHEC Sakai NleG 8.2 PLVQESVIKTLLDRINSNAFPVSLQDFSCTEEHLNCPITLHIPETGVFVRNARNSEICALYDQEALTE
196 243
S. Typhi Ty2 LIIDGATHPVSRAPLSLDMIINKNECYFDTTKGNFIIP.....
EPEC E2348/69 LVRDGGRHPLTREPITSSMIVSPEQCIYDQAKGNFVIKDK.....
EHEC Sakai NleG 2.2 LVGEGLPHPLTREPITASIIVKHEECIYDDTRGNFVIKGN.....
EHEC Sakai NleG 2.3 LVGEGLPHPLTREPITASIIVKHEECIYDDTRGNFIIKGN.....
EHEC Sakai NleG 5.1 LVKTRAAHPLSRESIAVSMIVGRDNCAFDPDRGNFVLKN.....
EHEC Sakai NleG 5.2 LVKTRAAHPLSRESIAVSMIVGRDNCAFDSDRGNFVLKN.....
EHEC Sakai NleG 6.1 LVETGGAHPLSREPITESMIMRKDECHFDTKREAFCCK.....
EHEC Sakai NleG 6.2 LVETGGTHPLSREPITESMIMRKDECHFDAKREAFCCK.....
EHEC EDL933 NleG 7 LTREHLPHPLSREKIVKEMIIERNMCYFDTISQHFIIMDADQQETAL.
EHEC Sakai NleG 8.1 LIRRNAPHPLSREPFVPEMIVSKDECHFNLIEQYFCILATQNICTRI.
EHEC Sakai NleG 8.2 LILRNALHPLSRDPFAPEMIISKDKCHFNITKQCFYALPIYPLQQNSI

StoE


1 65
S. Typhi Ty2 ..MKVSLDLVINSG.DDEIDMDYALQTLLGASGVTSIITEAILRGKVKENRHQSNEIRTNLKHSFT
Y. enterolitica YE177/02 ..MKVSLDLVINSG.EADVDMDYAIETLLGTSKVISIVSEAVLGGKVVSKRYASNPVRNKLKHSFT
S. marcescens 2880STDY5682999 ..MNINFDIVIKSG.DNDVDMDYGLKTLSGTSRVVSTLAEAILKKEVSERRTSINDVRTQLKQSFK
E. coli STEC S1191 ..MKVSYDVVIKSG.DQEVDMEYGLDTLSGTAEVTCILAEAILRKKIIKRRTHVNPARAVLKQSFK
K. pneumoniae K2746 MTGVVNYDVVIKSG.EEPVDMDYALDTLGGASEVTCLLAEAILQKKVVKRRTSANNARAVLHQSFQ
V. cholerae VC35 ..MCINFDVVIDTANEYSVDMKSGLDTLQGISEATRYIAETLLTDNVPKKLTHTKKVRTRLKKSFK
66 131
S. Typhi Ty2 GSFGQRFDVVISDRKVAARLSSMTRTVFAEVMSYYIYESLFLEGPALSDAAKKVVSGLDDIEDELT
Y. enterolitica YE177/02 GSYGQCFDLVISDTKMIDNLKRMGRSVFSEVISYYIYDALYLETKNLTPKALDIIKKLESIEEVLT
S. marcescens 2880STDY5682999 SSYGQNFCIEVNEPLLKRRLRKIGNDTFCEVMAFYIAESLFIPSDDLSPMAKEVVDDLEEVEDKLL
E. coli STEC S1191 SSYGQNFDLIVNEPELAAELKKMTRSVFSEVMGYFISESLYLETKELSPKAAGIIEELEEIEDELI
K. pneumoniae K2746 SSYGQNFALAIDDPIMKARLVEITNPVLAEIMGFYIAEAMYMEPSALSARARHYIDELDYLEDEIV
V. cholerae VC35 GSYGQVFGLDIEDDLLKRKFKDIGAEVFAELMGYFVSEALYQEPLKLSPKAEKIVTDLGEKEEALI
132 196
S. Typhi Ty2 KAIRN.RLKNMHKISTMCNYSVDLNYRKPGEKQKIITLNKNTALNITELIETNHDHQIEAIVTRFN
Y. enterolitica YE177/02 TKIRN.PLIDMHTISAMCGYSIDLNYRKPGEKQKLASLDHGTSKNITDLHESAKTHTIEAIITRFN
S. marcescens 2880STDY5682999 DVLRR.GLVDMHKITAMNSFNVELNHKPRGGHKRIATLTPKTAKHITETKEGDKDYEITAIFTRFN
E. coli STEC S1191 DRIRQ.PLVRMHRINLQKNFDVELNYKKPAGKQRIAKLDTMTATNLTQSKIMPGQVNINAVITRFN
K. pneumoniae K2746 SRIRN.PLIRMHKINYRCNWDVDFNFKPDGRQRKIVTLNTRTAANLTHTSVQRERFNIVAMVTRFN
V. cholerae VC35 NQLRKSSLEKIHEVSTKFGHDVKLRYRKSSVDQTVLAKFDKTTVYALKPISARNDVDITASITRLN
197 262
S. Typhi Ty2 TFTGNGRLLVRGEEKTTSFGFLNGLKYVTDAQTKKITSNLDANNRLAEEEREYLLLKVRDLTISNG
Y. enterolitica YE177/02 TFTGNGRLLVKGDKTTTSFGFTKAFKYVTEGQKKKITANQHENNTVSEENRKNIKLLVKNLSISTG
S. marcescens 2880STDY5682999 SMTGNGRLIVKDDDKTTAFGLAKGLRFVPLEFKKKITANLHSNNGLNKENWNYIKLKVKDLKLTSG
E. coli STEC S1191 ARTGNGRLVIEGEDDTVAFGFYMPLKAIPAAQKRLVSLNLHNNNGR.QDNYTYLKLTVSKVVVKSG
K. pneumoniae K2746 SRTGNGRLVLRDENETVAFGFAMPLGMVPPAQKKMVSLNLHNNNGR.GDNYIYLSMTVSRVVIMSG
V. cholerae VC35 INTGNGRLLLSGESETVAFGFSIEYKDVKIAAKKKFSENLNNNNGVHPDNWDVLKMIARPMKLKNG
263 276
S. Typhi Ty2 EVVKYLIIEVDGV.
Y. enterolitica YE177/02 EVIKYRVEEVE...
S. marcescens 2880STDY5682999 EVVKYFINEIA...
E. coli STEC S1191 DVVKYLIRMVETV.
K. pneumoniae K2746 ETVKYAVHSVRVLE
V. cholerae VC35 KIVKYIIKGIY...

Appendix 5

Amino acid sequence alignments of the novel effectors with homologues from other *S. enterica* serovars.

Sequences obtained from KEGG (Kanehisa et al. 2016), aligned using Clustal Omega (Sievers et al. 2011) and formatted using Strap (Gille et al. 2014).

StoB

```
                          1                                                                   71
S. Typhi Ty2              ........................................MGRLEAHATIKLTIDTQPSAEPTLGSTV
S. Paratyphi A ATCC9150   ...................................................MTIDTQPSAEPTLGSTV
S. Paratyphi B SPB7       ..........................................................MGSTV
S. Paratyphi C RKS4594    MDNSSLSIGWLTIDSTPPVRSMEDNSDIGSGGDNITNINTSTFIGSSEAHATIKLTIDTQPSAEPTLGSTV
S. Typhimurium ATCC14028 ...................................................MDTQPSAEPTLGSTV
S. Enteritidis EC200990135 MDNSSLSIGWLTIDSTPPVRSMKDNSDIGARGDNITNINTPTFIGSSEAHATIKLTIDTQPSAEPTLGSTV
                          72                                                                  142
S. Typhi Ty2              SSLDNTVSLKGVVEAHQDIQVKVTVDDTDYTASVDNDTGNWHVSVPQSAILSGENQYTITATDPAGNSAAA
S. Paratyphi A ATCC9150   SSLDNTVSLKGVVEAHQDIQVKVTVDDTDYTASVDNDTGNWHVSVPQSAILSGENQYTITATDPAGNSAAA
S. Paratyphi B SPB7       SSLDNTVTLKGVVEAHQDIQVKVTVNDTDYTASIDNDISN.............................
S. Paratyphi C RKS4594    NSLDNTVTLKGVVEAHQDIQVKVTVNDTDYTASIDNDISN.............................
S. Typhimurium ATCC14028 SSLDNTVTLKGVVEAHQDIQVKVTVNDTDYTAS....................................
S. Enteritidis EC200990135 NSLDNTVTLKGVVEAHQDIQVKVTVNDTDYTASIDNDISN.............................

                          143                                    184
S. Typhi Ty2              SVTFTGTSPTENPVNKSSGVDEMIMPDN.............
S. Paratyphi A ATCC9150   SVTFTGTSPTENPVNKSSGVDEMIMPDN.............
S. Paratyphi B SPB7       .........................................
S. Paratyphi C RKS4594    .........................................
S. Typhimurium ATCC14028 .GTFTGTSPTKNPVNKSSGVDEMISLSEATWHSVSVDEENHA
S. Enteritidis EC200990135 .........................................
```

StoC

```
                          1                                                                                                  71
S. Typhi Ty2              ...........................................................MPDGLESTLE
S. Paratyphi A ATCC9150   ...........................................................MPDGLESTLE
S. Paratyphi B SPB7       MNQKVLFFLSIIAYPGITQAINQNVMIEPLVIRDSTNYLVLPQAQQAEFSQCKSWPHDSTVIPAKYEATLL
S. Paratyphi C RKS4594    MNQKVLFFLSIIAYPGITQAINQNVMIEPLVIRDSTNYLVLPQAQQAEFSQCKSWPHDSTVIPAKYEATLL
S. Enteritidis EC20090135 MNQKVLFFLSIIAYPGITQAINQNVMIEPLVIRDSTNYLVLPQAQQAEFSQCKSWPHDSTVIPAKYEATLL
                          72                                                                                                 133
S. Typhi Ty2              FDPST.SFINTTAVDNGITY.SFTGEAVKATAHASCTANQATNS....AIC...VWDKSFSLPLTLLTKQN
S. Paratyphi A ATCC9150   FDPST.SFINTTAVDNGITY.SFTGEAVKATAHANCTANQATNS....AIC...VWDKSFSLPLTLLTKQN
S. Paratyphi B SPB7       NGSLISMFI......GGITVNLYTTADVKVNTDAQCTLLNGNFPGYYGITCFVTGYDTDKAVPV...RTDN
S. Paratyphi C RKS4594    NGSLISMFI......GGITVNLYTTADVKVNTDAQCTLLNGNFPGYYGITCFVTGYDTDKAVPV...RTDN
S. Enteritidis EC20090135 NGSLISMFI......GGITVNLYTTADVKVNTDAQCTLLNGNFPGYYGITCFVTGYDTDKAVPV...RTDN
                          134                                                                                                199
S. Typhi Ty2              GITINQQNLT.......VSVIPGGGNNDTNQYSSLSGHIIIDESVSSYTNYEPETSGIENLKLK......W
S. Paratyphi A ATCC9150   GITINQQNLT.......VSVIPGGGNNDTNQYSSLSGHIIIDESVSSYTNYEPETSGIENLKLK......W
S. Paratyphi B SPB7       GMSIIESKLYATGTMRYITEIPMDGSG..FQGMAIGGAVVINTGAI...TPTPNTGVISNITMPPLYDPGF
S. Paratyphi C RKS4594    GMSIIESKLYATGTMRYITEIPMDGSG..FQGMAIGGAVVINTGAI...TPPPNTGVISNITMPPLYDPGF
S. Enteritidis EC20090135 GMSIIESKLYATGTMRYITEIPMDGSG..FQGMAIGGAVVINTGAI...TPTPNTGVISNITMPPLYDPGF
                          200                                                                                                266
S. Typhi Ty2              TVTVTEDTEGDVGIW..NGSLVLNGSPASTLHRYLLPEILDASFSENAIAHSTEVAMTGAKNNVELASVYL
S. Paratyphi A ATCC9150   TVTVTEDTEGDVGIW..NGSLVLNGSPASTLHRYLLPEILDASFSENAIAHSTEVAMTGAKNNVELASVYL
S. Paratyphi B SPB7       IFTVP..GCGQYKYHSGTGSVFTNNNS..TYTVASPIGFITASLDKKSVLNYNELHYNDKAENIELGKIYL
S. Paratyphi C RKS4594    IFTVP..GCGQYKYHSGTGSVFTNNNS..TYTVASPIGFITASLDKNSVLNYNELHYNDKAENIELGKIYL
S. Enteritidis EC20090135 IFTVP..GCGQYKYHSGTGSVFTNNNS..TYTVASPIGFITASLDKNSVLNYNELHYNDKAENIELGKIYL
                          267                                                                                                337
S. Typhi Ty2              YHGNTPCDDTSLCNYSLNKTSVSLVCHDLNAQLNFSNTCNASGTTHCLNGKVGTIKGTWERVNIDTTCAIT
S. Paratyphi A ATCC9150   YHGNKPCDDTSLCNYSLNKTSVALVCHDLNAQLAFSSTCNASDTTHCLNGKVGTINGTWGKVSIDTTCAIT
S. Paratyphi B SPB7       MYKEKNVTWGEGFDYTLENSTINVVCADSRIKTNVDYQCRNGDMGACNNGELGRIIGNWERINVDTNCSVT
S. Paratyphi C RKS4594    MYKEKNVTWGEGFDYTLENSTINVVCADSRIKTNVDYQCRNGDMGACNNGELGRIIGNWERINVDTNCSVT
S. Enteritidis EC20090135 MYKEKNVTWGEGFDYTLENSTINVVCADSRIKTNVDYQCRNGDMGACNNGELGRIIGNWERINVDTNCSVT
                          338  343
S. Typhi Ty2              VLIPYE
S. Paratyphi A ATCC9150   VLIPYE
S. Paratyphi B SPB7       VILPWQ
S. Paratyphi C RKS4594    VILPWQ
S. Enteritidis EC20090135 VILPWQ
```

StoD

```
                          1                                                                                                  72
S. Typhi Ty2              MFLTFPNVAITRDNRIDKLSENDLELIRDTAIQNGGRKIQVQLRDLLYEVSNRAVEGDNNTFKVSFSTTDRA
S. Paratyphi B SPB7       ...........................................................MVPWREPGQV
                          73                                                                                                 139
S. Typhi Ty2              ..MFRERHIEWQGNAIRLERQLNTGLNVSRGNFLNMSTTSFSNNSQELAAHSSPGAPAIFD...TSNKQQLV
S. Paratyphi B SPB7       YSDIRRSYPERFSNAERLARQLNRTWNMPAPP....ASLTFSE.........SQNARYHFNTQPANIRDLLP
                          140                                                                                                211
S. Typhi Ty2              DKIDLCSFSPNVDELSCTEDNLTCPVMLVVPEKGVFVKTGPESNICQLFDETALIQLIIDGATHPVSRAPLS
S. Paratyphi B SPB7       VRINFCSFQVEAGSFACSEEHLTCPITLDIPTNGVFVKVSSQSDICCLFDKEAFLNLVCQGLEHPLSREPIC
                          212                   233
S. Typhi Ty2              LDMIINKNECYFDTTKGNFIIP
S. Paratyphi B SPB7       MGMIVRKSECFFNTERDKFTLK
```